Synthesis of Novel π-Conjugated Compounds Based on Tetrasubstituted [2.2]Paracyclophane

Masayuki GON

2016

Synthesis of Novel π-Conjugated Compounds Based on Tetrasubstituted [2.2]Paracyclophane

Masayuki GON

2016

Department of Polymer Chemistry
Graduate School of Engineering
Kyoto University

Preface

The studies presented in the thesis have been carried out under the direction of Professor Yoshiki Chujo at Department of Polymer Chemistry, Graduate School of Engineering, Kyoto University from April 2010 to January 2016. The studies are concerned with “Synthesis of Novel π-Conjugated Compounds Based on Tetrasubstituted [2.2]Paracyclophane”.

The author wishes to express his sincerest gratitude to Professor Yoshiki Chujo for his kind guidance, valuable suggestions and warm encouragement throughout this work. The author is deeply grateful to Professor Yasuhiro Morisaki for his constant advice and helpful discussions during this work. The author would like to thank Dr. Kazuo Tanaka, Dr. Yuichi Tsuji, Dr. Yuichi Kajiwara and Dr. Takahiro Kakuta for their valuable suggestions and discussion. The author is indebted to Ms. Risa Sawada, Mr. Hiroto Kozuka and Mr. Keita Sato for their great contributions to this work. The author wishes to acknowledge all members of Professor Chujo's group. The author is obliged to Ms. Masako Kakutani for her assistance during the author's laboratory life.

Furthermore, the author would like to thank Professor Kazuo Akagi, Professor Susumu Kitagawa, Professor Norihiro Tokitoh, Dr. Takashi Uemura, Dr. Takahiro Sasamori, Dr. Nobuhiro Yanai, Dr. Munehiro Inukai and Dr. Kazuyoshi Watanabe for their great collaborations in this study. The author wishes to express thanks to Professor Kenneth J. Wynne and Dr. Orga Zolotarskaya at Department of Chemical and Life Science Engineering, Virginia Commonwealth University for their support and valuable suggestions during the author's stay in the U.S. The author is grateful to Japan Society for the Promotion of Science (JSPS) for financial support.

Finally, the author expresses his deep appreciation to his friend and family, especially his parents, Jundo Gon and Sachiko Gon, and his brothers Hidetoshi Gon and Yasufumi Gon, for their continuous assistance and encouragement.

Masayuki Gon

Department of Polymer Chemistry
Kyoto University
January 2016

Contents

General Introduction ---------- 1

Part I: Conjugated Microporous Polymers Based on [2.2]Paracyclophanes

Chapter 1 ---------- 17

Synthesis and Characterization of [2.2]Paracyclophane-Containing Conjugated Microporous Polymers

Chapter 2 ---------- 35

Conjugated Microporous Polymers Consisting of Tetrasubstituted [2.2]Paracyclophane Junctions

Part II: π-Conjugated Compounds Based on Planar Chiral [2.2]Paracyclophanes

Chapter 3 ---------- 49

Planar Chiral Tetrasubstituted [2.2]Paracyclophane: Optical Resolution and Functionalization

Chapter 4 ---------- 67

Optically Active Cyclic Compounds Based on Planar Chiral [2.2]Paracyclophane: Extension of the Conjugated Systems and Chiroptical Properties

Chapter 5 ---------- 95

Optically Active Cyclic Compounds Based on Planar Chiral [2.2]Paracyclophane: Extension of π-Surface with Naphthalene Units

Chapter 6 ---------- 121

Highly Emissive Optically Active Conjugated Dimers Consisting of Planar Chiral [2.2]Paracyclophane Showing Circularly Polarized Luminescence

Chapter 7 ---------- 137

Enhancement of Circularly Polarized Luminescence Based on a Planar Chiral Tetrasubstituted [2.2]Paracyclophane Framework in Dilute Solution and Aggregation

Chapter 8 ---------- 167

Optically Active Phenylethene Dimers Based on Planar Chiral Tetrasubstituted [2.2]Paracyclophane

Part III: Optically Active Materials Based on Planar Chiral [2.2]Paracyclophanes

Chapter 9 ---------- 187

Control of Optical and Chiroptical Properties with Metal-Induced Higher-Ordered Structure Based on Planar Chiral Tetrasubstituted [2.2]Paracyclophane

Chapter 10 ---------- 213

Synthesis of Optically Active X-Shaped Conjugated Compounds and Dendrimers Based on Planar Chiral [2.2]Paracyclophane, Leading to Highly Emissive Circularly Polarized Luminescence Materials

List of Publications ---------- 237

General Introduction

1. Cyclophane Compounds

Cyclophanes are cyclic organic molecules which contain one or more aromatic rings in the main chain skeleton.[1] The aromatic rings provide rigidity, and in many cases the aliphatic linkers provide flexibility to the cyclic structure. Generally, the size of cyclic structure is important for the studies of cyclophanes. Large size cyclophanes are widely studied in the field of host-guest chemistry[2] and supramolecular assembly;[3] in addition, some natural products[4] have the large cyclophane structure. Such cyclophanes usually do not exhibit intramolecular π-π interaction of aromatic rings. Small size cyclophanes are well-investigated in the field of organic synthetic chemistry[1e,5] due to the specific π-electron system and the three-dimensionally rigid structure.[6] Such cyclophanes usually exhibit intramolecular π-π interaction of aromatic rings and have the restricted aromatic rings which cannot rotate freely. Almost all of the small cyclophanes are chemically synthesized and hardly observed in the natural products. Cyclophanes are classified as [n]orthocyclophane, [n]metacyclophane, and [n]paracyclophane depending on the substituent positions of aromatic rings; [n] means the number of carbon atoms in the aliphatic linkers. Several cyclophanes have two or more aromatic rings and aliphatic linkers. Especially, [2.2]orthocyclophane, [2.2]metacyclophane, and [2.2]paracyclophane are actively studied for a long time because of the clarity of the structure. The structures are shown in Figure 1. Among such [2.2]cyclophanes,

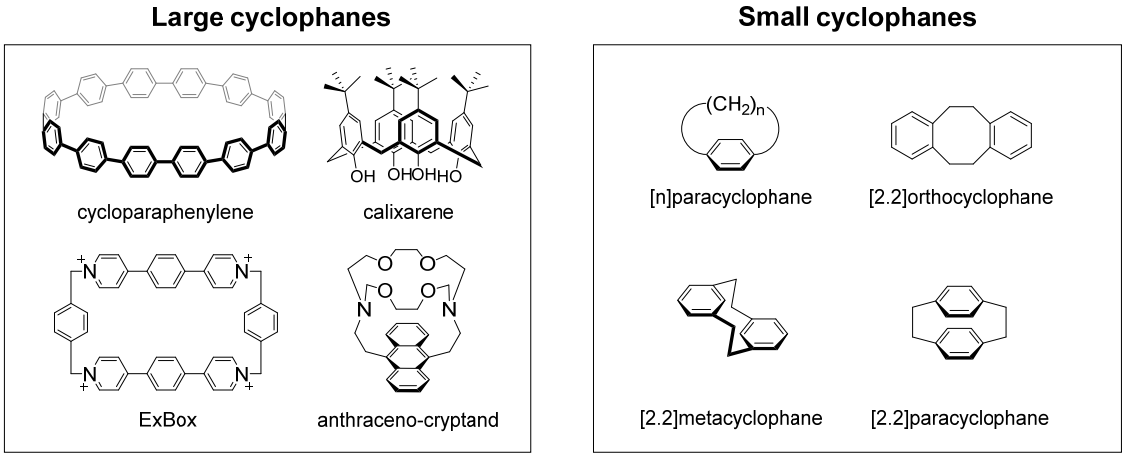

Figure 1. Cyclophane families.

[2.2]paracyclophanes are received much attention as the system having the strong π-π interaction and delocalized π-electrons between two benzene rings. A lot of [2.2]paracyclophane derivatives have been synthesized so far, and the physical properties and reactivities have been elucidated.

2. [2.2]Paracyclophane

[2.2]Paracyclophane was firstly discovered by Brown and Farthing in 1949. They synthesized and isomerized the trace amounts by high temperature pyrolysis of *p*-xylene, and the structure was confirmed by X-ray crystallography.[7] In 1951, Cram and co-workers reported the synthesis of [2.2]paracyclophane with Wrutz-type intramolecular reaction of 1,4-bis(bromomethyl)benzene.[8] After these discovery, this unique hydrocarbon had been received much attention, and numerous research projects were carried out.[9] [2.2]Paracyclophane has the face-to-face oriented two benzene rings which are connected by two ethylene units at the *para*-position. The distance of two benzene rings is approximately 3 Å, and the benzene rings are slightly bent like a boat structure. The π-electrons are delocalized between two benzene rings and this π-π interaction is called though-space conjugation. The highest occupied molecular orbital (HOMO), lowest unoccupied molecular orbital (LUMO) and nomenclature (numbering) of pseudo-*ortho*-[2.2]paracyclophane are shown in Figure 2. Using these unique structure and properties, a lot of functionalizations and functional materials have been developed. Examples of functionalized 4-monosubstituted [2.2]paracyclophanes are shown in Figure 3.

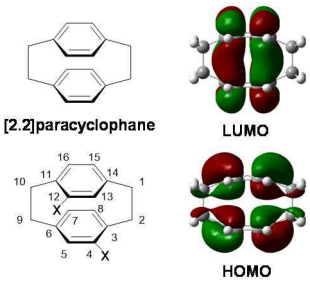

Figure 2. HOMO-LUMO orbitals and nomenclature.

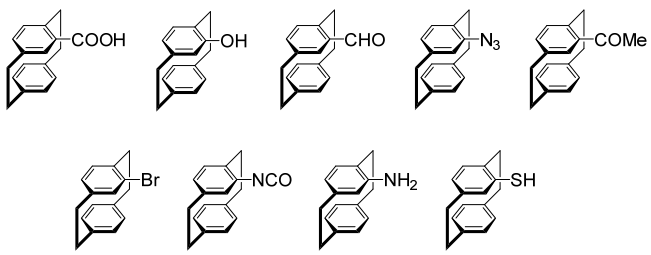

Figure 3. Examples of functionalized 4-monosubstituted [2.2]paracyclophanes.

First investigation of the chemical behaviors of [2.2]paracyclophane was carried out by Cram and co-workers in 1960s.[10] Recently, Hopf and co-workers developed synthetic method of [2.2]paracyclophanes having ethynyl groups at various positions.[11] These polyethynyl[2.2]paracyclophanes are available for π-conjugated building block (Figure 4). Bazan, Mukamel and co-workers investigated π-conjugated systems based on [2.2]paracyclophane in detail.[12] The π-conjugation system varied drastically with the π-conjugation length and the position of through-space conjugation of a [2.2]paracyclophane unit. Chujo, Morisaki and co-workers firstly applied [2.2]paracyclophane to π-conjugated polymer chemistry.[13] They reported synthesis and optical properties of though-space π-conjugated polymer including a [2.2]paracyclophane unit in the main chain, and excitation energy was migrated to entire the polymer chain. The bridge ethylene units of [2.2]paracyclophane decompose over 200 ˚C to produce benzyl radicals (Figure 5).[10a] If the [2.2]paracyclophane is chiral, racemization occurs. Gorham reported that [2.2]paracyclophane was quantitatively cleaved by vacuum vapor-phase pyrolysis at 600 ˚C to generate two molecules of *p*-xylene biradical.[14] The highly reactive *p*-xylene biradical was polymerized on surfaces (metals, glass, paper, plastics, ceramics etc.) maintained below 30 ˚C. He called the polymer 'parylene' (Figure 6). Recently, the bond cleavage proceeded with metal supported and catalytic system.[15] Rigid structure of [2.2]paracyclophanes is also applied to fast photochromic molecules.[16] In [2.2]paracyclophane chemistry, the fundamental properties have been actively investigated since the discovery. Recently, the unique properties started to be applied to polymer and materials chemistry.

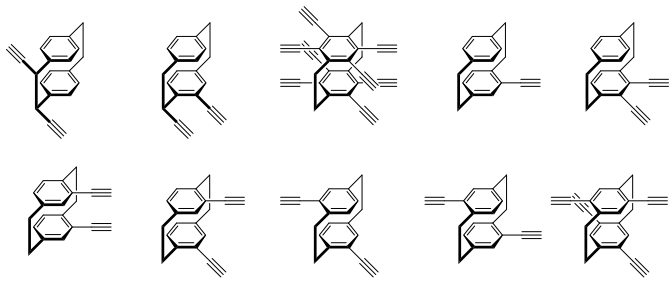

Figure 4. Examples of polyethynyl[2.2]paracyclophanes.

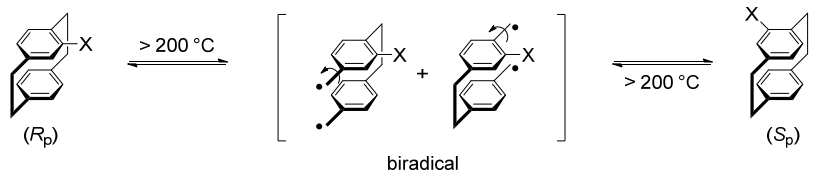

Figure 5. Bridge cleavage and racemization of [2.2]paracyclophane over 200 ˚C.

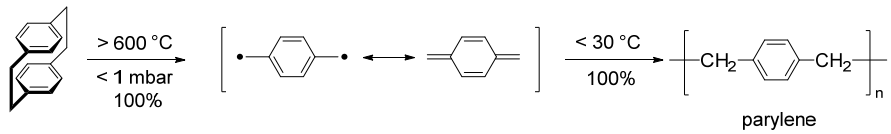

Figure 6. Bridge cleavage and polymerization of [2.2]paracyclophane over 600 ˚C by Gorham.

3. π-Conjugation System Based on [2.2]Paracyclophane

Detailed investigations on π-conjugation systems including the [2.2]paracyclophane unit were carried out by Bazan, Mukamel and co-workers[12] using the phenylene-vinylene systems. The features of π-conjugation system based on [2.2]paracyclophane are divided into two factors. One is the difference of the staking position with [2.2]paracyclophane in the monomer unit. The other is the π-conjugation length of the monomer unit. Monomer unit means one of the two stacked chromophores with [2.2]paracyclophane. In the case of the π-conjugation system stacked at the terminal aromatic ring, when the π-conjugation length is short, monomers strongly interact each other and photoluminescence is observed from mainly through-space (TS) level of [2.2]paracyclophane unit. It is called 'phane state'. The absorption occurs in the through-bond (TB) level of the monomer state because the phane state is forbidden transition band. On the other hand, when the π-conjugation length is long, the interaction is weak and photoluminescence is observed from mainly TB level of the monomer unit. In the case of the π-conjugation system stacked at central position, the strong interaction of the stacked monomers occurs and the absorbance and photoluminescence are observed from mixed monomer and phane state (Figure 7). Hopf and co-workers reported the optical properties of cyclic π-conjugation system including [2.2]paracyclophane (Figure 8).[17] Especially, in

4,7,12,15-tatrasubstituted [2.2]paracyclophane, the cyclic π-conjugation system effectively exhibited three-dimensional π-conjugation system via through-space conjugation of [2.2]paracyclophane. The UV-vis and photoluminescence spectra drastically changed compared with non-cyclic compounds. Chujo, Morisaki and co-workers reported phenylene-ethynylene-stacked optically active cyclic compounds with planar chiral [2.2]paracyclophane scaffolds (Figure 8).[18] Through-space conjugation behaviors in polymer[19] and oligomer[20] systems were actively investigated. The photo-excited energy was transferred to the terminal unit via through-space conjugation of [2.2]paracyclophane (Figure 9). In the case of poly(*p*-phenylene-ethynylene) system, the effective π-conjugation length of through-space π-conjugation system was longer than that of through-bond π-conjugation one. In addition, making advantage of designability of the stacked π-conjugation unit and effective fluorescence resonance energy transfer, it is expected to apply for single molecular wire as energy transfer media. Knorr, Harvey and co-workers also reported the features of Dexter type energy transfer behavior via [2.2]paracyclophane.[21] Martín and co-workers reported the photo-excited electron transfer through [2.2]paracyclophane.[22]

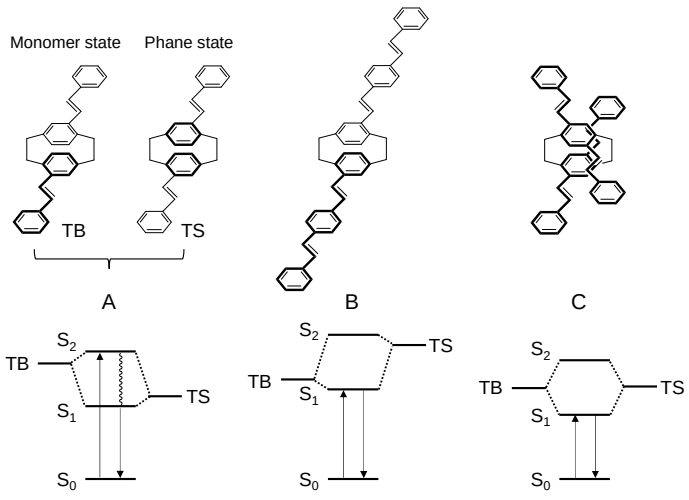

Figure 7. Qualitative electronic description of bichromophoric [2.2]paracyclophane molecules. In **A**, absorption occurs via the stilbene fragment, as shown by the excitation from S_0 to S_2. Internal conversion populates S_1, which is primarily TS in character, and emission occurs from there. In **B**, TB has lower energy, relative to TS. In **C**, TB and TS are mixed by interchromophore contact.

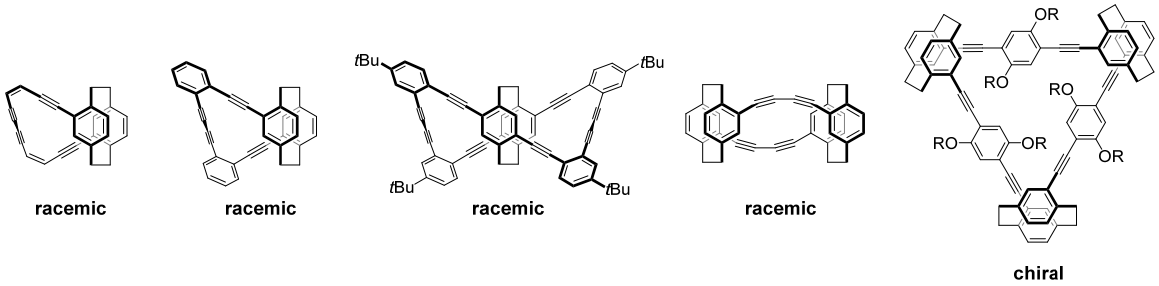

Figure 8. Examples of [2.2]paracyclophane-containing cyclic compounds.

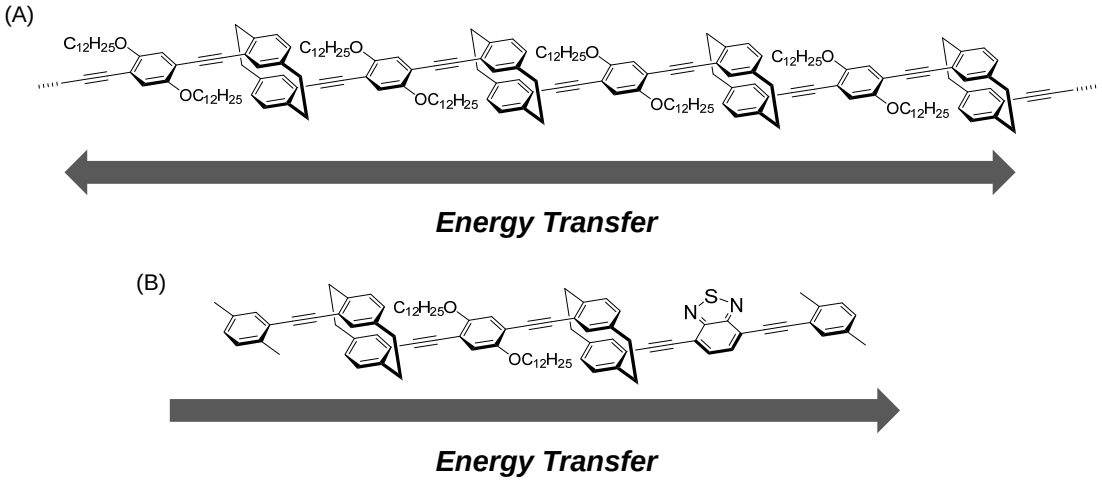

Figure 9. Energy transfer through molecules via [2.2]paracyclophane. (A) Excited energy is transferred entire the polymer chain. (B) Excited energy is transferred unidirectionally.

4. Planar Chirality of [2.2]Paracyclophane

[2.2]Paracyclophanes with substituent(s) exhibit planar chirality because the benzene rings cannot rotate. Numerous researches were carried out to obtain enantiopure planar chiral [2.2]paracyclophane so far.[23-25] Definition of the planar chirality is shown in Figure 10; first, a pilot atom, which is nearest atom to chiral plane, is decided; second, go to chiral plane from the pilot atom, then turn to a prior atom (an arrow in Figure 10). When the rotation is right, the planar chirality is (R_p), and when the rotation is left, the planar chirality is (S_p). Rowlands and co-workers reported the general optical resolution method of 4-monosubstituted [2.2]paracyclophane.[23g] They used optically

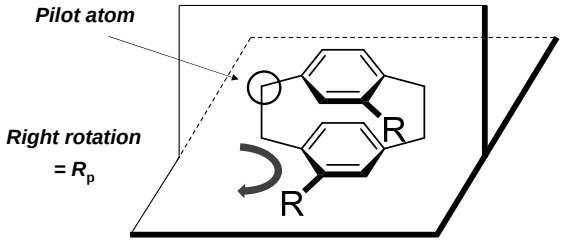

Figure 10. Definition of planar chirality.

active sulfoxide with an optical resolution agent and converted the sulfoxide to functional groups such as formyl and azide groups with sulfoxide-metal exchange method by *t*-butyllithium. Chujo, Morisaki and co-workers reported the general optical resolution method of pseudo-*ortho*-[2.2]paracyclophane[24h] in reference to the report of Rowlands.[23g] In addition, they developed the transformation to planar chiral ethynyl[2.2]paracyclophane, leading to the planar chiral π-conjugated compounds. The other planar chiral [2.2]paracyclophanes already synthesized are described in Figure 11. Thus, a lot of planar chiral [2.2]paracyclophanes have been synthesized and one of them was applied to an optically active phosphine ligand "PHANEPHOS",[24a,b] which was commercially available. Functionalized planar chiral [2.2]paracyclophane has a potential to be a novel optically active building block. Binaphthyl groups[26] (axial chirality) and helicene groups[27] (helical chirality) are famous as candidates for optically active building blocks. The main character of planar chirality of [2.2]paracyclophane is planarity, which is different from binaphthyl or helicene. The chirality of [2.2]paracyclophane is derived from restricted rotation of benzene rings. On the other hand, those of binaphthyl and helicene are derived from torsions. Therefore, planar chiral [2.2]paracyclophane has rigid structure and has the potential to extend π-conjugation length effectively. In addition, the [2.2]paracyclophane possesses good designability, as can be seen in a wide variety of functionalized [2.2]paracyclophane derivatives. The properties are advantage for opto-electronic materials and various applications.

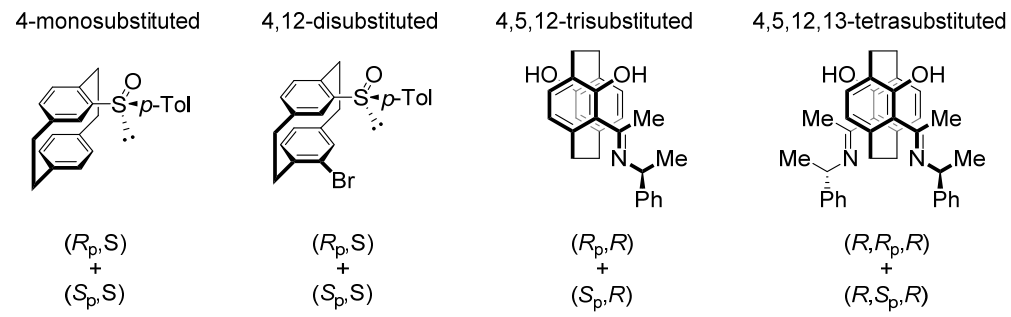

Figure 11. Planar chiral multi-substituted [2.2]paracyclophanes already reported.

5. Summary of This Thesis

The author has carried out the research to elucidate the properties of [2.2]paracyclophane and to suggest the potential applications to functionalized materials. The author has focused on 4,7,12,15-tetrasubstituted [2.2]paracyclophane which is one of the tetrasubstituted [2.2]paracyclophanes. The π-conjugation system using 4,7,12,15-tetrasubstituted [2.2]paracyclophane exhibits though-space conjugation at central position. The properties of these derivatives were investigated by Bazan, Mukamel and co-workers in detail. However, only several *p*-arylene-vinylene-based derivatives have been reported, and the planar chirality has not been investigated. Considering the unique properties of 4,7,12,15-tetrasubstituted [2.2]paracyclophane, it is important to synthesize many derivatives and investigate the chiroptical properties for various applications. One of the reasons why there has not been many researches on 4,7,12,15-tetrasubstituted [2.2]paracyclophane is a difficulty of the synthesis. Firstly, the author developed gram-scale synthesis of 4,7,12,15-tetrabromo[2.2]paracyclophane which is converted to a lot of functionalized [2.2]paracyclophanes. In reference to synthetic method previously reported,[28] the reaction process and purification method were optimized (Scheme 1). As a result, over 10 g synthesis was achieved in total 50% yield from a commercially available compound. Especially, the yield of the final dimerization process was improved from 20% to 68%, and the insoluble polymeric byproducts were reduced. Recrystallization is the only purification method and SiO_2 column chromatography is not necessary.

Scheme 1. Gram-scale synthesis of 4,7,12,15-tetrabromo[2.2]paracyclophane

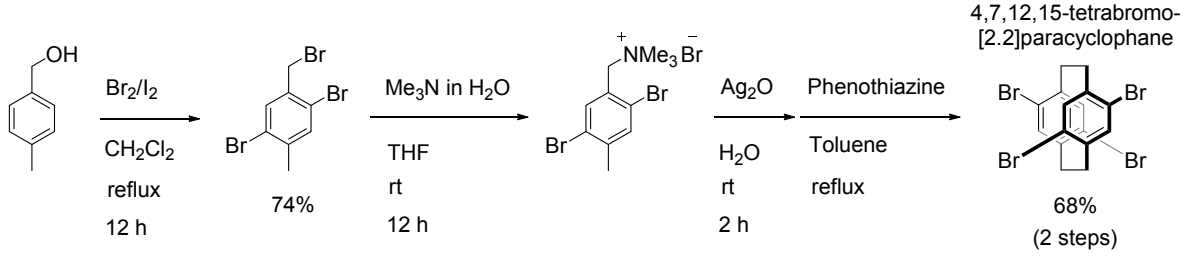

In Chapter 1, conjugated microporous polymers (CMPs) were prepared from disubstituted and tetrasubstituted [2.2]paracyclophane monomers by a Sonogashira-Hagihara coupling. The polymers obtained exhibited a type I nitrogen gas adsorption profile and H4-like hysteresis loops, indicating that the [2.2]paracyclophane containing CMPs possess slit-like mesopores. Their Brunauer-Emmett-Teller surface areas were estimated to be over 500 m^2g^{-1}. The step and stacked structure of the [2.2]paracyclophane unit affects the morphology of the polymers because of the contribution of two-dimensional expansion of the polymer network.

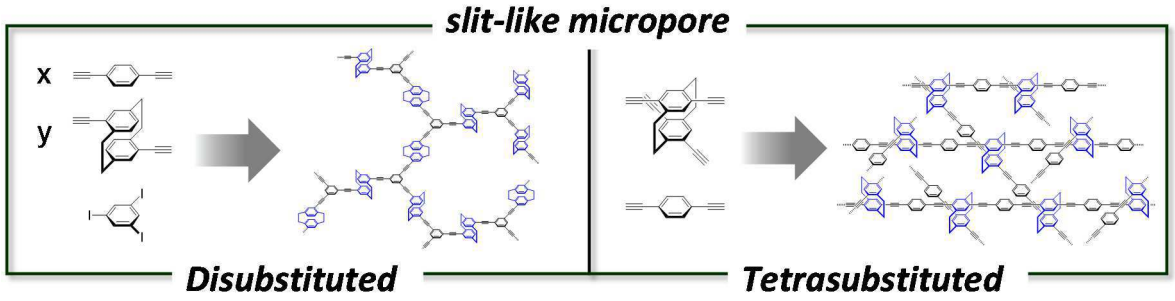

In Chapter 2, conjugated microporous polymers (CMPs) were synthesized from the tetrasubstituted [2.2]paracyclophane skeleton as a tetra-functional building block using Hay coupling, Sonogashira-Hagihara cross-coupling, and Yamamoto coupling. The CMPs exhibited microporosity (less than 2 nm) and large surface areas (up to approximately 1000 m^2g^{-1}). The CMPs consisted of relatively uniform particles and dispersed in organic solvents. These results suggest their possible applications in the fields of opto-electronics and catalyst chemistry.

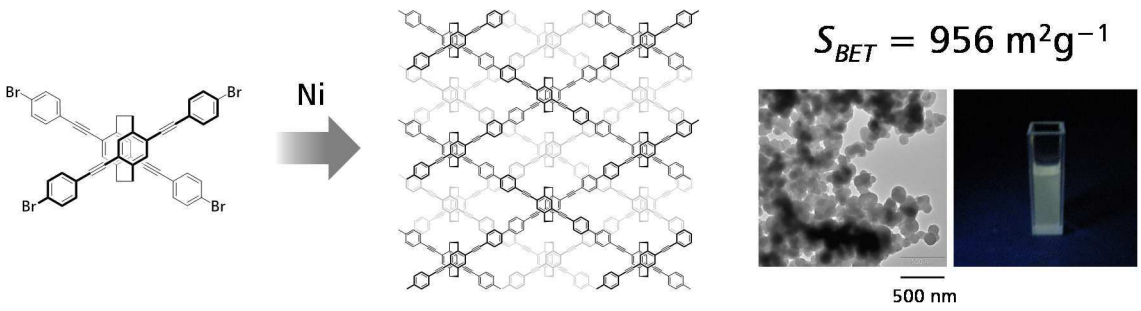

In Chapter 3, the author achieved optical resolution of 4,7,12,15-tetrasubstituted [2.2]paracyclophane and subsequent transformation to planar chiral building blocks. An optically active propeller-shaped macrocyclic compound containing a planar chiral cyclophane core was synthesized, showing excellent chiroptical properties such as high fluorescence quantum efficiency and a large circularly polarized luminescence dissymmetry factor.

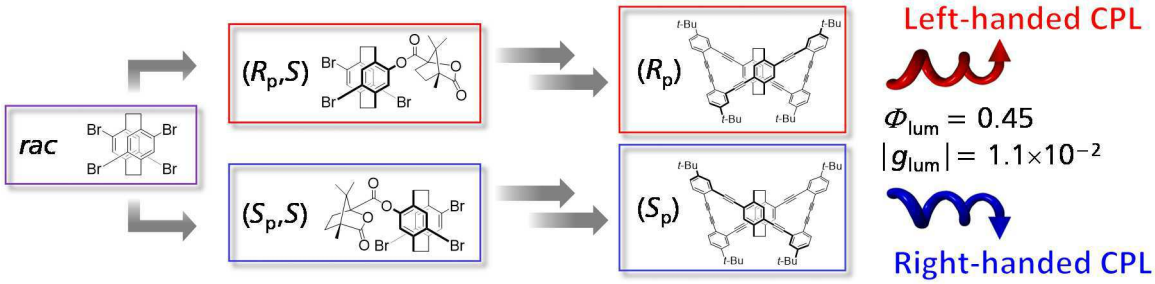

In Chapter 4, a series of optically active cyclic compounds based on the planar chiral tetrasubstituted [2.2]paracyclophane core were synthesized to obtain luminescent materials with excellent chiroptical properties in both the ground and excited states. The obtained cyclic compounds were composed of the optically active propeller-shaped structures created by the [2.2]paracyclophane core with *p*-phenylene-ethynylene moieties. The compounds exhibited good optical profiles, with a large molar extinction coefficient (ε) and photoluminescence quantum efficiency (Φ_{lum}). This optically active higher-ordered structure provided chiroptical properties of high performance, such as intense circularly polarized luminescence (CPL) with large dissymmetry factors (g_{lum}) in the excited state.

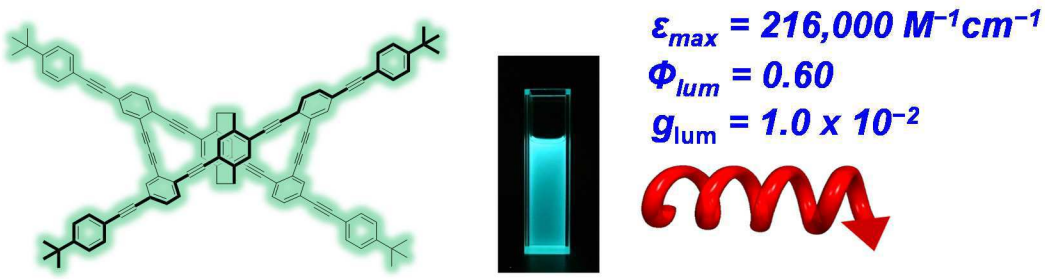

In Chapter 5, the author synthesized optically active cyclic compounds with extension of π-surface with naphthalene units based on a planar chiral 4,7,12,15-tetrasubstituted [2.2]paracyclophane framework. Hypsochromic effect was observed in the absorption and photoluminescence (PL) spectra of naphthalene-containing cyclic derivatives compared with those of benzene ones. Density functional theory (DFT) indicated that HOMO-LUMO band gap increased by introducing naphthalene units. Optimized structures showed that one of reasons of the hypsochromic effect was torsions of the cyclic structure.

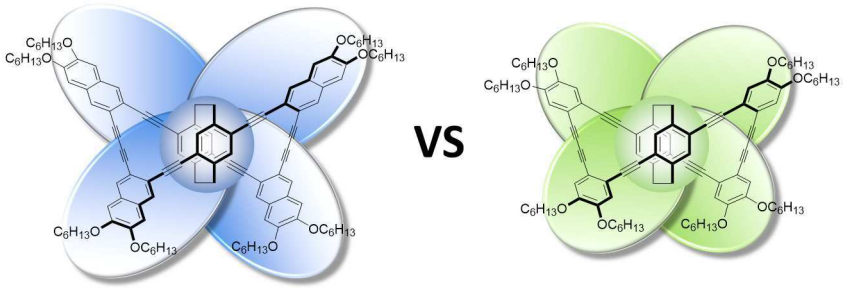

In Chapter 6, optically active π-conjugated dimers based on a planar chiral 4,7,12,15-tetrasubstituted [2.2]paracyclophane were synthesized. The π-conjugated dimers were functionalized by arylethynyl groups, such as phenyl, naphthyl and anthryl units. When the monomer had small aromatic unit, such as benzene and naphthalene, the dimer exhibited typical dimer-like optical properties. On the other hand, when anthracene was used, the dimer exhibited monomer-like optical properties. In the circular dichroism (CD) and circularly polarized luminescence (CPL) spectra, they exhibited unique chiroptical properties.

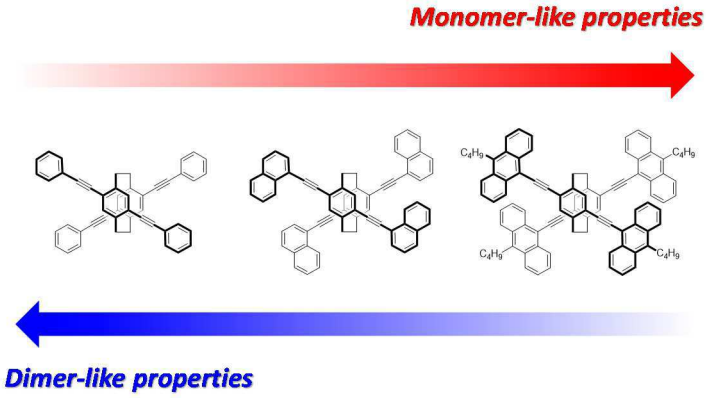

In Chapter 7, optically active π-conjugated oligo(phenylene-ethynylene) dimers with a planar chiral 4,7,12,15-tetrasubstituted [2.2]paracyclophane were synthesized. In the dilute solution, the dimers exhibited good chiroptical properties; *i.e.* 10^{-3} order dissymmetry factors (g_{abs} and g_{lum}). In the aggregation state, using kinetically stable preparing methods, one of dimers formed J-aggregates and the others formed parallel H-aggregates or inclined H-aggregates. The spin-coated films and drop-cast films exhibited opposite CPL signal each other with 10^{-2} order dissymmetry factor. Annealing method moves the films to the thermodynamically stable forms. The g_{lum} values of drop-cast thick films were drastically enhanced after annealing and the g_{lum} values reached 10^{-1} order.

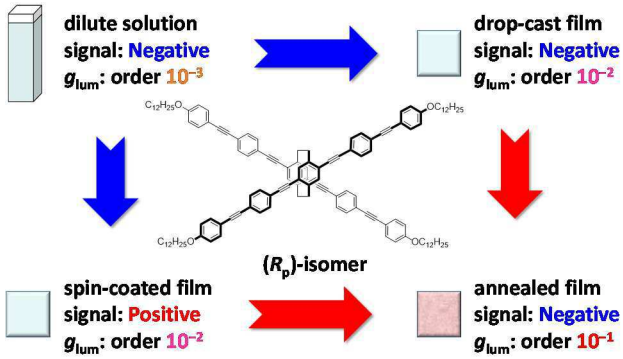

In Chapter 8, optically active phenylethene dimers based on a planar chiral 4,7,12,15-tetrasubstituted [2.2]paracyclophane were synthesized. The author succeeded in the synthesis of optically active photoluminescent compounds both in the dilute solution and in the aggregation state by attaching an aggregation-induced emission (AIE) active monomer to the [2.2]paracyclophane framework. The photoluminescent property in the dilute solution was obtained because the molecular motion of the AIE active monomers was suppressed by the rigid [2.2]paracyclophane framework.

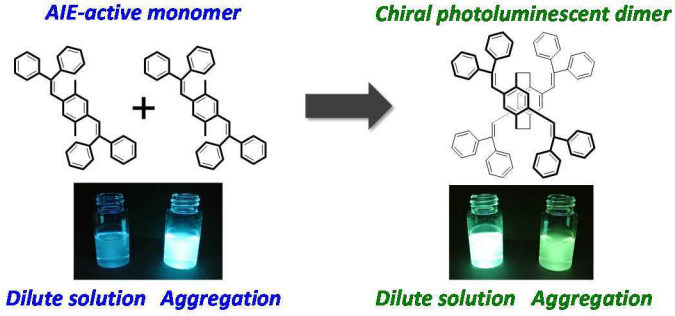

In Chapter 9, optically active *meta*-arylene-ethynylenes with pyridine groups based on a planar chiral 4,7,12,15-tetrasubstituted [2.2]paracyclophane were synthesized. The enantiopure higher-ordered structures were controlled by pyridine-Ag(I) complexation or an excimer formation. After Ag(I) coordination, the structural change was observed. The intramolecular interaction of the terminal pyrene units was observed in the ground state, and static excimer properties were observed because of the rigid π-π interaction in the excited state. Titration of Ag(I) revealed that the different coordination number of the compounds from two to four Ag(I) ions. Optical and chiroptical properties suggested the existence of intramolecular Ag(I)-π interaction.

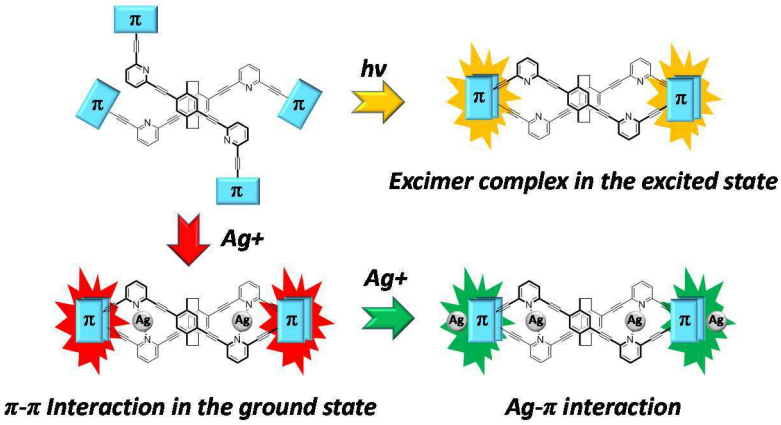

In Chapter 10, the author synthesized optically active dendrimers with a planar chiral 4,7,12,15-tetrasubstituted [2.2]paracyclophane as a core unit. Light-harvesting effect and steric protection of the dendrimer structure enhanced photoluminescence property both in the dilute solution and in the film state with excellent CPL profiles (dissymmetry factor: $g_{lum} \approx 0.002$, and absolute fluorescence quantum efficiency: $\Phi_{lum} \approx 0.60$).

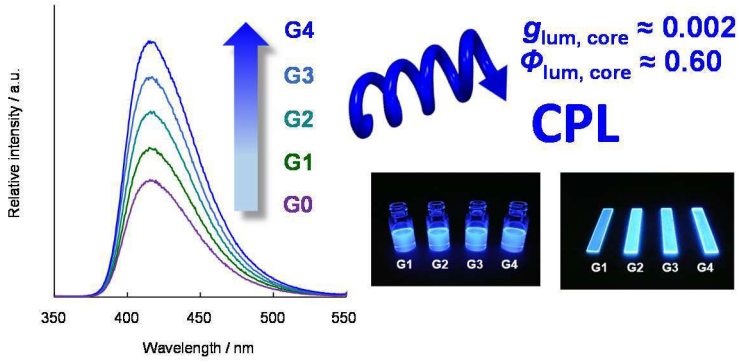

References and Notes

(1) (a) Kotha, S.; Shirbhate, M. E.; Waghule, G. T. **2015**, *11*, 1274–1331. (b) Hirst, E. S.; Jasti, R. *J. Org. Chem.* **2012**, *77*, 10473–10478. (c) Ikeda, A.; Shinkai, S. *Chem. Rev.* **1997**, *97*, 1713–1734. (d) Strutt, N. L.; Zhang, H.; Schneebeli, S. T.; Stoddart, J. F. *Acc. Chem. Res.* **2014**, *47*, 2631–2642. (e) Ghasemabadi, P. G.; Yao, T.; Bodwell, G. J. *Chem. Soc. Rev.* **2015**, *44*, 6494–6518.

(2) (a) Iwamoto, T.; Watanabe, Y.; Sadahiro, T.; Haino, T.; Yamago, S. *Angew. Chem., Int. Ed.* **2011**, *50*, 8342–8344. (b) Wald, P.; Schneider, H.-J. *Eur. J. Org. Chem.* **2009**, 3450–3453. (c) Takemura, H.; Nakata, S.; Inoue, A.; Mishima, A. **2013**, *77*, 483–487. (d) Fages, F.; Desvergne, J. P.; Bouas-Laurent, H.; Marsau, P.; Lehn, J. M.; Kotzyba-Hibert, F.; Albrecht-Gary, A. M.; Al-Joubbeh, M. *J. Am. Chem. Soc.* **1989**, *111*, 8672–8680. (e) Barnes, J. C.; Juríček, M.; Strutt, N. L.; Frasconi, M.; Sampath, S.; Giesener, M. A.; McGrier, P. L.; Bruns, C. J.; Stern, C. L.; Sarjeant, A. A.; Stoddart, J. F. *J. Am. Chem. Soc.* **2013**, *135*, 183–192. (f) Masci, B.; Pasquale, S.; Thuéry, P. *Org. Lett.* **2008**, *10*, 4835–4838. (g) Araki, K.; Shimizu, H.; Shinkai, S. *Chem. Lett.* **1993**, *22*, 205–208.

(3) (a) Juríček, M.; Barnes, J. C.; Dale, E. J.; Liu, W.-G.; Strutt, N. L.; Bruns, C. J.; Vermeulen, N. A.; Ghooray, K. C.; Sarjeant, A. A.; Stern, C. L.; Botros, Y. Y.; Goddard, W. A.; Stoddart, J. F. *J. Am. Chem. Soc.* **2013**, *135*, 12736–12746. (b) Abe, H.; Ohtani, K.; Suzuki, D.; Chida, Y.; Shimada, Y.; Matsumoto, S.; Inouye, M. *Org. Lett.* **2014**, *16*, 828–831. (c) Schmitt, A.; Perraud, O.; Payet, E.; Chatelet, B.; Bousquet, B.; Valls, M.; Padula, D.; Di Bari, L.; Dutasta, J.-P.; Martinez, A. *Org. Biomol. Chem.* **2014**, *12*, 4211−4217. (d) Ishihara, S.; Takeoka, S. *Tetrahedron Lett.* **2006**, *47*, 181–184.

(4) (a) Ploutno, A.; Carmeli, S. *J. Nat. Prod.* **2000**, *63*, 1524–1526. (b) Graupner, P. R.; Carr, A.; Clancy, E.; Gilbert, J.; Bailey, K. L.; Derby, J.-A.; Gerwick, B. C. *J. Nat. Prod.* **2003**, *66*, 1558–1561. (c) Ridley, D. D.; Ritchie, E.; Taylor, W. C. *Aust. J. Chem.* **1970**, *23*, 147–183.

(5) (a) Nishimura, J.; Okada ,Y.; Inokuma, S.; Nakamura, Y.; Gao, S. R. Synlett **1994**, *11*, 884–894. (b) Nishimura, J.; Nakamura, Y.; Hayashida, Y.; Kudo, T. *Acc. Chem. Res.* **2000**, *33*, 679-686.

(6) (a) *Cyclophane Chemistry: Synthesis, Structures and Reactions*; Vögtle, F., Ed.; John Wiley & Sons: Chichester, 1993. (b) *Modern Cyclophane Chemistry*; Gleiter, R., Hopf, H., Eds.; Wiley-VCH: Weinheim, 2004.

(7) Brown, C. J.; Farthing, A. C. *Nature* **1949**, *164*, 915–916.

(8) Cram, D. J.; Steinberg, H. *J. Am. Chem. Soc.* **1951**, *73*, 5691–5704.

(9) (a) Paradies, J. *Synthesis* **2011**, *23*, 3749–3766. (b) Meijere, A.; König, B. *Synlett* **1997**, *11*, 1221–1232. (c) Hopf, H. *Angew. Chem., Int. Ed.* **2008**, *47*, 9808–9812. (d) Elacqua, E.; MacGillivray, L. R. *Eur. J. Org. Chem.* **2010**, *2010*, 6883–6894. (e) Schneider, J. F.; Fröhlich, R.; Paradies, J. *Isr. J. Chem.* **2012**, *52*, 76–91. (f) Starikova, Z. A.; Fedyanin, I. V.; Antipin, M. Y. *Russ. Chem. Bull. Int. Ed.* **2004**, *53*, 1779–1805. (g) MacGillivray, L. R. *J. Org. Chem.* **2008**, *73*, 3311–3317. (h) Rowlands, G. J. *Isr. J. Chem.* **2012**, *52*, 60–75. (i) Elacqua, E.; Friščić, T.; MacGillivray, L. R. *Isr. J. Chem.* **2012**, *52*, 53–59. (J) Rowlands, G. J. *Org. Biomol. Chem.* **2008**, *6*, 1527–1534. (k) Gibson, S. E.; Knight, J. D. *Org. Biomol. Chem.* **2003**, *1*, 1256–1269. (l) Dyson, P. J.; Johnson, B. F. G.; Martin, C. M. *Coord. Chem. Rev.* **1998**, *175*, 59–89. (m) Aly, A. A.; Brown, A. B. *Tetrahedron* **2009**, *65*, 8055–8089. (n) David, O. R. P. *Tetrahedron* **2012**, *68*, 8977–8993.

(10) (a) Reich, H. J.; Cram, D. J. *J. Am. Chem. Soc.* **1969**, *91*, 3505–3516. (b) Reich, H. J.; Cram, D. J. *J. Am. Chem. Soc.* **1968**, *90*, 1365–1367. (c) Cram, D. J.; Fischer, H. P. *J. Org. Chem.* **1965**, *30*, 1815–1819. (d) Cram, D. J.; Dalton, C. K.; Knox, G. R. *J. Am. Chem. Soc.* **1963**, *85*, 1088–1093. (e) Cram, D. J.; Singer, L. A. *J. Am. Chem. Soc.* **1963**, *85*, 1084–1088. (f) Singer, L. A.; Cram, D. J. *J. Am. Chem. Soc.* **1963**, *85*, 1080–1084. (g) Cram, D. J.; Singer, L. A. *J. Am. Chem. Soc.* **1963**, *85*, 1075–1079. (h) Cram, D. J.; Wilkinson, D. I. *J. Am. Chem. Soc.* **1960**, *82*, 5721–5723.

(11) Bondarenko, L.; Dix, I.; Hinrichs, H.; Hopf, H. *Synthesis* **2004**, *16*, 2751–2759.

(12) (a) Bazan,G. C.; Oldham Jr, W. J.; Lachicotte,R. J.; Tretiak, S.; Chernyak, V.; Mukamel, S. *J. Am. Chem. Soc.* **1998**, *120*, 9188–9204. (b) Wang, S.; Bazan, G. C.; Tretiak, S.; Mukamel, S. *J. Am. Chem. Soc.* **2000**, *122*, 1289–1297. (c) Zyss, J.; Ledoux, I.; Volkov, S.; Chernyak, V.; Mukamel, S.; Bartholomew, G. P.; Bazan, G. C. *J. Am. Chem. Soc.* **2000**, *122*, 11956–11962. (d) Bartholomew, G. P.; Bazan, G. C. *Acc. Chem. Res.* **2001**, *34*, 30–39. (e) Bartholomew G. P.; Bazan, G. C. *Synthesis* **2002**, 1245–1255. (f) Bartholomew G. P.; Bazan, G. C.; *J. Am. Chem. Soc.* **2002**, *124*, 5183–5196. (g) Seferos, D. S.; Banach, D. A.; Alcantar, N. A.; Israelachvili, J. N.; Bazan, G. C. *J. Org. Chem.* **2004**, *69*, 1110–1119. (h) Bartholomew, G. P.; Rumi, M.; Pond, S. J. K.; Perry, J. W.; Tretiak, S.; Bazan, G. C. *J. Am. Chem. Soc.* **2004**, *126*, 11529–11542. (i) Hong, J. W.; Woo H. Y.; Bazan, G. C. *J. Am. Chem. Soc.* **2005**, *127*, 7435–7443. (j) Bazan, G. C. *J. Org. Chem.*, **2007**, *72*, 8615–8635.

(13) (a) Morisaki, Y.; Chujo, Y. *Angew. Chem., Int. Ed.* **2006**, *45*, 6430–6437. (b) Morisaki, Y.; Chujo, Y. *Polym. Chem.* **2011**, *2*, 1249–1257. (c) Morisaki, Y.; Chujo, Y. *Chem. Lett.* **2012**, *41*, 840–846.

(14) Gorham, W. F. *J. Polym. Sci. A-1 Polym. Chem.* **1966**, *4*, 3027–3039.

(15) (a) Eisch, J. J.; Dutta, S.; Gitua, J. N. *Organometallics* **2005**, *24*, 6291–6294. (b) To, C. T.; Choi, K. S.; Chan, K. S. *J. Am. Chem. Soc.* **2012**, *134*, 11388–11391.

(16) Kishimoto, Y.; Abe, J. *J. Am. Chem. Soc.* **2009**, *131*, 4227–4229.

(17) (a) Hinrichs, H.; Boydston, A. J.; Jones, P. G.; Hess, K.; Herges, R.; Haley, M. M.; Hopf, H. *Chem.–Eur. J.* **2006**, *12*, 7103–7115. (b) Dix, I.; Bondarenko, L.; Jones, P. G.; Oeser, T.; Hopf, H. **2014**, *10*, 2013–2020.

(18) Morisaki, Y.; Hifumi, R.; Lin, L.; Inoshita, K.; Chujo, Y. *Polym. Chem.* **2012**, *3*, 2727–2730.

(19) (a) Morisaki, Y.; Ueno, S.; Saeki, A.; Asano, A.; Seki, S.; Chujo, Y. *Chem.–Eur. J.* **2012**, *18*, 4216–4224. (b) Morisaki, Y.; Ueno, S.; Chujo, Y. *J. Polym. Sci. A Polym. Chem.* **2013**, *51*, 334–339.

(20) (a) Morisaki, Y.; Kawakami, N.; Shibata, S.; Chujo, Y. *Chem.–Asian J.* **2014**, *9*, 2891–2895. (b) Morisaki, Y.; Kawakami, N.; Nakano, T.; Chujo, Y. *Chem.–Eur. J.* **2013**, *19*, 17715–17718. (c) Morisaki, Y.; Kawakami, N.; Nakano, T.; Chujo, Y. *Chem. Lett.* **2014**, *43*, 426–428.

(21) Clement, S.; Goudreault, T.; Bellows, D.; Fortin, D.; Guyard, L.; Knorr, M.; Harvey, P. D. *Chem. Commun.* **2012**, *48*, 8640–8642.

(22) Wielopolski, M.; Molina-Ontoria, A.; Schubert, C.; Margraf, J. T.; Krokos, E.; Kirschner, J.; Gouloumis, A.; Clark, T.; Guldi, D. M.; Martín, N. *J. Am. Chem. Soc.* **2013**, *135*, 10372–10381.

(23) Optical resolution of 4-monosubstituted [2.2]paracyclophane: (a) Rozenberg, V.; Danilova, T.; Sergeeva, E.; Vorontsov, E.; Starikova, Z.; Korlyukov, A.; Hopf, H. *Eur. J. Org. Chem.* **2002**, 468–477. (b) Cipiciani, A.; Fringuelli, F.; Mancini, V.; Piermatti, O.; Pizzo, F.; Ruzziconi, R. *J. Org. Chem.* **1997**, *62*, 3744–3747. (c) Banfi, S.; Manfredi, A.; Montanari, F.; Pozzi, G.; Quici, S. *J. Mol. Catal. A: Chem.* **1996**, *113*, 77–86.

(d) Minuti, L.; Taticchi, A.; Marrocchi, A. *Tetrahedron: Asymmetry* **2000**, *11*, 4221–4225. (e) Pamperin, D.; Ohse, B.; Hopf H.; Pietzsch, M. J. *Mol. Catal. B: Enzym.* **1998**, *5*, 317–319. (f) Cipiciani, A.; Bellezza, F.; Fringuelli, F.; Silvestrini, M. G. *Tetrahedron: Asymmetry* **2001**, *12*, 2277–2281. (g) Hitchcock, P. B.; Rowlands, G. J.; Parmar, R. *Chem. Commun.* **2005**, 4219−4221.

(24) Optical resolution of pseudo-*ortho*-[2.2]paracyclophane (4,12-disubstituted [2.2]paracyclophane): (a) Pye, P. J.; Rossen, K.; Reamer, R. A.; Tsou, N. N.; Volante, R. P.; Reider, P. J. *J. Am. Chem. Soc.* **1997**, *119*, 6207−6208. (b) Rossen, K.; Pye, P. J.; Maliakal, A.; Volante, R. P. *J. Org. Chem.* **1997**, *62*, 6462−6463. (c) Zhuravsky, R.; Starikova, Z.; Vorontsov, E.; Rozenberg, V. *Tetrahedron: Asymmetry* **2008**, *19*, 216−222. (d) Jiang, B.; Zhao, X.-L. *Tetrahedron: Asymmetry* **2004**, *15*, 1141−1143. (e) Jones, P. G.; Hillmer, J.; Hopf, H. *Acta Crystallogr.* **2003**, *E59*, o24−o25. (f) Pamperin, D.; Hopf, H.; Syldatk, C.; Pietzsch, M. *Tetrahedron: Asymmetry* **1997**, *8*, 319−325. (g) Braddock, D. C.; MacGilp, I. D.; Perry, B. G. *J. Org. Chem.* **2002**, *67*, 8679−8681. (h) Morisaki, Y.; Hifumi, R.; Lin, L.; Inoshita, K.; Chujo, Y. *Chem. Lett.* **2012**, *41*, 990−992. (i) Meyer-Eppler, G.; Vogelsang, E.; Benkhaüser, C.; Schneider, A.; Schnakenburg, G.; Lützen, A. *Eur. J. Org. Chem.* **2013**, 4523−4532.

(25) Optical resolutions of 4,5,12-trisubstituted [2.2]paracyclophane and 4,5,12,13-tetrasubstituted [2.2]paracyclophane: Vorontsova, N. V.; Rozenberg, V. I.; Sergeeva, E. V.; Vorontsov, E. V.; Starikova, Z. A.; Lyssenko, K. A.; Hopf, H. *Chem.−Eur. J.* **2008**, *14*, 4600−4617.

(26) (a) Pu, L. *Chem. Rev.* **1998**, *98*, 2405−2494. (b) Pereira, M. M.; Calvete, M. J. F.; Carrilho, R. M. B.; Abreu, A. R. *Chem. Soc. Rev.* **2013**, *42*, 6990−7027. (c) Caricato, M.; Sharma, A. K.; Coluccini, C.; Pasini, D. *Nanoscale* **2014**, *6*, 7165−7174.

(27) (a) Urbano, A. *Angew. Chem., Int. Ed.* **2003**, *42*, 3986−3989. (b) Shen, Y.; Chen, C.-F. *Chem. Rev.* **2012**, *112*, 1463−1535.

(28) Chow, H.-F.; Low, K.-H.; Wong, K. Y. *Synlett* **2005**, *14*, 2130−2134. (b) Karakaya, B.; Claussen, W.; Gessler, K.; Saenger, W.; Schlüter, A.-D. *J. Am. Chem. Soc.* **1997**, *119*, 3296−3301.

Part I

Conjugated Microporous Polymers

Based on [2.2]Paracyclophanes

Chapter 1

Synthesis and Characterization of [2.2]Paracyclophane-Containing Conjugated Microporous Polymers

Abstract

Conjugated microporous polymers (CMPs) were prepared from disubstituted and tetrasubstituted [2.2]paracyclophane monomers by a Sonogashira-Hagihara coupling. The polymers obtained exhibited a type I nitrogen gas adsorption profile and H4-like hysteresis loops, indicating that the [2.2]paracyclophane containing CMPs possess slit-like mesopores. Their Brunauer-Emmett-Teller surface areas were estimated to be above 500 m^2g^{-1}. The step and stacked structure of the [2.2]paracyclophane unit affects the morphology of the polymers because of the contribution of two-dimensional expansion of the polymer network.

Introduction

Microporous polymers such as porous coordination polymers (PCPs),[1] metal organic frameworks (MOFs),[1] and microporous organic polymers (MOPs)[2] have potential applications as catalysts,[3] gas storage materials,[2f,k,m,4] and gas separation materials[3a,5] owing to their microporosity and large surface area. They consist of organic compounds, whose functional groups can be changed to easily design and produce organic frameworks. The sizes and shapes of the micropores can be controlled precisely at the molecular levels. Thus, organic compounds are ideal building blocks for preparing microporous materials for the following reasons; they can be prepared easily, modified easily, and imparted with a variety of functional characteristics.

Over the past three decades, conjugated polymers have attracted considerable attention in polymer chemistry as well as in materials chemistry since the discovery of the conductivity of polyacetylene through chemical doping.[6] In general, organic polymers, including conjugated polymers, possess film-forming properties, high processability, and light weightedness.[7–9] Therefore, conjugated polymers have been used widely as optoelectronic materials such as light-emitting devices,[7] field-effect transistors,[8] and photovoltaic cells.[9] Advances in transition-metal-catalyzed coupling reactions have facilitated the preparation of various conjugated polymers with conformationally stable rigid structures.[10] Recently, conjugated frameworks have been incorporated into network polymers using multifunctional conjugated compounds as monomers. Consequently, network polymers comprising only rigid conjugated skeletons with micropores can be fabricated. This new class of microporous polymers is called conjugated microporous polymers (CMPs).[11,12] CMPs are of interest to researchers because they possess π-electrons delocalized throughout their framework; therefore, they have received considerable attention for their potential applications in the field of optoelectronics.[12m]

[2.2]Paracyclophane is an attractive aromatic compound, in which two benzene rings are π-stacked and fixed together with a face-to-face distance of approximately 3 Å.[13] In this chapter, the author attempted to synthesize CMPs containing [2.2]paracyclophane units in their conjugated main chain. The author focused on the structure of [2.2]paracyclophane rather than its through-space conjugated π-electron system[14] in light of the fact that the incorporation of the pseudo-*para*-disubstituted [2.2]paracyclophane as well as 4,7,12,15-tetrasubstituted [2.2]paracyclophane units results in the formation of a conformationally stable step structure. The author investigated the effects of the step structure on the properties of the poly(*p*-arylene-ethynylene)-based CMPs.

Results and Discussion

Target CMPs were prepared by a Sonogashira-Hagihara coupling[15] of monomers 1,4-diethynylbenzene **1**, pseudo-*para*-diethynyl[2.2]paracyclophane **2**, and 1,3,5-triiodobenzene (**3**), as shown in Scheme 1. The ratio (*x*:*y*) of monomers **1** and **2** was changed, by which eleven CMPs (**CMP-0** to **CMP-10**) were obtained (Table 1).[16] In general, the isolated yield of a CMP synthesized by palladium-catalyzed coupling is over 100% as a result of the presence of non-reacted halogens. For example, **CMP-10** was obtained in 114% isolated yield, and elemental analysis revealed that **CMP-10** contained 3.40 wt% iodine (Table 1). Scheme 2 shows the synthesis of **CMP-11** containing 4,7,12,15-tetrasubstituted [2.2]paracyclophane as a crossing point in the polymer network. The treatment of 4,7,12,15-tetraethynyl[2.2]paracyclophane **4** with 1,4-diiodobenzene **5** in the presence of a catalytic amount of $Pd(PPh_3)_4$ and CuI afforded the corresponding polymer **CMP-11** in 116% isolated yield.

Scheme 1. Synthesis of **CMP-0** to **CMP-10**

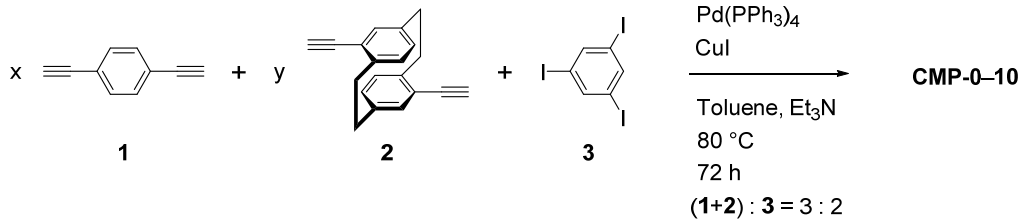

Scheme 2. Synthesis of **CMP-11**

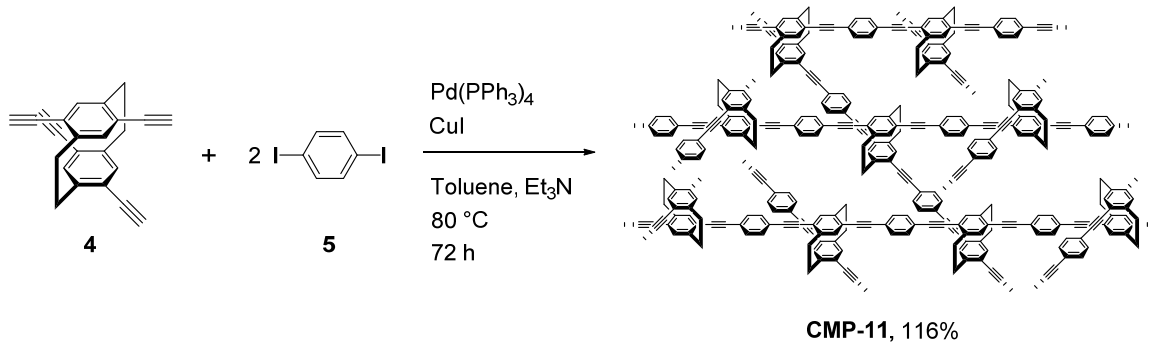

Table 1. The results of polymerization of monomers **1**, **2**, and **3**

CMP	Monomer ratio[a]		Yield / %	Elemental analysis / wt%		
	1	**2**		H(calcd)	C(calcd)	I
CMP-0	10	0	117	3.68 (3.47)	82.56 (96.53)	5.63
CMP-1	9	1	117	3.69 (3.77)	80.78 (96.23)	5.87
CMP-2	8	2	118	3.92 (4.03)	83.07 (95.97)	5.78
CMP-3	7	3	107	4.15 (4.25)	84.33 (95.75)	4.78
CMP-4	6	4	122	4.25 (4.46)	85.09 (95.54)	4.17
CMP-5	5	5	114	4.54 (4.63)	84.23 (95.37)	4.41
CMP-6	4	6	108	4.61 (4.79)	86.23 (95.21)	3.57
CMP-7	3	7	120	4.68 (4.94)	84.24 (95.06)	4.53
CMP-8	2	8	110	4.89 (5.07)	82.63 (94.93)	5.00
CMP-9	1	9	104	4.97 (5.19)	82.83 (94.81)	6.72
CMP-10	0	10	114	4.94 (5.30)	85.33 (94.70)	3.40

[a] Monomer **3** was added with the ratio of (**1**+**2**):**3** = 3:2

The structures of **CMP-0** to **CMP-11** were confirmed by solid-state CP/MAS ^{13}C NMR and FT-IR spectroscopy. Figure 1A shows the solid-state CP/MAS ^{13}C NMR spectra of **CMP-0** to **CMP-10**. Assignments were carried out by referring to the ^{13}C NMR spectrum of the model compound,[17] as shown in Figure 2. The signals for carbon-carbon triple bonds "*a*" for **CMP-0** to **CMP-10** were observed at around 90 ppm, and those attributable to their aromatic carbons "*b*" and "*c*" appeared at 120-145 ppm. The signals of the bridge methylene carbons "*d*" and aromatic carbons "*e*" in the [2.2]paracyclophane unit appeared at around 35 and 142 ppm, respectively.

The FT-IR spectra of **CMP-0** to **CMP-10** (Figure 1B) were obtained from KBr pellets. For all samples, the peaks of the stretching vibration of the carbon-carbon triple bond and the double bond of the aromatic groups appeared at around 2200 cm^{-1} and at around 1580 cm^{-1} in combination with 1480 cm^{-1}, respectively. In the spectra of CMPs containing cyclophane units, the peaks attributable to the C–H stretching vibration were observed at 2850-2960 cm^{-1}, which increased against the transmittance of the aromatic C−H stretching vibration with increasing content of the [2.2]paracyclophane units in the CMP backbone. Figure 3 shows the IR spectra of **CMP-11**; the peak appeared at 3288 cm^{-1} derived from the C−H stretching vibration of non-reacted terminal alkynes.

Figure 4 shows the nitrogen adsorption-desorption isotherms of **CMP-0** to **CMP-11** as measured at 77 K. According to the IUPAC classification reported in 1985,[18] all of the isotherms exhibited a type I nitrogen gas sorption profile. In the isotherms of **CMP-8** to **CMP-11**, a H4-like hysteresis loop appeared around $0.5P/P_0$ with the higher content of [2.2]paracyclophane. This result implies the possibility of the existence of narrow slit-like mesopores, which seemed to be formed by the incorporation of the step structure of the [2.2]paracyclophane moiety. The Brunauer-Emmett-Teller (BET) surface areas (S_{BET}) of **CMP-0** to **CMP-11** were estimated, and the results are summarized with the Langmuir surface

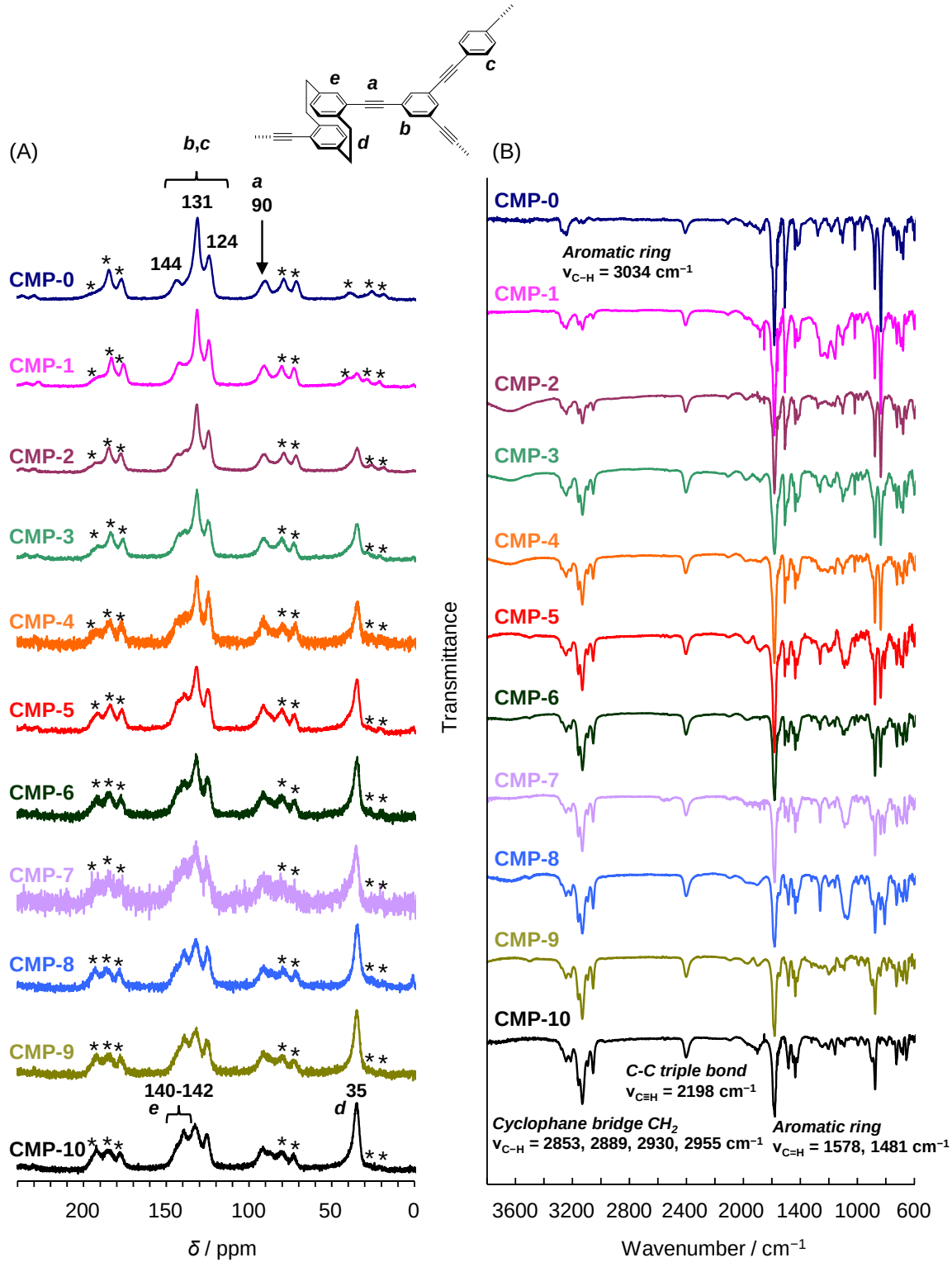

Figure 1. (A) CP/MAS ^{13}C NMR spectra of **CMP-0** to **CMP-10**. Spectra were recorded at a MAS rate of 4 kHz relative to adamantane. Asterisks denote spinning side bands. (B) FT-IR spectra of **CMP-0** to **CMP-10** (KBr).

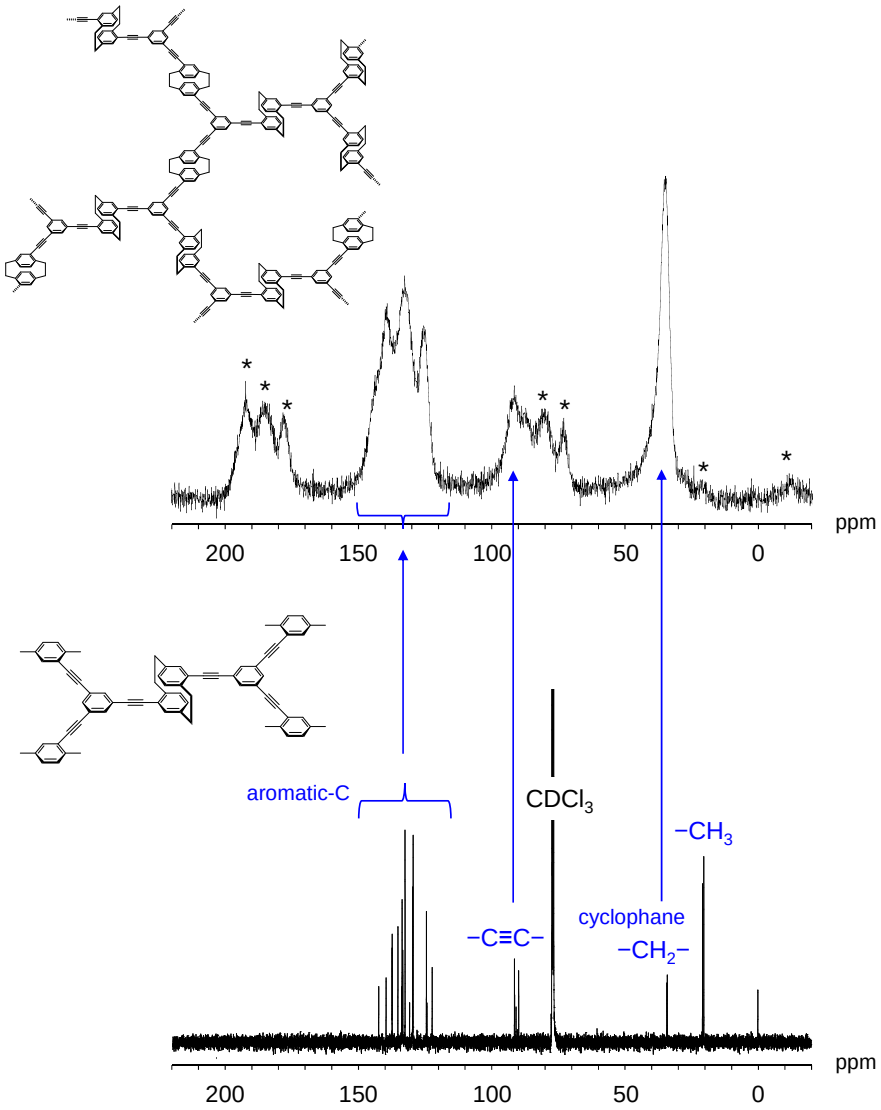

Figure 2. Comparison of the solid state CP/MAS ^{13}C NMR spectrum of **CMP-10** with the ^{13}C NMR spectrum of the model compound in $CDCl_3$. Asterisks denote spinning sidebands.

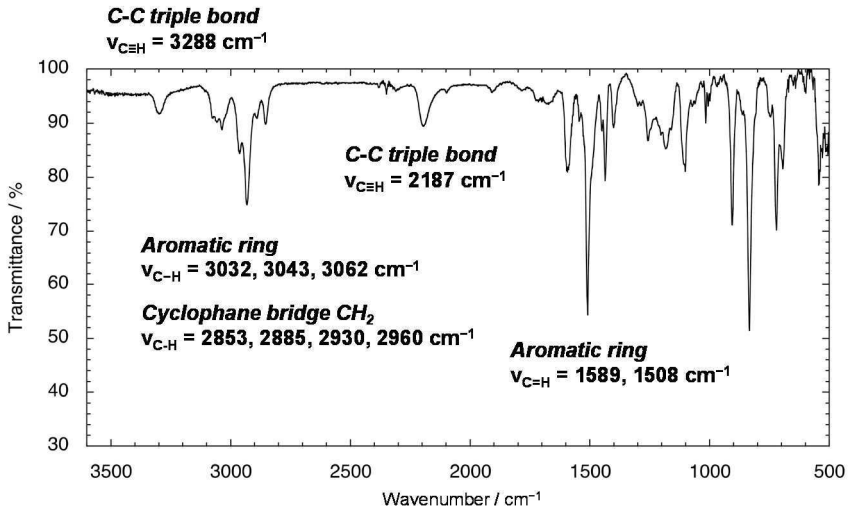

Figure 3. FT-IR spectrum of **CMP-11** (KBr).

areas ($S_{Langmuir}$) in Table 2. The S_{BET} value of **CMP-0** was found to be 822 m^2g^{-1}, which is consistent with the reported S_{BET} value of 834 m^2g^{-1} of the CMP prepared from monomers 1,4-diiodobenzene and 1,3,5-triethynylbenzene.[12a,c] Although incorporation of the [2.2]paracyclophane moiety resulted in a decrease in the surface area, the S_{BET} values were relatively high, above 500 m^2g^{-1}, as listed in Table 2. The isotherm for **CMP-11** consisted of the tetrasubstituted [2.2]paracyclophane unit as a crossing point in the polymer network. This isotherm revealed that **CMP-11** was also microporous and had a BET surface area of 640 m^2g^{-1} (Figure 3 and Table 2).

Table 2. Surface area of CMPs

CMP	S_{BET} / m^2g^{-1}	Pressure range / P/P_0	C	$S_{Langmuir}$ / m^2g^{-1}
CMP-0	822	0.011-0.054	769	1068
CMP-1	687	0.023-0.053	613	894
CMP-2	702	0.026-0.055	575	948
CMP-3	650	0.032-0.086	810	865
CMP-4	710	0.042-0.062	412	929
CMP-5	581	0.062-0.073	330	788
CMP-6	617	0.048-0.13	259	816
CMP-7	561	0.044-0.063	228	692
CMP-8	502	0.010-0.11	241	673
CMP-9	520	0.026-0.14	216	672
CMP-10	501	0.021-0.081	277	630
CMP-11	640	0.049-0.064	369	806

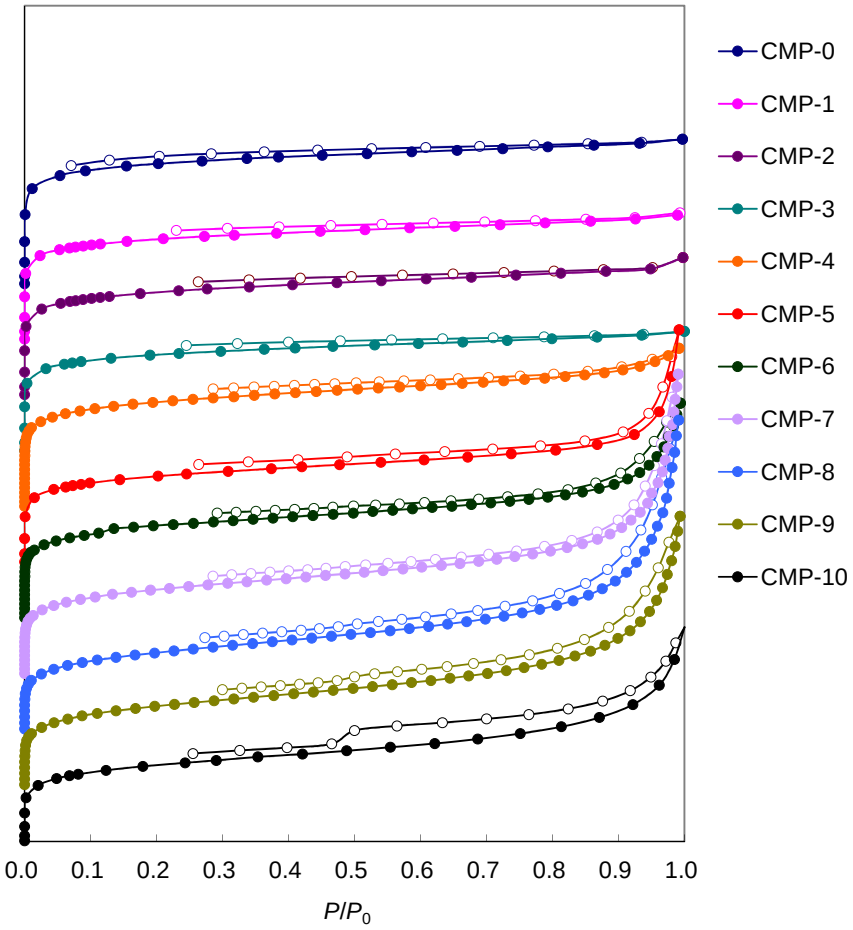

Figure 4. Nitrogen adsorption-desorption isotherms of **CMP-0** to **CMP-11** at 77 K; a filled circle and an open circle indicate adsorption and desorption isotherms, respectively.

A three-dimensional (3D) network structure formed effectively in **CMP-0** owing to the bending of the struts, leading to a larger surface area. However, [2.2]paracyclophane creates partially a two-dimensional (2D) stacked structure of π-electron systems, which covered the nanopores in the CMP in comparison with **CMP-0**. The differences in these structures derived from the [2.2]paracyclophane units reflected their morphologies as seen by SEM.[19] Figure 5 shows the SEM images of **CMP-0**, **CMP-3**, **CMP-6**, and **CMP-10** as representative examples.[20] SEM observation of **CMP-0** reveals the presence of mainly aggregates of spherical particles with submicrometer diameters; such spherical particles generally form in the case of a CMP grown in three dimensions. As the [2.2]paracyclophane content increased, the morphologies changed gradually. For example, aggregates of masses and plates were observed

for **CMP-10** (Figure 5). The morphologies of the CMPs with a high [2.2]paracyclophane content were considered to be derived from the contribution of the step and stacked structure of the [2.2]paracyclophane moieties. [2.2]Paracyclophanes construct partially 2D stacked structures and slit-like pores rather than the layered structure of π-conjugated planes according to the X-ray diffraction (XRD) patterns (Figure 6), which indicated the amorphous feature of CMPs.

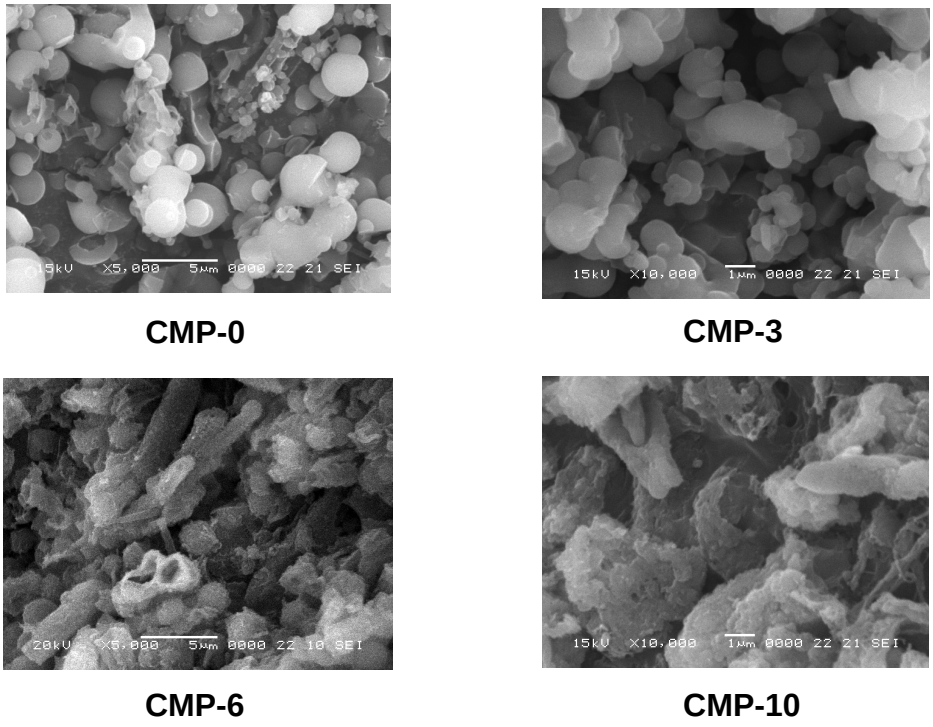

Figure 5. SEM images of **CMP-0**, **CMP-3**, **CMP-6**, and **CMP-10**.

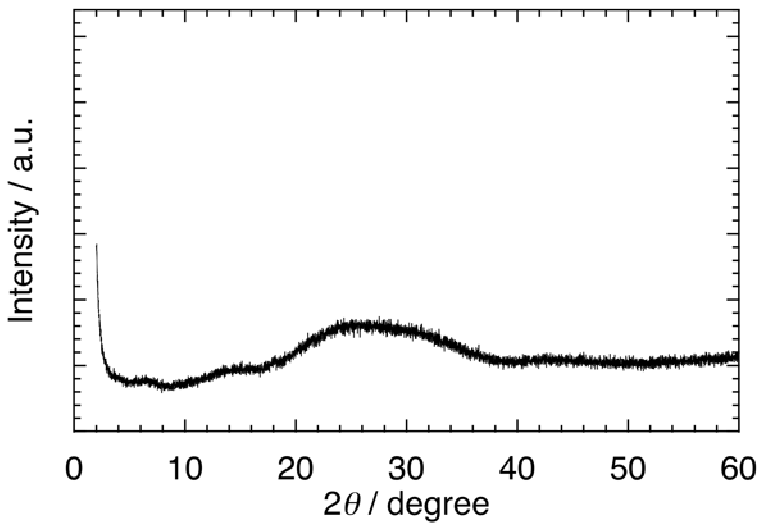

Figure 6. XRD pattern of **CMP-10**.

Conclusions

In summary, the author synthesized a new type of CMP by taking advantage of the structure of the [2.2]paracyclophane skeleton. All of the CMPs exhibited a type I nitrogen gas adsorption profile, and H4-like hysteresis loops were observed for CMPs with high [2.2]paracyclophane content. This result indicates that the [2.2]paracyclophane-containing CMPs possess slit-like mesopores. The BET surface areas of the CMPs were estimated to be above 500 m^2g^{-1}. As the [2.2]paracyclophane content increased in the CMPs, their morphologies changed gradually, and aggregates of masses and plates were observed, attributable to the contribution of partial 2D expansion of the polymer network created by the step and stacked structure of the [2.2]paracyclophane moieties. [2.2]Paracyclophane compounds with substituents have a conformationally stable planar chirality. CMPs consisting of such optically active [2.2]paracyclophane units should possess chiral micropores. Therefore, they have potential for use as optical resolving reagents and light-harvesting matrices for achieving circularly polarized luminescence.

Experimental Section

General. Solid state cross-polarization/magic-angle-sample-spinning (CP/MAS) ^{13}C NMR spectra were obtained on a JEOL JNM-LA300WB spectrometer operated at 75.6 MHz, and were recorded at the MAS rate of 4 kHz with the ^{1}H decoupling field amplitude of 75 kHz and reported relative to adamantane. The contact time and the repetition time were fixed as 2 ms and 6 s, respectively. FT-IR spectra were obtained on a SHIMADZU IRPrestige-21 spectrophotometer. The adsorption isotherms of nitrogen at 77 K were measured with a BELSORP-18PLUS instrument, and N_2 gas of high purity (99.9999%) was used. Prior to the adsorption measurements, the sample was treated under reduced pressure ($< 10^{-2}$ Pa) at 373 K for 5 h. Scanning electron microscopy (SEM) measurement was carried out on a JEOL JSM-5600B system. Samples were placed on a conducting carbon tape attached to a SEM grid, and then coated with platinum. X-Ray diffraction (XRD) data were obtained on a Rigaku MiniFlex diffractometer using CuKα radiation in a range of $3° \leq 2\theta \leq 60°$ at intervals of 0.01° at a scanning rate of 0.25 deg min^{-1} in the θ-2θ Bragg-Brentano geometry. Elemental analyses were performed at the Microanalytical Center of Kyoto University.

Materials. Dehydrated toluene was purchased commercially and used without further purification. Et_3N was purchased and purified by passage through a purification column under Ar pressure.[21] $Pd(PPh_3)_4$ (> 97%, Tokyo Chemical Industry = TCI), CuI (95%, Wako), and 1,4-diiodobenzene **5** (>98%, TCI) were purchased commercially and used without further purification. 1,4-Diethynylbenzene **1** (>98%) was purchased from TCI and purified by sublimation. Pseudo-*para*-diethynyl[2.2]paracyclophane **2** was synthesized from pseudo-*para*-dibromo[2.2]paracyclophane according to the literature procedure.[14i] 1,3,5-Triiodobenzene **3** was synthesized from 1,3,5-tribromobenzene (>98%, TCI) according to the literature procedure.[22] 4,7,13,16-Tetraethynyl[2.2]paracyclophane **4** was synthesized from 4,7,13,16-tetrabromo[2.2]paracyclophane according to the literature procedure.[23] All reactions were performed under Ar atmosphere.

Synthesis of Synthesis of CMP-0 to CMP-10. A typical procedure is as follows. A mixture of **1** (31.5 mg, 0.25 mmol), **2** (64.1 mg, 0.25 mmol), **3** (151.9 mg, 0.33 mmol), $Pd(PPh_3)_4$ (28.9 mg, 0.025 mmol), CuI (4.8 mg, 0.025 mmol), Et_3N (2.0 mL), and toluene (3.0 mL) was placed in a round-bottom flask equipped with a magnetic stirring bar and a reflux condenser. After degassing the reaction mixture several times, the reaction was carried out at 80 °C for 72 h with stirring. The reaction mixture was cooled to room temperature and 1.0 N HCl (10 mL) was added to the mixture. The pale yellow solid was collected by filtration and washed with $CHCl_3$, H_2O, and MeOH. The solid was then further washed

with $CHCl_3$ for 24 h and MeOH for 24 h using a Soxhlet extractor. The solid was dried at 70 °C in a vacuum oven for 24 h to afford **CMP-5** (163.6 mg, 114%). The results of the CMP syntheses are summarized in Table 1.

CMP-0. Solid state CP/MAS ^{13}C NMR: δ 144, 131, 124, 90 ppm. FT-IR (KBr): ν = 3034, 2200, 1581, 1508 cm^{-1}.

CMP-1. Solid state CP/MAS ^{13}C NMR: δ 142, 131, 124, 91, 35 ppm. FT-IR (KBr): ν = 3038, 2940, 2926, 2850, 2197, 1581, 1508 cm^{-1}.

CMP-2. Solid state CP/MAS ^{13}C NMR: δ 142, 138, 132, 124, 91, 35 ppm. FT-IR (KBr): ν = 3040, 2954, 2926, 2887, 2853, 2199, 1581, 1508 cm^{-1}.

CMP-3. Solid state CP/MAS ^{13}C NMR: δ 142, 138, 132, 125, 90, 34 ppm. FT-IR (KBr): ν = 3040, 2940, 2926, 2889, 2853, 2199, 1582, 1508 cm^{-1}.

CMP-4. Solid state CP/MAS ^{13}C NMR: δ 142, 135, 132, 125, 91, 34 ppm. FT-IR (KBr): ν = 3042, 3009, 2939, 2930, 2889, 2853, 2199, 1582, 1508, 1480 cm^{-1}.

CMP-5. Solid state CP/MAS ^{13}C NMR: δ 142, 139, 132, 125, 91, 35 ppm. FT-IR (KBr): ν = 3042, 3011, 2940, 2928, 2891, 2853, 2199, 1582, 1508, 1481 cm^{-1}.

CMP-6. Solid state CP/MAS ^{13}C NMR: δ 142, 139, 131, 125, 91, 35 ppm. FT-IR (KBr): ν = 3042, 3009, 2957, 2928, 2889, 2853, 2200, 1582, 1508, 1481 cm^{-1}.

CMP-7. Solid state CP/MAS ^{13}C NMR: δ 141, 138, 132, 125, 91, 35 ppm. FT-IR (KBr): ν = 3044, 3009, 2939, 2930, 2891, 2853, 2199, 1582, 1508, 1481 cm^{-1}.

CMP-8. Solid state CP/MAS ^{13}C NMR: δ 142, 139, 132, 125, 91, 34 ppm. FT-IR (KBr): ν = 3040, 3009, 2957, 2928, 2889, 2853, 2195, 1578, 1481 cm^{-1}.

CMP-9. Solid state CP/MAS ^{13}C NMR: δ 142, 140, 132, 126, 91, 35 ppm. FT-IR (KBr): ν = 3044, 3011, 2955, 2928, 2891, 2853, 2199, 1578, 1481 cm^{-1}.

CMP-10. Solid state CP/MAS ^{13}C NMR: δ 142, 139, 133, 126, 92, 35 ppm. FT-IR (KBr): ν = 3042, 3009, 2955, 2930, 2889, 2853, 2198, 1578, 1481 cm^{-1}.

Synthesis of CMP-11. A mixture of **4** (72.3 mg, 0.24 mmol), **5** (156.7 mg, 0.48 mmol), $Pd(PPh_3)_4$ (27.4 mg, 0.024 mmol), CuI (4.5 mg, 0.024 mmol), Et_3N (2.0 mL), and toluene (3.0 mL) was placed in a round-bottom flask equipped with a magnetic stirring bar and a reflux condenser. After degassing the reaction mixture several times, the reaction was carried out at 80 °C for 72 h with stirring. The reaction mixture was cooled to room temperature and 1.0 N HCl (10 mL) was added to the mixture. The yellow solid was collected by filtration and washed with $CHCl_3$, H_2O, and MeOH. The solid was then further

washed with $CHCl_3$ for 24 h and MeOH for 24 h using a Soxhlet extractor. The solid was dried at 70 °C in a vacuum oven for 24 h to afford **CMP-11** (124.2 mg, 116%). Solid state CP/MAS ^{13}C NMR (δ): 144, 133, 126, 94, 35. FT-IR (KBr): ν = 3288, 3062, 3043, 3032, 2960, 2930, 2885, 2853, 2187, 1589, 1508 cm^{-1}. Anal. calcd. for $C_{36}H_{20}$: C 95.54, H 4.46; found: C 79.83, H 4.60, I 6.76.

References and Notes

(1) (a) Li, H.; Eddaoudi, M.; O'Keeffe, M.; Yaghi, O. M. *Nature* **1999**, *402*, 276−279. (b) Cheetham, A. K.; Férey, G.; Loiseau, T. *Angew. Chem., Int. Ed.* **1999**, *38*, 3268−3292. (c) Eddaoudi, M.; Kim, J.; Rosi, N.; Vodak, D.; O'Keeffe, M.; Yaghi, O. M. *Science* **2002**, *295*, 469−472. (d) Yaghi, O. M.; O'Keeffe, M.; Ockwig, N. W.; Chae, H. K.; Eddaoudi, M.; Kim, J. *Nature* **2003**, *423*, 705−714. (e) Chae, H. K.; Siberio-Perez, D. Y.; Kim, J.; Go, Y. B.; Eddaoudi, M.; Matzger, A. J.; O'Keeffe, M.; Yaghi, O. M. *Nature* **2004**, *427*, 523−527. (f) Chae, H. K.; Siberio-Perez, D. Y.; Kim, J.; Go, Y. B.; Eddaoudi, M.; Matzger, A. J.; O'Keeffe, M.; Yaghi, O. M. *Nature* **2004**, *427*, 523−527. (g) Kitagawa, S.; Kitaura, R.; Noro, S. *Angew. Chem., Int. Ed.* **2004**, *43*, 2334−2375. (h) Kitagawa, S.; Noro, S.; Nakamura, T. *Chem. Commun.* **2006**, 701−707. (i) Maji, T. K.; Kitagawa, S. *Pure Appl. Chem.* **2007**, *79*, 2155−2177. (j) Kitagawa, S.; Matsuda, R. *Coord. Chem. Rev.* **2007**, *251*, 2490−2509. (k) Ferey, G. *Chem. Soc. Rev.* **2008**, *37*, 191−214.

(2) Recent reviews, see: (a) Jiang, J.-X.; Cooper, A. I. **2010**, *293*, 1−33. (b) Thomas, A. *Angew. Chem., Int. Ed.* **2010**, *49*, 8328−8344. (c) Thomas, A.; Kuhn, P.; Weber, J.; Titirici, M.-M.; Antonietti, M. *Macromol. Rapid Commun.* **2009**, *30*, 221−236. (d) McKeown, N. B.; Budd, P. M. *Chem. Soc. Rev.* **2006**, *35*, 675−683. and also see for intrinsic microporosity (PIM): (e) Budd, P. M.; Ghanem, B. S.; Makhseed, S.; McKeown, N. B.; Msayib, K. J.; Tattershall, C. E. *Chem. Commun.* **2004**, 230−231. (f) McKeown, N. B.; Gahnem, B.; Msayib, K. J.; Budd, P. M.; Tattershall, C. E.; Mahmood, K.; Tan, S.; Book, D.; Langmi, H. W.; Walton, A. *Angew. Chem., Int. Ed.* **2006**, *45*, 1804−1807. (g) Budd, P. M.; Butler, A.; Selbie, J.; Mahmood, K.; McKeown, N. B.; Ghanem, B.; Msayib, K.; Book, D.; Walton, A. *Phys. Chem. Chem. Phys.* **2007**, *9*, 1802−1808. (h) Ghanem, B. S.; Msayib, K. J.; McKeown, N. B.; Harris, K. D. M.; Pan, Z.; Budd, P. M.; Butler, A.; Selbie, J.; Book, D.; Walton, A. *Chem. Commun.* **2007**, 67−69. see for covalent organic frameworks (COF): (i) Côté, A. P.; Benin, A. I.; Ockwig, N. W.; O'Keeffe, M.; Matzger, A. J.; Yaghi, O. M. *Science* **2005**, *310*, 1166−1170. (j) El-Kaderi, H. M.; Hunt, J. R.; Mendoza-Cortés, J. L.; Côté, A. P.; Taylor, R. E.; O'Keeffe, M.; Yaghi, O. M. *Science* **2007**, *316*, 268−272. see for hyper-crosslinked polymer (HCP): (k) Lee, J.-Y.; Wood, C. D.; Bradshaw, D.; Rosseinsky, M. J.; Cooper, A. I. *Chem. Commun.* **2006**, 2670−2672. (l) Tsyurupa, M. P.; Davankov, V. A. *React. Func. Polym.* **2006**, *66*, 768−779. (m) Wood, C. D.; Tan, B.; Trewin, A.; Niu, H.; Bradshaw, D.; Rosseinsky, M. J.; Khimyak, Y. Z.; Campbell, N. L.; Kirk, R.; Stöckel, E.; Cooper, A. I. *Chem. Mater.* **2007**, *19*, 2034−2048.

(3) (a) McKeown, N. B.; Budd, P. M.; Msayib, K. J.; Ghanem, B. S.; Kingston, H. J.; Tattershall, C. E.; Makhseed, S.; Reynolds, K. J.; Fritsch, D. *Chem. Eur.−J.* **2005**, *11*, 2610−2620. (b) Taguchi, A.; Schüth, F. *Micropor. Mesopor. Mater.* **2005**, *77*, 1−45. (c) Hartmann, M. *Chem. Mater.* **2005**, *17*, 4577−4593. (d) Corma, A.; Garcia, H. *Adv. Synth. Catal.* **2006**, *348*, 1391−1412. (e) Du, X.; Sun, Y.; Tan, B.; Teng, Q.; Yao, X.; Su, C.; Wang, W. *Chem. Commun.* **2010**, *46*, 970−972.

(4) (a) McKeown, N. B.; Budd, P. M.; Msayib, K. J.; Ghanem, B. S.; Kingston, H. J.; Tattershall, C. E.; Makhseed, S.; Reynolds, K. J.; Fritsch, D. *Chem. Eur.−J.* **2005**, *11*, 2610−2620. (b) Wood, C. D.; Tan, B.; Trewin, A.; Su, F.; Rosseinsky, M. J.; Bradshaw, D.; Sun, Y.; Zhou, L.; Cooper, A. I. *Adv. Mater.* **2008**, *20*, 1916−1921. (c) Furukawa, H.; Yaghi, O. M. *J. Am. Chem. Soc.* **2009**, *131*, 8875−8883. (d) Czaja, A. U.; Trukhan, N.; Muller, U. *Chem. Soc. Rev.* **2009**, *38*, 1284−1293. (e) Germain, J.; Fréchet, J. M. J.; Svec, F. *Small* **2009**, *5*, 1098−1111. (f) Li, A.; Lu, R.-F.; Wang, Y.; Wang, X.; Han, K.-L.; Deng, W.-Q. *Angew. Chem., Int. Ed.* **2010**, *49*, 3330−3333.

(5) (a) Park, H. B.; Jung, C. H.; Lee, Y. M.; Hill, A. J.; Pas, S. J.; Mudie, S. T.; Van Wagner, E.; Freeman, B. D.; Cookson, D. J. *Science* **2007**, *318*, 254−258. (b) Ren, H.; Ben, T.; Wang, E.; Jing, X.; Xue, M.; Liu, B.; Cui, Y.; Qiu, S.; Zhu, G. *Chem. Commun.* **2010**, *46*, 291−293.

(6) (a) Shirakawa, H.; Louis, E. J.; MacDiarmid, A. G.; Chiang, C. K.; Heeger, A. J. *J. Chem. Soc. Chem. Commun.* **1977**, 578−580. (b) Chang, L. L. *Physics Letters A* **1969**, *29*, 125−126. (c) Shirakawa, H. *Angew. Chem., Int. Ed.* **2001**, *40*, 2574−2580. (d) MacDiarmid, A. G. *Angew. Chem., Int. Ed.* **2001**, *40*, 2581−2590. (e) Heeger, A. J. *Angew. Chem., Int. Ed.* **2001**, *40*, 2591−2611.

(7) (a) Kraft, A.; Grimsdale, A. C.; Holmes, A. B. *Angew. Chem., Int. Ed.* **1998**, *37*, 402−428. (b) Friend, R. H.; Gymer, R. W.; Holmes, A. B.; Burroughes, J. H.; Marks, R. N.; Taliani, C.; Bradley, D. D. C.; Santos, D. A. D.; Bredas, J. L.; Logdlund, M.; Salaneck, W. R. *Nature* **1999**, *397*, 121−128. (c) Mitschke, U.; Bauerle, P. *J. Mater. Chem.* **2000**, *10*, 1471−1507. (d) Bernius, M. T.; Inbasekaran, M.; O'Brien, J.; Wu, W. *Adv. Mater.* **2000**, *12*, 1737−1750. (e) Akcelrud, L. *Prog. Polym. Sci.* **2003**, *28*, 875−962.; *Organic Light Emitting Devices: Synthesis, Properties and Application*; Müellen, K., Scherf, U., Eds.; Wiley-VCH, Weinheim 2006.

(8) (a) Sirringhaus, H. *Adv. Mater.* **2005**, *17*, 2411−2425.; (b) *Organic Field-Effect Transistors*; Groza, J. R., Locklin, J. J., Eds.; CRC Press Taylor & Francis Group, New York 2007.; (c) Murphy, A. R.; Fréchet, J. M. J. *Chem. Rev.* **2007**, *107*, 1066−1096. (d) Takimiya, K.; Kunugi, Y.; Otsubo, T. *Chem. Lett.* **2007**, *36*, 578−583. (e) Anthony, J. E. *Angew. Chem., Int. Ed.* **2008**, *47*, 452−483.

(9) (a) O'Regan, B.; Gratzel, M. *Nature* **1991**, *353*, 737−740. (b) *Organic Photovoltaics: Materials, Device Physics, and Manufacturing Technologies*; Brabec, C., Dyakonov, V., Scherf, U., Eds.; Wiley-VCH, Weinheim 2008.

(10) For example, see: (a) *Design and Synthesis of Conjugated Polymers*; Leclerc, M., Morin, J.-F., Eds.; Wiley-VCH: Weinheim, 2010. (b) *Conjugated Polymer Synthesis: Methods and Reactions*; Chujo Y., Ed.; Wiley-VCH: Weinheim 2010.

(11) Cooper, A. I. *Adv. Mater.* **2009**, *21*, 1291−1295.

(12) (a) Jiang, J.-X.; Su, F.; Trewin, A.; Wood, C. D.; Campbell, N. L.; Niu, H.; Dickinson, C.; Ganin, A. Y.; Rosseinsky, M. J.; Khimyak, Y. Z.; Cooper, A. I. *Angew. Chem., Int. Ed.* **2007**, *46*, 8574−8578. (b) Germain, J.; Frechet, J. M. J.; Svec, F. *J. Mater. Chem.* **2007**, *17*, 4989−4997. (c) Jiang, J.-X.; Su, F.; Trewin, A.; Wood, C. D.; Niu, H.; Jones, J. T. A.; Khimyak, Y. Z.; Cooper, A. I. *J. Am. Chem. Soc.* **2008**, *130*, 7710−7720. (d) Weber, J.; Thomas, A. *J. Am. Chem. Soc.* **2008**, *130*, 6334−6335. (e) Jiang, J.-X.; Su, F.; Niu, H.; Wood, C. D.; Campbell, N. L.; Khimyak, Y. Z.; Cooper, A. I. *Chem. Commun.* **2008**, 486−488. (f) Dawson, R.; Su, F.; Niu, H.; Wood, C. D.; Jones, J. T. A.; Khimyak, Y. Z.; Cooper, A. I. *Macromolecules* **2008**, *41*, 1591−1593. (g) Rose, M.; Bohlmann, W.; Sabo, M.; Kaskel, S. *Chem. Commun.* **2008**, 2462−2464. (h) Kuhn, P.; Antonietti, M.; Thomas, A. *Angew. Chem., Int. Ed.* **2008**, *47*, 3450−3453. (i) Schwab, M. G.; Fassbender, B.; Spiess, H. W.; Thomas, A.; Feng, X.; Müllen, K. *J. Am. Chem. Soc.* **2009**, *131*, 7216−7217. (j) Farha, O. K.; Spokoyny, A. M.; Hauser, B. G.; Bae, Y.-S.; Brown, S. E.; Snurr, R. Q.; Mirkin, C. A.; Hupp, J. T. *Chem. Mater.* **2009**, *21*, 3033−3035. (k) Zhang, Y.; Riduan, S. N.; Ying, J. . Y. *Chem. Eur.−J.* **2009**, *15*, 1077−1081. (l) Palkovits, R.; Antonietti, M.; Kuhn, P.; Thomas, A.; Schüth, F. *Angew. Chem., Int. Ed.* **2009**, *48*, 6909−6912. (m) Chen, L.; Honsho, Y.; Seki, S.; Jiang, D. *J. Am. Chem. Soc.* **2010**, *132*, 6742−6748. (n) Choi, J. H.; Choi, K. M.; Jeon, H. J.; Choi, Y. J.; Lee, Y.; Kang, J. K.

Macromolecules **2010**, *43*, 5508−5511. (o) Jiang, J.-X.; Laybourn, A.; Clowes, R.; Khimyak, Y. Z.; Bacsa, J.; Higgins, S. J.; Adams, D. J.; Cooper, A. I. *Macromolecules* **2010**, *43*, 7577−7582. (p) Dawson, R.; Laybourn, A.; Khimyak, Y. Z.; Adams, D. J.; Cooper, A. I. *Macromolecules* **2010**, *43*, 8524−8530. (q) Jiang, J.-X.; Wang, C.; Laybourn, A.; Hasell, T.; Clowes, R.; Khimyak, Y. Z.; Xiao, J.; Higgins, S. J.; Adams, D. J.; Cooper, A. I. *Angew. Chem., Int. Ed.* **2011**, *50*, 1072−1075. (r) Dawson, R.; Adams, D. J.; Cooper, A. I. *Chem. Sci.* **2011**, *2*, 1173−1177. (s) Zhang, K.; Tieke, B.; Vilela, F.; Skabara, P. J. *Macromol. Rapid Commun.* **2011**, *32*, 825−830.

(13) (a) *Cyclophane Chemistry: Synthesis, Structures and Reactions*; Vögtle, F., Ed.; John Wiley & Sons, Chichester, 1993. (b) *Modern Cyclophane Chemistry*; Gleiter, R., Hopf, H., Eds.; Wiley-VCH: Weinheim 2004. (c) Hopf, H. *Angew. Chem., Int. Ed.* **2008**, *47*, 9808−9812.

(14) (a) Morisaki, Y.; Chujo, Y. *Angew. Chem., Int. Ed*. **2006**, *45*, 6430−6437. (b) Morisaki, Y.; Chujo, Y. *Prog. Polym. Sci.* **2008**, *33*, 346−364. (c) Morisaki, Y.; Chujo, Y. *Bull. Chem. Soc. J.* **2009**, *82*, 1070−1082. (d) Morisaki, Y.; Chujo, Y. *Polym. Chem.* **2011**, *2*, 1249−1257. (e) Morisaki, Y.; Chujo, Y. *Macromolecules* **2002**, *35*, 587−589. (f) Morisaki, Y.; Ishida, T.; Chujo, Y. *Macromolecules* **2002**, *35*, 7872−7877. (g) Morisaki, Y.; Fujimura, F.; Chujo, Y. *Organometallics* **2003**, *22*, 3553−3557. (h) Morisaki, Y.; Chujo, Y. *Macromolecules* **2003**, *36*, 9319−9324. (i) Morisaki, Y.; Chujo, Y. *Macromolecules* **2004**, *37*, 4099−4103. (j) Morisaki, Y.; Murakami, T.; Chujo, Y. *Macromolecules* **2008**, *41*, 5960−5963. (k) Morisaki, Y.; Murakami, T.; Sawamura, T.; Chujo, Y. *Macromolecules* **2009**, *42*, 3656−3660.

(15) Tohda, Y.; Sonogashira, K.; Hagihara, N. *Synthesis* **1977**, 777−778. Sonogashira, K. In *Handbook of Organopalladium Chemistry for Organic Synthesis*; Negishi, E., Ed.; Wiley-Interscience: New York, 2002; pp 493−529.

(16) Recently, we synthesized only CMP-10 during our investigation of the π-stacked molecule; see, Morisaki, Y.; Gon, M.; Tsuji, Y.; Kajiwara, Y.; Chujo, Y. *Tetrahedron Lett.* **2011**, *52*, 5504−5507.

(17) Structure, synthetic procedure, spectral data, and ^{1}H and ^{13}C NMR spectra of the model compound and the related compounds are shown in the Supporting Information in the paper.

(18) Sing, K. S. W.; Everett, D. H.; Haul, R. A. W.; Moscou, L.; Pierotti, R. A.; Rouquérol, J.; Siemieniewska, T. *Pure Appl. Chem.* 1**985**, *57*, 603−619.

(19) The SEM image of **CMP-0** is almost identical to the reported CMP; see reference 11a.

(20) The SEM image of **CMP-11** is shown in Figure S12 in the Supporting Information in the paper.

(21) Pangborn, A. B.; Giardello, M. A.; Grubbs, R. H.; Rosen, R. K.; Timmers, F. J. *Organometallics* **1996**, *15*, 1518−1520.

(22) (a) Beinhoff, M.; Karakaya, B.; Schlüter, A. D. *Synthesis* **2003**, 79−90. (b) Mechtler, C.; Zirngast, M.; Gaderbauer, W.; Wallner, A.; Baumgartner, J.; Marschner, C. *J. Organomet. Chem.* **2006**, *691*, 150−158.

(23) Bondarenko, L.; Dix, I.; Hinrichs, H.; Hopf, H. *Synthesis* **2004**, 2751−2759.

Chapter 2

Conjugated Microporous Polymers Consisting of Tetrasubstituted [2.2]Paracyclophane Junctions

Abstract

Conjugated microporous polymers (CMPs) were synthesized from the tetrasubstituted [2.2]paracyclophane compounds as tetra-functional building blocks using Hay coupling, Sonogashira-Hagihara cross-coupling, and Yamamoto coupling. The CMPs exhibited microporosity (less than 2 nm) and large surface areas (up to approximately 1000 m^2g^{-1}). The CMPs consisted of relatively uniform particles and dispersed in organic solvents. These results suggest their possible applications in the fields of opto-electronics and catalyst chemistry.

Introduction

[2.2]Paracyclophane, which contains two benzene rings, has attracted considerable attention with regard to its structure, reactivity, and physical properties.[1] A number of [2.2]paracyclophane derivatives have been prepared so far, and their unique properties derived from the characteristic interactions between the stacked π-electron systems have been investigated in detail.[1-3] Recently, through-space conjugated oligomers and polymers by incorporating [2.2]paracyclophane into the conjugated polymer backbone have been synthesized.[4-7] These polymers exhibited an extension of π-conjugation length via the through-space interaction.[8] In addition, end-capping of the through-space conjugated polymers allowed for fluorescence resonance energy transfer (FRET) from the stacked π-electron systems to the end-capped π-electron systems.[8,9]

Microporous polymers such as metal organic frameworks (MOFs),[10-20] porous coordination polymers (PCPs),[10-20] and microporous organic polymers (MOPs)[21-33] have been extensively investigated. Because these polymers possess micropores and large surface areas, it is expected that they can be applied as catalysts,[34-38] gas storage materials,[26,31,33,39-43] and gas separation materials.[34,44,45] Generally, they are composed of organic compounds whose functional groups can be readily designed; thus, the sizes and shapes of the micropores can be controlled at the molecular level. Recently, π-conjugated frameworks have been used for network polymers. This new class of microporous network polymers is called conjugated microporous polymers (CMPs),[46,47] and they consist of only rigid π-conjugated skeletons and of micropores that can be readily fabricated. CMPs have received considerable attention owing to their potential application in the field of optoelectronics[48,49] because of the presence of delocalized π-electrons throughout their frameworks as well as their rigid micropores.

In this chapter, the author focused on the structure of [2.2]paracyclophane to construct a network for a CMP. In particular, the author selected a 4,7,12,15-tetrasubstituted

[2.2]paracyclophane skeleton with a crisscross structure as the junction of the CMP. Three types of CMPs consisting of tetrasubstituted [2.2]paracyclophane junctions were synthesized from [2.2]paracyclophane monomers with different sizes by Hay coupling,[50] Sonogashira-Hagihara cross-coupling,[51,52] and Yamamoto coupling.[53] All CMPs were found to be microporous with large surface areas on the basis of nitrogen gas sorption studies. Further characterization of the obtained CMPs by cross-polarization magic angle spinning (CP/MAS) ^{13}C NMR, FT-IR, X-ray diffraction (XRD), and scanning electron microscopy (SEM) were also performed.

Results and Discussion

[2.2]Paracyclophane-based monomer **1** was prepared from 4,7,12,15-tetrasubstituted [2.2]paracyclophane[54] using the procedure reported in the literature.[55] The Sonogashira-Hagihara cross-coupling[51,52] of compound **1** with 1-bromo-4-iodobenzene **2** proceeded chemoselectively to give monomer **3** in 43% isolated yield, as shown in Scheme 1. Schemes 2-4 show the synthesis of target CMPs **1**-**3**. Hay coupling[50] of **1** (Scheme 2), Sonogashira-Hagihara cross-coupling of **1** with **4** (Scheme 3), and Yamamoto coupling[53] of **3** (Scheme 4) afforded the corresponding CMPs **1**-**3**, respectively. After the coupling reaction, the crude products were washed with organic solvents and H_2O using a Soxhlet extractor to yield the CMPs as pale yellow powders. The polymerization results are listed in Table 1. The reaction efficiencies of the CMPs were calculated according to the FT-IR absorption peak of C−H stretching vibration of the terminal alkyne (CMP **1**) and the elemental analysis data (CMP **2** and **3**). Generally, the isolated yield of a CMP synthesized by palladium-catalyzed cross-coupling is over 100% because of the presence of unreacted halogens such as bromine and iodine. Thus, in our case, CMP **2** possessed 3.37 wt% iodine according to the result of elemental analysis. On the other hand, Yamamoto coupling proceeded smoothly to provide CMP **3**

(Scheme 4) with high reaction efficiency (>99%), although this reaction required a stoichiometric amount of Ni. Almost all of the Br species reacted, and the elemental analysis showed that only 0.24 wt% of Br remained in the sample. It is desirable to remove residual halogens from the viewpoint of the possible application of the CMPs.

Scheme 1. Synthesis of **3**

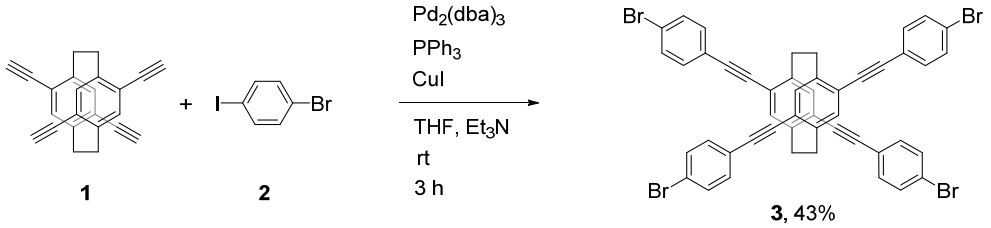

Scheme 2. Synthesis of **CMP 1**

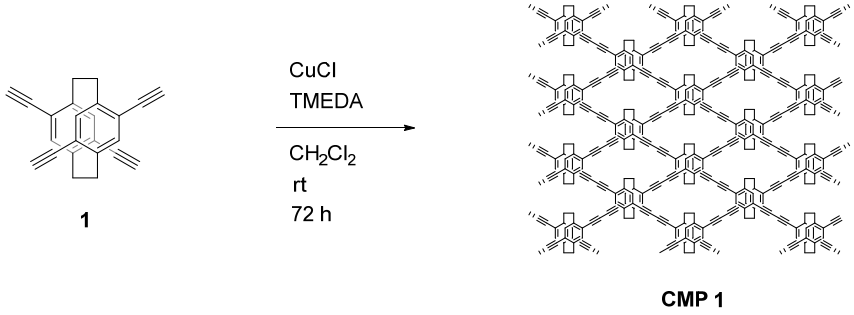

Scheme 3. Synthesis of **CMP 2**

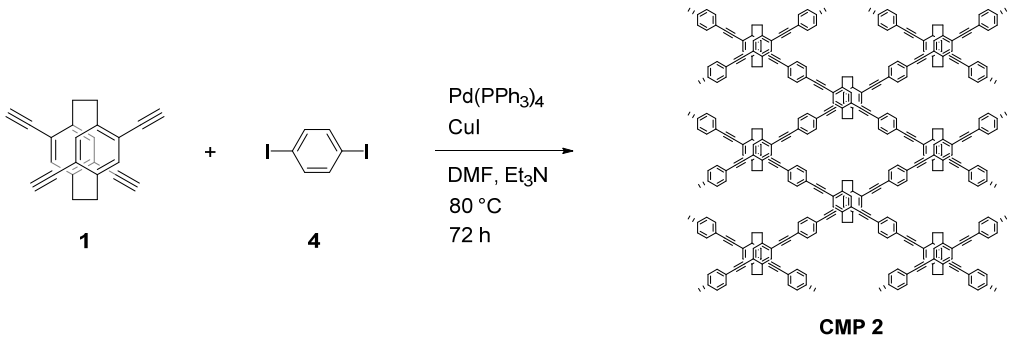

Scheme 4. Synthesis of **CMP 3**

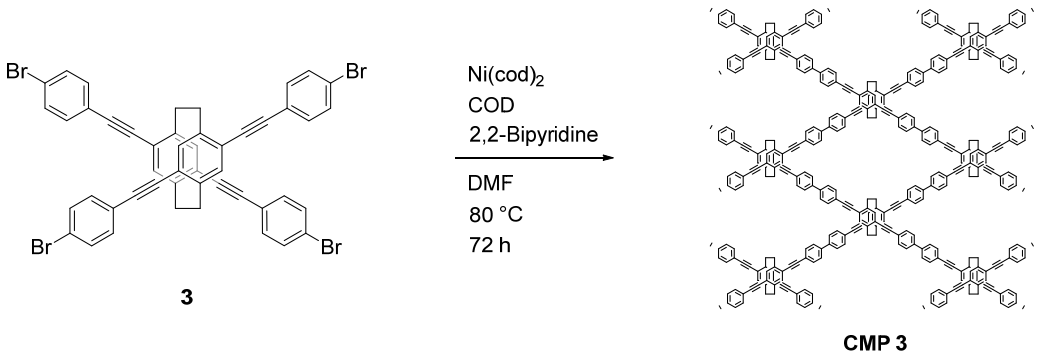

Table 1. Results of Polymerization and Surface Areas of CMPs

CMP	Yield[a] (%)	Reaction Efficiency[b]	Elemental analysis			S_{BET} (m^2g^{-1})	$S_{Langmuir}$ (m^2g^{-1})
			H (%) Found, Calcd.	C (%) Found, Calcd.	Halogen (%) Found, Calcd.		
1	90	0.72	4.05, 4.03	82.99, 95.97	−	889	1,156
2	116	0.94	4.72, 4.46	85.32, 95.54	Iodine:3.37, 0	840	1,285
3	91	>0.99	4.98, 4.67	87.93, 95.33	Bromine:0.24, 0	956	1,231

[a] Isolated yield calculated on the basis of weight. [b] Calculated from the elemental analysis data for CMPs **2** and **3** from the FT-IR absorption peak of the terminal alkyne C−H stretching for CMP **1**.

The structures of the obtained CMPs were confirmed by solid-state CP/MAS ^{13}C NMR and FT-IR spectroscopies. The solid-state CP/MAS ^{13}C NMR spectra of CMPs **1**-**3** are shown in Figure 1. As a representative example, the signal positions of CMP **2** for various types of carbons are as follows. The relatively sharp peak at 31.7 ppm was assigned to the bridge methylene carbons of cyclophane units. The small signals of the C−C triple bond carbons appeared at around 95 ppm. Finally, the peaks at 120-145 ppm were assignable to the aromatic carbons. The FT-IR spectra were obtained using KBr pellets of the CMPs. The spectra of the CMPs **1**-**3** are shown in Figure 2. For all samples, the peaks of the stretching vibration of the C−C triple bond appeared around 2200 cm^{-1} and those of the C−C double bonds of phenylenes appeared around 1580 and 1480 cm^{-1}. The peaks attributable to the stretching vibrations of the C−H bonds in the cyclophane units were observed at 2850-2950 cm^{-1}. In the FT-IR spectra of CMPs **1**and **2**, the C−H stretching vibration of unreacted terminal alkynes appeared at around 3250 cm^{-1}. Thus, the reaction efficiencies of CMPs **1**and **2** could be calculated from the absorbance of the terminal alkyne C−H stretching.

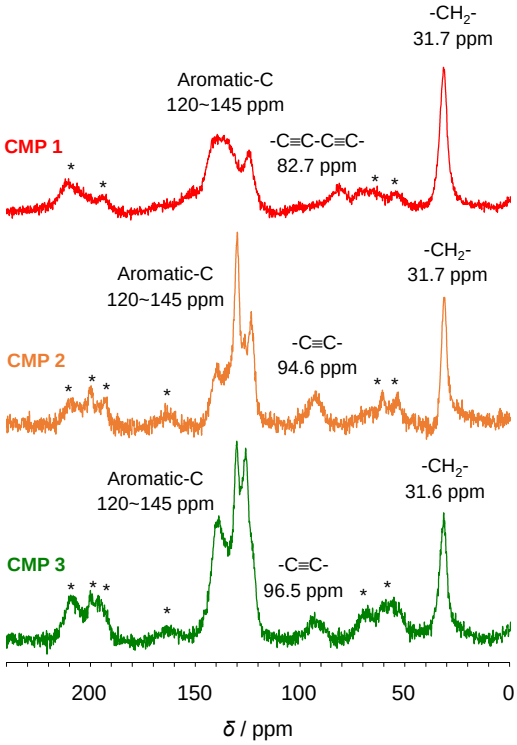

Figure 1. Solid state CP/MAS ^{13}C NMR spectra of CMPs **1-3**; CP/MAS 7 kHz, asterisks denote spinning sidebands.

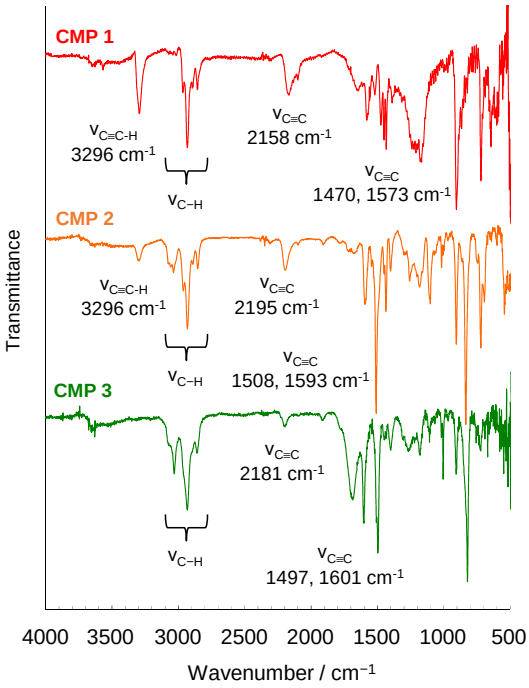

Figure 2. FT-IR spectra of CMPs **1-3**.

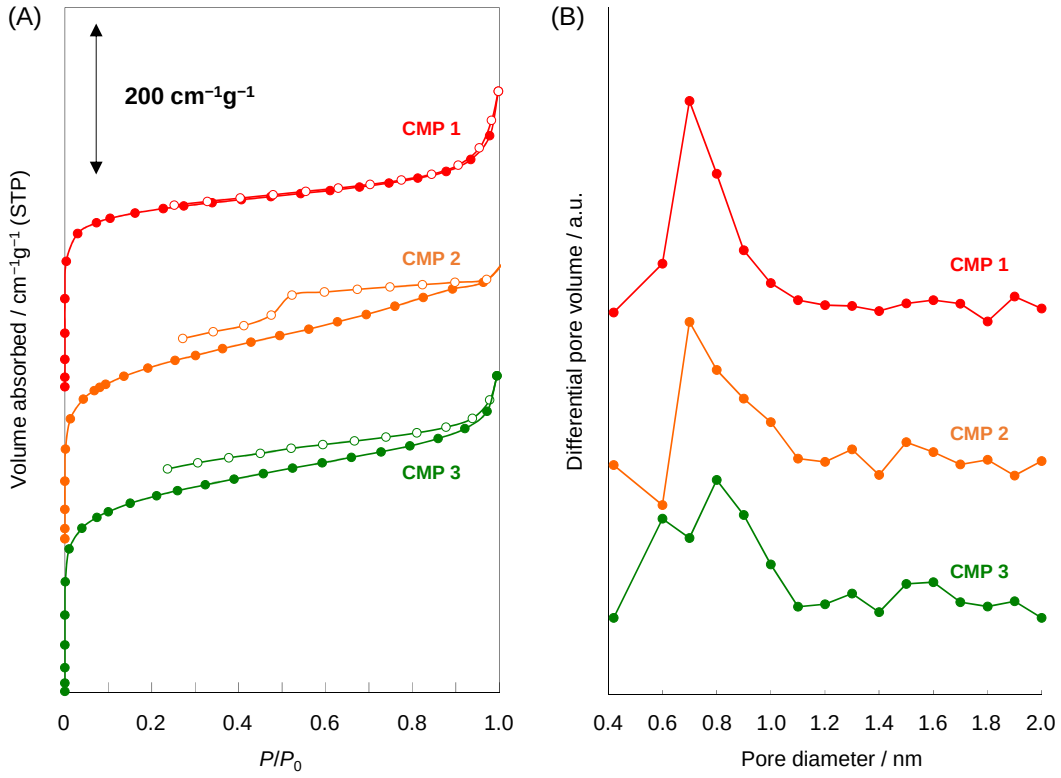

Figure 3. (A) Nitrogen adsorption-desorption isotherms of CMPs **1-3**. (B) Pore size distribution curves of CMPs **1-3**.

The CMPs were analyzed by nitrogen gas sorption. The nitrogen adsorption/desorption isotherms of CMPs **1**-**3** obtained at 77 K are shown in Figure 3A. According to the IUPAC classification reported in 1985,[57] all isotherms of CMPs **1**-**3** exhibited a type I nitrogen gas sorption profile. This result clearly indicates that the obtained CMPs are microporous network polymers comprised only micropores with diameters of less than 2 nm. The Brunauer-Emmett-Teller (BET) surface areas (S_{BET}) and Langmuir surface areas ($S_{Langmuir}$) of CMPs **1**-**3** were estimated, and the results are shown in Table 1. All of the CMPs exhibited large BET surface areas (> 840 m^2g^{-1}). CMP **3**, which was obtained by Yamamoto coupling, exhibited the highest S_{BET} value of approximately 1000 m^2g^{-1}. Pore size distribution curves of CMPs **1**-**3** were obtained by the micropore method, and they are shown in Figure 3B. The pores were mainly observed in the mesopores range from 0.5 to 1.1 nm. The pore diameters of the CMPs increased as the distance between [2.2]paracyclophane junctions became longer. For example, the pore diameters of CMPs **2** and **3** were estimated to be approximately 1.0 nm.

The powder XRD patterns of CMPs **1**-**3** exhibited the hollow peaks as shown in Figure 4, indicating that they were completely amorphous. SEM images of CMPs **1**-**3** are shown in Figure 5, respectively. The morphology of CMP **2** obtained by cross-coupling polymerization suggested the presence of various chunks consisting of small plates and blocks. In contrast, the SEM image of CMP **1** showed aggregates consisting of small blocks, and that of CMP **3**, which was prepared by the Yamamoto coupling, showed relatively uniform particles with approximately 0.2 μm in size. Thus, CMP **3** was readily dispersed in common organic solvents such as $CHCl_3$ and CH_2Cl_2. In addition, there was little residual Br in CMP **3**; therefore its optical properties were investigated. As shown in Figure 6A, CMP **3** dispersed in CH_2Cl_2 exhibited a broad absorption band with a peak top at around 420 nm. As shown in Figure 6B, upon excitation at the absorption peak maximum, a broad and featureless emission spectrum

was observed with a peak top at around 530 nm (fluorescence quantum yield of 2%) derived from the stacked and aggregated structures of the π-conjugated frameworks.

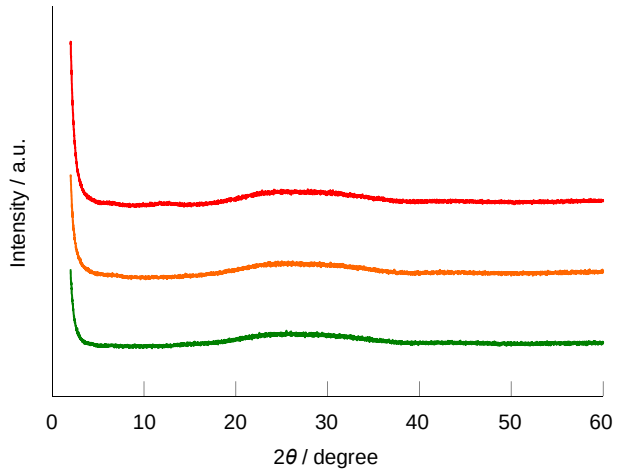

Figure 4. XRD patterns of CMPs **1**-**3**.

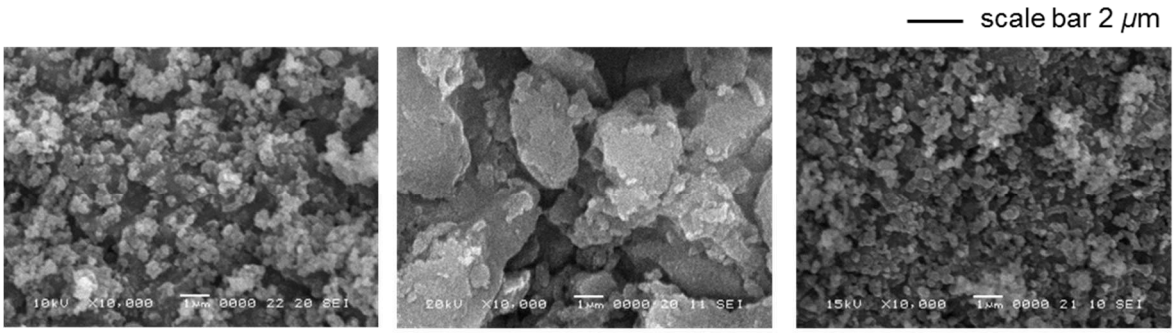

Figure 5. SEM images of CMPs **1**-**3**.

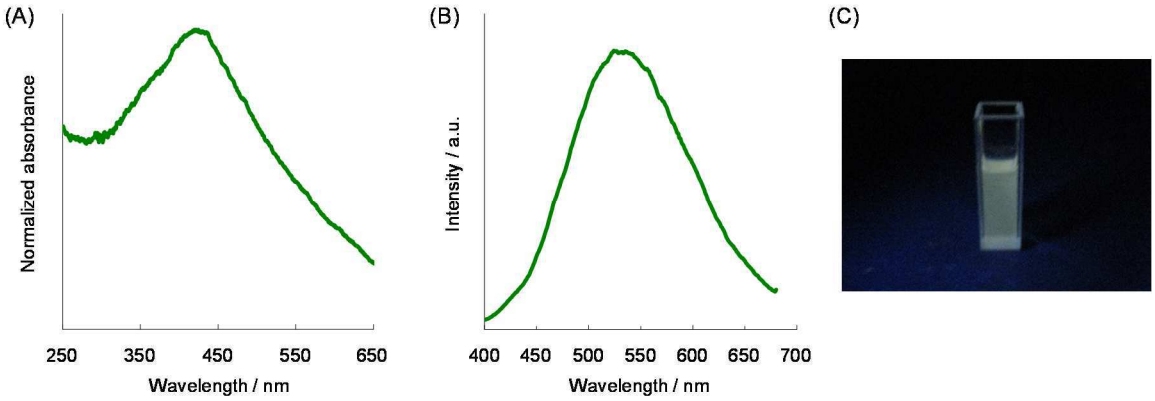

Figure 6. (A) UV-vis absorption spectrum of CMP **3** dispersed in CH_2Cl_2. (B) PL spectrum of CMP **3** dispersed in CH_2Cl_2 (excited at absorption maximum). (C) PL of the CMP dispersed in CH_2Cl_2, irradiated with UV lamp (365 nm).

Conclusions

In summary, the author prepared CMPs containing tetrasubstituted [2.2]paracyclophane units as the junctions of the network structure by Hay coupling, Sonogashira-Hagihara cross-coupling, and Yamamoto coupling. All CMPs comprised micropores with diameters of less than 2 nm. Moreover, they exhibited large surface areas; in particular, the BET surface area (S_{BET} value) of the CMPs synthesized by Yamamoto coupling reached 1000 m^2g^{-1}. The morphology of this CMP was relatively uniform and the particles had diameters of approximately 0.2 μm; therefore, it was readily dispersed in common organic solvents.

Experimental Section

General. ^{1}H and ^{13}C NMR spectra were recorded on a JEOL JNM-EX400 instrument at 400 and 100 MHz, respectively. Samples were analyzed in $CDCl_3$, and the chemical shift values were expressed relative to Me_4Si as an internal standard. Solid state cross-polarization/magic-angle-sample-spinning (CP/MAS) ^{13}C NMR spectra were obtained on a Bruker Avance III spectrometer operated at 100 MHz, and CP/MAS spectra were recorded at the MAS rate of 7 kHz with the ^{1}H decoupling field amplitude of 57 kHz. The contact time and the repetition time were fixed as 2 ms and 5 s, respectively. Analytical thin layer chromatography (TLC) was performed with silica gel 60 Merck F254 plates. Column chromatography was performed with Wakogel C-300 SiO_2. High-resolution mass spectra (HRMS) were obtained on a Thermo Scientific MALDI LTQ Orbitrap XL hybrid mass spectrometer. The adsorption isotherms of nitrogen at 77 K were measured with a BELSORP-18PLUS instrument, and N_2 gas of high purity (99.9999%) was used. Prior to the adsorption measurements, the sample was treated under reduced pressure ($< 10^{-2}$ Pa) at 423 K for 5 h. Scanning electron microscopy (SEM) measurement was carried out on a JEOL JSM-5600B system. Samples were put on a conducting carbon tape attached by a SEM grid, and then coated with platinum. X-Ray diffraction (XRD) data were obtained on a Rigaku MiniFlex diffractometer using CuKα radiation in a range of $3° \leq 2\theta \leq 60°$ at intervals of 0.01° at a scanning rate of 0.25° min^{-1}. Elemental analyses were performed at the Microanalytical Center of Kyoto University.

Materials. THF and Et_3N were purchased and purified by passage through purification column under Ar pressure.[57] Dehydrated CH_2Cl_2 and DMF were obtained commercially, and used after degassing. $Pd_2(dba)_3$, $Pd(PPh_3)_4$, $Ni(cod)_2$, PPh_3, CuI, *N*,*N*,*N*',*N*'-tetramethylethylenediamine (TMEDA), 2,2'-bipyridine, cyclooctadiene (COD), 1-bromo-4-iodobenzene (**2**), and 1,4-diiodobenzene (**4**) were obtained commercially, and used without further purification. 4,7,12,15-Tetraethynyl[2.2]paracyclophane (**1**)[54] was prepared from the corresponding tetrabromo[2.2]paracyclophane[55] as described in the literature.

Synthesis of 4,7,12,15-Tetrakis(4-bromophenylethynyl)[2.2]paracyclophane 3. A mixture of **1** (0.363 g, 1.19 mmol), **2** (1.486 g, 5.25 mmol), $Pd_2(dba)_3$ (109 mg, 0.12 mmol), PPh_3 (125 mg, 0.45 mmol), and CuI (46 mg, 0.24 mmol) was placed in a 50 mL Pyrex flask equipped with a magnetic stirrer bar. The equipment was purged with Ar, followed by adding THF (40 mL) and NEt_3 (10 mL) at 0 °C. The reaction was carried out at room temperature for 3 h. The reaction mixture was concentrated in vacuo to afford the crude product, which was purified by SiO_2 column chromatography (hexane/$CHCl_3$,

v/v = 8/1 as an eluent) and recrystallization from $CHCl_3$ and MeOH to afford **3** as a pale yellow solid (476 mg, 0.52 mmol, 43%). R_f = 0.24 (hexane/$CHCl_3$, v/v = 8/1). ^{1}H NMR ($CDCl_3$, 400 MHz): δ 3.07 (t, J = 8.0 Hz, 4H), 3.54 (t, J = 8.0 Hz, 4H), 7.10 (s, 4H), 7.41 (d, J = 8.0 Hz, 8H), 7.53 (d, J = 8.0 Hz, 8H); ^{13}C NMR ($CDCl_3$, 100 MHz): δ 32.7, 90.3, 93.6, 122.3, 122.7, 125.0, 131.7, 132.8, 134.6, 141.8. HRMS (MALDI) calcd for $C_{48}H_{28}Br_4$ $[M]^+$: 919.8919, found 919.8878. Elemental analysis calcd. for $C_{48}H_{28}Br_4$: C 62.37 H 3.05 Br 34.58, found: C 62.64 H 3.27 Br 34.48.

Synthesis of CMP 1. $CuCl_2$ (99 mg, 1.00 mmol), TMEDA (116 mg, 1.00 mmol), and CH_2Cl_2 (5.0 mL) were placed in a 50 mL Pyrex flask equipped with a magnetic stirrer bar, and the mixture was bubbled with dry O_2 (air) for 30 min. Compound **1** (126 mg, 0.42 mmol) in CH_2Cl_2 (2.0 mL) was added to this solution. After the reaction was carried out at room temperature for 72 h, aqueous NH_3 (28%) was added. The pale yellow solid was collected by filtration and washed with THF, hexane, $CHCl_3$, H_2O, and MeOH. Then, the solid was further washed with $CHCl_3$ for 24 h and MeOH for 24 h using a Soxhlet extractor. The solid was dried at 150 °C in a vacuum oven for 24 h to afford CMP **1** (112 mg, 90%). Solid state CP/MAS ^{13}C NMR: δ 31.7, 82.7, 125.2, 141.1 ppm. FT-IR (KBr): 903, 1470, 1573, 2158, 2929, 3290 cm^{-1}.

Synthesis of CMP 2. A mixture of **1** (72 mg, 0.24 mmol), **4** (157 mg, 0.48 mmol), $Pd(PPh_3)_4$ (27.4 mg, 0.024 mmol), CuI (4.5 mg, 0.024 mmol), Et_3N (1.9 mL), and DMF (2.85 mL) was placed in a round-bottom flask equipped with a magnetic stirring bar and a reflux condenser. After degassing the reaction mixture several times, the reaction was carried out at 80 °C for 72 h with stirring. The reaction mixture was cooled to room temperature, and 1.0 N HCl (10 mL) was added to the mixture. The pale yellow solid was collected by filtration and washed with THF, hexane, $CHCl_3$, H_2O, and MeOH. Then, the solid was further washed with $CHCl_3$ for 24 h and MeOH for 24 h using a Soxhlet extractor. The solid was dried at 150 °C in a vacuum oven for 24 h to afford CMP **2** (124 mg, 116 %). Solid state CP/MAS ^{13}C NMR: δ 31.7, 94.6, 123.4, 130.1, 140.2 ppm. FT-IR (KBr): 833, 905, 1508, 1593, 2195, 2930, 3032, 3296 cm^{-1}.

Synthesis of CMP 3. A mixture of $Ni(cod)_2$ (309 mg, 1.12 mmol), and 2,2'-bipyridine (175.7 mg, 1.12 mmol) was placed in a round-bottom flask equipped with a magnetic stirring bar and a reflux condenser. The equipment was purged with Ar, followed by adding DMF (30 mL) and COD (0.14 mL, 1.12 mmol), and then, the mixture was stirred for 1 h at 80 °C. To the mixture was added compound **3** (200 mg, 0.22 mmol). The reaction was carried out at 80 °C for 72 h. To the mixture, conc. HCl aq. (6.0 mL) was added, and the mixture was stirred for 8 h at room temperature. The pale yellow solid was collected by

filtration and washed with THF, hexane, $CHCl_3$, H_2O, and MeOH. Then, the solid was further washed with $CHCl_3$ for 24 h and MeOH for 24 h using a Soxhlet extractor. The solid was dried at 150 °C in a vacuum oven for 24 h to afford CMP **3** (120 mg, 91%). Solid state CP/MAS ^{13}C NMR: δ 31.6, 96.5, 126.1, 130.5, 140.1 ppm. FT-IR (KBr): 822, 1497, 1601, 2181, 2930, 3028 cm^{-1}.

References and Notes

(1) Brown, C. J.; Farthing, A. C. *Nature* **1949**, *164*, 915–916.

(2) Vögtle, F., Ed., C*yclophane Chemistry: Synthesis, Structures and Reactions*; John Wiley & Sons: Chichester, 1993.

(3) Gleiter, R.; Hopf, H., Eds., *Modern Cyclophane Chemistry*; Wiley-VCH: Weinheim, Germany, 2004.

(4) Morisaki, Y.; Chujo, Y. *Angew. Chem., Int. Ed.* **2006**, *45*, 6430–6437.

(5) Morisaki, Y.; Chujo, Y. *Prog. Polym. Sci.* **2008**, *33*, 346–364.

(6) Morisaki, Y.; Chujo Y. *Polym. Chem.* **2011**, *2*, 1249–1257.

(7) Morisaki, Y.; Chujo, Y. In *Conjugated Polymer Synthesis: Methods and Reactions*; Chujo, Y., Ed.; Wiley-VCH: Weinheim; 2010, Chapter 5, pp 133–163.

(8) Morisaki, Y.; Ueno, S.; Saeki, A.; Asano, A.; Seki, S.; Chujo Y. *Chem.–Eur. J.* **2012**, *18*, 4216–4224.

(9) Morisaki, Y.; Ueno, S.; Chujo Y. *J. Polym. Sci. Part A Polym. Chem.* **2013**, *51*, 334–339.

(10) Li, H.; Eddaoudi, M.; O'Keeffe, M.; Yaghi, O. M. *Nature* **1999**, 402, 276–279.

(11) Cheetham, A. K.; Férey, G.; Loiseau, T. *Angew. Chem., Int. Ed.* **1999**, *38*, 3268–3292.

(12) Eddaoudi, M.; Kim, J.; Rosi, N.; Vodak, D.; O'Keeffe, M.; Yaghi, O. M. *Science* **2002**, *295*, 469–472.

(13) Yaghi, O. M.; O'Keeffe, M.; Ockwig, N. W.; Chae, H. K.; Eddaoudi, M.; Kim, J. *Nature* **2003**, *423*, 705–714.

(14) Matzger, A.; O'Keeffe, M.; Yaghi, O. M. *Nature* **2004**, *427*, 523–527.

(15) Kitagawa, S.; Kitaura, R.; Noro, S. *Angew. Chem., Int. Ed.* **2004**, *43*, 2334–2375.

(16) Kitagawa, S.; Noro, S.; Nakamura, T. *Chem. Commun.* **2006**, 701–707.

(17) Kitagawa, S.; Matsuda, R. *Coord. Chem. Rev.* **2007**, *251*, 2490–2509.

(18) Maji, T. K.; Kitagawa, S. *Pure Appl. Chem.* **2007**, *79*, 2155–2177.

(19) Férey, G. *Chem. Soc. Rev.* **2008**, *37*, 191–214.

(20) Uemura, T.; Yanai, N.; Kitagawa, S. *Chem. Soc. Rev.* **2009**, *38*, 1228–1236.

(21) Jiang, J.-X.; Cooper, A. I. *Top. Curr. Chem.* **2010**, *293*, 1–33.

(22) Thomas, A. *Angew. Chem., Int. Ed.* **2010**, *49*, 8328–8344.

(23) Thomas, A.; Kuhn, P.; Weber, J.; Titirici, M.-M.; Antonietti, M. *Macromol. Rapid Commun.* **2009**, *30*, 221–236.

(24) McKeown, N. B.; Budd, P. M. *Chem. Soc. Rev.* **2006**, *35*, 675–683.

(25) Budd, P. M.; Ghanem, B. S.; Makhseed, S.; McKeown, N. B.; Msayib, K. J.; Tattershall, C. E. *Chem. Commun.* **2004**, 230–231.

(26) McKeown, N. B.; Gahnem, B. M.; Msayib, K.; Budd, P. M.; Tattershall, C. E.; Mahmood, K.; Tan, S.; Book, D.; Langmi, H. W.; Walton, A. *Angew. Chem., Int. Ed.* **2006**, *45*, 1804–1807.

(27) Budd, P. M.; Butler, A.; Selbie, J.; Mahmood, K.; McKeown, N. B.; Ghanem, B.; Msayib, K.; Book, D.; Walton, A. *Phys. Chem. Chem. Phys.* **2007**, *9*, 1802–1808.

(28) Ghanem, B. S.; Msayib, K. J.; McKeown, N. B.; Harris, K. D. M.; Pan, Z.; Budd, P. M.; Butler, A.; Selbie, J.; Book, D.; Walton, A. *Chem. Commun.* **2007**, 67–69.

(29) Côté, A. P.; Benin, A. I.; Ockwig, N. W.; O'Keeffe, M.; Matzger, A. J.; Yaghi, O. M. *Science* **2005**, *310*, 1166–1170.

(30) El-Kaderi, H. M.; Hunt, J. R.; Mendoza-Cortés, J. L.; Côté, A. P.; Taylor, R. E.; O'Keeffe, M.; Yaghi, O. M. *Science* **2007**, *316*, 268–272.

(31) Lee, J. Y.; Wood, C. D.; Bradshaw, D.; Rosseinsky, M. J.; Cooper, A. I. *Chem. Commun.* **2006**, 2670–2672.

(32) Tsyurupa, M. P.; Davankov, V. A. *React. Funct. Polym.* **2006**, *66*, 768–779.

(33) Wood, C. D.; Tan, B.; Trewin, A.; Niu, H. J.; Bradshaw, D.; Rosseinsky, M. J.; Khimyak, Y. Z.; Campbell, N. L.; Kirk, R.; Stockel, E.; Cooper, A. I. *Chem. Mater.* **2007**, *19*, 2034–2048.

(34) McKeown, N. B.; Budd, P. M.; Msayib, K. J.; Ghanem, B. S.; Kingston, H. J.; Tattershall, C. E.; Makhseed, S.; Reynolds, K. J.; Fritsch, D. *Chem.–Eur. J.* **2005**, *11*, 2610–2620.

(35) Taguchi, A.; Schüth, F. *Micropor. Mesopor. Mater.* **2005**, *77*, 1–45.

(36) Hartmann, M. *Chem. Mater.* **2005**, *17*, 4577–4593.

(37) Corma, A.; Garcia, H. *Adv. Synth. Catal.* **2006**, *348*, 1391–1412.

(38) Du, X.; Sun, Y. L.; Tan, B. E.; Teng, Q. F.; Yao, X. J.; Su, C. Y.; Wang, W. *Chem. Commun.* **2010**, *46*, 970–972.

(39) Wood, C. D.; Tan, B.; Trewin, A.; Su, F.; Rosseinsky, M. J.; Bradshaw, D.; Sun, Y.; Zhou, L.; Cooper, A. I. *Adv. Mater.* **2008**, *20*, 1916–1921.

(40) Furukawa, H.; Yaghi, O. M. *J. Am. Chem. Soc.* **2009**, *131*, 8875–8883.

(41) Czaja, A. U.; Trukhan, N.; Müller, U. *Chem. Soc. Rev.* **2009**, *38*, 1284–1293.

(42) Svec, F.; Germain, J.; Fréchet, J. M. J. *Small* **2009**, *5*, 1098–1111.

(43) Li, A.; Lu, R. F.; Wang, Y.; Wang, X.; Han, K. L.; Deng, W. Q. *Angew. Chem., Int. Ed.* **2010**, *49*, 3330–3333.

(44) Park, H. B.; Jung, C. H.; Lee, Y. M.; Hill, A. J.; Pas, S. J.; Mudie, S. T.; Van Wagner, E.; Freeman, B. D.; Cookson, D. J. *Science* **2007**, *318*, 254–258.

(45) Ren, H.; Ben, T.; Wang, E. S.; Jing, X. F.; Xue, M.; Liu, B. B.; Cui, Y.; Qiu, S. L.; Zhu, G. S.; *Chem. Commun.* **2010**, *46*, 291–293.

(46) Cooper, A. I. *Adv. Mater.* **2009**, *21*, 1291–1295.

(47) McKeown, N. B.; Budd, P. M. *Macromolecules* **2010**, *43*, 5163–5176.

(48) Chen, L.; Honsho, Y.; Seki, S.; Jiang, D.-L. *J. Am. Chem. Soc.* **2010**, *132*, 6742–6748.

(49) Liu, X.; Xu, Y.; Jiang, D.-L. *J. Am. Chem. Soc.* **2012**, *134*, 8738–8741.

(50) Hay, A. S. *J. Org. Chem.* **1962**, *27*, 3320–3321.

(51) Tohda, Y.; Sonogashira, K.; Hagihara, N. *Synthesis* **1977**, 777–778.

(52) Sonogashira K. in *Handbook of Organopalladium Chemistry for Organic Synthesis*; Negishi, E. Ed.; Wiley-VCH, New York, 2002, pp. 493–529.

(53) Yamamoto, T.; Morita, A.; Miyazaki, Y.; Maruyama, T.; Wakayama, H.; Zhou, Z.-h.; Nakamura, Y.; Kanbara, T. *Macromolecules* **1992**, *25*, 1214–1223.

(54) Bondarenko, L.; Dix, I.; Hinrichs, H.; Hopf, H. *Synthesis* **2004**, 2751–2759.

(55) Chow, H.-F.; Low, K.-H.; Wong, K. Y. *Synlett* **2005**, 2130–2134.

(56) Sing, K. S. W.; Everett, D. H.; Haul, R. A. W.; Moscou, L.; Pierotti, R. A.; Rouquérol, J.; Siemieniewska, T. *Pure Appl. Chem.* **1985**, *57*, 603–619.

(57) Pangborn, A. B.; Giardello, M. A.; Grubbs, R. H.; Rosen, R. K.; Timmers, F. J. *Organometallics* **1996**, *15*, 1518–1520.

Part II

π-Conjugated Compounds

Based on Planar Chiral [2.2]Paracyclophanes

Chapter 3

Planar Chiral Tetrasubstituted [2.2]Paracyclophane: Optical Resolution and Functionalization

Abstract

Optical resolution of 4,7,12,15-tetrasubstituted [2.2]paracyclophane and subsequent transformation to planar chiral building blocks are described. An optically active propeller-shaped macrocyclic compound containing a planar chiral cyclophane core was synthesized, showing excellent chiroptical properties such as high fluorescence quantum efficiency and a large circularly polarized luminescence dissymmetry factor.

Introduction

Planar chiral [2.2]paracyclophanes provide a conformationally stable chiral environment due to suppression of the rotation of phenylenes.[1] Optical resolutions of various [2.2]paracyclophanes have been conducted,[1-3] and the resulting optically active [2.2]paracyclophane compounds have mainly been used as chiral auxiliaries. For example, aryl-PHANEPHOS[3a,b] are well-known commercially available compounds; they are widely used as chiral ligands for transition metal-catalyzed asymmetric reactions.

There have been several reports on optical resolution of disubstituted [2.2]paracyclophane;[3] however, only one report on that of a tetrasubstituted [2.2]paracyclophane compound exists.[4] Considering the potential applications of [2.2]paracyclophane skeletons in polymer and materials chemistry,[5] as well as organic and organometallic chemistry, further development and modification of optical resolution methods for planar chiral tetrasubstituted [2.2]paracyclophanes would be valuable. Herein, the author reports optical resolution of *rac*-4,7,12,15-tetrabromo[2.2]paracyclophane and subsequent transformations to produce planar chiral building blocks for through-space carbon-rich compounds.[6] In this chapter, an optically active macrocycle[7] based on a tetrasubstituted [2.2]paracyclophane was synthesized. The excellent chiroptical properties, in particular, circularly polarized luminescence (CPL), are also reported.

Results and Discussion

Optical resolution of tetrasubstituted [2.2]paracyclophane was carried out by a diastereomer method beginning with 4,7,12,15-tetrabromo[2.2]paracyclophane[8] *rac*-**1**, as shown in Figure 1. One of bromides in *rac*-**1** was converted to a hydroxyl group to obtain *rac*-**2** in 69% isolated yield,[3c-e] which was reacted with (−)-(1*S*,4*R*)-camphanoyl chloride **3** to obtain a mixture of diastereomers. These were readily separated by SiO_2 column chromatography and purified by recrystallization to obtain (S_p,1*S*,4*R*)-**4** and (R_p,1*S*,4*R*)-**4** in 38% and 34% isolated yield, respectively (each diastereomer ratio (dr) > 99.5%).[9] The structures were confirmed by NMR spectroscopy, mass analysis, elemental analysis, and X-ray crystallography (Figure 1).

Hydrolysis and subsequent transformation of (S_p,1*S*,4*R*)-**4** are shown in Scheme 1. Treatment of (S_p,1*S*,4*R*)-**4** with KOH afforded (S_p)-**2**. This compound was used for the next transformation to OTf without purification, and enantiopure (S_p)-**5** was obtained in 92% isolated yield. Sonogashira-Hagihara coupling[10] of (S_p)-**5** with trimethylsilylacetylene using a $Pd_2(dba)_3$/(*t*-Bu)$_3$P catalysis gave only (S_p)-**6** in 83% isolated yield. Interestingly, bromide was selectively reacted, and tetra(trimethylsilylethynyl)[2.2]paracyclophane (S_p)-**7** was not detected by thin-layer chromatography. Reacting (S_p)-**6** with trimethylsilylacetylene using a $PdCl_2$(dppf) catalysis afforded (S_p)-**7**. Removal of the trimethylsilyl group was carried out with K_2CO_3/MeOH afforded the corresponding tetrayne[11] (S_p)-**8** in 91% isolated yield. The enantiomer (R_p)-**8** was also synthesized by the same route.

Tetrasubstituted [2.2]paracyclophanes **5** and **8** can be employed as conformationally stable chiral building blocks for various optically active carbon-rich compounds. In this study, the author synthesized an optically active propeller-shaped macrocycle[12] from **8**, as shown in Scheme 1. The reaction of (S_p)-**8** with 5-*tert*-butyl-2-[(trimethylsilyl)ethynyl]iodobenzene afforded the corresponding optically active compound (S_p)-**9** in 89% isolated yield. Desilylation of (S_p)-**9** with K_2CO_3/MeOH and a subsequent oxidative coupling reaction using

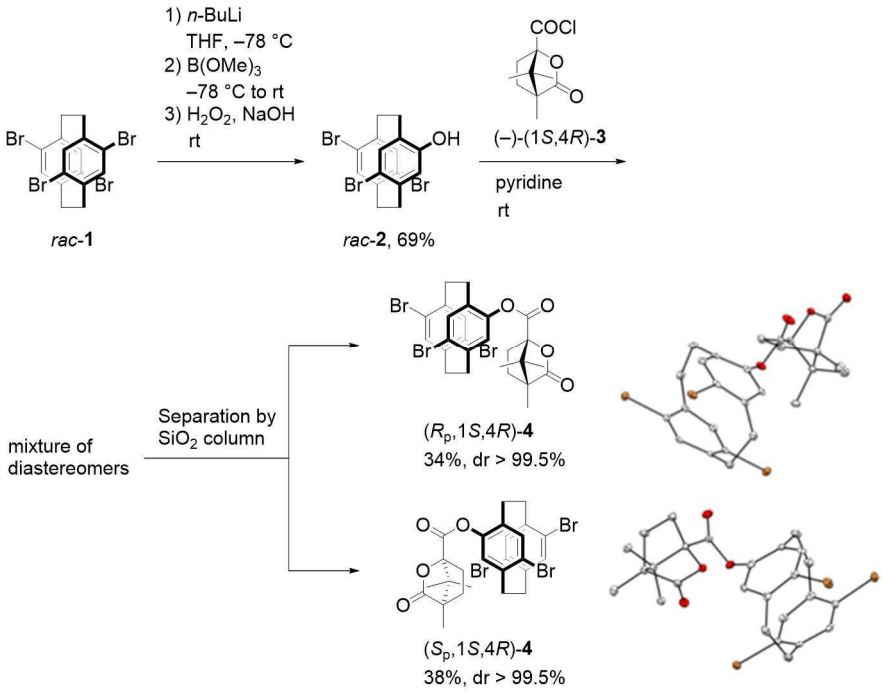

Figure 1. Optical resolution of *rac*-**1**. Crystal structures of (S_p,1*S*,4*R*)-**4** and (R_p,1*S*,4*R*)-**4** with ellipsoids at 30% probability. Hydrogen atoms and solvent ($CHCl_3$ in (R_p,1*S*,4*R*)-**4**) are omitted for clarity.

Scheme 1. Synthesis of Optically Active Macrocycle

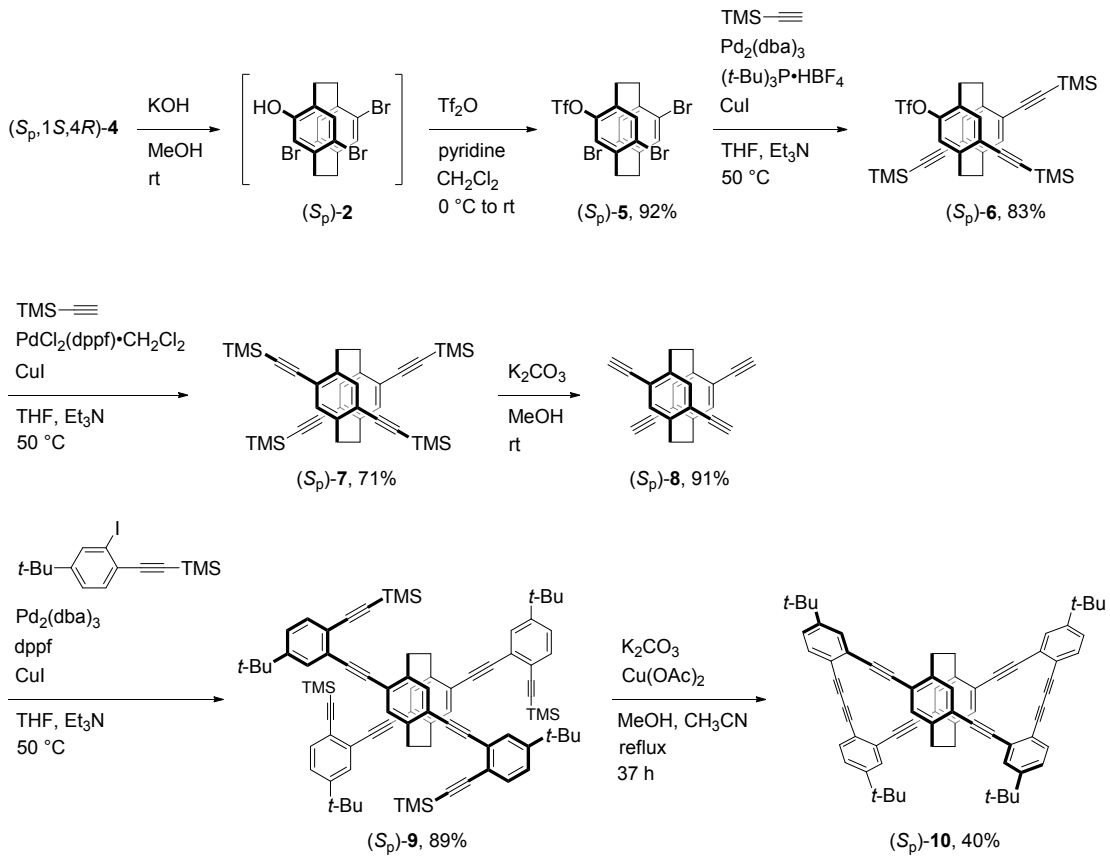

$Cu(OAc)_2$ gave the target macrocycle (S_p)-**10** in 40% isolated yield. Enantiomer (R_p)-**10** was also prepared, and their structures were confirmed by NMR spectroscopy and mass analysis. A single crystal of *rac*-**10** was obtained by recrystallization with $CHCl_3$ and MeOH, and the molecular structure is shown in Figure 2. The enantiomers co-crystallized into a single crystal, and the bowtie-shaped[13] structure was confirmed from the top view. As shown in the front and side views, the structure seems like a two-blade propeller owing to the planar chiral [2.2]paracyclophane core. This structure has previously been synthesized by Hopf, Haley, and co-workers as a racemic compound,[12] although the positions of the *tert*-butyl groups were different.

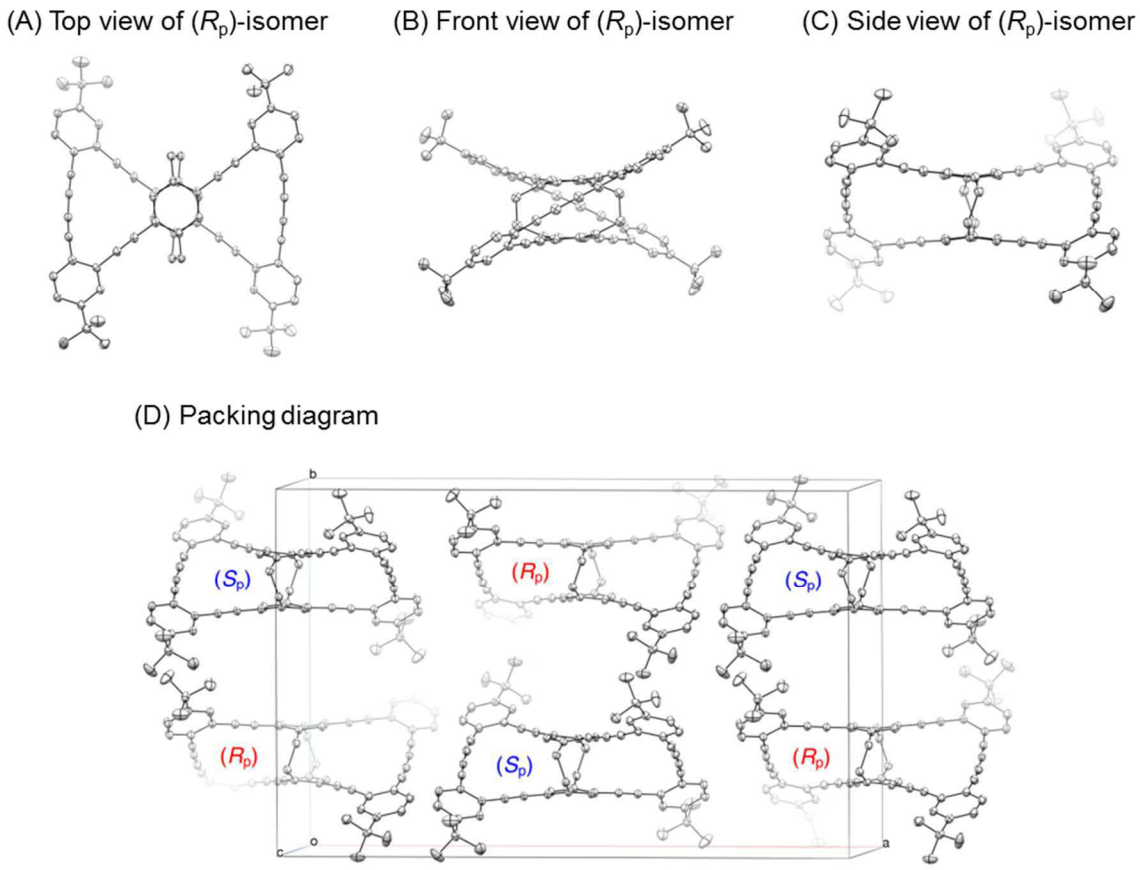

Figure 2. Preliminary X-ray structure of *rac*-**10** and its packing diagram. Thermal ellipsoids are scaled to the 30% probability level. Hydrogen atoms and solvents are omitted for clarity.

The optical properties of (R_p)- and (S_p)-**10** were investigated; the UV-vis absorption, circularly dichroism (CD), photoluminescence (PL), and CPL spectra of (R_p)- and (S_p)-**10** in the dilute $CHCl_3$ solution (1.0×10^{-5} M) are shown in Figure 3. The UV-vis absorption spectrum of **10** (Figure 3A) was identical to that of the cyclic compound prepared by Hopf, Haley, and co-workers.[12] Thus, there was no difference in the electronic structure of the ground state between these compounds regardless of the positions of the *tert*-butyl groups.[14] In the CD spectra of (R_p)- and (S_p)-**10**, intense and mirror image Cotton effects were observed in the absorption bands of the UV-vis spectra (Figure 3A). The molar ellipticity ([θ]) was very large, with a [θ] for (S_p)-**10** of 2.7×10^6 deg cm^2 dmol^{-1}. The dissymmetry factor of absorbance, $g_{abs} = 2(\Delta\varepsilon/\varepsilon)$, is another parameter indicating chirality in the ground state; a large g_{abs} value of 0.9×10^{-2} was obtained. The specific rotation $[\alpha]^{23}_D$ (*c* 0.5, $CHCl_3$) of (S_p)-**10** was estimated to be −1494.9, whereas that of (S_p)-**9** was +44.1. In all cases, the chiroptical data for (S_p)-**10** were considerably enhanced compared with those for (S_p)-**9** in the ground state.

As shown in Figure 3B, compound **10** exhibited a vibronic emission peak at around 460 nm with an absolute PL quantum efficiency (Φ_{lum}) of 0.45 for (S_p)-**10**. The PL decay curve was fitted with a single exponential relationship ($\chi^2 = 1.18$), and the PL lifetime (τ) was calculated to be 3.71 ns (Figure 4). This efficient PL arose from criss-cross delocalization across the entire molecule via the strong through-space interaction of the [2.2]paracyclophane core.[15]

Intense and mirror image CPL signals for (R_p)- and (S_p)-**10** were observed in the emission region (Figure 3B) with a large CPL dissymmetry factor, $g_{lum} = 2(I_{left} - I_{right})/(I_{left} + I_{right})$, where I_{left} and I_{right} are the PL intensities of left- and right-handed CPL, respectively. The maximum $|g_{lum}|$ value was estimated to be 1.1×10^{-2} (Figure 5). It is rare that a monodispersed chiral hydrocarbon exhibits such a large g_{lum} on the order of 10^{-2}.[16d,f,g] Recently, small molecules that exhibit CPL in the dilute solution have been extensively studied; helically and axially chiral compounds have been known to have CPL with large g_{lum} values on the order of 10^{-3}-10^{-2}.[16] A

conformationally stable chiral structure of the emitting species, such as a helical structure, in the excited state is essential to obtain CPL with a large g_{lum}. Macrocycle **10** possesses a conformationally stable chiral second-ordered structure (propeller-shaped structure) due to complete fixation by the [2.2]paracyclophane bridge methylenes, resulting in intense CPL with a large g_{lum}.[17] There were only small differences between the g_{abs} and g_{lum} for (R_p)- and (S_p)-**10**, indicating little conformational change between the ground and the excited states.[18]

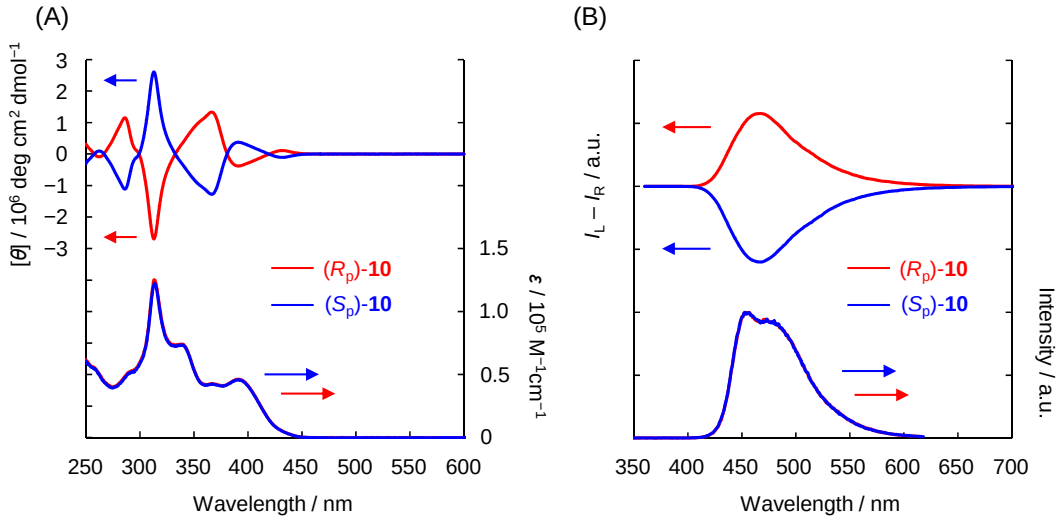

Figure 3. (A) UV-vis absorption and CD spectra of (R_p)- and (S_p)-**10** in $CHCl_3$ (1.0×10^{-5} M) at room temperature. (B) PL and CPL spectra of (R_p)- and (S_p)-**10** in $CHCl_3$ (1.0×10^{-6} M for PL and 1.0×10^{-5} for CPL) at room temperature, excited at 314 nm.

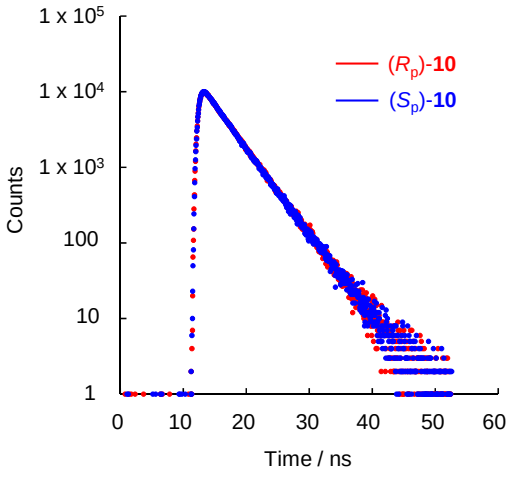

Figure 4. PL decay curves of (R_p)- and (S_p)-**10** in $CHCl_3$ (1.0×10^{-5} M) at room temperature, excited at 375 nm LED laser.

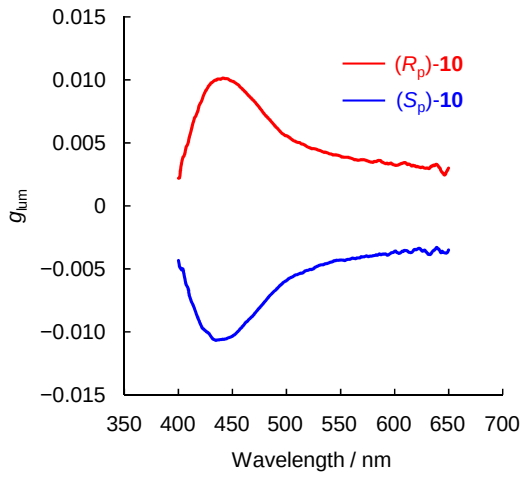

Figure 5. Charts of g_{lum} of (R_p)- and (S_p)-**10** in $CHCl_3$ (1.0×10^{-5} M) at room temperature.

Conclusions

In conclusion, the author have developed a practical method for optical resolution of planar chiral tetrasubstituted [2.2]paracyclophane. The obtained enantiopure 4,7,12,15-tetrafunctional cyclophane was readily modified to the corresponding planar chiral compounds. In the present study, a propeller-shaped macrocyclic compound was synthesized through coupling reactions. The obtained macrocycle exhibited a chiral environment in the ground and excited state. In particular, the macrocycle exhibited PL with a high Φ_{lum} of 0.45 and CPL with a large g_{lum} of 1.1×10^{-2}. A conformationally stable higher-ordered structure in the excited state is required for CPL with a large g_{lum}, and the theoretical supports in the excited state will be the next target. From the conformational viewpoint, [2.2]paracyclophane is the ideal scaffold and provides new design guidelines for CPL materials in addition to helically and axially chiral compounds. Various functionalizations of planar chiral tetrasubstituted [2.2]paracyclophanes, such as **5** and **8**, are available to obtain a variety of optically active emissive molecules.

Experimental Section

General. ^{1}H and ^{13}C NMR spectra were recorded on JEOL EX400 and AL400 instruments at 400 and 100 MHz, respectively. Samples were analyzed in $CDCl_3$, and the chemical shift values were expressed relative to Me_4Si as an internal standard. Analytical thin layer chromatography (TLC) was performed with silica gel 60 Merck F254 plates. Column chromatography was performed with Wakogel C-300 SiO_2. High-resolution mass (HRMS) spectrometry was performed at the Technical Support Office (Department of Synthetic Chemistry and Biological Chemistry, Graduate School of Engineering, Kyoto University), and the HRMS spectra were obtained on a JEOL JMS-MS700 spectrometer for electron ionization (EI), a Thermo Fisher Scientific EXACTIVE spectrometer for electrospray ionization (ESI), and a JEOL JMS-HX110A spectrometer for fast atom bombardment (FAB). Recyclable preparative high-performance liquid chromatography (HPLC) was carried out on a Japan Analytical Industry Co. Ltd., Model LC918R (JAIGEL-1H and 2H columns) and LC9204 (JAIGEL-2.5H and 3H columns) using $CHCl_3$ as an eluent. UV-vis spectra were recorded on a SHIMADZU UV-3600 spectrophotometer, and samples were analyzed in $CHCl_3$ at room temperature. Fluorescence emission spectra were recorded on a HORIBA JOBIN YVON Fluoromax-4 spectrofluorometer, and samples were analyzed in $CHCl_3$ at room temperature. PL lifetime measurement was performed on a Horiba FluoroCube spectrofluorometer system; excitation was carried out using a UV diode laser (NanoLED 375 nm). Specific rotations ($[\alpha]^{t}_{D}$) were measured with a HORIBA SEPA-500 Polarimeter. Diastereomer ratio (dr) was confirmed by a HPLC (TOSOH UV-8020) equipped with a Daicel CHIRALPAK IA column (0.46 cm × 25 cm, solvent flow rate 0.5 mL/min). Circular dichroism (CD) spectra were recorded on a JASCO J-820 spectropolarimeter with $CHCl_3$ as a solvent at room temperature. Circularly polarized luminescence (CPL) spectra were recorded on a JASCO CPL-200S with $CHCl_3$ as a solvent at room temperature. Elemental analyses were performed at the Microanalytical Center of Kyoto University.

Materials. *n*-BuLi (1.65 M in hexane), $B(OMe)_3$, H_2O_2 (30 w/v% in H_2O), NaOH, (–)-(1S,4R)-camphanoyl chloride (3), KOH, Tf_2O, trimethylsilylacetylene, $Pd_2(dba)_3$ (dba = dibenzylideneacetone), $(t\text{-Bu})_3P{\cdot}HBF_4$, CuI, K_2CO_3, MeOH, $PdCl_2(dppf){\cdot}CH_2Cl_2$ (dppf = 1,1'-bis(diphenylphosphino)ferrocene), and $Cu(OAc)_2$ were purchased and used without further purification. Anhydrous CH_2Cl_2 and CH_3CN were purchased and used without further purification. Pyridine was purchased and purified by distillation with KOH. THF and Et_3N were purchased and purified by passage through solvent purification columns under Ar pressure.[19] *rac*-4,7,12,15-Tetrabromo[2.2]paracyclophane *rac*-**1** was prepared as described in the literature.[8] 4,7,12,15-

Tetra(trimethylsilylethynyl)[2.2]paracyclophane *rac*-**7**,[11] 4,7,12,15-tetraethynyl[2.2]paracyclophane *rac*-**8**,[11] 2-bromo-4-*tert*-butyl-1-iodobenzene **s1**,[20] and 1-bromo-5-*tert*-butyl-2-[(trimethylsilyl)ethynyl]benzene **s2** have previously been reported.[21]

Synthesis of *rac*-2. A solution of *n*-BuLi (1.65 M in hexane, 6.9 mL, 11 mmol) was slowly added to a solution of *rac*-4,7,12,15-tetrabromo[2.2]paracyclophane *rac*-**1** (5.24 g, 10 mmol) in THF (80 mL) at −78 °C. After 30 min, $B(OMe)_3$ (16.7 mL, 150 mmol) was added and the mixture was stirred 1 h at −78 °C to room temperature. Subsequently, aqueous 2 M NaOH (20 mL, 40 mmol) and aqueous 30% H_2O_2 (33.4 mL, 0.30 mol) were added and the mixture was stirred overnight at room temperature. To the yellow reaction mixture was added saturated aqueous NH_4Cl solution, and the organic layer was extracted three times with CH_2Cl_2. The combined organic layer was washed with brine and dried over $MgSO_4$. $MgSO_4$ was removed by filtration, and the solvent was removed with a rotary evaporator. The crude residue was purified by column chromatography on SiO_2 ($CHCl_3$ as an eluent, R_f = 0.38) to afford *rac*-**2** (3.19 g. 6.91 mmol, 69%) as a light yellow crystal. ^{1}H NMR ($CDCl_3$, 400 MHz) δ 2.80-3.00 (m, 4H), 3.12-3.26 (m, 4H), 4.61 (s, 1H), 6.35 (s, 1H), 7.06 (s, 1H), 7.13 (s, 1H), 7.14 (s, 1H) ppm; ^{13}C NMR ($CDCl_3$, 100 MHz) δ 28.1, 32.6, 32.9, 33.2, 117.3, 119.4, 125.0, 125.7, 127.0, 134.1, 134.7, 134.9, 140.0, 140.3, 141.2, 153.7 ppm. HRMS (ESI) calcd. for $C_{16}H_{13}Br_3ClO$ $[M+Cl]^-$: 492.8200, found: 492.8186. Elemental analysis calcd. for $C_{16}H_{13}Br_3O$: C 41.69 H 2.84, found: C 42.48 H 2.90.

Optical resolution of *rac*-2: Synthesis of (S_p,1*S*,4*R*)-4 and (R_p,1*S*,4*R*)-4. A mixture of *rac*-**2** (3.19 g, 6.9 mmol) and (1*S*)-(−)-camphanoyl chloride (2.06 g, 9.51 mmol) was placed in a round-bottom flask equipped with a magnetic stirring bar. After degassing the reaction mixture several times, dehydrated pyridine (40 mL) was added and the mixture was stirred at room temperature for 9 h. After addition of 5 M HCl (100 mL), the organic layer was extracted with CH_2Cl_2 and washed with 1 M HCl, saturated aqueous $NaHCO_3$ and brine. The combined organic layer was dried over $MgSO_4$. $MgSO_4$ was removed by filtration, and the solvent was removed with a rotary evaporator. The crude residue was purified by column chromatography on SiO_2 ($CHCl_3$/hexane = 9/1 v/v as an eluent) to give the mixture of (S_p,1*S*,4*R*)-**4** and (R_p,1*S*,4*R*)-**4**. as a crystal. Recrystallization was carried out to obtain each diastereomer; (S_p,1*S*,4*R*)-**4** (1.70 g, 2.65 mmol, 38%) from toluene and hexane (good and poor solvent, respectively), (R_p,1*S*,4*R*)-**4** (1.49 g, 2.33 mmol, 34%) from $CHCl_3$ and MeOH (good and poor solvent, respectively). (S_p,1*S*,4*R*)-**4**. R_f = 0.30 ($CHCl_3$/hexane = 9/1 v/v). Pale yellow block crystal. ^{1}H NMR ($CDCl_3$, 400 MHz) δ 1.15 (s, 3H), 1.21 (s, 3H), 1.25 (s, 3H), 1.75-1.81 (m, 1H), 1.97-2.05 (m, 1H), 2.13-2.20 (m, 1H), 2.53-2.60 (m, 1H), 2.88-3.03 (m, 5H), 3.20-3.30 (m, 3H) 6.83 (s, 1H), 7.01 (s, 1H),

7.13 (s, 1H), 7.30 (s, 1H) ppm; ^{13}C NMR ($CDCl_3$, 100 MHz) δ 9.81, 16.7, 17.4, 28.7, 28.8, 30.8, 32.6, 32.9, 33.8, 54.7, 55.1, 90.8, 123.8, 125.1, 125.3, 125.6, 132.2, 134.7, 134.8, 135.6, 140.3, 140.7, 140.8, 148.1, 165.3, 178.0 ppm. HRMS (ESI) calcd. for $C_{26}H_{25}Br_3ClO_4$ $[M+Cl]^-$: 672.8986, found: 672.8968. Elemental analysis calcd. for $C_{26}H_{25}Br_3O_4$: C 48.70 H 3.93 Br 37.39, found: C 48.46 H 3.80 Br 37.41. $[\alpha]^{23}_D$ = +80.6 (*c* 0.5, $CHCl_3$). Retention time of HPLC: *t* = 11.3 min (CHIRALPAK IA, hexane/THF = 8/2 v/v). (R_p,1*S*,4*R*)-**4**. R_f = 0.21 ($CHCl_3$/hexane = 9/1 v/v). Colorless needle crystal. ^{1}H NMR ($CDCl_3$, 400 MHz) δ 1.12 (s, 3H), 1.20 (s, 3H), 1.23 (s, 3H), 1.80-1.87 (m, 1H), 2.02-2.09 (m, 1H), 2.27-2.34 (m, 1H), 2.56-2.63 (m, 1H), 2.83-3.04 (m, 5H), 3.21-3.31 (m, 3H), 6.87 (s, 1H), 7.03 (s, 1H), 7.14 (s, 1H), 7.29 (s, 1H) ppm; ^{13}C NMR ($CDCl_3$, 100 MHz) δ 9.80, 16.9, 17.0, 28.8, 29.1, 31.3, 32.6, 33.0, 33.9, 54.4, 54.9, 90.7, 123.7, 125.0, 125.1, 125.5, 132.0, 134.6, 134.8, 135.4, 140.3, 140.6, 140.7, 147.9, 164.8, 177.6 ppm. HRMS (ESI) calcd. for $C_{26}H_{25}Br_3ClO_4$ $[M+Cl]^-$: 672.8986, found: 672.8968. Elemental analysis calcd. for $C_{26}H_{25}Br_3O_4$: C 48.70 H 3.93 Br 37.39, found: C 48.46 H 3.78 Br 37.10. $[\alpha]^{23}_D$ = −86.1 (*c* 0.5, $CHCl_3$). Retention time of HPLC: *t* = 12.5 min (CHIRALPAK IA, hexane/THF = 8/2 v/v).

Synthesis of 5. KOH (1.42 g, 2.41 mmol) in H_2O (15 mL) was added to a solution of (S_p,1*S*,4*R*)-**4** (1.55 g, 2.41 mmol) in EtOH (70 mL). After the mixture was stirred for 10 h at room temperature, the reaction mixture was quenched by the addition of 1 M HCl (30 mL). The organic layer was extracted with CH_2Cl_2 and washed with saturated aqueous $NaHCO_3$ and brine. The combined organic layer was dried over $MgSO_4$. $MgSO_4$ was removed by filtration, and the solvent was evaporated. Compound (S_p)-**2** was obtained and used for the next reaction without purification. Dehydrated pyridine (2.0 mL, 25 mmol) and Tf_2O (1.0 mL, 5.94 mmol) were added to a stirred solution of (S_p)-2 in dehydrated CH_2Cl_2 (30 mL) at 0 °C. After being stirred for 2 h at room temperature, the reaction mixture was quenched by the addition of 5 M HCl (5 mL). The organic layer was extracted with CH_2Cl_2 and washed with 1 M HCl, saturated aqueous $NaHCO_3$, and brine. The combined organic layer was dried over $MgSO_4$. $MgSO_4$ was removed by filtration, and the solvent was evaporated. The residue was purified by column chromatography on SiO_2 (hexane as an eluent) to afford (S_p)-**5** (1.31 g, 2.22 mmol, 92%) as a colorless crystal. (S_p)-**5**. R_f = 0.23 (hexane). 1 H NMR ($CDCl_3$, 400 MHz) δ 2.85-3.08 (m, 4H), 3.19-3.35 (m, 4H), 6.95 (s, 1H), 6.96 (s, 1H), 7.15 (s, 1H), 7.33 (s, 1H) ppm; ^{13}C NMR ($CDCl_3$, 100 MHz) δ 28.8, 32.6, 32.8, 33.6, 118.7 (q, J_{C-F} = 319 Hz), 125.1, 125.4, 125.5, 126.2, 133.4, 134.7, 135.4, 135.5, 140.46, 140.49, 141.9, 147.5 ppm. HRMS (FAB) calcd. for $C_{17}H_{12}Br_3F_3OS$ $[M]^+$: 589.8009, found: 589.8009. Elemental analysis calcd. for $C_{17}H_{12}Br_3F_3OS$: C 34.43 H 2.04 F 9.61 S 5.41 Br 40.42, found: C 34.62

H 2.03 F 9.85 S 5.34 Br 39.60. $[\alpha]^{23}_{D}$ = +90.5 (*c* 0.5, $CHCl_3$). (R_p)-**5**. Yield: 85% from (R_p,1*S*,4*R*)-**4**. HRMS (FAB) calcd. for $C_{17}H_{12}Br_3F_3OS$ $[M]^+$: 589.8009, found: 589.8006. Elemental analysis calcd. for $C_{17}H_{12}Br_3F_3OS$: C 34.43 H 2.04 F 9.61 S 5.41 Br 40.42, found: C 34.33 H 2.06 F 9.66 S 5.43 Br 39.83. $[\alpha]^{23}_{D}$ = –90.6 (*c* 0.5, $CHCl_3$). Racemic compound *rac*-**5** was synthesized from *rac*-**2** in 92% isolated yield.

Synthesis of 6. A mixture of (S_p)-**5** (1.31 g, 2.22 mmol), $Pd_2(dba)_3$ (0.203 g, 0.222 mmol), *t*-$Bu_3P\cdot HBF_4$ (0.258 g, 0.888), CuI (0.085 g, 0.44 mmol), THF (25 mL) and Et_3N (25 mL) was placed in a round-bottom flask equipped with a magnetic stirring bar. After degassing the reaction mixture several times, trimethylsilylacetylene (3.14 mL, 22.2 mmol) was added to the mixture via a syringe. The reaction was carried out at 50 °C for 17 h with stirring. After the reaction mixture was cooled to room temperature, precipitates were removed by filtration, and the solvent was removed with a rotary evaporator. The residue was purified by column chromatography on SiO_2 ($CHCl_3$/hexane = 1/9 v/v as an eluent) to afford (S_p)-**6** (1.18 g, 1.83 mmol, 83%) as a light brown solid. R_f = 0.26 ($CHCl_3$/hexane = 1/9 v/v). ^{1}H NMR ($CDCl_3$, 400 MHz) δ 0.30 (s, 9H), 0.31 (s, 9H), 0.32 (s, 9H), 2.82-2.98 (m, 4H), 3.22-3.27 (m, 1H), 3.39-3.46 (m, 3H), 6.76 (s, 1H), 6.87 (s, 1H), 6.99 (s, 1H), 7.10 (s, 1H) ppm; ^{13}C NMR ($CDCl_3$, 100 MHz) δ −0.18, −0.06, −0.05, 29.3, 31.9, 31.9, 32.4, 99.8, 100.4, 100.5, 103.1, 104.1, 104.1, 118.7 (q, J_{C-F} = 320 Hz), 124.4, 125.4, 125.4, 125.6, 131.9, 134.4, 134.9, 136.7, 142.0, 142.0, 145.6, 148.1 ppm. HRMS (FAB) calcd. for $C_{32}H_{40}O_3F_3Si_3S$ $[M+H]^+$: 645.1958, found: 645.1940. Elemental analysis calcd. for $C_{32}H_{39}O_3F_3Si_3S$: C 59.59 H 6.10, found: C 59.54 H 6.04. (R_p)-**6** and *rac*-**6** were obtained by the same procedure in 90% and 63% isolated yields, respectively. (S_p)-**6**: $[\alpha]^{23}_{D}$ = −24.9 (*c* 0.5, $CHCl_3$). (R_p)-**6**: $[\alpha]^{23}_{D}$ = +28.9 (*c* 0.5, $CHCl_3$).

Synthesis of 7. A mixture of (S_p)-**6** (1.18 g, 1.83 mmol), $PdCl_2(dppf)\cdot CH_2Cl_2$ (0.300 g, 0.367 mmol), CuI (0.070 g, 0.37 mmol), THF (20 mL), and Et_3N (20 mL) was placed in a round-bottom flask equipped with a magnetic stirring bar. After degassing the reaction mixture several times, trimethylsilylacetylene (2.59 mL, 18.3 mmol) was added to the mixture via a syringe. The reaction was carried out at 50 °C for 12 h. After the reaction mixture was cooled to room temperature, precipitates were removed by filtration, and the solvent was evaporated. The residue was purified by column chromatography on SiO_2 ($CHCl_3$/hexane = 1/9 v/v as an eluent) to afford (S_p)-**7** (0.769 g, 1.30 mmol, 71%) as a pale yellow crystal. The NMR data were matched with the literature's value.[11] R_f = 0.35 ($CHCl_3$/hexane = 1/9 v/v). HRMS (ESI) calcd. for $C_{36}H_{49}Si_4$ $[M+H]^+$: 593.2906, found: 593.2906. (R_p)-**7** was obtained by the same procedure in 76% isolated yield. Racemic compound *rac*-**7** was obtained by the same procedure, and

used for the next reaction to prepare *rac*-**8** without purification. (S_p)-**7**: $[\alpha]^{23}_D$ = −59.4 (*c* 0.5, $CHCl_3$). (R_p)-**7**: $[\alpha]^{23}_D$ = +59.4 (*c* 0.5, $CHCl_3$).

Synthesis of 8. K_2CO_3 (1.08 g, 7.77 mmol) was added to a suspension of (S_p)-**7** (0.769 g, 1.30 mmol) in MeOH (40 mL). After the mixture was stirred for 12 h at room temperature, H_2O was added to the reaction mixture. The organic layer was extracted with $CHCl_3$ and washed with brine. The combined organic layer was dried over $MgSO_4$. $MgSO_4$ was removed by filtration, and the solvent was evaporated. The residue was purified by column chromatography on SiO_2 ($CHCl_3$/hexane = 1/4 v/v as an eluent) to afford (S_p)-**8** (0.360 g, 1.18 mmol, 91%) as a colorless crystal. The NMR data were matched with the literature's value.[11] R_f = 0.17 ($CHCl_3$/hexane = 1/9 v/v). HRMS (EI) calcd. for $C_{24}H_{15}$ $[M-H]^+$: 303.1168, found 303.1172. (R_p)-**8** was obtained by the same procedure in 91% isolated yield. Racemic compound *rac*-**8** was obtained by the same procedure in 94% isolated yield (from *rac*-**6**). (S_p)-**8**: $[\alpha]^{23}_D$ = +141.6 (*c* 0.5, $CHCl_3$). (R_p)-**8**: $[\alpha]^{23}_D$ = −146.0 (*c* 0.5, $CHCl_3$).

Scheme 2. Synthesis of **s3**

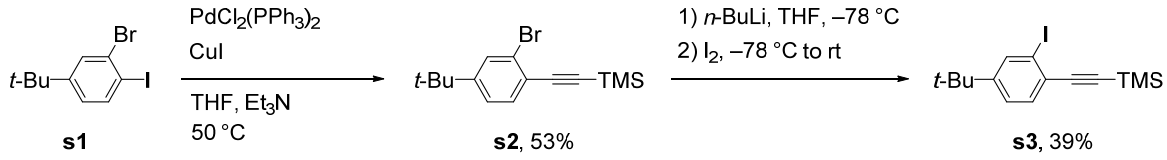

Synthesis of s3. 2-Bromo-4-*tert*-butyl-1-iodobenzene (**s1**) was prepared according to the literature.[21] A mixture of **s1** (3.73g, 11.0 mmol), $PdCl_2(PPh_3)_2$ (0.386 g, 0.550 mmol), CuI (0.105 g, 0.550 mmol), THF (45 mL), and Et_3N (15 mL) was placed in a round-bottom flask equipped with a magnetic stirring bar. After degassing the reaction mixture several times, trimethylsilylacetylene (1.71 mL, 12.1 mmol) was added to the mixture via a syringe. The reaction was carried out at room temperature. After the reaction for 6 h, precipitates were removed by filtration, and the solvent was evaporated. The residue was purified by column chromatography on SiO_2 (R_f = 0.34, hexane as an eluent) to afford **s2** (1.79 g, 5.79 mmol, 53%) as a pale yellow oil. The product **s2** was used for the next reaction without further purification. A solution of *n*-BuLi (1.65 M in hexane, 3.98 mL, 6.57 mmol) was slowly added to a solution of **s2** (1.79 g, 5.79 mmol) in THF (40 mL) at −78 °C. After 15 min, a solution of iodine (2.20 g, 8.69 mmol) in THF (20 mL) was added and the mixture was stirred for 1 h at −78 °C to room temperature. The reaction mixture was quenched by the addition of aqueous $NaHSO_3$ solution and the organic layer was extracted three times with hexane. The combined organic layer was washed with

brine and dried over $MgSO_4$. $MgSO_4$ was removed by filtration, and the solvent was evaporated. The residue was purified by column chromatography on SiO_2 (R_f = 0.39, hexane as an eluent) to afford **s3** (0.811 g. 2.28 mmol, 39%) as a light yellow oil. ^{1}H NMR ($CDCl_3$, 400 MHz) δ 0.27 (s, 9H), 1.28 (s, 9H), 7.29 (dd, *J* = 8.1 Hz, 2.0 Hz, 1H), 7.38 (d, *J* = 8.1 Hz, 1H), 7.82 (d, *J* = 1.7 Hz, 1H) ppm; ^{13}C NMR ($CDCl_3$, 100 MHz) δ −0.1, 31.0, 34.7, 97.8, 101.4, 196.7, 125.0, 126.7, 132.24, 135.8, 153.4 ppm. HRMS (EI) calcd. for $C_{15}H_{21}ISi$ $[M]^+$: 356.0457, found: 356.0464. Elemental analysis calcd. for $C_{15}H_{21}ISi$: C 50.56 H 5.94, found: $C_{15}H_{21}ISi$: C 50.78; H 5.72.

Synthesis of 9. A mixture of (S_p)-**8** (20 mg, 0.0657 mmol), **s3** (103.0 mg, 0.289 mmol), $Pd_2(dba)_3$ (6.0 mg, 0.066 mmol), dppf (7.3 mg, 0.013 mmol), CuI (2.5 mg, 0.013 mmol), THF (2 mL), and Et_3N (2 mL) was placed in a round-bottom flask equipped with a magnetic stirring bar. After degassing the reaction mixture several times, the reaction was carried out at 50 °C for 64 h. After the reaction mixture was cooled to room temperature, precipitates were removed by filtration, and the solvent was evaporated. The residue was purified by column chromatography on SiO_2 ($CHCl_3$/hexane = 1/3 v/v as an eluent) to afford (S_p)-**9** (71.0 mg, 0.0583 mmol, 89%) as a light yellow solid. R_f = 0.20 ($CHCl_3$/hexane = 1/4 v/v). ^{1}H NMR ($CDCl_3$, 400 MHz) δ 0.21 (s, 36H), 1.27 (s, 36H), 3.19-3.26, (m, 4H), 3.71-3.78 (m, 4H), 7.29 (dd, *J* = 8.3 Hz, 2.0 Hz, 4H), 7.35 (s, 4H), 7.46 (d, *J* = 8.3 Hz, 4H), 7.56 (d, *J* = 2.0 Hz, 4H) ppm; ^{13}C NMR ($CDCl_3$, 100 MHz) δ 0.1, 31.0, 32.7, 34.7, 92.4, 93.7, 97.6, 104.2, 122.5, 125.2, 125.4, 125.7, 129.3 (d, *J* = 9.9 Hz), 132.8, 135.3 (d, *J* = 9.9 Hz), 142.0, 151.6 ppm. HRMS (ESI) calcd. for $C_{84}H_{97}Si_4$ $[M+H]^+$: 1217.6662, found 1217.6694. Elemental analysis calcd. for $C_{84}H_{96}Si_4$: C 82.83 H 7.94, found: C 82.74 H 7.78. (R_p)-**9** and *rac*-**9** were obtained by the same procedure in 77% and 67% isolated yields, respectively. (S_p)-**9**: $[\alpha]^{23}_D$ = +44.1 (*c* 0.5, $CHCl_3$). (R_p)-**9**: $[\alpha]^{23}_D$ = −45.4 (*c* 0.5, $CHCl_3$).

Synthesis of 10. K_2CO_3 (28.4 mg, 0.205 mmol) and $Cu(OAc)_2$ (148.9 mg, 0.820 mmol) were added to a solution of (S_p)-**9** (25.0 mg, 0.0205 mmol) in MeOH (50 mL) and CH_3CN (50 mL). The mixture was heated at reflux temperature for 37 h. After the reaction mixture was cooled to room temperature, aqueous NH_3 (28%) was added to the reaction mixture, and the organic layer was extracted three times with CH_2Cl_2. The combined organic layer was washed with brine and dried over $MgSO_4$. $MgSO_4$ was removed by filtration, and the solvent was evaporated. The residue was purified by column chromatography on SiO_2 (eluent: $CHCl_3$/hexane = 1/1 v/v). Further purification was carried out by HPLC and recrystallization with $CHCl_3$ and MeOH (good and poor solvent, respectively) to afford (S_p)-**10** (7.5 mg, 0.0081 mmol, 40%) as a yellow solid. R_f = 0.25 ($CHCl_3$/hexane = 1/4 v/v). ^{1}H NMR ($CDCl_3$, 400 MHz) δ 1.34 (s, 36H), 3.13-3.21 (m, 4H), 3.57-3.65, (m, 4H), 7.22 (s, 4H), 7.35 (dd, *J* = 8.3 Hz,

2.0 Hz, 4H), 7.46 (d, J = 8.0 Hz, 4H), 7.54 (d, J = 2.0 Hz, 4H) ppm; ^{13}C NMR ($CDCl_3$, 100 MHz) δ 31.1, 33.3, 35.0, 78.2, 81.9, 92.5, 93.3, 121.3, 124.3, 125.5, 128.1, 129.1, 130.8, 133.9, 143.0, 152.4 ppm. HRMS (FAB) calcd. for $C_{72}H_{60}$ $[M]^+$: 924.4695 found 924.4712. (R_p)-**10** and *rac*-**10** were obtained by the same procedure in 71% and 58% isolated yields, respectively. (S_p)-**10**: $[\alpha]^{23}_D$ = −1494.9 (*c* 0.5, $CHCl_3$). (R_p)-**10**: $[\alpha]^{23}_D$ = +1501.0 (*c* 0.5, $CHCl_3$).

X-ray crystal structure analysis of *rac*-10. The intensity data were collected on a Rigaku Saturn70 CCD with VariMax Mo Optic using MoKα radiation (λ = 0.71070 Å). Single crystals of $[C_{72}H_{60}(H_2O)_4]$ suitable for X-ray analysis were obtained by slow recrystallization from $CHCl_3$/MeOH. A single crystal was mounted on a glass fiber. The structures were solved by direct methods (SHELXS-97) and refined by full-matrix least-squares procedures on F^2 for all reflections (SHELXL-97).[22] The solvated H_2O molecules in the unit cell were found to be severely disordered. The coordinates of the hydrogen atoms of the H_2O molecules were fixed as ideal positions, and Uij of the oxygen atoms were restricted with ISOR instruction. All of Alerts A and B pointed out by Check-Cif systems would be due to the severe disorder of H_2O molecules, which could not be perfectly resolved because of the low quality of the obtained crystals. However, the author believes the analysis has been well done with sufficient accuracy. All hydrogen atoms other than those of H_2O molecules were placed using AFIX instructions, while all other atoms were refined anisotropically.

References and Notes

(1) (a) *Cyclophane Chemistry: Synthesis, Structures and Reactions*; Vögtle, F., Ed.; John Wiley & Sons: Chichester, 1993. (b) *Modern Cyclophane Chemistry*; Gleiter, R., Hopf, H., Eds.; Wiley-VCH: Weinheim, 2004.

(2) (a) Cram, D. J.; Allinger, N. L. *J. Am. Chem. Soc.* **1955**, *77*, 6289–6294. (b) Rozenberg, V.; Sergeeva, E.; Hopf, H. *In Modern Cyclophane Chemistry*, Gleiter, R.; Hopf, H., Eds.; Wiley-VCH: Weinheim, 2004; pp 435–462. (c) Rowlands, G. *J. Org. Biomol. Chem.* **2008**, *6*, 1527–1534. (d) Gibson, S. E.; Knight, J. D. *Org. Biomol. Chem.* **2003**, *1*, 1256–1269. (e) Aly, A. A.; Brown, A. B. *Tetrahedron* **2009**, *65*, 8055–8089. (f) Paradies, J. *Synthesis* **2011**, 3749–3766.

(3) For optical resolution of pseudo-*ortho*-disubstituted [2.2]paracyclophane, see: (a) Pye, P. J.; Rossen, K.; Reamer, R. A.; Tsou, N. N.; Volante, R. P.; Reider, P. J. *J. Am. Chem. Soc.* **1997**, *119*, 6207–6208. (b) Rossen, K.; Pye, P. J.; Maliakal, A.; Volante, R. P. *J. Org. Chem.* **1997**, 62, 6462–6463. (c) Zhuravsky, R.; Starikova, Z.; Vorontsov, E.; Rozenberg, V. *Tetrahedron: Asymmetry* **2008**, *19*, 216–222. (d) Jiang, B.; Zhao, X.-L. *Tetrahedron: Asymmetry* **2004**, *15*, 1141–1143. (e) Jones, P. G.; Hillmer, J.; Hopf, H. *Acta Crystallogr.* **2003**, E59, o24–o25. (f) Pamperin, D.; Hopf, H.; Syldatk, C.; Pietzsch, M. *Tetrahedron: Asymmetry* **1997**, *8*, 319–325. (g) Pamperin, D.; Ohse, B.; Hopf, H.; Pietzsch, M. *J. Mol. Catal. B: Enzymatic* **1998**, *5*, 317–319. (h) Braddock, D. C.; MacGilp, I. D.; Perry, B. G. *J. Org. Chem.* **2002**, *67*, 8679–8681. (i) Morisaki, Y.; Hifumi, R.; Lin, L.; Inoshita, K.; Chujo, Y. *Chem. Lett.* **2012**, *41*, 990–992. (j) Meyer-Eppler, G.; Vogelsang, E.; Benkhäuser, C.; Schneider, A.; Schnakenburg, G.; Lützen, A. *Eur. J. Org. Chem.* **2013**, 4523–4532.

(4) Optical resolution of *rac*-4,5,15,16-tetrasubstituted [2.2]paracyclophane was reported: Vorontsova, N. V.; Rozenberg, V. I.; Sergeeva, E. V.; Vorontsov, E. V.; Starikova, Z. A.; Lyssenko, K. A.; Hopf, H. *Chem.–Eur. J.* **2008**, 14, 4600–4617.

(5) Hopf, H. *Angew. Chem., Int. Ed.* **2008**, *47*, 9808–9812.

(6) *Carbon-Rich Compounds*; Haley, M. M.; Tykwinski, R. R., Eds.; Wiley-VCH: Weinheim, 2006.

(7) Review on chiral carbon-rich macrocycles: Campbell, K.; Tykwinski, R. R. *In Carbon-Rich Compounds: From Molecules to Materials*; Haley, M. M.; Tykwinski, R. R., Eds.; Wiley-VCH: Weinheim, 2006; pp 229–294.

(8) Chow, H.-F.; Low, K.-H.; Wong, K. Y. *Synlett* **2005**, 2130–2134.

(9) Diastereomer ratio was determined by HPLC.

(10) (a) Tohda, Y.; Sonogashira, K.; Hagihara, N. *Tetrahedron Lett.* **1975**, 16, 4467–4470. (b) Sonogashira, K. In *Handbook of Organopalladium Chemistry for Organic Synthesis*; Negishi, E., Ed.; Wiley-Interscience: New York, 2002; pp 493–529.

(11) Bondarenko, L.; Dix, I.; Hinrichs, H.; Hopf, H. *Synthesis* **2004**, 2751–2759.

(12) Hinrichs, H.; Boydston, A. J.; Jones, P. G.; Hess, K.; Herges, R.; Haley, M. M.; Hopf, H. *Chem.–Eur. J.* **2006**, *12*, 7103–7115.

(13) Schultz, A.; Li, X.; Barkakaty, B.; Moorefield, C. N.; Wesdemiotis, C.; Newkome, G. R. *J. Am. Chem. Soc.* **2012**, *134*, 7672–7675.

(14) Theoretical Cotton effect patterns were also identical.

(15) Electronic delocalization between chromophores connected to [2.2]paracyclophane has been elucidated by Bazan and co-workers: (a) Wang, S.; Bazan, G. C.; Tretiak, S.; Mukamel, S. *J. Am. Chem. Soc.* **2000**, *122*, 1289–1297. (b) Bartholomew, G. P.; Bazan, G. C. *Acc. Chem. Res.* **2001**, *34*, 30–39. (c) Bartholomew, G. P.; Bazan, G. C. *Synthesis* **2002**, 1245–1255. (d) Hong, J. W.; Woo, H. Y.; Bazan, G. C. *J. Am. Chem. Soc.* **2005**, 127, 7435–7443. (e) Bazan, G. C. *J. Org. Chem.* **2007**, *72*, 8615–8635.

(16) (a) For bridged triarylamine helicene ($g_{lum} = 1.1 \times 10^{-3}$): Field, J. E.; Muller, G.; Riehl, J. P.; Venkataraman, D. *J. Am. Chem. Soc.* **2003**, *125*, 11808–11809. (b) For perylene-diimide-substituted binaphthyl ($g_{lum} = 3 \times 10^{-3}$): Kawai, T.; Kawamura, K.; Tsumatori, H.; Ishikawa, M.; Naito, M.; Fujiki, M.; Nakashima, T. *ChemPhysChem* **2007**, *8*, 1465–1468. (c) Tsumatori, H.; Nakashima, T.; Kawai, T. *Org. Lett.* **2010**, *12*, 2362–2365. (d) For phthalhydrazide-functionalized helicene ($g_{lum} = 2.1 \times 10^{-2}$): Kaseyama, T.; Furumi, S.; Zhang, X.; Tanaka, K.; Takeuchi, M. *Angew. Chem., Int. Ed.* **2011**, *50*, 3684–3687. (e) For BINOL-containing dipyrrolyl diketone with anion responsibility ($g_{lum} = 2 \times 10^{-3}$): Maeda, H.; Bando, Y.; Shimomura, K.; Yamada, I.; Naito, M.; Nobusawa, K.; Tsumatori, H.; Kawai, T. *J. Am. Chem. Soc.* **2011**, 133, 9266–9269. (f) For helical π-conjugated-receptor-anion complex ($g_{lum} = 1.3 \times 10^{-2}$): Haketa, Y.; Bando, Y.; Takaishi, K.; Uchiyama, M.; Muranaka, A.; Naito, M.; Shibaguchi, H.; Kawai, T.; Maeda, H. *Angew. Chem., Int. Ed.* **2012**, *51*, 7967–7971. (g) For helically chiral bitriphenylene ($g_{lum} = 3.2 \times 10^{-2}$): Sawada, Y.; Furumi, S.; Takai, A.; Takeuchi, M.; Noguchi, K.; Tanaka, K. *J. Am. Chem. Soc.* **2012**, *134*, 4080–4083. (h) For sila[7]helicene ($g_{lum} = 3.5 \times 10^{-3}$): Oyama, H.; Nakano, K.; Harada, T.; Kuroda, R.; Naito, M.; Nobusawa, K.; Nozaki, K. *Org. Lett.* **2013**, *15*, 2104–2107. (i) Review, see: Maeda, H.; Bando, Y. *Pure Appl. Chem.* **2013**, *85*, 1967–1978.

(17) The g_{lum} values of (R_p)- and (S_p)-**9** were sufficiently large, $|g_{lum}| = 1.2\text{-}1.3 \times 10^{-3}$.

(18) No thermochromism and solvatochromism were observed in UV, CD, PL, and CPL spectra for **10** as well as **9**.

(19) Pangborn, A. B.; Giardello, M. A.; Grubbs, R. H.; Rosen, R. K.; Timmers, F. J. *Organometallics* **1996**, *15*, 1518–1520.

(20) Lee, S. H.; Jang, B.-B.; Kafafi, Z. H. *J. Am. Chem. Soc.* **2005**, *127*, 9071–9078.

(21) Chen, T.-A.; Liu, R.-S. *Chem.–Eur. J.* **2011**, *17*, 8023–8027.

(22) (a) Sheldrick, G. M. Acta Crystallogr. Sect. A **1990**, *46*, 467. (b) Sheldrick, G. M. SHELX-97 Program for Crystal Structure Solution and the Refinement of Crystal Structures, Institüt für Anorganische Chemie der Universität Göttingen, Tammanstrasse 4, D-3400 Göttingen, Germany, 1997.

Chapter 4

Optically Active Cyclic Compounds Based on Planar Chiral [2.2]Paracyclophane: Extension of the Conjugated Systems and Chiroptical Properties

Abstract

A series of optically active cyclic compounds based on the planar chiral tetrasubstituted [2.2]paracyclophane core were synthesized to obtain luminescent materials with excellent chiroptical properties in both the ground and excited states. The obtained cyclic compounds were composed of the optically active propeller-shaped structures created by the [2.2]paracyclophane core with *p*-phenylene-ethynylene moieties. The compounds exhibited good optical profiles, with a large molar extinction coefficient (ε) and photoluminescence quantum efficiency (Φ_{lum}). The emission occurred mainly from the propeller-shaped cyclic structures. This optically active higher-ordered structure provided chiroptical properties of high performance, such as a large specific rotation ($[\alpha]_D$) and molar ellipticity ($[\theta]$) in the ground state and intense circularly polarized luminescence (CPL) with large dissymmetry factors (g_{lum}) in the excited state. The results suggest that planar chiral [2.2]paracyclophane-based optically active higher-ordered structures, such as the propeller-shaped cyclic structure, are promising scaffolds for obtaining CPL and that appropriate modifications can enhance the CPL characteristics.

Introduction

The importance of conjugated compounds has been increasing owing to their conductive, luminescent, and charge transfer properties, leading to their potential applications in various opto-electronic devices.[1] Both industrial and academic researchers have extensively studied the design and construction of novel conjugated systems. [2.2]Paracyclophane is a typical cyclophane compound containing two stacked phenylenes in close proximity. This compound was first prepared by Brown and Farthing in 1949 by pyrolysis of *p*-xylene.[2] In 1951, Cram and Steinberg reported its direct synthesis by a Wurtz-type intramolecular cyclization of 1,4-bis(bromomethyl)benzene.[3] Since then, considerable attention has been paid in the field of organic chemistry to the synthesis, reactivity, and opto-electronic properties of this unique conjugated system.[4]

One of the interesting features of [2.2]paracyclophane compounds is undoubtedly the π-π interactions between the stacked aromatic rings, as well as the resulting stacked π-electron systems. Bazan, Mukamel, and co-workers reported the characteristic optical properties of 4,12-disubstituted and 4,7,12,15-tetrasubstituted [2.2]paracyclophane compounds.[5] They disclosed that the stacked position of the two π-electron systems affects the conjugation system in the ground and excited states. In particular, the two stacked π-electron systems found in the 4,7,12,15-tetrasubstituted [2.2]paracyclophane skeleton, *i.e.* interchromophore interactions between the two π-electron systems, exhibit strong through-space conjugation in addition to the common through-bond conjugation.[5b,d,e,i,j] Hopf, Haley, and co-workers synthesized cyclic compounds that have an propeller-shaped structure based on the 4,7,12,15-tetrasubstituted [2.2]paracyclophane unit.[6]

The stacked structures of [2.2]paracyclophanes result in three-dimensional molecules. In Chapter 3, inspired by the synthesis of the propeller-shaped cyclic compounds based on 4,7,12,15-tetrasubstituted [2.2]paracyclophane and its unique π-conjugation system, the author

attempted to introduce chirality into this cyclic structure.[7] Some [2.2]paracyclophanes with substituents are planar chiral compounds due to the suppression of the rotary motion of the phenylenes.[8] The author achieved optical resolution of 4,7,12,15-tetrasubstituted [2.2]paracyclophane compounds[7,9] using the diastereomer method, followed by transformation to obtain the enantiopure precursors (R_p)- and (S_p)-**3Ph** and the propeller-shaped cyclic compounds (R_p)- and (S_p)-**3PhC** (Figure 1).[7] It should be noted that the obtained optically active cyclic compounds exhibited intense circularly polarized luminescence (CPL)[10] with a large dissymmetry factor (g_{lum}) on the order of 10^{-2}.

Further development of planar chiral [2.2]paracyclophane-based optically active compounds is expected to afford luminescent materials with excellent chiroptical properties in both the ground and excited states. In this chapter, the author focused his attention on the propeller-shaped skeleton containing the planar chiral tetrasubstituted [2.2]paracyclophane core. To obtain superior CPL emitters, the author designed cyclic compounds with extended π-conjugation moieties; herein, the synthesis and optical properties of these compounds are discussed.

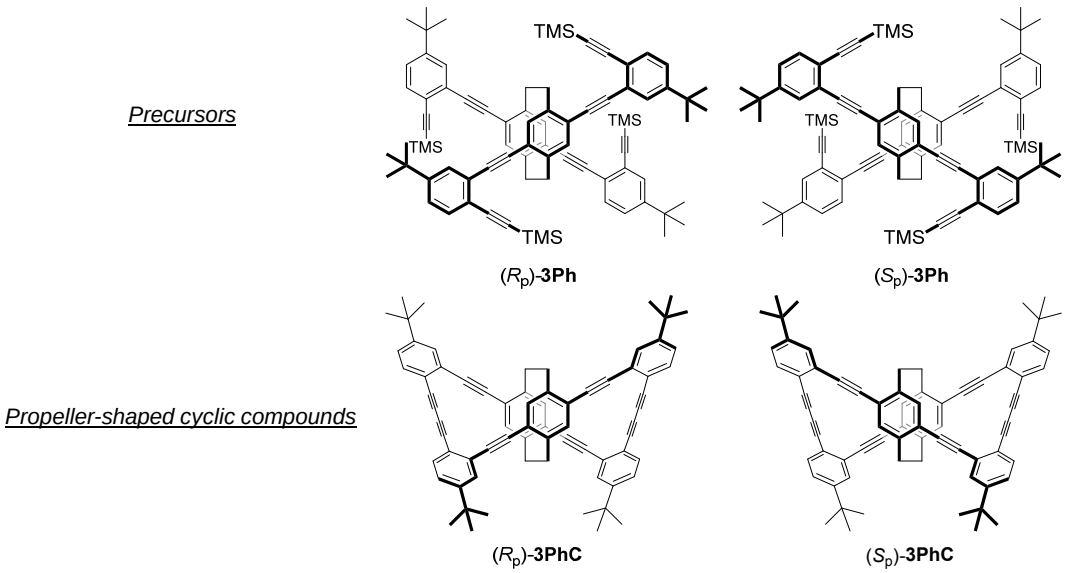

Figure 1. Precursors and the corresponding propeller-shaped cyclic compounds.

Results and Discussion

Synthesis

The optical resolution of planar chiral 4,7,12,15-tetrasubstituted [2.2]paracyclophane was carried out using the diastereomer method developed in Chapter 3, and the obtained enantiopure compounds were converted to the corresponding (R_p)- and (S_p)-4,7,12,15-tetraethynyl[2.2]paracyclophanes.[7] The synthetic routes to the target optically active cyclic compounds are shown in Schemes 1-4. Initially, the author prepared phenylene-ethynylene compounds **4** and **11** as arm units for light-harvesting moieties (Schemes 1 and 2, respectively). The *tert*-butyl groups in **4** and **11** were introduced to provide the target compounds with solubility in organic solvents, such as THF, $CHCl_3$, CH_2Cl_2, and toluene; in particular, two *tert*-butyl groups were required in **11** to dissolve the extended π-conjugation system of this cyclic compound in these solvents.

As shown in Scheme 1, 4-*tert*-butylethynylbenzene **1** was reacted with 2-bromo-4-iodoaniline in the presence of a catalytic amount of $PdCl_2(PPh_3)_2$ to obtain compound **2** in 89% isolated yield; this reaction occurred chemoselectively at the iodine substituent of **2**. Sonogashira-Hagihara coupling[11] of **2** with trimethylsilylacetylene (TMS-acetylene) afforded compound **3** in 59% isolated yield. The amino group in **3** was converted to an iodo group using the Sandmeyer reaction[12] to obtain compound **4** in 61% isolated yield.

The chemoselective Sonogashira-Hagihara coupling of 3,5-di(*tert*-butyl)ethynylbenzene **5** with *p*-iodobromobenzene afforded compound **6** in 68% isolated yield (Scheme 2). The successive Sonogashira-Hagihara coupling of **6** with TMS-acetylene gave compound **7** in 80% isolated yield. The TMS group in **7** was readily removed by the reaction with K_2CO_3/MeOH to prepare compound **8** quantitatively. Compound **8** was reacted with 2-bromo-4-iodoaniline in the same manner as described for compound **1** (Scheme 1); successive Sonogashira-Hagihara coupling with TMS-acetylene to obtain compound **10** in 71% isolated yield and the

Scheme 1. Synthesis of compound **4** (arm unit for **5PhC**)

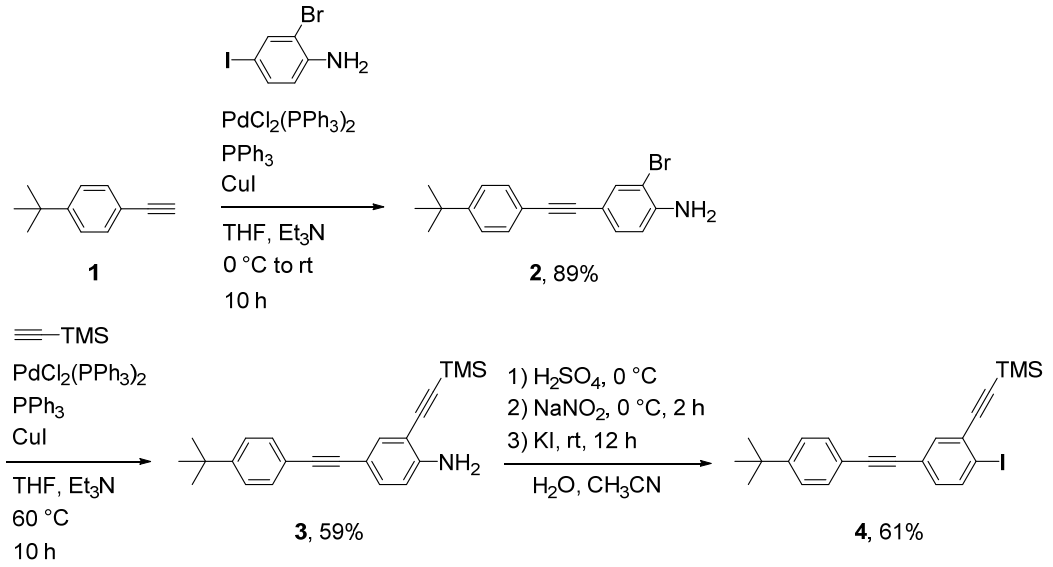

Scheme 2. Synthesis of compound **11** (arm unit for **7PhC**)

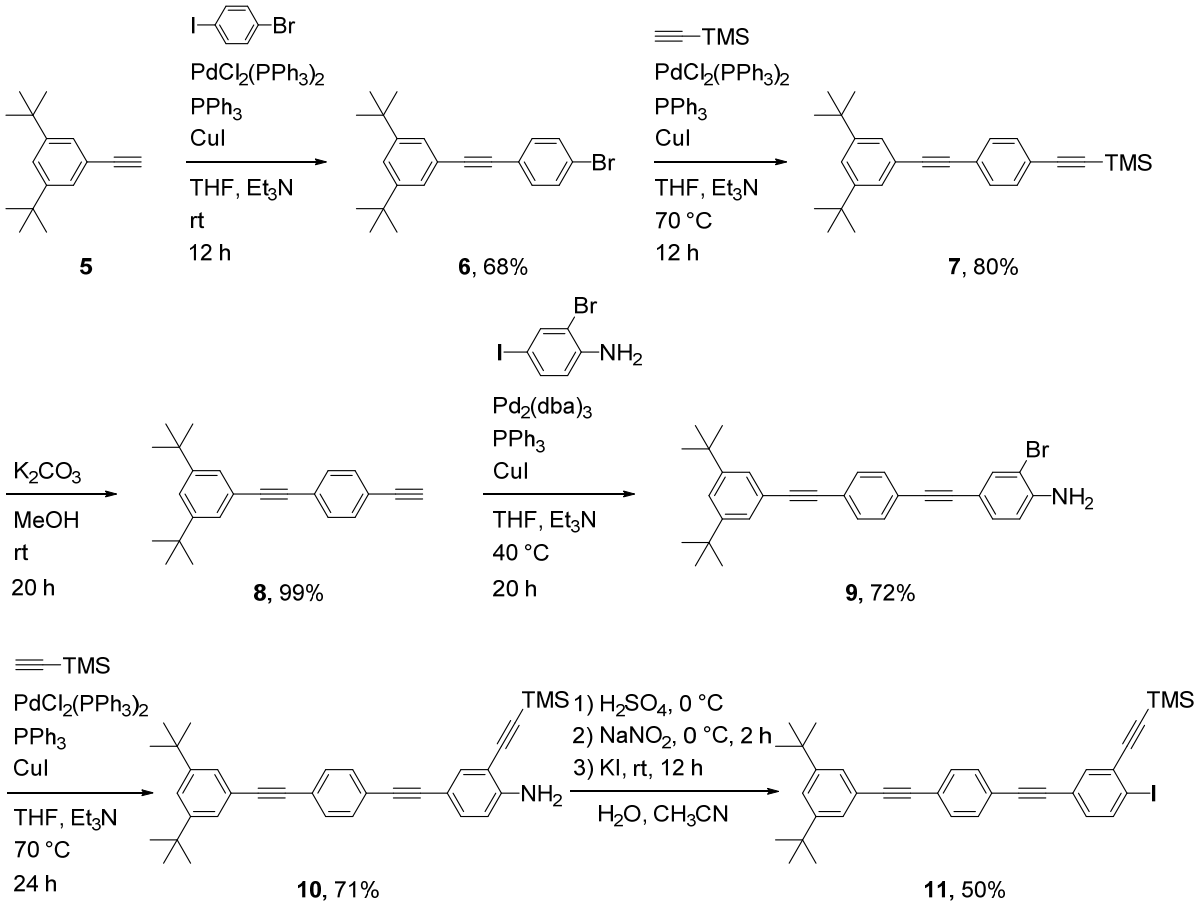

Sandmeyer reaction afforded the corresponding compound **11** in 50% isolated yield.

Schemes 3 and 4 show the syntheses of the target cyclic compounds **5PhC** and **7PhC**, respectively. In these Schemes, only the reactions of the (R_p)-isomers are shown in these reactions; the (S_p)-isomers were prepared under identical conditions from (S_p)-**12**. The treatment of (R_p)-4,7,12,15-tetraethynyl[2.2]paracyclophane (R_p)-**12** with compound **4** in the presence of the $Pd_2(dba)_3$/CuI catalytic system using di(1-adamantyl)-*n*-butylphosphine[13] (cataCXium® A) as a phosphine ligand afforded compound (R_p)-**5Ph** in 64% isolated yield (Scheme 3). After deprotection of the four TMS groups in (R_p)-**5Ph** using NBu_4F, a Pd-mediated alkyne coupling was carried out *in situ* to obtain cyclic compound (R_p)-**5PhC** in 18% isolated yield. Under the same reaction conditions, compounds (R_p)-**7Ph** and (R_p)-**7PhC** with the extended phenylene-ethynylene units were prepared by the reaction of **11** with (R_p)-**12**, as

Scheme 3. Synthesis of (R_p)-**5Ph** and (R_p)-**5PhC**

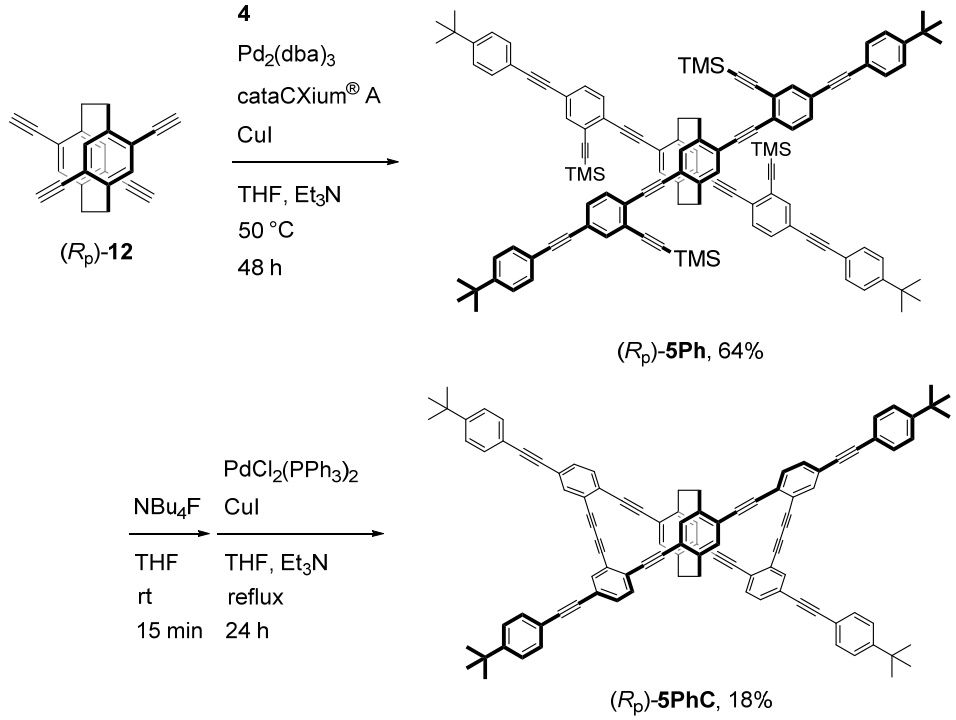

shown in Scheme 4. When cyclization was carried out, unidentified impurities such as oligomeric products by intermolecular reactions were formed. They could be readily removed by column chromatography on SiO_2, resulting in low isolated yields (18% and 30% for (R_p)-**5PhC** and (R_p)-**7PhC**, respectively). The structures of all new compounds in this study were confirmed by ^1H and ^{13}C NMR spectroscopy, high-resolution mass spectrometry (HRMS), and elemental analysis; the detailed synthetic procedures and NMR spectra data are shown in the experimental section.

Scheme 4. Synthesis of (R_p)-**7Ph** and (R_p)-**7PhC**

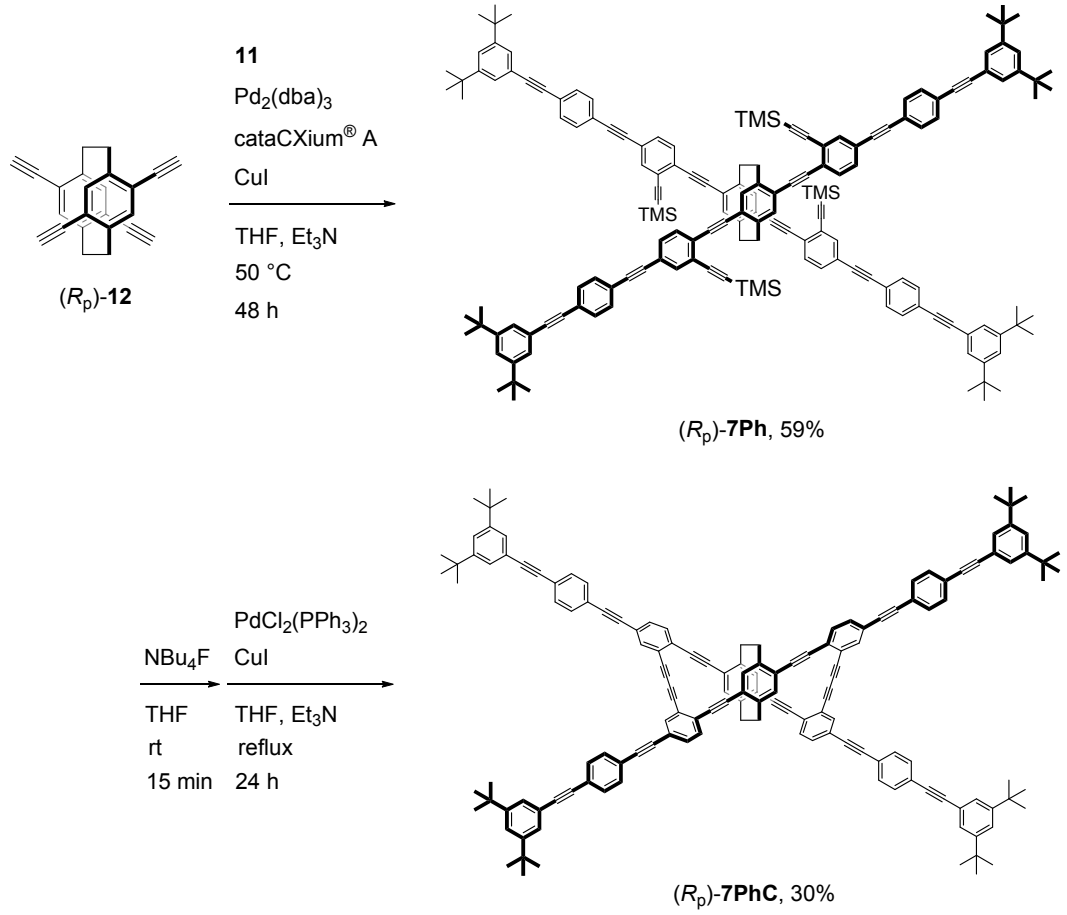

Optical Properties

The optical properties of both enantiomers of cyclic compounds **3PhC**, **5PhC**, and **7PhC** as well as their precursors **3Ph**, **5Ph**, and **7Ph** were evaluated. The data are summarized in Table 1. Although the optical and chiroptical properties of **3Ph** and **3PhC** were reported in Chapter 3, they are included herein for comparison.

Table 1. Optical properties: Spectroscopic data of (R_p)-isomers

	λ_{abs}[a]/nm (ε / 10^5 M^{-1} cm^{-1})	λ_{lum}[b]/nm	τ[c]/ns (χ^2)	Φ_{lum}[d]
(R_p)-**3Ph**	372 (0.44)	418	2.16 (1.04)	0.46
(R_p)-**5Ph**	398 (1.41)	438	1.05 (1.00)	0.80
(R_p)-**7Ph**	403 (1.79)	443	0.87 (1.00)	0.88
(R_p)-**3PhC**	314 (1.25), 391 (0.46)	453	3.75 (1.06)	0.41
(R_p)-**5PhC**	329 (2.16), 419 (1.06)	471	2.07 (1.01)	0.60
(R_p)-**7PhC**	355 (2.58), 422 (1.27)	474	2.00 (1.08)	0.70

[a] In $CHCl_3$ (1.0×10^{-5} M). [b] In $CHCl_3$ (1.0×10^{-6} M), excited at absorption maxima. [c] Emission life time at λ_{lum}. [d] Absolute PL quantum efficiency.

Figures 2A and B show the UV-vis absorption spectra and photoluminescence (PL) spectra of the (R_p)-precursors in the dilute $CHCl_3$ solutions (1.0×10^{-5} M for UV and 1.0×10^{-6} M for PL), respectively. The absorption spectra exhibited a hyperchromic effect and bathochromic shift with an extension of the π-conjugation length (Figure 2A). In the PL spectra (Figure 2B), a similar bathochromic shift was observed. The PL spectra of (R_p)-**5Ph** and (R_p)-**7Ph** exhibited vibrational structures, whereas that of (R_p)-**3Ph** was relatively broad; the same phenomena were observed in the case of *p*-phenylenevinylene-stacked [2.2]paracyclophane compounds reported previously by Bazan and co-workers.[5b,d,e,i,j] This result suggests that the excited energy migrates to the phane state[5] in (R_p)-**3Ph**; however, it is localized on the extended phenylene-ethynylene chromophores in (R_p)-**5Ph** and (R_p)-**7Ph**. Table 1 includes the PL decay data (PL lifetime (τ) and χ^2 parameters) for all compounds. Thus, it was supported by the shorter PL lifetimes of (R_p)-**5Ph** (τ = 1.05 ns) and (R_p)-**7Ph** (τ = 0.87 ns) than that of (R_p)-**3Ph** (τ = 2.16

ns); in other words, the PL of (R_p)-**5Ph** and (R_p)-**7Ph** occurred from the chromophore states[5] rather than the phane states.

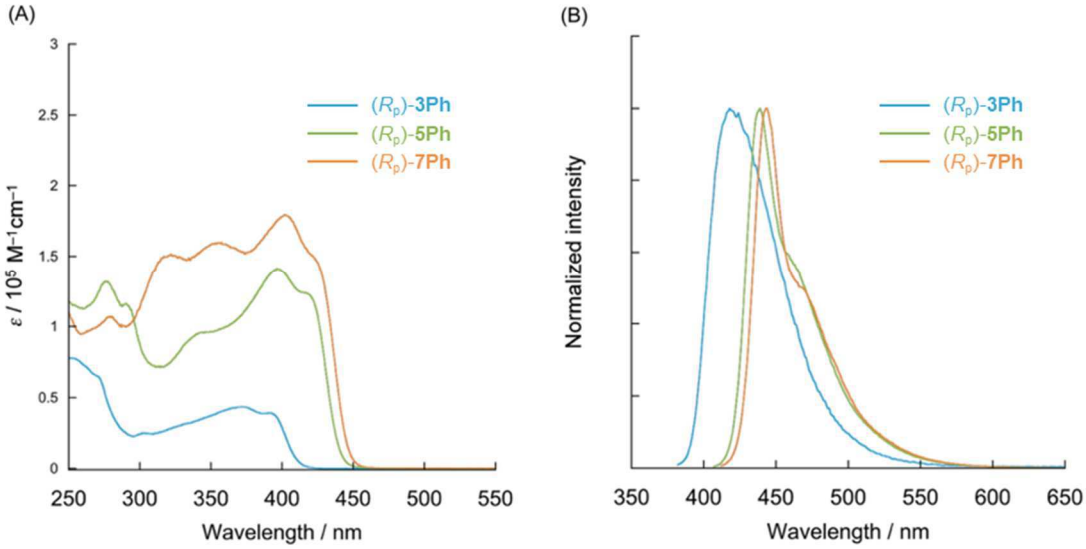

Figure 2. (A) UV-vis absorption spectra in the dilute $CHCl_3$ (1.0×10^{-5} M) and (B) PL spectra in the dilute $CHCl_3$ (1.0×10^{-5} M; excited at absorption maximum) of (R_p)-**3Ph**, (R_p)-**5Ph**, and (R_p)-**7Ph**.

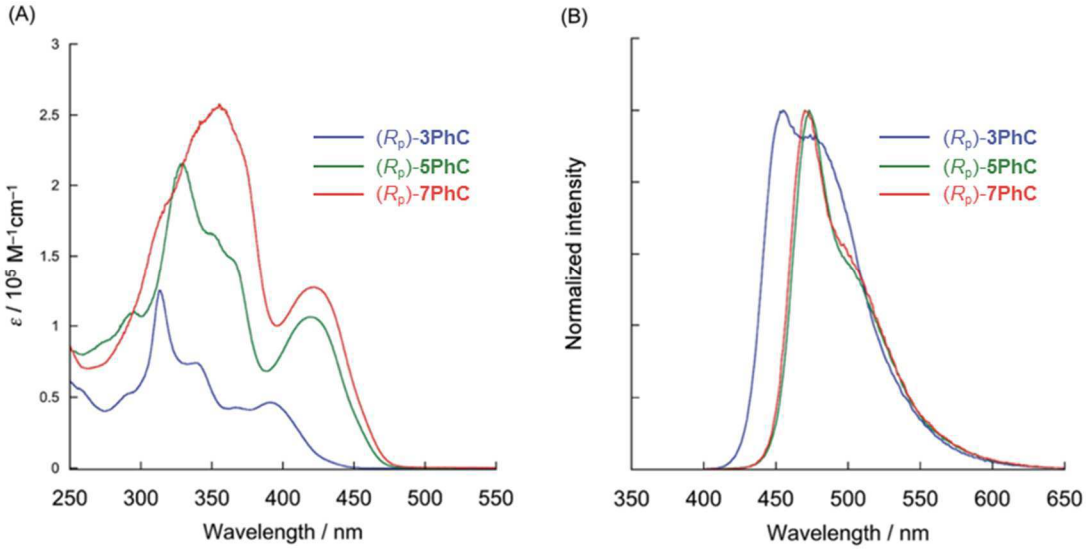

Figure 3. (A) UV-vis absorption spectra in the dilute $CHCl_3$ (1.0×10^{-5} M) and (B) PL spectra in the dilute $CHCl_3$ (1.0×10^{-5} M; excited at absorption maximum) of (R_p)-**3PhC**, (R_p)-**5PhC**, and (R_p)-**7PhC**.

As shown in Figures 3A and B, the same tendencies were observed in the absorption and PL spectra of cyclic compounds (R_p)-**3PhC**, (R_p)-**5PhC**, and (R_p)-**7PhC**. The absorption spectrum of (R_p)-**5PhC** exhibited a hyperchromic effect and was bathochromically shifted in comparison with that of (R_p)-**3PhC** (Figure 3A). Although the absorption spectrum of (R_p)-**7PhC** also showed a hyperchromic effect and was bathochromically shifted, the absorption bands of (R_p)-**5PhC** and (R_p)-**7PhC** near 425 nm were almost identical. As shown in Figure 3B, the PL spectra of (R_p)-**5PhC** and (R_p)-**7PhC** were identical and both exhibited vibrational structures. The absolute PL quantum efficiencies (Φ_{lum}) of (R_p)-**5PhC** and (R_p)-**7PhC** were determined to be 0.60 and 0.70, respectively. The lifetimes were lengthened by cyclization of the compounds and shortened by elongation of the conjugated systems. All compounds exhibited single exponential decay curves. The τ of (R_p)-**3PhC** was estimated to be 3.75 ns, which were longer than those of (R_p)-**5PhC** (τ = 2.07 ns) and (R_p)-**7PhC** (τ = 2.00 ns). In addition, the τ of (R_p)-**5PhC** and (R_p)-**7PhC** were identical, suggesting that the PL of (R_p)-**5PhC** and (R_p)-**7PhC** arose from similar emitting species.

Figure 4 shows the highest occupied molecular orbitals (HOMOs) and the lowest unoccupied molecular orbitals (LUMOs) of the cyclic compounds (R_p)-**3PhC**, (R_p)-**5PhC**, and (R_p)-**7PhC**; the molecular orbitals were obtained by density functional theory (DFT) at the TD-BHandHLYP/def2-TZVPP//BLYP/def2-TZVPP level. The longest wavelength absorption bands observed in the absorption spectra (Figure 3A) were assigned to the S_0 to S_1 transition (Figure 4); both the HOMO and LUMO are located mainly on the cyclic moieties of these compounds. The π-orbitals are somewhat extended to the *p*-phenylene-ethynylene arms in the HOMOs of (R_p)-**5PhC** and (R_p)-**7PhC**, whereas they were localized on the cyclic moieties in the LUMOs. As the π-conjugations of (R_p)-**5PhC** and (R_p)-**7PhC** did not extend to the LUMOs regardless of the length of the π-conjugated *p*-phenylene-ethynylenes, the properties of the

cyclic skeleton would predominately affect the absorption and emission, resulting in similar optical profiles observed for (R_p)-**5PhC** and (R_p)-**7PhC**.

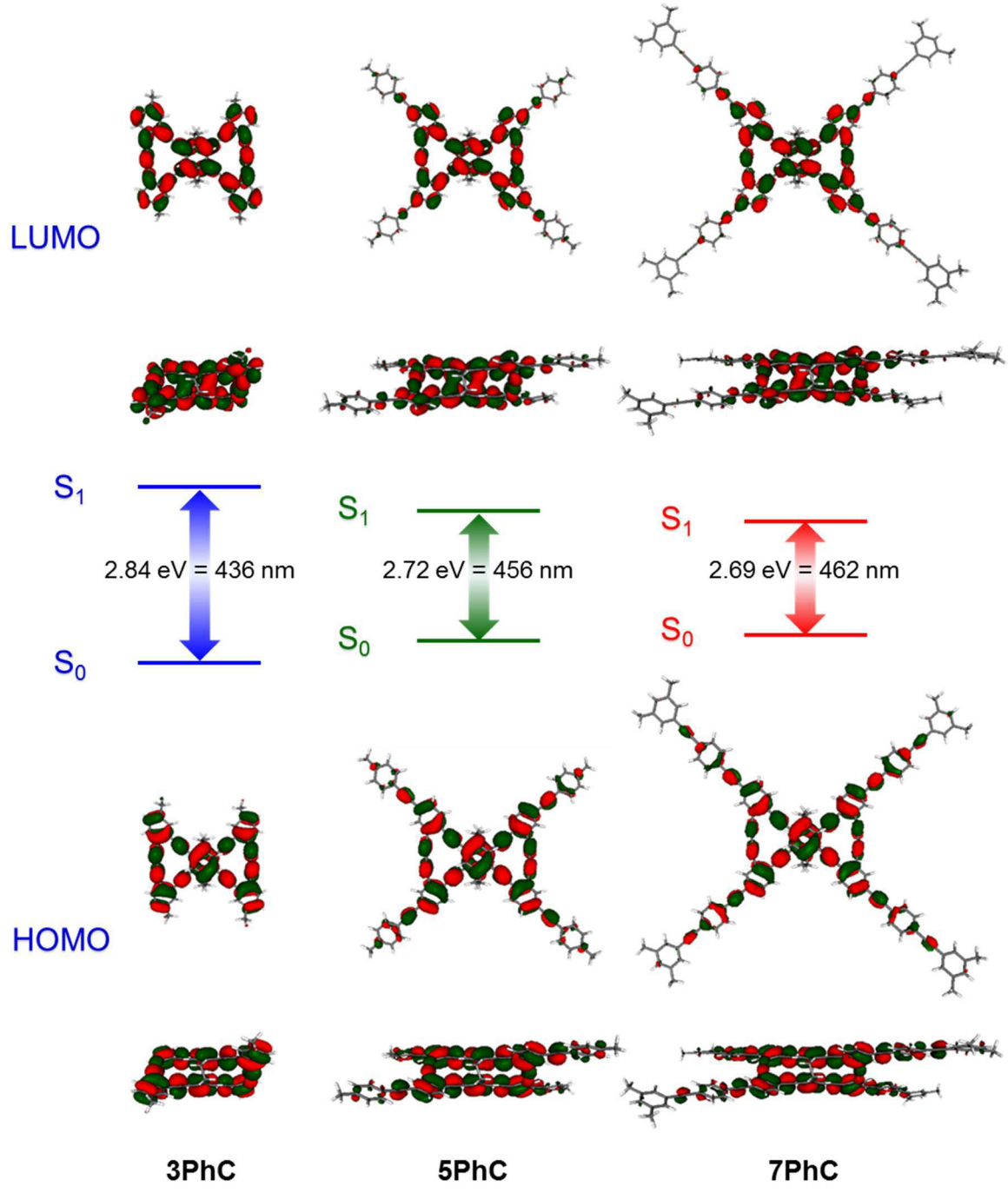

Figure 4. HOMOs and LUMOs of (R_p)-**3PhC**, (R_p)-**5PhC**, and (R_p)-**7PhC** obtained by density functional theory (DFT) at the TD-BHandHLYP/def2-TZVPP//BLYP/def2-TZVPP level.

Chiroptical Properties

The chiroptical properties of the ground and excited states of **3Ph**, **5Ph**, **7Ph**, **3PhC**, **5PhC**, and **7PhC** were investigated by circular dichroism (CD) and CPL spectroscopy, respectively. The chiroptical data, *i.e.* the maximum molar ellipticity ([θ]), specific rotation, and CPL dissymmetry factor[14] (g_{lum}) are summarized in Table 2. Figure 5 shows the CD and absorption spectra of both enantiomers of **3Ph**, **5Ph**, and **7Ph** in the dilute $CHCl_3$ (1.0×10^{-5} M). In all cases, mirror image Cotton effects were observed in the CD spectra, and the maximum [θ] values were estimated to be approximately $\pm 3.3 \times 10^5$ deg cm^2 dmol^{-1}. As can be seen in Figure 6, the [θ] values for **3PhC**, **5PhC**, and **7PhC** were larger than those of **3Ph**, **5Ph**, and **7Ph**, with the maximum values on the order of 10^6 deg cm^2 dmol^{-1}. The specific rotation $[\alpha]^{23}_D$ values for (R_p)-**3PhC**, **5PhC**, and **7PhC** were +1501.0, +855.6, and +467.9, respectively, and were much larger than those for (R_p)-**3Ph**, **5Ph**, and **7Ph** (Table 2). Thus, the construction of optically active higher-ordered (propeller-shaped) structures through cyclization affected the chiroptical properties of the ground state, and greater chirality was induced in the cyclic compounds.

Table 2. Chiroptical properties: Specific rotation and spectroscopic data of (R_p)-isomers

	$[\alpha]^{23}_D$[a]	g_{abs} / 10^{-2} at λ_{abs}[b]	g_{lum} / 10^{-2} at $\lambda_{lum, max}$[c]
(R_p)-**3Ph**	−45.4	−0.13	−0.14
(R_p)-**5Ph**	−42.5	−0.14	−0.12
(R_p)-**7Ph**	−62.9	−0.10	−0.10
(R_p)-**3PhC**	+1501.0	+0.88	+1.3
(R_p)-**5PhC**	+855.6	+1.0	+1.0
(R_p)-**7PhC**	+467.9	+0.75	+0.75

[a] Specific rotation (*c* 0.1, $CHCl_3$ at 23 °C). The $[\alpha]^{23}_D$ values of (S_p)-isomers are described in the experimental section. [b] $g_{abs} = 2\Delta\varepsilon/\varepsilon$, where $\Delta\varepsilon$ indicates differences of absorbance between left- and right-handed circularly polarized light, respectively. The g_{abs} value of the first peak top was estimated. [c] $g_{lum} = 2(I_{left} - I_{right})/(I_{left} + I_{right})$, where I_{left} and I_{right} indicate luminescence intensities of left- and right-handed CPL, respectively.

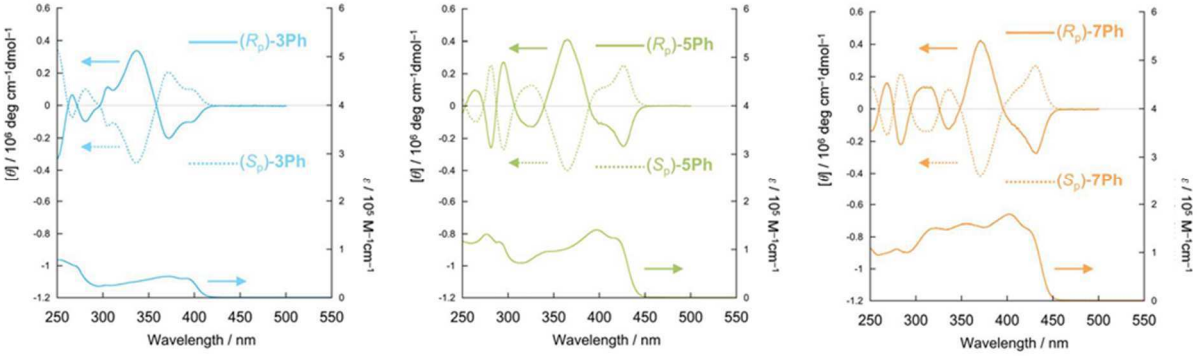

Figure 5. CD (top) and absorption (bottom) spectra of **3Ph**, **5Ph**, and **7Ph** in $CHCl_3$ (1.0×10^{-5} M).

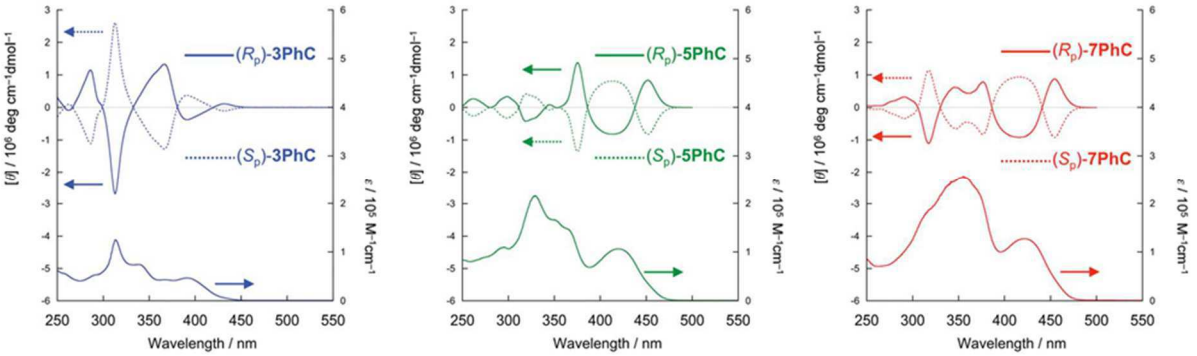

Figure 6. CD (top) and absorption (bottom) spectra of **3PhC**, **5PhC**, and **7PhC** in $CHCl_3$ (1.0×10^{-5} M).

The CPL spectra of the precursors and cyclic compounds in the dilute $CHCl_3$ (1.0×10^{-5} M) are shown in Figures 7 and 8, respectively. Intense and mirror image CPL signals were observed in the emission regions for the enantiomers of each compound, as shown in Figures 7 and 8. The g_{lum} values of **3Ph**, **5Ph**, and **7Ph** were very large (-0.14×10^{-2}, -0.12×10^{-2}, and -0.10×10^{-2} for the (R_p)-isomers, respectively; Table 2). The g_{lum} values for (R_p)-**3PhC**, **5PhC**, and **7PhC** were calculated to be $+1.3 \times 10^{-2}$, $+1.0 \times 10^{-2}$, and $+0.75 \times 10^{-2}$, respectively (Table 2). As expected, the values for the cyclic compounds were significantly larger than those for the precursors owing to the optically active propeller-shaped structures. Higher-ordered structures of the emitting species in the excited state, such as propeller-shaped,[7] V-shaped,[15] S-

shaped,[16] and helical structures,[15-18] are considered to be important for large g_{lum} values on the order of 10^{-2} to 10^{-3}.[19,20]

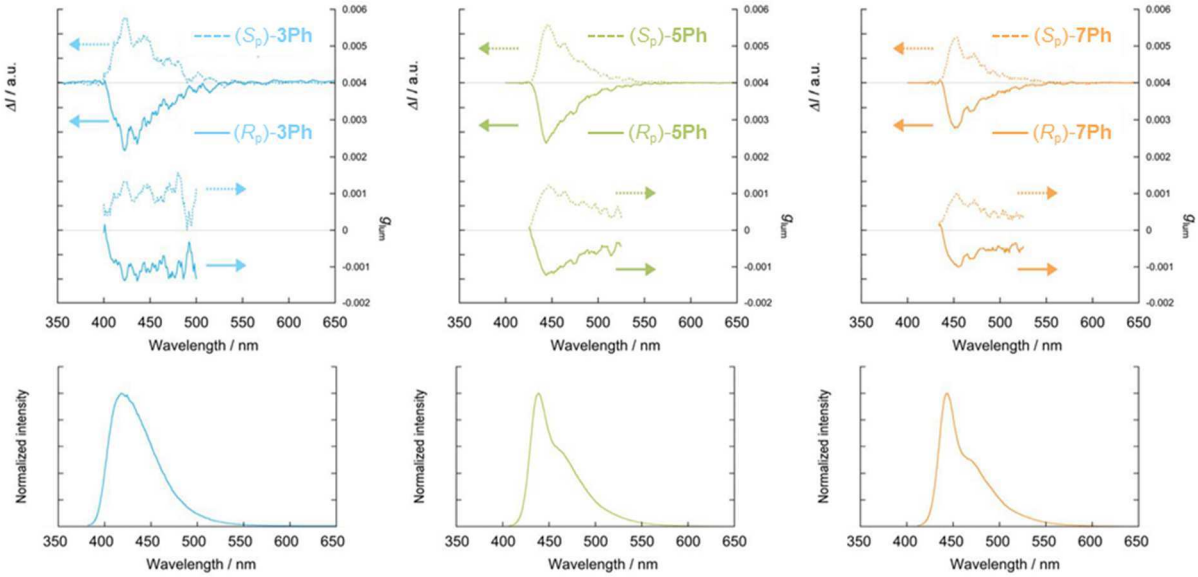

Figure 7. CPL (top), g_{lum} (middle), and PL (bottom) spectra of **3Ph**, **5Ph**, and **7Ph** in $CHCl_3$ (1.0×10^{-5} M for CPL and 1.0×10^{-6} M for PL). Excitation wavelength: 300 nm, 350 nm, and 350 nm for **3Ph**, **5Ph**, and **7Ph**, respectively.

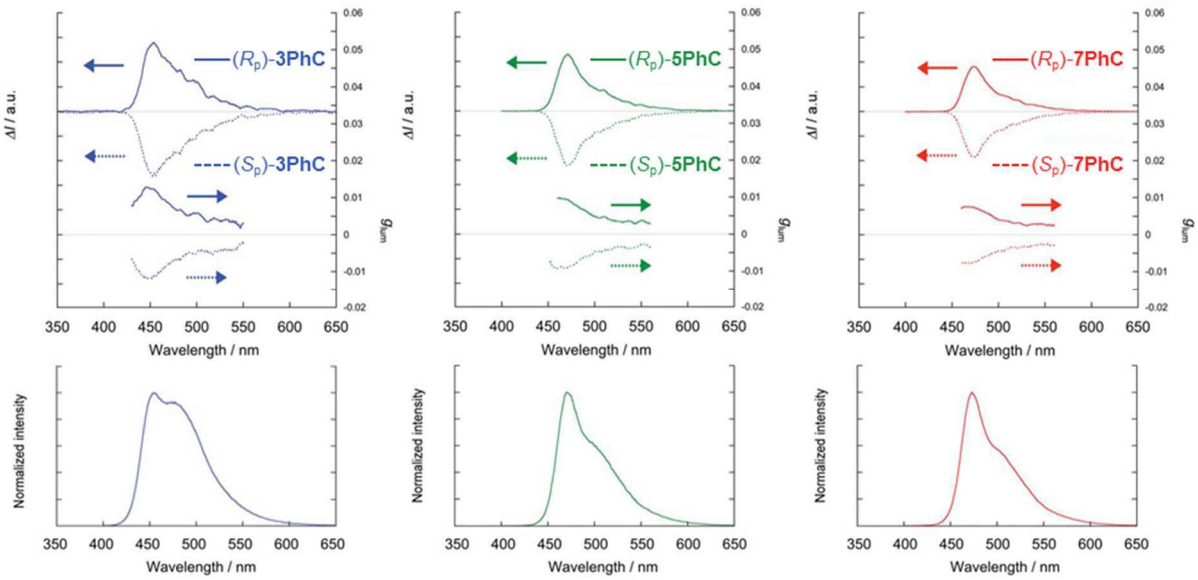

Figure 8. CPL (top), g_{lum} (middle), and PL (bottom) spectra of **3PhC**, **5PhC**, and **7PhC** in $CHCl_3$ (1.0×10^{-5} M for CPL and 1.0×10^{-6} M for PL). Excitation wavelength: 314 nm, 350 nm, and 355 nm for **3PhC**, **5PhC**, and **7PhC**, respectively.

The concentration effect (from 1.0×10^{-7} M to 1.0×10^{-3} M in $CHCl_3$) on CPL was studied for (R_p)-isomers, and the CPL profiles of their film fabricated by drop-casting from $CHCl_3$ solution (1.0×10^{-3} M) were also investigated. The CPL spectra were gradually red-shifted and the g_{lum} values decreased slightly, as the concentration increased. In Chapter 3, the g_{lum} value of **3PhC** was estimated to be 1.1×10^{-2} in $CHCl_3$ (1.0×10^{-5} M),[7] whereas the g_{lum} values in more diluted $CHCl_3$ solutions (1.0×10^{-6} and 10^{-7} M) were 1.3×10^{-2}. The solvent effect on CPL using good solvents such as CH_2Cl_2, toluene, and THF was not observed. The films exhibited almost the same g_{lum} values as those in solution, although Φ_{lum} decreased.

The g_{lum} values of **3PhC**, **5PhC**, and **7PhC** decreased as the Φ_{lum} values increased with the extension of the *p*-phenylene-ethynylene substituents; however, the g_{lum} values were sufficiently large in comparison with the values reported to date.[19,15-20] Generally, the achievement of both high Φ_{lum} and large g_{lum} values is challenging, because orientation of fluorophores tends to decrease the PL performance because of excimer-like emission. Helicene derivatives are considered to be one of the promising candidates for organic CPL materials, and many of them exhibit large g_{lum} values;[17] however, the Φ_{lum} values of helicene derivatives are by no means satisfactory.[21] Considering the applications of organic emitters, large ε, high Φ_{lum}, and large g_{lum} values are required. From this viewpoint, **5PhC** and **7PhC** possess well-balanced optical profiles (large ε values of $2.16\text{-}2.58 \times 10^5$ M^{-1} cm^{-1}, good Φ_{lum} values of 0.60-0.70, and large g_{lum} values of $0.75\text{-}1.0 \times 10^{-2}$), and these compounds show good potential for application in organic CPL materials.

Conclusions

In summary, planar chiral [2.2]paracyclophane-based cyclic compounds with extended π-conjugated systems were synthesized. Cyclization resulted in a significant enhancement of the optical and chiroptical properties compared with those of the non-cyclic precursors. The HOMOs of the cyclic compounds were mainly located on the cyclic skeletons, whereas the LUMOs were localized on the cyclic skeletons. Thus, the absorption and emission occurred from the propeller-shaped cyclic structures, resulting in similar optical profiles for both **5PhC** and **7PhC**. The optically active higher-ordered structure of these compounds provided chiroptical properties of high performance, and both large $[\alpha]_D$ and $[\theta]$ values were derived from the optically active propeller-shaped structure. The rigid propeller-shaped cyclic structures are maintained in the exited state unless carbon-carbon bonds are cleaved; hence, intense CPL with large g_{lum} values was observed for these compounds. The *p*-phenylene-ethynylene substituents introduced onto the propeller-shaped structure acted as light-harvesting antenna and improved the optical properties, leading to the large ε values and relatively high Φ_{lum} values for the cyclic compounds. Compound **5PhC** was, in particular, an outstanding CPL emitter, possessing well-balanced optical and chiroptical properties. The results of the present work suggest that planar chiral [2.2]paracyclophane-based optically active higher-ordered structures, such as the propeller-shaped cyclic structure, are promising scaffolds for emergent CPL materials and that appropriate modifications, *e.g.* extension of the π-conjugated system, can enhance the CPL characteristics.

Experimental Section

General. ^{1}H and ^{13}C spectra were recorded on a JEOL EX400 or AL400 instrument at 400 and 100 MHz, respectively. Samples were analyzed in $CDCl_3$, and the chemical shift values were expressed relative to Me_4Si as an internal standard. Analytical thin layer chromatography (TLC) was performed with silica gel 60 Merck F254 plates. Column chromatography was performed with Wakogel C-300 SiO_2. High-resolution mass (HRMS) spectrometry was performed at the Technical Support Office (Department of Synthetic Chemistry and Biological Chemistry, Graduate School of Engineering, Kyoto University), and the HRMS spectra were obtained on a Thermo Fisher Scientific EXACTIVE spectrometer for electrospray ionization (ESI), a Thermo Fisher Scientific EXACTIVE spectrometer for atmospheric pressure chemical ionization (APCI), and a Thermo Fisher Scientific orbitrapXL spectrometer for matrix assisted laser desorption/ionization (MALDI) using 1,8-dihydroxy-9,10-dihydroanthracen-9-one (DIT) as a matrix. Recyclable preparative high-performance liquid chromatography (HPLC) was carried out on a Japan Analytical Industry Model LC918R (JAIGEL-1H and 2H columns) using $CHCl_3$ as an eluent. UV-vis spectra were recorded on a SHIMADZU UV-3600 spectrophotometer, and samples were analyzed in $CHCl_3$ at room temperature. Photoluminescence (PL) emission spectra were recorded on a HORIBA JOBIN YVON Fluoromax-4 spectrofluorometer, and samples were analyzed in $CHCl_3$ at room temperature. PL lifetime measurement was performed on a Horiba FluoroCube spectrofluorometer system; excitation was carried out using a UV diode laser (NanoLED 375 nm). Specific rotations ($[\alpha]^{t}_{D}$) were measured with a HORIBA SEPA-500 polarimeter. Circular dichroism (CD) spectra were recorded on a JASCO J-820 spectropolarimeter with $CHCl_3$ as a solvent at room temperature. Circularly polarized luminescence (CPL) spectra were recorded on a JASCO CPL-200S with $CHCl_3$ as a solvent at room temperature. Elemental analyses were performed at the Microanalytical Center of Kyoto University.

Materials. Commercially available compounds used without purification: (Tokyo Chemical Industry Co, Ltd.) trimethylsilylacetylene, $PdCl_2(PPh_3)_2$, $Pd_2(dba)_3$ (dba = dibenzylideneacetone) tetra-*n*-butylammonium fluoride (NBu_4F, TBAF) (1 M in THF); (Wako Pure Chemical Industries, Ltd.) *p*-*t*-butylphenylacetylene (**1**), *p*-bromoiodobenzene, PPh_3, CuI, $NaNO_2$, concd. H_2SO_4, KI, K_2CO_3; (Sigma-Aldrich Co. LLC.) di(1-adamantyl)-*n*-butylphosphine (cataCXium® A). Commercially available solvents: CH_3CN and MeOH were used without purification. H_2O was purified by demineralizer. THF and Et_3N were purified by passage through solvent purification columns under Ar pressure.[24] Compounds prepared as described in the literatures: 4-Iodo-2-bromoaniline[23], 3,5-di-*t*-

butylethynylbenzene (**5**)[24], (R_p)-4,7,12,15-tetraethynyl[2.2]para-cyclophane ((R_p)-**12**)[7], cyclic compounds, **3Ph**[7] and **3PhC**.[7]

Computational Details. The Orca program package[25] was used for computation. We optimized the structures of **3PhC**, **5PhC**, and **7PhC** (methyl groups were used in place of *tert*-butyl groups) in the ground S_0 states and calculated their electric structures. The density functional theory (DFT) was applied for the optimization of the structures in the S_0 states at the BLYP/def2-TZVPP levels. We calculated the electric states and transitions from S_0 to S_1 of the **3PhC**, **5PhC**, and **7PhC** with the optimized geometries in the S_0 states by time-dependent DFT (TD-DFT) at the TD-BHandHLYP/def2-TZVPP levels.

Synthesis of 2. A mixture of 2-bromo-4-iodoaniline (4.16 g, 14.0 mmol), $PdCl_2(PPh_3)_2$ (0.490 g, 0.70 mmol), PPh_3 (0.366 g, 1.40 mmol), CuI (0.133 g, 0.70 mmol), THF (80 mL) and Et_3N (20 mL) was placed in a round-bottom flask equipped with a magnetic stirring bar. After degassing the reaction mixture several times, the mixture was cooled to 0 °C. *p*-*t*-butylphenylacetylene (**1**) (2.61 mL, 14.7 mmol) was added to the mixture via a syringe. The reaction was carried out at room temperature for 10 h with stirring. Precipitates were removed by filtration, and the solvent was removed with a rotary evaporator. The crude residue was purified by column chromatography on SiO_2 (EtOAc/hexane = 1/6 v/v as an eluent) to afford **2** (4.06 g, 12.4 mmol, 89%) as a pale brown crystal (R_f = 0.34 (EtOAc/hexane = 1/6 v/v)). The product **2** was used for the next reaction without further purification.

Synthesis of 3. A mixture of **2** (2.29 g, 7.0 mmol), $PdCl_2(PPh_3)_2$ (0.245 g, 0.35 mmol), dppf (0.194 g, 0.35 mmol), CuI (0.067 g, 0.35 mmol), THF (45 mL) and Et_3N (15 mL) was placed in a round-bottom flask equipped with a magnetic stirring bar. After degassing the reaction mixture several times, trimethylsilylacetylene (1.97 mL, 14.0 mmol) was added to the mixture via a syringe. The reaction was carried out at 60 °C for 10 h with stirring. After the reaction mixture was cooled to room temperature, precipitates were removed by filtration, and the solvent was removed with a rotary evaporator. The crude residue was purified by column chromatography on SiO_2 (EtOAc/hexane = 1/6 v/v as an eluent). Further purification was carried out by recrystallization with hexane to afford **3** (1.42 g, 4.11 mmol, 59%) as a light brown crystal. R_f = 0.43 (EtOAc/hexane = 1/6 v/v). ^{1}H NMR ($CDCl_3$, 400 MHz) δ 0.26 (s, 9H), 1.32 (s, 9H), 4.38, (s, 2H), 6.64 (d, J = 8.5 Hz, 1H), 7.28 (d, J = 1.9 Hz, 1H) 7.34 (d, J = 8.5 Hz, 2H), 7.41 (d, J = 8.5 Hz, 2H), 7.49 (d, J = 1.9 Hz, 1H) ppm; ^{13}C NMR ($CDCl_3$, 100 MHz) δ 0.1, 31.2, 34.7, 87.5, 88.6, 100.3, 100.8, 107.8, 112.4, 114.0, 120.7, 125.3, 131.1, 133.2, 135.6, 148.0, 151.0

ppm. HRMS (ESI) calcd. for $C_{23}H_{28}NSi$ $[M+H]^+$: 346.1986, found: 346.1977. Elemental analysis calcd. for $C_{23}H_{27}NSi$: C 79.94 H 7.88 N 4.05, found: C 79.86 H 7.94 N 4.03.

Synthesis of 4. A mixture of **3** (0.628 g, 1.82 mmol), CH_3CN (100 mL), H_2O (30 mL) and concentrated H_2SO_4 (8.0 mL) was placed in a round-bottom flask at 0 °C, equipped with a magnetic stirring bar. To the reaction mixture, $NaNO_2$ (0.163 g, 2.36 mmol) in H_2O (4 mL) was slowly added at 0 °C. After stirring for 2 h, the mixture was added into a solution of KI (1.87 g, 11.3 mmol) in CH_3CN (50 mL) and H_2O (50 mL) at 0 °C. The reaction mixture was stirred at room temperature for 12 h. The mixture was quenched by the addition of aqueous $NaHSO_3$ solution, and the organic layer was extracted three times with CH_2Cl_2. The combined organic layer was washed with brine and dried over $MgSO_4$. $MgSO_4$ was removed by filtration, and the solvent was evaporated. The residue was purified by column chromatography on SiO_2 (hexane as an eluent). Further purification was carried out by recrystallization with $CHCl_3$ and MeOH (good and poor solvent, respectively) to afford **4** (0.734 g, 1.62 mmol, 61%) as a colorless crystal. R_f = 0.23 (hexane). ^{1}H NMR ($CDCl_3$, 400 MHz) δ 0.29 (s, 9H), 1.30 (s, 9H), 7.08, (dd, J = 8.2 Hz, J = 2.1 Hz, 1H), 7.34 (d, J = 8.6 Hz, 2H), 7.42 (d, J = 8.6 Hz, 2H), 7.61 (d, J = 2.1 Hz, 1H), 7.76 (d, J = 8.0 Hz, 1H) ppm; ^{13}C NMR ($CDCl_3$, 100 MHz) δ −0.1, 31.2, 34.8, 87.1, 91.4, 99.4, 100.5, 105.8, 119.6, 123.5, 125.3, 129.9, 131.3, 132.0, 135.3, 138.6, 151.8 ppm. HRMS (APCI) calcd. for $C_{23}H_{26}ISi$ $[M+H]^+$: 457.0843, found: 457.0840. Elemental analysis calcd. for $C_{23}H_{25}ISi$: C 60.52 H 5.52 I 27.80, found: C 60.49 H 5.57 I 27.79.

Synthesis of 6. A mixture of **5** (3.79 g, 17.7 mmol), *p*-bromoiodobenzene (5.26 g, 18.6 mmol), $PdCl_2(PPh_3)_2$ (0.621 g, 0.885 mmol), PPh_3 (0.464 g, 1.77 mmol), CuI (0.169 mg, 0.885 mmol), THF (75 mL) and Et_3N (25 mL) was placed in a round-bottom flask equipped with a magnetic stirring bar. After degassing the reaction mixture several times, the reaction was carried out at room temperature for 12 h with stirring. After the reaction, precipitates were removed by filtration, and the solvent was removed with a rotary evaporator. The crude residue was purified by column chromatography on SiO_2 (hexane as an eluent). Further purification was carried out by recrystallization with $CHCl_3$ and MeOH (good and poor solvent, respectively) to afford **6** (4.45 g, 12.0 mmol, 68%) as a colorless block crystal. R_f = 0.39 (hexane). ^{1}H NMR ($CDCl_3$, 400 MHz) δ 1.33 (s, 18H), 7.37-7.41 (m, 5H), 7.47 (d, J = 8.8 Hz, 2H) ppm; ^{13}C NMR ($CDCl_3$, 100 MHz) δ 31.3, 34.8, 87.0, 91.7, 121.9, 122.2, 122.5, 123.0, 125.8, 131.6, 133.0, 150.9 ppm. HRMS (APCI) calcd. for $C_{22}H_{26}Br$ $[M+H]^+$: 369.1212, found: 369.1206. Elemental analysis calcd. for $C_{22}H_{25}Br$: C 71.54 H 6.82, found: C 71.48 H 6.81.

Synthesis of 7. A mixture of **6** (4.21 g, 11.4 mmol), $PdCl_2(PPh_3)_2$ (0.400 g, 0.57 mmol), PPh_3 (0.299 g, 1.14 mmol), CuI (0.109 g, 0.57 mmol), THF (40 mL) and Et_3N (40 mL) was placed in a round-bottom flask equipped with a magnetic stirring bar. After degassing the reaction mixture several times, trimethylsilylacetylene (2.42 mL, 17.1 mmol) was added to the mixture via a syringe. The reaction was carried out at 70 °C for 12 h with stirring. After the reaction mixture was cooled to room temperature, precipitates were removed by filtration, and the solvent was removed with a rotary evaporator. The crude residue was purified by column chromatography on SiO_2 ($CHCl_3$/hexane = 1/9 v/v as an eluent). Further purification was carried out by recrystallization with $CHCl_3$ and MeOH (good and poor solvent, respectively) to afford **7** (3.54 g, 9.15 mmol, 80%) as a light yellow needle crystal. R_f = 0.50 ($CHCl_3$/hexane = 1/9 v/v). ^{1}H NMR ($CDCl_3$, 400 MHz) δ 0.25 (s, 9H), 1.33 (s, 18H), 7.38-7.48 (m, 7H) ppm; ^{13}C NMR ($CDCl_3$, 100 MHz) δ −0.1, 31.3, 34.8, 87.8, 92.5, 96.1, 104.7, 121.9, 122.7, 123.0, 123.6, 125.9, 131.4, 131.9, 150.9 ppm. HRMS (APCI) calcd. for $C_{27}H_{35}Si$ $[M+H]^+$: 387.2503, found: 387.2491. Elemental analysis calcd. for $C_{27}H_{34}Si$: C 83.87 H 8.86, found: C 83.71 H 8.79.

Synthesis of 8. K_2CO_3 (1.80 g, 13.1 mmol) was added to a suspension of **7** (3.36 g, 8.70 mmol) in MeOH (100 mL). After the mixture was stirred for 20 h at room temperature, H_2O was added to the reaction mixture. The organic layer was extracted with $CHCl_3$ and washed with brine. The combined organic layer was dried over $MgSO_4$. $MgSO_4$ was removed by filtration, and the solvent was removed with a rotary evaporator. The crude residue was purified by column chromatography on SiO_2 ($CHCl_3$/hexane = 1/9 v/v as an eluent) to afford **8** (2.71 g, 8.62 mmol, 99%) as a colorless crystal. R_f = 0.48 ($CHCl_3$/hexane = 1/9 v/v). ^{1}H NMR ($CDCl_3$, 400 MHz) δ 0.25 (s, 9H), 1.33 (s, 18H), 7.38 (d, J = 2.0 Hz, 2H), 7.41 (t, J = 1.8 Hz, 1H), 7.46 (d, J = 8.1 Hz, 2H), 7.50 (d, J = 8.1 Hz, 2H) ppm; ^{13}C NMR ($CDCl_3$, 100 MHz) δ 31.4, 34.9, 78.7, 83.4, 87.6, 92.6, 121.6, 121.8, 123.0, 124.0, 125.8, 131.4, 132.0, 150.9 ppm. HRMS (APCI) calcd. for $C_{24}H_{27}$ $[M+H]^+$: 315.2107, found: 315.2102. Elemental analysis calcd. for $C_{24}H_{26}$: C 91.67 H 8.33, found: C 91.43 H 8.56.

Synthesis of 9. A mixture of 2-bromo-4-iodoaniline (2.34 g, 7.88 mmol), **8** (2.48 g, 7.88 mmol), $Pd_2(dba)_3$ (0.180 g, 0.197 mmol), PPh_3 (0.207 g, 0.788 mmol), CuI (0.075 g, 0.39 mmol), THF (40 mL) and Et_3N (40 mL) was placed in a round-bottom flask equipped with a magnetic stirring bar. After degassing the reaction mixture several times, the reaction was carried out at 40 °C for 20 h with stirring. Precipitates were removed by filtration, and the solvent was removed with a rotary evaporator. The crude residue was purified by column chromatography on SiO_2 (EtOAc/hexane = 1/4 v/v as an eluent)

to afford **9** (2.74 g, 5.65 mmol, 72%) as a pale brown crystal (R_f = 0.48 (EtOAc/hexane = 1/6 v/v)). The product **9** was used for the next reaction without further purification.

Synthesis of 10. A mixture of **9** (2.74 g, 5.65 mmol), $PdCl_2(PPh_3)_2$ (0.270 g, 0.385 mmol), dppf (0.213 g, 0.385 mmol), CuI (0.073 g, 0.39 mmol), THF (40 mL) and Et_3N (40 mL) was placed in a round-bottom flask equipped with a magnetic stirring bar. After degassing the reaction mixture several times, trimethylsilylacetylene (2.17 mL, 15.4 mmol) was added to the mixture via a syringe. The reaction was carried out at 70 °C for 24 h with stirring. After the reaction mixture was cooled to room temperature, precipitates were removed by filtration, and the solvent was removed with a rotary evaporator. The crude residue was purified by column chromatography on SiO_2 (EtOAc/hexane = 1/4 v/v as an eluent). Further purification was carried out by recrystallization with hexane to afford **10** (2.01 g, 4.00 mmol, 71%) as a light brown needle crystal. R_f = 0.59 (EtOAc/hexane = 1/4 v/v). ^{1}H NMR ($CDCl_3$, 400 MHz) δ 0.27 (s, 9H), 1.34 (s, 18H), 4.42, (s, 2H), 6.64 (d, J = 8.6 Hz, 1H), 7.28 (dd, J = 8.6 Hz, J = 2.0 Hz, 1H) 7.38-7.45 (m, 5H), 7.49-7.51 (m, 3H) ppm; ^{13}C NMR ($CDCl_3$, 100 MHz) δ 0.1, 31.3, 34.8, 87.3, 88.0, 91.2, 92.2, 100.4, 100.6, 107.9, 111.9, 114.0, 122.0, 122.8, 122.9, 123.4, 125.9, 131.2, 131.5, 133.2, 135.7, 148.3, 150.9 ppm. HRMS (ESI) calcd. for $C_{35}H_{40}NSi$ $[M+H]^+$: 502.2925, found: 502.2911. Elemental analysis calcd. for $C_{35}H_{39}NSi$: C 83.78 H 7.83 N 2.79, found: C 83.52 H 7.85 N 2.53.

Synthesis of 11. A mixture of **10** (0.878 g, 1.75 mmol), CH_3CN (150 mL), H_2O (50 mL) and concentrated H_2SO_4 (24 mL) was placed in a round-bottom flask at 0 °C, equipped with a magnetic stirring bar. To the reaction mixture, $NaNO_2$ (0.224 g, 3.25 mmol) in H_2O (4 mL) was slowly added at 0 °C. After stirring for 2 h, the mixture was added into a solution of KI (2.57 g, 15.5 mmol) in CH_3CN (50 mL) and H_2O (50 mL) at 0 °C. The reaction mixture was stirred at room temperature for 12 h. The mixture was quenched by the addition of aqueous $NaHSO_3$ solution, and the organic layer was extracted three times with CH_2Cl_2. The combined organic layer was washed with brine and dried over $MgSO_4$. $MgSO_4$ was removed by filtration, and the solvent was evaporated. The residue was purified by column chromatography on SiO_2 ($CHCl_3$/hexane = 1/7 v/v as an eluent). Further purification was carried out by recrystallization with $CHCl_3$ and MeOH (good and poor solvent, respectively) to afford **11** (0.443 g, 0.883 mmol, 50%) as a colorless solid. R_f = 0.44 ($CHCl_3$/hexane = 1/7 v/v). ^{1}H NMR ($CDCl_3$, 400 MHz) δ 0.29 (s, 9H), 1.34 (s, 18H), 7.11, (dd, J = 8.0 Hz, J = 2.0 Hz, 1H), 7.39 (d, J = 1.7 Hz, 2H), 7.42 (d, J = 1.7 Hz, 1H), 7.47 (d, J = 8.5 Hz, 2H), 7.52 (d, J = 8.3 Hz, 2H), 7.63 (d, J = 2.0 Hz, 1H), 7.81 (d, J = 8.0 Hz, 1H) ppm; ^{13}C NMR ($CDCl_3$, 100 MHz) δ −0.3, 31.3, 34.8, 87.8, 89.4, 90.9, 92.7, 99.6, 101.0, 105.6, 121.9, 122.2, 123.0, 123.1, 123.8, 125.9, 130.0, 131.5, 131.6, 132.0, 135.4, 138.8, 150.9 ppm.

HRMS (ESI) calcd. for $C_{35}H_{37}ISi$ $[M]^+$: 612.1704, found: 612.1688. Elemental analysis calcd. for $C_{35}H_{37}ISi$: C 68.62 H 6.09, found: C 68.31 H 5.99.

Synthesis of 5Ph. A mixture of (R_p)-**12** (20 mg, 0.0657 mmol), **4** (132 mg, 0.289 mmol), $Pd_2(dba)_3$ (6.0 mg, 0.066 mmol), cataCXium® A (9.4 mg, 0.026 mmol), CuI (2.5 mg, 0.013 mmol), THF (2 mL) and Et_3N (2 mL) was placed in a round-bottom flask equipped with a magnetic stirring bar. After degassing the reaction mixture several times, the reaction was carried out at 50 °C for 48 h with stirring. After the reaction mixture was cooled to room temperature, precipitates were removed by filtration, and the solvent was removed with a rotary evaporator. The crude residue was purified by column chromatography on SiO_2 ($CHCl_3$/hexane = 1/2 v/v as an eluent). Further purification was carried out by HPLC to afford (R_p)-**5Ph** (68 mg, 0.042 mmol, 64%) as a light yellow solid. R_f = 0.53 ($CHCl_3$/hexane = 1/3 v/v). ^{1}H NMR ($CDCl_3$, 400 MHz) δ 0.24 (s, 36H), 1.33 (s, 36H), 3.19, (m, 4H), 3.73 (m, 4H), 7.26 (s, 4H) 7.38 (d, J = 8.6 Hz, 8H), 7.45 (dd, J = 8.0 Hz, 1.6 Hz, 4H), 7.48 (d, J = 8.6 Hz, 8H), 7.52 (d, J = 8.0 Hz, 4H), 7.73 (d, J = 1.6 Hz, 4H) ppm; ^{13}C NMR ($CDCl_3$, 100 MHz) δ 0.1, 31.2, 32.8, 34.9, 87.8, 92.0, 93.4, 94.8, 99.2, 103.0, 119.8, 123.3, 125.3, 125.4, 125.4, 125.4, 131.0, 131.4, 132.3, 135.2, 135.7, 141.9, 151.9 ppm. HRMS (ESI) calcd. for $C_{116}H_{116}Si_4N$ $[M+NH_4]^+$: 1634.8179, found: 1634.8173. Elemental analysis calcd. for $C_{116}H_{112}Si_4$: C 86.08 H 6.98, found: C 86.06 H 6.93. (S_p)-**5Ph** and *rac*-**5Ph** were obtained by the same procedure in 69% and 66% isolated yields, respectively. (R_p)-**5Ph**: $[\alpha]^{23}_D$ = −42.5 (c 0.1, $CHCl_3$). (S_p)-**5Ph**: $[\alpha]^{23}_D$ = +42.6 (c 0.1, $CHCl_3$).

Synthesis of 5PhC. (R_p)-**5Ph** (53.6 mg, 0.0331 mmol) in THF (5.0 mL) was placed in a round-bottom flask equipped with a magnetic stirring bar. After degassing several times, TBAF (1 M in THF, 0.2 mL, 0.2 mmol) was added to the solution at room temperature for 15 min with stirring. The mixture was quenched by the addition of H_2O, and the organic layer was extracted three times with $CHCl_3$. The combined organic layer was washed with brine and dried over $MgSO_4$. $MgSO_4$ was removed by filtration, and the solvent was evaporated. The residue was purified by flash column chromatography on SiO_2 ($CHCl_3$ as an eluent). A mixture of the residue, $PdCl_2(PPh_3)_2$ (217 mg, 0.309 mmol), CuI (58.8 mg, 0.309 mmol), THF (200 mL) and Et_3N (50 mL) was placed in a round-bottom flask equipped with a magnetic stirring bar. The mixture was heated at reflux temperature for 24 h under open air. After the reaction mixture was cooled to room temperature, the solvent was evaporated. The residue was purified by column chromatography on SiO_2 ($CHCl_3$/hexane = 1/2 v/v as an eluent). Further purification was carried out by HPLC to afford (R_p)-**5PhC** (7.7 mg, 0.0058 mmol, 18%) as a light yellow solid. R_f = 0.30 ($CHCl_3$/hexane = 1/3 v/v). ^{1}H NMR ($CDCl_3$, 400 MHz) δ 1.34 (s, 36H), 3.13, (m, 4H), 3.55 (m, 4H),

7.21 (s, 4H) 7.40 (d, *J* = 8.6 Hz, 8H), 7.50 (d, *J* = 8.6 Hz, 8H), 7.51 (m, 8H), 7.69 (m, 4H) ppm; ^{13}C NMR ($CDCl_3$, 100 MHz) δ 31.2, 33.2, 34.9, 79.0, 81.5, 87.5, 92.5, 93.0, 94.8, 119.6, 123.7, 124.2, 124.3, 125.4, 127.7, 131.4, 131.8, 132.2, 133.9, 133.9, 143.3, 152.1 ppm. HRMS (APCI) calcd. for $C_{104}H_{77}$ $[M+H]^+$: 1325.6020, found: 1325.6032. (S_p)-**5PhC** and *rac*-**5PhC** were obtained by the same procedure in 18% and 9% isolated yields, respectively. (R_p)-**5PhC**: $[\alpha]^{23}_D$ = +855.59 (*c* 0.1, $CHCl_3$). (S_p)-**5PhC**: $[\alpha]^{23}_D$ = −849.61 (*c* 0.1, $CHCl_3$).

Synthesis of 7Ph. A mixture of (R_p)-**12** (20 mg, 0.0657 mmol), **11** (177 mg, 0.289 mmol), $Pd_2(dba)_3$ (6.0 mg, 0.066 mmol), cataCXium® A (9.4 mg, 0.026 mmol), CuI (2.5 mg, 0.013 mmol), THF (2 mL) and Et_3N (2 mL) was placed in a round-bottom flask equipped with a magnetic stirring bar. After degassing the reaction mixture several times, the reaction was carried out at 50 °C for 48 h with stirring. After the reaction mixture was cooled to room temperature, precipitates were removed by filtration, and the solvent was removed with a rotary evaporator. The crude residue was purified by column chromatography on SiO_2 ($CHCl_3$/hexane = 1/3 v/v as an eluent). Further purification was carried out by HPLC to afford (R_p)-**7Ph** (87 mg, 0.039 mmol, 59%) as a light yellow solid. R_f = 0.26 ($CHCl_3$/hexane = 1/3 v/v). ^{1}H NMR ($CDCl_3$, 400 MHz) δ 0.25 (s, 36H), 1.34 (s, 72H), 3.21, (m, 4H), 3.75 (m, 4H), 7.28 (s, 4H) 7.41-7.43 (m, 12H), 7.47 (dd, *J* = 8.2 Hz, 1.5 Hz, 4H), 7.51-7.57 (m, 20H), 7.76 (d, *J* = 1.6 Hz, 4H), ppm; ^{13}C NMR ($CDCl_3$, 100 MHz) δ 0.0, 31.3, 32.7, 34.8, 87.8, 90.1, 91.6, 92.8, 93.4, 95.0, 99.4, 102.9, 121.9, 122.3, 122.9, 123.0, 123.8, 125.5, 125.6, 125.7, 125.9, 131.1, 131.6, 131.6, 132.4, 135.3, 135.9, 142.0, 150.9 ppm. HRMS (APCI) calcd. for $C_{164}H_{161}Si_4$ $[M+H]^+$: 2242.1670, found: 2242.1710. Elemental analysis calcd. for $C_{164}H_{160}Si_4$: C 87.80 H 7.19, found: C 87.70 H 7.16. (S_p)-**7Ph** and *rac*-**7Ph** were obtained by the same procedure in 63% and 70% isolated yields, respectively. (R_p)-**7Ph**: $[\alpha]^{23}_D$ = −62.9 (*c* 0.1, $CHCl_3$). (S_p)-**7Ph**: $[\alpha]^{23}_D$ = +59.6 (*c* 0.1, $CHCl_3$).

Synthesis of 7PhC. A typical procedure is as follows. (R_p)-**7Ph** (70.0 mg, 0.0312 mmol) in THF (5.0 mL) was placed in a round-bottom flask equipped with a magnetic stirring bar. After degassing several times, TBAF (1 M in THF, 0.3 mL, 0.3 mmol) was added to the solution at room temperature for 15 min with stirring. The mixture was quenched by the addition of H_2O, and the organic layer was extracted three times with $CHCl_3$. The combined organic layer was washed with brine and dried over $MgSO_4$. $MgSO_4$ was removed by filtration, and the solvent was evaporated. The residue was purified by flash column chromatography on SiO_2 ($CHCl_3$ as an eluent). A mixture of the residue, $PdCl_2(PPh_3)_2$ (219 mg, 0.312 mmol), CuI (59.4 mg, 0.312 mmol), THF (300 mL) and Et_3N (50 mL) was placed in a round-bottom flask equipped with a magnetic stirring bar. The mixture was heated at reflux temperature for

24 h under open air. After the reaction mixture was cooled to room temperature, the solvent was evaporated. The residue was purified by column chromatography on SiO_2 ($CHCl_3$/hexane = 1/1 v/v as an eluent). Further purification was carried out by HPLC to afford (R_p)-**7PhC** (18.1 mg, 0.00928 mmol, 30%) as a light yellow solid. R_f = 0.26 ($CHCl_3$/hexane = 1/3 v/v). ^{1}H NMR ($CDCl_3$, 400 MHz) δ 1.35 (s, 72H), 3.14, (m, 4H), 3.56 (m, 4H), 7.21 (s, 4H) 7.40-7.43 (m, 12H), 7.48-7.56 (m, 24H), 7.69 (m, 4H) ppm; ^{13}C NMR ($CDCl_3$, 100 MHz) δ 31.3, 33.2, 34.8, 79.1, 81.5, 87.8, 89.8, 92.1, 92.9, 93.0, 95.0, 121.9, 122.2, 123.1, 123.3, 124.0, 124.3, 124.4, 125.9, 128.1, 131.6, 131.6, 131.9, 132.4, 134.0, 134.0, 143.4, 150.9 ppm. HRMS (MALDI, DIT) calcd. for $C_{152}H_{124}$ $[M]^+$: 1948.9703, found: 1948.9756. (S_p)-**7PhC** and *rac*-**7PhC** were obtained by the same procedure in 27% and 27% isolated yields, respectively. (R_p)-**7PhC**: $[\alpha]^{23}_D$ = +467.90 (*c* 0.1, $CHCl_3$). (S_p)-**7PhC**: $[\alpha]^{23}_D$ = −463.35 (*c* 0.1, $CHCl_3$).

References and Notes

(1) For example: (a) *Handbook of Conducting Polymers*; Skotheim, T. A., Elsenbaumer R. L., Reynolds J. R., Eds.; Marcel Dekker: New York, 3rd edn, 2006. (b) *Organic Light Emitting Devices: Synthesis, Properties and Application*; Müellen K., Scherf, U., Eds.; Wiley-VCH: Weinheim, 2006. (c) *Organic Field-Effect Transistors*; Groza, J. R., Locklin, J. J., Eds.; CRC Press Taylor & Francis Group: New York, 2007. (d) *Organic Photovoltaics: Materials, Device Physics, and Manufacturing Technologies*; Brabec, C., Dyakonov V., Scherf, U., Eds.; Wiley-VCH, Weinheim, 2008.

(2) Brown, C. J.; Farthing, A. C. *Nature* **1949**, *164*, 915–916.

(3) Cram, D. J.; Steinberg, H. *J. Am. Chem. Soc.* **1951**, *73*, 5691–5704.

(4) (a) *Cyclophane Chemistry: Synthesis, Structures and Reactions*; Vögtle, F., Ed.; John Wiley & Sons: Chichester, 1993. (b) *Modern Cyclophane Chemistry*; Gleiter, R., Hopf, H., Eds.; Wiley-VCH: Weinheim, 2004.

(5) (a) Bazan,G. C.; Oldham Jr, W. J.; Lachicotte,R. J.; Tretiak, S.; Chernyak, V.; Mukamel, S. *J. Am. Chem. Soc.* **1998**, *120*, 9188–9204. (b) Wang, S.; Bazan, G. C.; Tretiak, S.; Mukamel, S. *J. Am. Chem. Soc.* **2000**, *122*, 1289–1297. (c) Zyss, J.; Ledoux, I.; Volkov, S.; Chernyak, V.; Mukamel, S.; Bartholomew, G. P.; Bazan, G. C. *J. Am. Chem. Soc.* **2000**, *122*, 11956–11962. (d) Bartholomew, G. P.; Bazan, G. C. *Acc. Chem. Res.* **2001**, *34*, 30–39. (e) Bartholomew, G. P.; Bazan, G. C. *Synthesis* **2002**, 1245–1255. (f) Bartholomew G. P.; Bazan, G. C.; *J. Am. Chem. Soc.* **2002**, *124*, 5183–5196. (g) Seferos, D. S.; Banach, D. A.; Alcantar, N. A.; Israelachvili, J. N.; Bazan, G. C. *J. Org. Chem.* **2004**, *69*, 1110–1119. (h) Bartholomew, G. P.; Rumi, M.; Pond, S. J. K.; Perry, J. W.; Tretiak, S.; Bazan, G. C. *J. Am. Chem. Soc.* **2004**, *126*, 11529–11542. (i) Hong, J. W.; Woo H. Y.; Bazan, G. C. *J. Am. Chem. Soc.* **2005**, *127*, 7435–7443. (j) Bazan, G. C. *J. Org. Chem.*, **2007**, *72*, 8615–8635.

(6) Hinrichs, H.; Boydston, A. J.; Jones, P. G.; Hess, K.; Herges, R.; Haley M. M.; Hopf, H. *Chem.–Eur. J.* **2006**, *12*, 7103–7115.

(7) Morisaki, Y.; Gon, M.; Sasamori, T.; Tokitoh, N.; Chujo, Y. *J. Am. Chem. Soc.* **2014**, *136*, 3350–3353.

(8) (a) Cram, D. J.; Allinger, N. L. *J. Am. Chem. Soc.* **1955**, *77*, 6289–6294. (b) Rozenberg, V., Sergeeva, E., Hopf, H. In *Modern Cyclophane Chemistry*; Gleiter R., Hopf, H., Eds.; Wiley-VCH, Weinheim, Germany, 2004, pp. 435–462. (c) Rowlands, G. J. *Org. Biomol. Chem.* **2008**, *6*, 1527–1534. (d) Gibson, S. E.; Knight, J. D. *Org. Biomol. Chem.* **2003**, *1*, 1256–1269. (e) Aly, A. A.; Brown, A. B. *Tetrahedron* **2009**, *65*, 8055–8089. (f) Paradies, J. *Synthesis* **2011**, 3749–3766.

(9) Optical resolution of *rac*-4,5,15,16-tetrasubstituted [2.2]paracyclophane has already been achieved: Vorontsova, N. V.; Rozenberg, V. I.; Sergeeva, E. V.; Vorontsov, E. V.; Starikova, Z. A.; Lyssenko, K. A.; Hopf, H. *Chem.–Eur. J.* **2008**, *14*, 4600–4617.

(10) (a) Riehl, J. P.; Richardson, F. S. *Chem. Rev.* **1986**, *86*, 1–16. (b) *Comprehensive Chiroptical Spectroscopy*; Riehl J. P., Muller, F., Eds.; Wiley and Sons, New York, 2012.

(11) (a) Tohda, Y.; Sonogashira, K.; Hagihara, N. *Tetrahedron Lett.* **1975**, *16*, 4467–4470. (b) Sonogashira, K. In *Handbook of Organopalladium Chemistry for Organic Synthesis*; Negishi, E., Ed.; Wiley-Interscience: New York, 2002; pp 493−529.

(12) (a) Sandmeyer, T. *Ber. Dtsch. Chem. Ges.* **1884**, *17*, 1633–1635. (b) Sandmeyer, T. *Ber. Dtsch. Chem. Ges.* **1884**, *17*, 2650–2653.

(13) Zapf, A.; Ehrentraut, A.; Beller, M. *Angew. Chem., Int. Ed.* **2000**, *39*, 4153–4155.

(14) CPL dissymmetry factor is defined as $g_{lum} = 2(I_{left} - I_{right})/(I_{left} + I_{right})$, where I_{left} and I_{right} indicate luminescence intensities of left- and right-handed CPL, respectively.

(15) Morisaki, Y.; Inoshita, K.; Chujo, Y. *Chem.–Eur. J.* **2014**, *20*, 8386–8390.

(16) Nakamura, K.; Furumi, S.; Takeuchi, M.; Shibuya, T.; Tanaka, K. *J. Am. Chem. Soc.* **2014**, *136*, 5555–5558.

(17) (a) Field, J. E.; Muller, G.; Riehl, J. P.; Venkataraman, D. *J. Am. Chem. Soc.* **2003**, *125*, 11808–11809. (b) Kaseyama, T.; Furumi, S.; Zhang, X.; Tanaka, K.; Takeuchi, M. *Angew. Chem., Int. Ed.* **2011**, *50*, 3684–3687. (c) Sawada, Y.; Furumi, S.; Takai, A.; Takeuchi, M.; Noguchi, K.; Tanaka, K. *J. Am. Chem. Soc.* **2012**, *134*, 4080–4083. (d) Oyama, H.; Nakano, K.; Harada, T.; Kuroda, R.; Naito, M.; Nobusawa, K.; Nozaki, K. *Org. Lett.* **2013**, *15*, 2104–2107.

(18) (a) Maeda, H.; Bando, Y.; Shimomura, K.; Yamada, I.; Naito, M.; Nobusawa, K.; Tsumatori, H.; Kawai, T. *J. Am. Chem. Soc.* **2011**, *133*, 9266–9269. (b) Haketa, Y.; Bando, Y.; Takaishi, K.; Uchiyama, M.; Muranaka, A.; Naito, M.; Shibaguchi, H.; Kawai, T.; Maeda, H. *Angew. Chem., Int. Ed.* **2012**, *51*, 7967–7971.

(19) Review, see: (a) Maeda, H.; Bando, Y. *Pure Appl. Chem.* **2013**, *85*, 1967–1978. (b) CPL was observed from chiral orientation of flurophores. Based on axially chiral scaffolds: Kawai, T.; Kawamura, K.; Tsumatori, H.; Ishikawa, M.; Naito, M.; Fujiki, M.; Nakashima, T. *ChemPhysChem* **2007**, *8*, 1465–1468. (c) Tsumatori, H.; Nakashima, T.; Kawai, T.; *Org. Lett.* **2010**, *12*, 2362–2365. (d) Kimoto, T.; Tajima, N.; Fujiki, M.; Imai, Y.; *Chem.–Asian J.* **2012**, *7*, 2836–2841. (e) Amako, T.; Kimoto, T.; Tajima, N.; Fujiki, M.; Imai, Y. *RSC Adv.* **2013**, *3*, 6939–6944. (f) Amako, T.; Kimoto, T.; Tajima, N.; Fujiki, M.; Imai, Y. *Tetrahedron* **2013**, *69*, 2753–2757. (g) Kimoto, T.; Amako, T.; Tajima, N.; Kuroda, R.; Fujiki, M.; Imai, Y. *Asian J. Org. Chem.* **2013**, *2*, 404–410. (h) Kumar, J.; Nakashima, T.; Tsumatori, H.; Kawai, T. *J. Phys. Chem. Lett.* **2014**, *5*, 316–321. (i) Kitayama, Y.; Amako, T.; Suzuki, N.; Fujiki, M.; Imai, Y. *Org. Biomol. Chem.* **2014**, *12*, 4342–4346. (j) Based on centrally chiral scaffold: Kumar, J.; Nakashima, T.; Tsumatori, H.; Mori, M.; Naito, M.; Kawai, T. *Chem.–Eur. J.* **2013**, *19*, 14090–14097. (k) CPL from inherently achiral monochromophore systems is recently reported: Sánchez-Carnerero, E. M.; Moreno, F.; Maroto, B. L.; Agarrabeitia, A. R.; Ortiz, M. J.; Vo, B. G.; Muller, G.; de la Moya, S. *J. Am. Chem. Soc.* **2014**, *136*, 3346–3349.

(20) Some optically active conjugated polymers exhibit CPL. For polymers emitting CPL in their film or aggregation states: (a) Peeters, E.; M. Christiaans, P. T.; Janssen, R. A. J.; Schoo, H. F. M.; Dekkers H. P. J. M.; Meijer, E. W. *J. Am. Chem. Soc.* **1997**, *119*, 9909–9910. (b) Satrijio, A.; Meskers, S. C. J.; Swager, T. M. *J. Am. Chem. Soc.*, **2006**, *128*, 9030–9031. (c) Wilson, J. N.; Steffen, W.; McKenzie, T. G.; Lieser, G.; Oda, M.; Neher, D.; Bunz, U. H. F.; *J. Am. Chem. Soc.* **2002**, *124*, 6830–6831. (d) Langeveld-Voss, B. M. W.; Janssen, R. A.; Christiaans, M. P. T.; Meskers, S. C. J.; Dekkers, H. P. J. M.; Meijer, E. W. *J. Am. Chem. Soc.* **1996**, *118*, 4908–4909. (e) Oda, M.; Nothofer, H.-G.; Lieser, G.; Scherf, U.; Meskers, S. C. J.; Neher, D. *Adv. Mater.* **2000**, *12*, 362–365. (f) Oda, M.; Nothofer, H.-G.; Scherf, U.; Šunjić, V.; Richter, D.; Regenstein, W.; Meskers, S. C. J.; Neher, D. *Macromolecules* **2002**, *35*, 6792–6798. (g) Goto, H.; Akagi, K. *Angew. Chem., Int. Ed.* **2005**, *44*, 4322–4328. (h) Hayasaka, H.; Miyashita, T.; Tamura, K.; Akagi, K. *Adv. Funct.. Mater.* **2010**, *20*, 1243–1250. (i) Fukao S.; Fujiki, M. *Macromolecules* **2009**, *42*,

8062–8067. (j) Yu, J.-M.; Sakamoto, T.; Watanabe, K.; Furumi, S.; Tamaoki, N.; Chen, Y.; Nakano, T. *Chem. Commun.* **2011**, *47*, 3799–3801. (k) Watanabe, K.; Sakamoto, T.; Taguchi, M.; Fujiki, M.; and T. Nakano, *Chem. Commun.* **2011**, *47*, 10996–10998. (l) Hirahara, T.; Yoshizawa-Fujita, M.; Takeoka, Y.; Rikukawa, M. *Chem. Lett.* **2012**, *41*, 905–907. (m) Watanabe, K.; Koyama, Y.; Suzuki, N.; Fujiki, M.; Nakano, T. *Polym. Chem.* **2014**, *5*, 712–717. (n) For polymer aggregates in optically active solvents: Nakano, Y.; Liu, Y.; Fujiki, M. *Polym. Chem.* **2010**, *1*, 460–469. (o) Kawagoe, Y.; Fujiki, M.; Nakano, Y. *New J. Chem.* **2010**, *34*, 637–647. (p) For polymers emitting CPL in solution: Morisaki, Y.; Hifumi, R.; Lin, L.; Inoshita, K.; Chujo, Y. *Polym. Chem.* **2012**, *3*, 2727–2730. (q) Nagata, Y.; Nishikawa, T.; Suginome, M. *Chem. Commun.* **2014**, *50*, 9951–9953. (r) For CPL created by polymer–polymer complexation: Shiraki, T.; Tsuchiya, Y.; Noguchi, T.; Tamaru, S.; Suzuki, N.; Taguchi, M.; Fujiki, M.; Shinkai, S. *Chem.–Asian J.* **2014**, *9*, 218–222.

(21) Optically active helicene can be used as a chiral dopant for a conjugated polymer film, resulting in induced circularly polarized electroluminescence (CPEL): Yang, Y.; da Costa, R. C.; Smilgies, D.-M.; Campbell, A. J.; Fuchter, M. J. *Adv. Mater.* **2013**, *25*, 2624–2628.

(22) Pangborn, A. B.; Giardello, M. A.; Grubbs, R. H.; Rosen, R. K.; Timmers, F. J. *Organometallics* **1996**, *15*, 1518–1520.

(23) Hirose, K.; Miura, S.; Senda, Y.; Tobe, Y. *Chem. Commun*. **2012**, *48*, 6052–6054.

(24) Miura, Y.; Matsumoto, M.; Ushitani, Y. *Macromolecules*, **1993**, *26*, 6673–6675.

(25) Neese, F. *WIREs Comput. Mol. Sci.* **2012**, *2*, 73–78.

Chapter 5

Optically Active Cyclic Compounds Based on Planar Chiral [2.2]Paracyclophane: Extension of π-Surface with Naphthalene Units

Abstract

The author synthesized optically active cyclic compounds with extension of π-surface with naphthalene units based on a planar chiral 4,7,12,15-tetrasubstituted [2.2]paracyclophane framework. Tuning of the properties of the cyclic compounds was possible changing aromatic moieties. Hypsochromic effect was observed by absorption and photoluminescence (PL) spectra of naphthalene-containing cyclic derivatives compared with those of benzene-containing compounds. As a result, light blue and light green emission were observed in the naphthalene- and the benzene-containing cyclic compounds, respectively. Density functional theory (DFT) indicated that HOMO-LUMO band gap increased with introducing naphthalene units. Optimized structures showed that one of reasons of the hypsochromic effect was torsions of the cyclic structure. The naphthalene-containing cyclic derivatives had larger molar extinction coefficient (ε) and photoluminescence quantum efficiency (Φ_{lum}) and benzene-containing cyclic derivatives had larger g_{lum} values. These results are useful for the design of cyclic compounds and CPL materials.

Introduction

It is necessary to design π-conjugated compounds with conductive, luminescent, and charge transfer properties for various material applications, such as opto-electronic devices.[1] Among π-conjugated compounds, [2.2]paracyclophane has been widely studied as a three-dimensional π-conjugation building block owing to its unique structure of face-to-face oriented two benzene rings.[2] [2.2]Paracyclophane was firstly prepared by Brown and Farthing in 1949 by pyrolysis of *p*-xylene,[3] and Cram and Steinberg reported its direct synthesis by a Wurtz-type intramolecular cyclization of 1,4-bis(bromomethyl)benzene in 1951.[4] Representative properties of [2.2]paracyclophane are through-space conjugation and planar chirality derived from the interaction of the two benzene rings and the suppression of the rotation of the benzene rings, respectively. The author focused on these unique properties and developed an optical resolution method of 4,7,12,15-tetrasubstituted [2.2]paracyclophane, as shown in Chapter 3.[5] Especially in the research of a planar chiral 4,7,12,15-tetrasubstituted [2.2]paracyclophane, the author revealed that propeller-shaped cyclic compounds exhibited high performance of circular dichroism (CD) and circularly polarized luminescence (CPL) properties.[5] In Chapter 4, the author tried to enhance the properties of the planar chiral cyclic compounds using phenylene-ethynylene substituents. As a result, the author succeeded in the synthesis of the compounds exhibiting excellent CD and CPL properties.[6] In this case, a bathochromic effect was observed owing to extension of the π-conjugation. Therefore, it is important to obtain the compounds which exhibit a hypsochromic effect for the diversity of designability of the cyclic compounds. In this chapter, the author observed the hypsochromic effect using naphthalene units in place of benzene units as a cyclic linker. In addition, molar extinction coefficient (ε) and photoluminescence quantum efficiency (Φ_{lum}) were improved in comparison with the benzene-containing compounds. These are very important factors for applications for optical materials. Details were investigated with density functional theory (DFT), showing that a HOMO-LUMO

band gap of naphthalene-containing cyclic derivatives became larger than that of benzene-containing compounds. Optimized structures indicated torsions of the cyclic structure affected the extension of the π-conjugation. Herein, the synthesis and optical properties of these compounds are discussed.

Results and Discussion

Synthesis

The optical resolution of planar chiral 4,7,12,15-tetrasubstituted [2.2]paracyclophane was carried out using the diastereomer method developed in Chapter 3, and the obtained enantiopure compounds were converted to the corresponding (R_p)- and (S_p)-4,7,12,15-tetraethynyl[2.2]paracyclophanes.[5] The synthetic routes to the target optically active cyclic compounds are shown in Schemes 1-5. Initially, the author prepared iodinated naphthalene compounds **3** and **9** to prepare the cyclic compounds (Schemes 1 and 2, respectively). Compound **10** was synthesized according to the literature (see the experimental section). The hexyloxy groups in **3** and **10**, and butyl groups in **9** were introduced to provide the target compounds with solubility in organic solvents, such as THF, $CHCl_3$, CH_2Cl_2 and toluene.

As shown in Scheme 1, one of bromides of 2,3-dibromo-6,7-bis(hexyloxy)naphthalene **1** was reacted with trimethylsilylacetylene in the presence of a catalytic amount of $PdCl_2(PPh_3)_2$ to obtain compound **2** in 26% isolated yield. The other bromide of **2** was converted to an iodide, and then iodinated compound **3** was obtained in 73% isolated yield. As shown in Scheme 2, 1,2,4,5-tetraboromobenzene **4** was reacted with 2,5-dibutylfuran **5** in the presence of *n*-butyllithium to obtain compound **6** in 71% isolated yield, which was reacted with sodium iodide and trimethysilyl chloride to obtain compound **7** in 83% isolated yield. One of bromides in compound **7** was reacted with trimethylsilylacetylene in the presence of a catalytic amount

Scheme 1. Synthesis of compound **3** (cyclic linker of **NpC**)

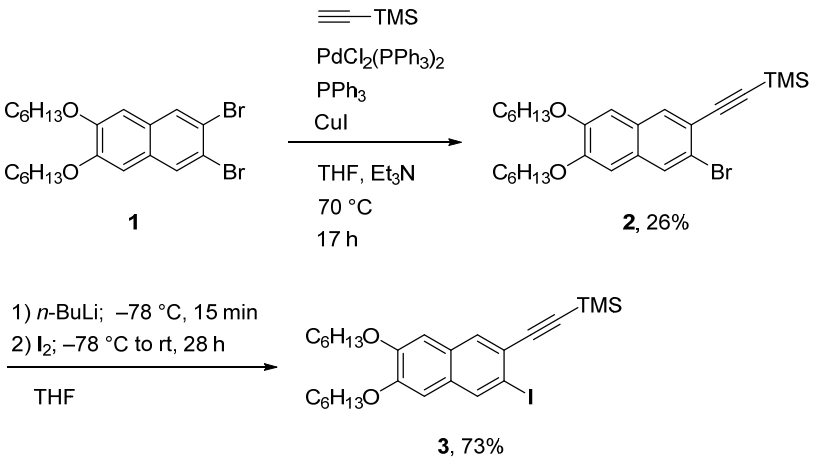

Scheme 2. Synthesis of compound **9** (cyclic linker of **NpBu$_2$C**)

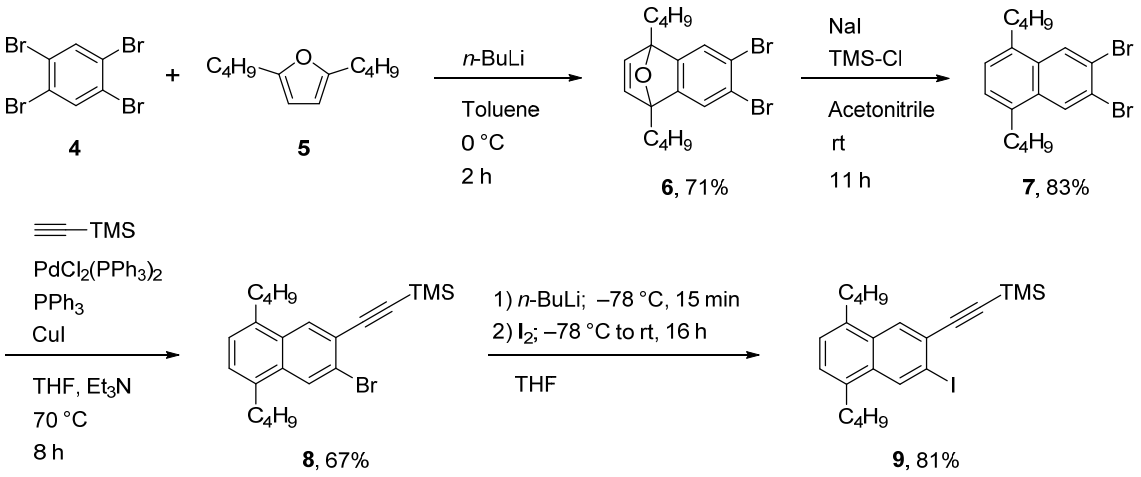

of $PdCl_2(PPh_3)_2$ to obtain compound **8** in 67% isolated yield. The other bromide of **8** was converted to an iodide, and then iodinated compound **9** was obtained in 81% isolated yield.

Schemes 3, 4 and 5 show the syntheses of the target cyclic compounds **NpC**, **PhC** and **NpBu$_2$C**, respectively. In these Schemes, only the reactions of the (R_p)-isomers are shown; the (S_p)-isomers were synthesized under identical conditions from (S_p)-**Cp**. The treatment of (R_p)-4,7,12,15-tetraethynyl[2.2]paracyclophane (R_p)-**Cp** with compound **3** in the presence of the $Pd_2(dba)_3$/CuI catalytic system using dppf as a phosphine ligand afforded compound (R_p)-**Np-**

TMS in 61% isolated yield (Scheme 3). After deprotection of the four TMS groups in (R_p)-**Np-TMS** using NBu_4F, a Pd-mediated alkyne homo-coupling was carried out *in situ* to obtain cyclic compound (R_p)-**NpC** in 29% isolated yield. Under the same reaction conditions, compounds (R_p)-**PhC** and (R_p)-**NpBu$_2$C** were prepared by the reaction of **10** with (R_p)-**Cp** and by the reaction of **9** with (R_p)-**Cp** as shown in Schemes 4 and 5, respectively. In order to improve the reactivity, di(1-adamantyl)-*n*-butylphosphine[7] (cataCXium® A) was used as a phosphine ligand. Cyclization was carried out, unidentified impurities such as oligomeric products by intermolecular reactions were formed. They could be readily removed by column chromatography on SiO_2, resulting in low isolated yields (29%, 20% and 18% for (R_p)-**NpC**, (R_p)-**PhC** and (R_p)-**NpBu$_2$C**, respectively). The structures of all new compounds in this study were confirmed by ^1H and ^{13}C NMR spectroscopy, high-resolution mass spectrometry (HRMS), and elemental analysis; the detailed synthetic procedures and NMR spectra data are shown in the experimental section.

Scheme 3. Synthesis of (R_p)-**NpC**

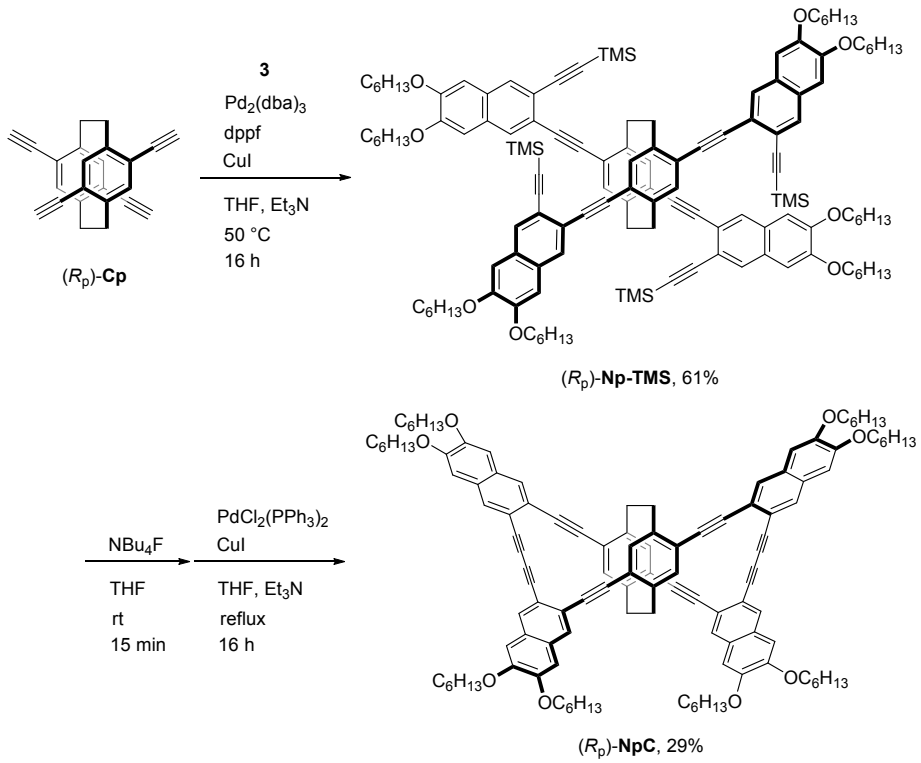

Scheme 4. Synthesis of (R_p)-**PhC**

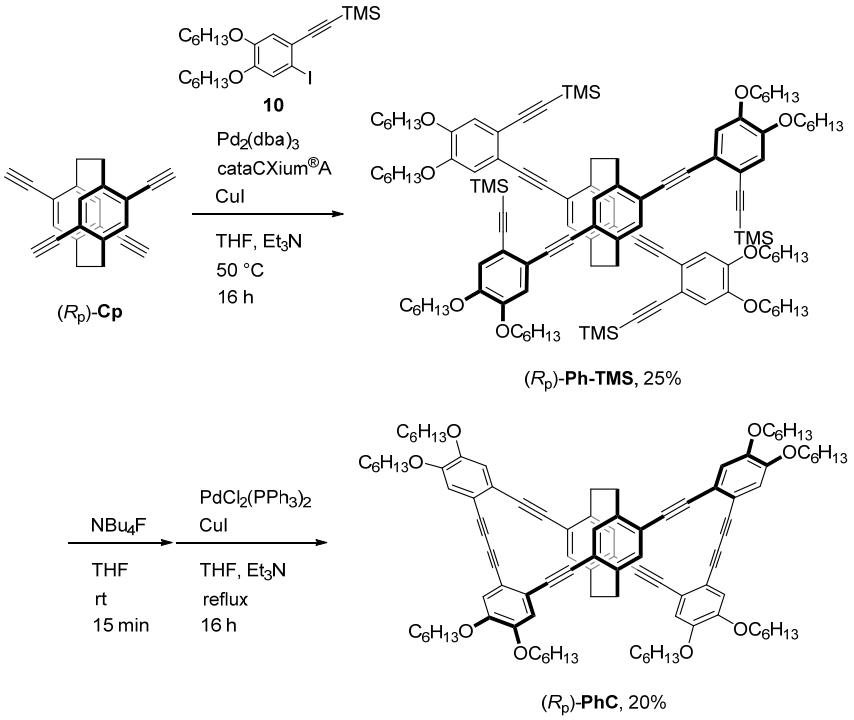

Scheme 5. Synthesis of (R_p)-**NpBu$_2$C**

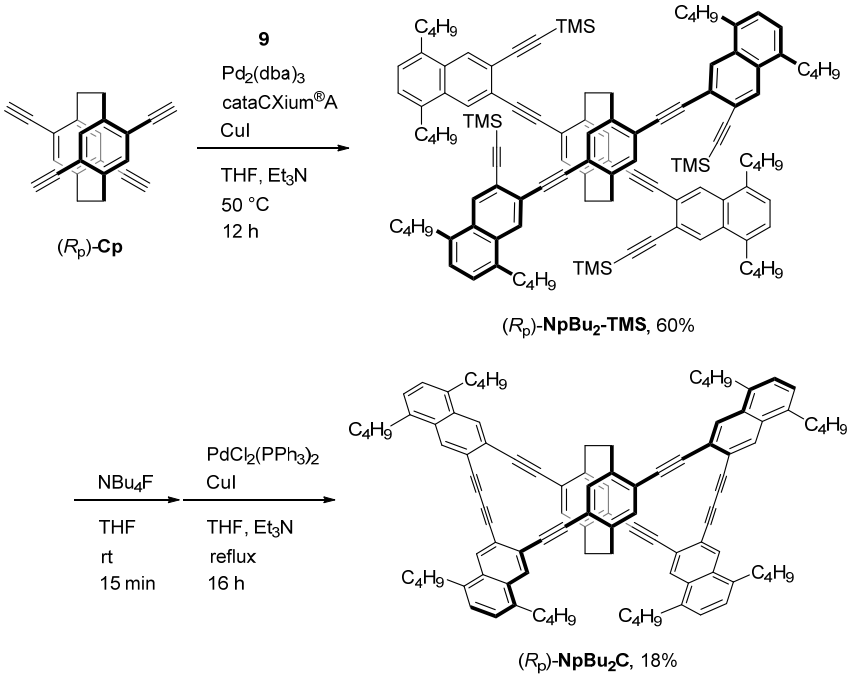

Optical Properties

The optical properties of both enantiomers of cyclic compounds **NpC**, **PhC**, and **NpBu$_2$C** as well as their precursors **Np-TMS**, **Ph-TMS** and **NpBu$_2$-TMS** were evaluated. The data are summarized in Table 1. Although the optical and chiroptical properties of **PhtBu-TMS** and **PhtBuC** were shown in Chapter 3, they are included herein for comparison.

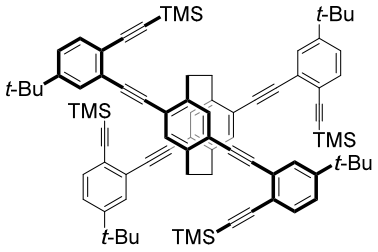

PhtBu-TMS

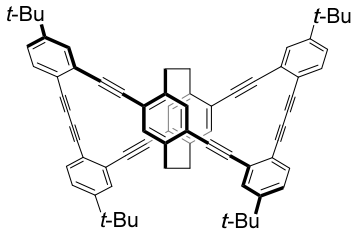

PhtBuC

Table 1. Optical properties: Spectroscopic data of (R_p)-isomers

	λ_{abs}[a]/nm (ε / 10^5 M^{-1} cm^{-1})	λ_{lum}[b]/nm	τ[c]/ns (χ^2)	Φ_{lum}[d]
(R_p)-**Np-TMS**	382 (0.96)	426	1.33 (1.01)	0.65
(R_p)-**Ph-TMS**	384 (0.58)	428	1.71 (1.07)	0.59
(R_p)-**NpBu$_2$-TMS**	388 (0.86)	424	1.54 (1.03)	0.77
(R_p)-**PhtBu-TMS**	372 (0.44)	418	2.16 (1.04)	0.46
(R_p)-**NpC**	353 (1.29)	446	1.83 (1.06)	0.51
(R_p)-**PhC**	325 (1.18), 401 (0.49)	482	4.67 (1.18)	0.44
(R_p)-**NpBu$_2$C**	348 (1.63), 412 (0.57)	438	2.00 (1.12)	0.81
(R_p)-**PhtBuC**	314 (1.25), 391 (0.46)	453	3.75 (1.06)	0.41

[a] In $CHCl_3$ (1.0×10^{-5} M). [b] In $CHCl_3$ (1.0×10^{-6} M), excited at absorption maxima. [c] Emission life time at λ_{lum}. [d] Absolute PL quantum efficiency.

Figures 1A and 1B show the UV-vis absorption spectra and photoluminescence (PL) spectra of the (R_p)-precursors in the dilute $CHCl_3$ solutions (1.0×10^{-5} M for UV and 1.0×10^{-6} M for PL), respectively. The absorption spectra exhibited a hyperchromic effect with extension of the π-surface from (Figure 1A). Bathochromic shift was caused by two factors; attaching naphthalene unit in place of benzene unit and attaching alkoxy groups. On the other hand, absorption edge was almost identical between (R_p)-**Np-TMS** and (R_p)-**NpBu$_2$-TMS** because

alkoxy groups were relatively far from alkyne unit attached the [2.2]paracyclophane core in the ground state. In the PL spectra (Figure 1B), a similar bathochromic shift was observed with extension of the π-conjugation unit and the introducing alkoxy group. A little bathochromic shift was observed in (R_p)-**Np-TMS** compared with (R_p)-**NpBu$_2$-TMS**. This result showed alkoxy groups in the naphthalene unit worked in the excited state.

As shown in Figures 2A and B, the interesting tendencies were observed in the absorption and PL spectra of cyclic compounds (R_p)-**NpC**, (R_p)-**PhC**, (R_p)-**NpBu$_2$C** and (R_p)-**PhtBuC**. In the absorption spectra, bathochromic shift was observed by the cyclization and introducing alkoxy groups. The alkoxy groups in the naphthalene unit affected the spectra in the cyclic form. In addition, a hypsochromic shift was observed with an extension of the π-surface by the naphthalene unit. It is interesting phenomenon, considering that the precursors exhibited the similar absorption edge ((R_p)-**Np-TMS**, (R_p)-**Ph-TMS** and (R_p)-**NpBu$_2$-TMS**). In the PL spectra (Figure 2B), a similar bathochromic shift and hypsochromic shift were observed. In this case, a hypsochromic shift from (R_p)-**PhtBuC** to (R_p)-**NpBu$_2$C** was clearly observed. In addition, Stokes shifts of (R_p)-**PhC** and (R_p)-**PhtBuC** were larger than those of (R_p)-**NpC** and (R_p)-**NpBu$_2$C**.

PL lifetime measurement was carried out to support optical data. Table 1 includes the PL decay data (PL lifetime (τ) and χ^2 parameters) for all compounds. PL lifetime of the cyclization compounds was longer than that of the precursors. In addition, the difference of lifetime of naphthalene derivatives between the cyclic compounds and the precursors is smaller than that of benzene compounds. Therefore, naphthalene-containing cyclic compounds were relatively similar to the precursors compared with benzene-containing compounds. This may be one of the reasons of the hypsochromic shift.

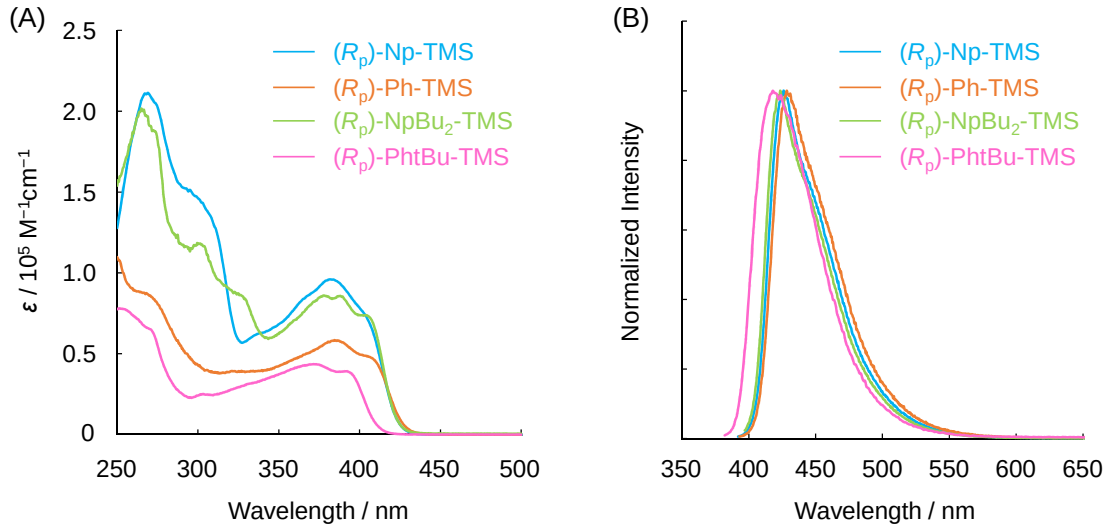

Figure 1. (A) UV-vis absorption spectra in the dilute $CHCl_3$ (1.0×10^{-5} M) and (B) PL spectra in the dilute $CHCl_3$ (1.0×10^{-6} M; excited at absorption maximum from 350 to 500 nm) of (R_p)-**Np-TMS**, **Ph-TMS**, **NpBu$_2$-TMS**, and **PhtBu-TMS**.

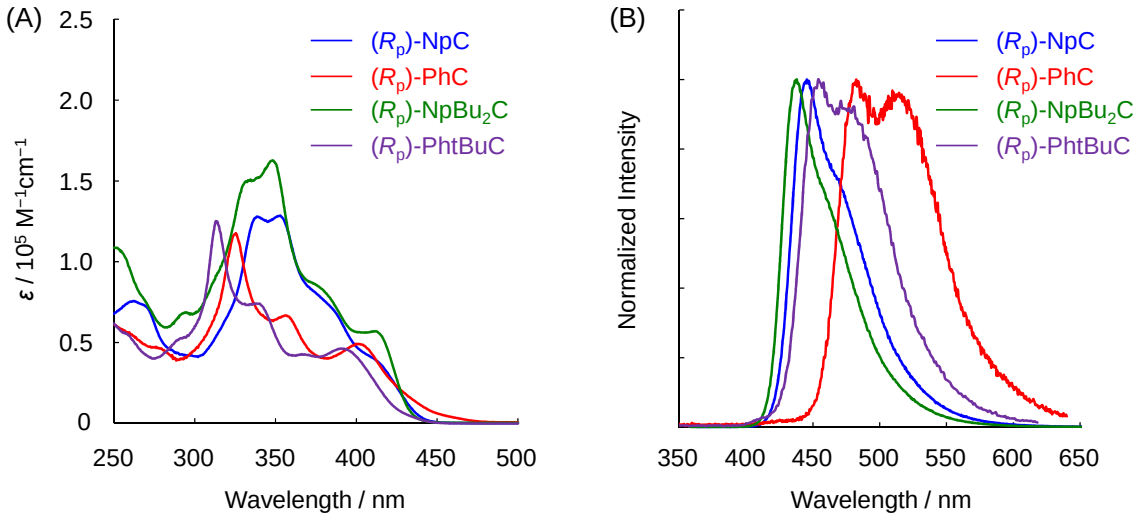

Figure 2. (A) UV-vis absorption spectra in the dilute $CHCl_3$ (1.0×10^{-5} M) and (B) PL spectra in the dilute $CHCl_3$ (1.0×10^{-6} M; excited at absorption maximum) of (R_p)-**NpC**, **PhC**, **NpBu$_2$C**, and **PhtBuC**.

Chiroptical Properties

The chiroptical properties of the ground and excited states of **Np-TMS**, **Ph-TMS**, **NpBu$_2$-TMS**, **NpC**, **PhC**, and **NpBu$_2$C** were investigated by circular dichroism (CD) and CPL spectroscopy, respectively. Chiroptical data, such as specific rotation, CD and CPL dissymmetry factors[8] (g_{abs} and g_{lum}, respectively) are summarized in Table 2. The chiroptical data of **PhtBu-TMS** and **PhtBuC** are shown in the same table. Figure 3 shows the CD and absorption spectra of both enantiomers of **Np-TMS**, **Ph-TMS**, **NpBu$_2$-TMS** and **PhtBu-TMS** in the dilute $CHCl_3$ (1.0×10^{-5} M). In all cases, mirror image Cotton effects were observed in the CD spectra, and the g_{abs} values of the first cotton effect were estimated to be approximately -1.5×10^{-3} for (R_p)-isomers. The g_{abs} values were enhanced by the cyclization and the values for (R_p)-**NpC**, **PhC**, **NpBu$_2$C** and **PhtBuC** were estimated to be, $+3.3 \times 10^{-3}$, $+3.9 \times 10^{-3}$, $+0.67 \times 10^{-3}$, and $+8.8 \times 10^{-3}$, respectively (Figure 4). The specific rotation $[\alpha]^{23}_D$ values for (R_p)-**NpC**, **PhC**, **NpBu$_2$C** and **PhtBuC** were +789.4, +1086.4, +1040.13, +1501.0, respectively. They were much larger than those of (R_p)-**Np-TMS**, **Ph-TMS**, **NpBu$_2$-TMS** and **PhtBu-TMS** (Table 2). It is suggested that optically active higher-ordered (propeller-shaped) structures by cyclization induced chirality strongly in the cyclic compounds in the ground state.

The CPL spectra of the precursors and cyclic compounds in the dilute $CHCl_3$ (1.0×10^{-5} M) are shown in Figures 5 and 6 respectively. Intense and mirror image CPL spectra were observed for the enantiomers, as shown in Figures 5 and 6. The g_{lum} values of (R_p)-**Np-TMS**, **Ph-TMS**, **NpBu$_2$-TMS** and **PhtBu-TMS** were large (approximately, -1.4×10^{-3} for the (R_p)-isomers, respectively; Table 2). On the other hand, the g_{lum} values for (R_p)-**NpC**, **PhC**, **NpBu$_2$C** and **PhtBuC** were calculated to be $+3.5 \times 10^{-3}$, $+8.4 \times 10^{-3}$, $+0.84 \times 10^{-3}$, and $+13 \times 10^{-3}$, respectively (Table 2). **NpBu$_2$C** exhibited very weak CPL signals. Considering that **NpBu$_2$C** had the similar structure with **NpC**, this is a very interesting phenomenon. As expected, the g_{lum} values for the cyclic compounds were enhanced in comparison with those for the

precursors by the optically active propeller-shaped structures. The emitting species with higher-ordered structures have a potential to exhibit good CPL properties in the excited state. For example, propeller-shaped,[5,6] V-shaped,[9] S-shaped,[10] and helical structures[11] have been reported previously.

Table 2. Chiroptical properties: Specific rotation and spectroscopic data of (R_p)-isomers

	$[\alpha]^{23}_D$[a]	g_{abs} / 10^{-3} at λ_{abs}[b]	g_{lum} / 10^{-3} at $\lambda_{lum,\,max}$[c]
(R_p)-**Np-TMS**	−41.2	−1.4	−1.4
(R_p)-**Ph-TMS**	−17.9	−1.3	−1.5
(R_p)-**NpBu$_2$-TMS**	−183.7	−1.8	−1.4
(R_p)-**PhtBu-TMS**	−45.4	−1.3	−1.4
(R_p)-**NpC**	+789.4	+3.3	+3.5
(R_p)-**PhC**	+1086.4	+3.9	+8.4
(R_p)-**NpBu$_2$C**	+1040.1	+0.67	+0.84
(R_p)-**PhtBuC**	+1501.0	+8.8	+13

[a] Specific rotation (*c* 0.1, $CHCl_3$ at 23 °C). The $[\alpha]^{23}_D$ values of (S_p)-isomers are described in the experimental section. [b] $g_{abs} = 2\Delta\varepsilon/\varepsilon$, where $\Delta\varepsilon$ indicates differences of absorbance between left- and right-handed circularly polarized light, respectively. The g_{abs} value of the first peak top was estimated. [c] $g_{lum} = 2(I_{left} - I_{right})/(I_{left} + I_{right})$, where I_{left} and I_{right} indicate luminescence intensities of left- and right-handed CPL, respectively.

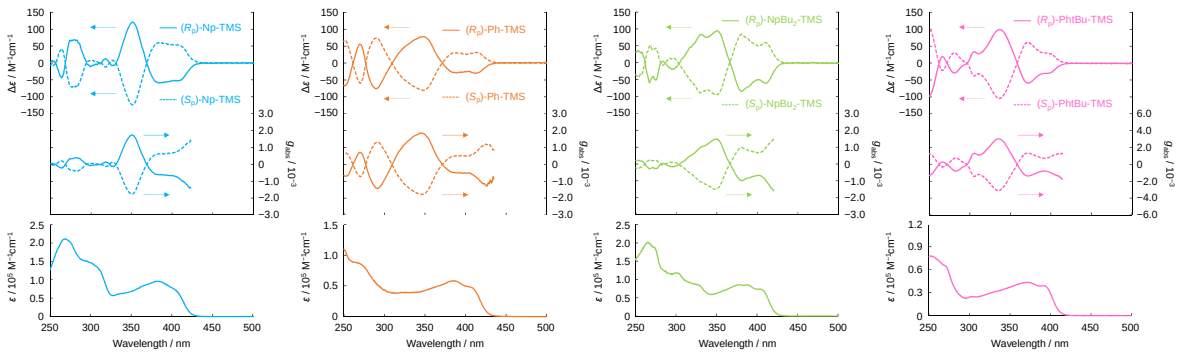

Figure 3. CD (top), g_{abs} (middle), and UV-vis absorption (bottom) spectra of **Np-TMS**, **Ph-TMS**, **NpBu$_2$-TMS**, and **PhtBu-TMS** in the dilute $CHCl_3$ (1.0×10^{-5} M).

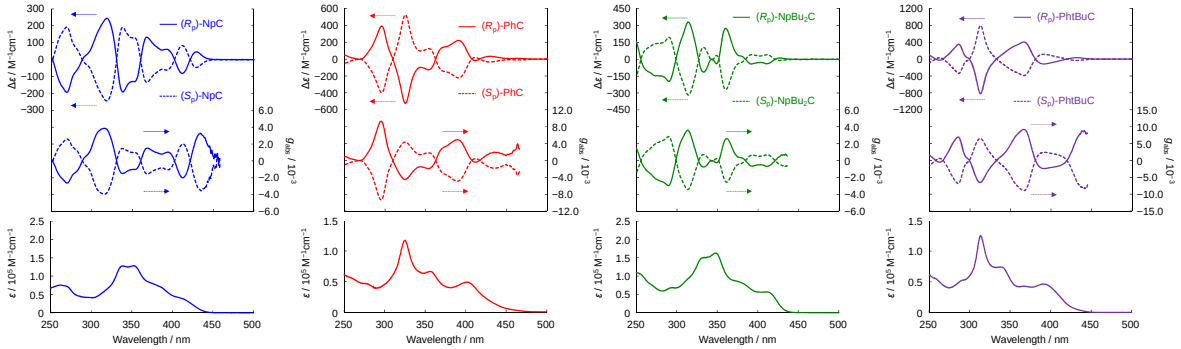

Figure 4. CD (top), g_{abs} (middle), and UV-vis absorption (bottom) spectra of **NpC**, **PhC**, **NpBu$_2$C**, and **PhtBuC** in the dilute $CHCl_3$ (1.0×10^{-5} M).

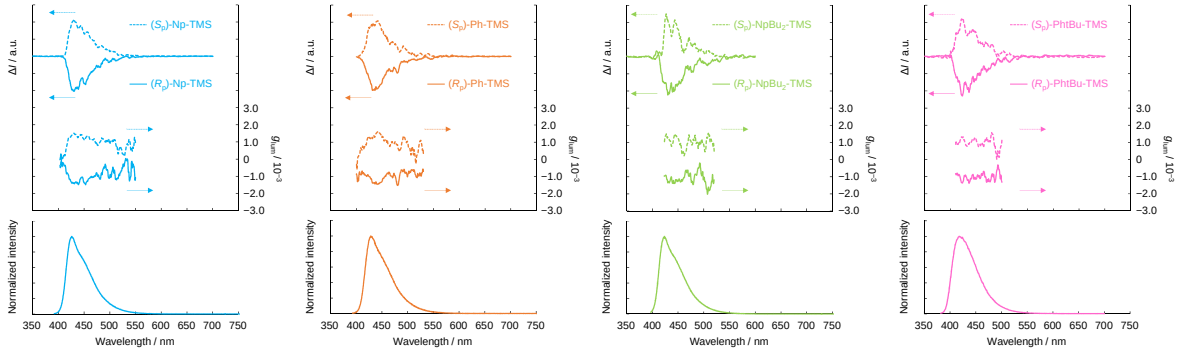

Figure 5. CPL (top), g_{lum} (middle), and PL (bottom) spectra of **Np-TMS**, **Ph-TMS**, **NpBu$_2$-TMS**, and **PhtBu-TMS** in the dilute $CHCl_3$ (1.0×10^{-5} M for CPL and 1.0×10^{-6} M for PL). Excitation wavelength was 300 nm, 350 nm 300 nm and 300 nm for **NpC**, **PhC**, **NpBu$_2$C**, and **PhtBuC**, respectively.

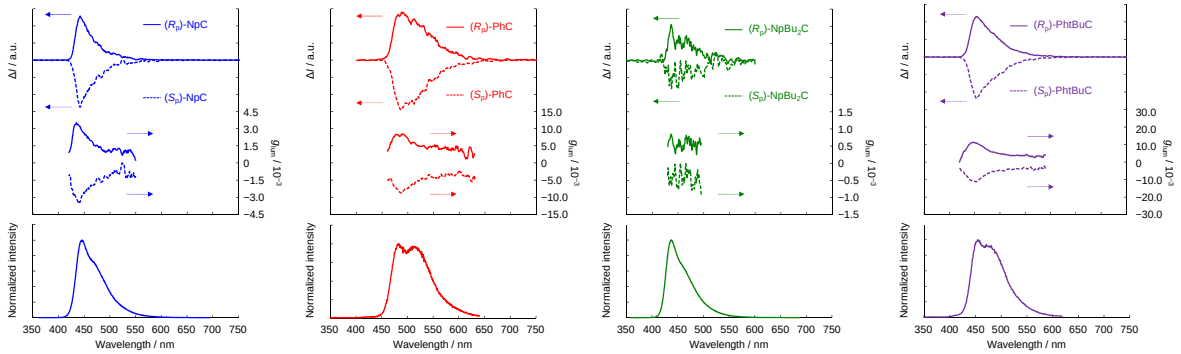

Figure 6. CPL (top), g_{lum} (middle), and PL (bottom) spectra of **NpC**, **PhC**, **NpBu$_2$C**, and **PhtBuC** in the dilute $CHCl_3$ (1.0×10^{-5} M for CPL and 1.0×10^{-6} M for PL). Excitation wavelength was 300 nm, 350 nm, 300 nm, and 314 nm for **NpC**, **PhC**, **NpBu$_2$C**, and **PhtBuC**, respectively.

Figure 7 shows the highest occupied molecular orbitals (HOMOs) and the lowest unoccupied molecular orbitals (LUMOs) of the cyclic compounds **NpC**, **PhC**, **NpBu$_2$C** and **PhtBuC**; methyl groups were used in place of hexyl and butyl groups to simplify the calculation. The molecular orbitals were obtained by density functional theory (DFT) at the TD-BHandHLYP/def2-TZVPP//BLYP/def2-TZVPP level. Only in the case of **NpBu$_2$C**, the HOMO orbital did not form a cyclic π-conjugation system and the HOMO−1 orbital was delocalized whole of the molecule. The energies of the HOMO and HOMO−1 were very close, resulting in the weak CPL of **NpBu$_2$C**. Figure 7 shows that naphthalene derivatives had low HOMO levels and high LUMO levels and that alkoxy groups increased HOMO and LUMO levels, especially HOMO levels. The first Cotton effects in the CD spectra (Figure 4) were assigned to the S_0 to S_1 transition (Table 3). Experimental data of wavelength of the first Cotton effect in the CD spectra are shown in Table 3. The hypsochromic shift by the naphthalene unit was almost identified between calculation and experimental data. In order to investigate the cause of the hypsochromic shift, the author focused on the torsion of the cyclic compounds. Calculated torsion angles, θ_1 and θ_2 are shown in Figure 8, and the parameters are shown in Table 3. The torsions of the naphthalene-containing cyclic compounds were relatively larger than those of benzene-containing compounds. Therefore, it is difficult to extend π-conjugation in the naphthalene derivatives. Those results support the lifetime measurement which indicated that the properties were similar to the precursors. As a result, the hypsochromic shift was caused by shorter π-conjugation length of the naphthalene substituents.

Comparing with the compounds having benzene and naphthalene units in the cyclic structures, the benzene unit can enhance *g* values and the naphthalene unit can enhance a molar extinction coefficient and absolute fluorescence quantum efficiency (Φ_{lum}) (Tables 1 and 2), which are very important factors for CPL applications. In addition, the naphthalene unit induced the hypsochromic shift compared with the benzene unit. These results indicate the

possibility to tune the optical properties of the cyclic compounds exhibiting good chiroptical properties.[12,13]

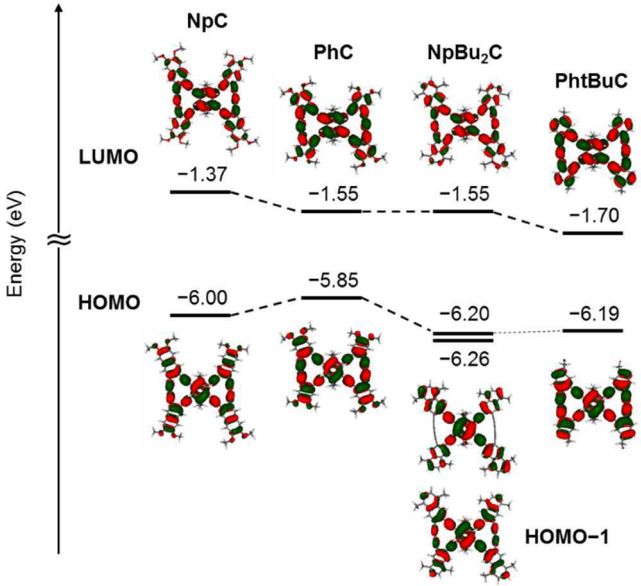

Figure 7. HOMOs (HOMO−1) and LUMOs of model compounds, **NpC**, **PhC**, **NpBu$_2$C**, and **PhtBuC** obtained by density functional theory (DFT) at the TD-BHandHLYP/def2-TZVPP//BLYP/def2-TZVPP level.

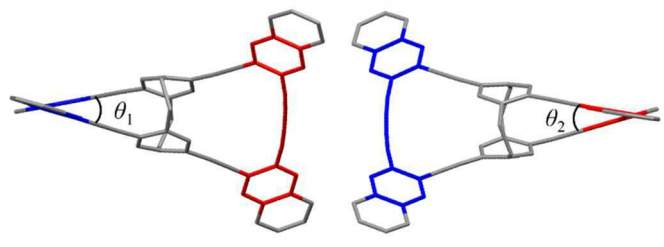

Figure 8. Torsion angles, θ_1 and θ_2, of cyclic compounds.

Table 3. Calculated parameter from TD-DFT and experimental wavelength obtained from CD spectra

	S_0 to S_1[a]/eV (nm)	λ_{abs}[b]/nm	θ_1[c]	θ_2[c]
NpC	3.02 (411)	429	24.55˚	22.78˚
PhC	2.72 (456)	464	22.96˚	23.17˚
NpBu$_2$C	3.05 (406)	428	24.68˚	23.12˚
PhtBuC	2.84 (436)	431	22.30˚	21.79˚

Calculated at TD-BHandHLYP/def2-TZVPP//BLYP/def2-TZVPP level. [a] Energy band gap of transition from S_0 to S_1. [b] Wavelength observed from first Cotton effect of CD spectra of **NpC**, **PhC**, **NpBu$_2$C**, and **PhtBuC**, respectively (Figure 5). [c] Estimated torsion angles of each optimized molecular structure (Figure 8).

Conclusions

In summary, planar chiral [2.2]paracyclophane-based cyclic compounds with extended π-surface were synthesized. Cyclization enhanced the optical and chiroptical properties compared with those of the non-cyclic precursors because of the optically active higher-ordered structure. The optical and chiroptical properties could be tuned by the benzene and naphthalene units. Introduction of the naphthalene unit enhanced a molar extinction coefficient and absolute fluorescence quantum efficiency; however g_{lum} values decreased in comparison with induction of the benzene unit. Another interesting property was hypsochromic shift by the introduction of the naphthalene unit. As a result, **NpC** exhibited light blue emission, and **PhC** exhibited light green emission. DFT supported this phenomenon; cyclic structure including a naphthalene unit decreased HOMO levels and increased LUMO levels in spite of the large π-surface. Calculated molecular structure indicated that the torsion was one of the reasons of the hypsochromic shift. These results are useful for the molecular design not only of the cyclic [2.2]paracyclophane derivatives but of various optically active compounds.

Experimental Section

General. ^{1}H and ^{13}C NMR spectra were recorded on JEOL EX400 and AL400 instruments at 400 and 100 MHz, respectively. Samples were analyzed in $CDCl_3$, and the chemical shift values were expressed relative to Me_4Si as an internal standard. Analytical thin layer chromatography (TLC) was performed with silica gel 60 Merck F254 plates. Column chromatography was performed with Wakogel C-300 silica gel. High-resolution mass (HRMS) spectrometry was performed at the Technical Support Office (Department of Synthetic Chemistry and Biological Chemistry, Graduate School of Engineering, Kyoto University), and the HRMS spectra were obtained on a Thermo Fisher Scientific EXACTIVE spectrometer for atmospheric pressure chemical ionization (APCI). Recyclable preparative high-performance liquid chromatography (HPLC) was carried out on a Japan Analytical Industry Co. Ltd., Model LC918R (JAIGEL-1H and 2H columns) and LC9204 (JAIGEL-2.5H and 3H columns) using $CHCl_3$ as an eluent. UV-vis spectra were recorded on a SHIMADZU UV-3600 spectrophotometer, and samples were analyzed in $CHCl_3$ at room temperature. Fluorescence emission spectra were recorded on a HORIBA JOBIN YVON Fluoromax-4 spectrofluorometer, and samples were analyzed in $CHCl_3$ at room temperature. The PL lifetime measurement was performed on a Horiba FluoroCube spectrofluorometer system; excitation was carried out using a UV diode laser (NanoLED 375 nm). Specific rotations ($[\alpha]^{t}_{D}$) were measured with a HORIBA SEPA-500 polarimeter. Circular dichroism (CD) spectra were recorded on a JASCO J-820 spectropolarimeter with $CHCl_3$ as a solvent at room temperature. Circularly polarized luminescence (CPL) spectra were recorded on a JASCO CPL-200S with $CHCl_3$ as a solvent at room temperature. Elemental analyses were performed at the Microanalytical Center of Kyoto University.

Materials. Commercially available compounds used without purification: (Wako Pure Chemical Industries, Ltd.) PPh_3, CuI, K_2CO_3, NaI; (Tokyo Chemical Industry Co, Ltd.) trimethylsilylacetylene (TMS-acetylene), $PdCl_2(PPh_3)_2$, $Pd_2(dba)_3$ (dba = dibenzylideneacetone), 1,1'-bis(diphenylphosphino)ferrocene (dppf), tetra-*n*-butylammonium fluoride (NBu_4F, TBAF, 1 M in THF), trimethylsilyl chloride (TMS-Cl); (Kanto Chemical Co., Inc.) *n*-butyllithium (*n*-BuLi, 1.6 M in hexane); (Sigma-Aldrich Co. LLC.) di(1-adamantyl)-*n*-butylphosphine (cataCXium® A). Commercially available solvents: MeOH (Wako Pure Chemical Industries, Ltd.), toluene (deoxygenated grade, Wako Pure Chemical Industries, Ltd.) and acetonitrile (deoxygenated grade, Wako Pure Chemical Industries, Ltd.) used without purification. THF (Wako Pure Chemical Industries, Ltd.) and Et_3N (Kanto Chemical Co., Inc.), purified by passage through solvent purification columns under Ar pressure.[14] Compounds

prepared according to the literatures: 2,3-Dibromo-6,7-bis(hexyloxy)naphthalene (**1**)[15], 2,5-di-*n*-butylfuran (**5**)[16], 1,2-bis(hexyloxy)-4-iodo-5-[2-(trimethylsilyl)ethynyl]benzene (**10**)[17], (R_p)- and (S_p)-4,7,12,15-tetraethynyl[2.2]paracyclophane ((R_p)- and (S_p)-**Cp**).[5]

Computational Details. The Orca program package[18] was used for computation. The author optimized the structures of **NpC**, **PhC**, **NpBu$_2$C** and **PhtBuC** (methyl groups were used in place of hexyl and butyl groups) in the ground S_0 states and calculated their electric structures. The density functional theory (DFT) was applied for the optimization of the structures in the S_0 states at the BLYP/def2-TZVPP levels. The author calculated the electric states and transitions from S_0 to S_1 of the **NpC**, **PhC** and **PhtBuC**, and from S_0 to S_1 and S_0 to S_2 states of the **NpBu$_2$C** with the optimized geometries in the S_0 states by time-dependent DFT (TD-DFT) at the TD-BHandHLYP/def2-TZVPP levels.

Synthesis of 2. A mixture of 2,3-dibromo-6,7-bis(hexyloxy)naphthalene (**1**) (3.93 g, 8.1 mmol), $PdCl_2(PPh_3)_2$ (0.284 g, 0.405 mmol), CuI (0.0770 g, 0.405 mmol), THF (180 mL) and Et_3N (60 mL) was placed in a round-bottom flask equipped with a magnetic stirring bar. After degassing the reaction mixture several times, TMS-acetylene (1.20 mL, 8.49 mmol) was added to the mixture via a syringe. The reaction was carried out at 70 °C for 17 h with stirring. After the reaction mixture was cooled to room temperature, precipitates were removed by filtration, and the solvent was removed with a rotary evaporator. The residue was purified by column chromatography on SiO_2 ($CHCl_3$/hexane = 1/2 v/v as an eluent) to afford **2** (1.06 g, 2.11 mmol, 26%) as a yellow solid. R_f = 0.33 ($CHCl_3$/hexane = 1/2 v/v). ^{1}H NMR ($CDCl_3$, 400 MHz) δ 0.29 (s, 9H), 0.91 (t, J = 7.1 Hz, 6H), 1.34-1.38 (m, 8H), 1.50 (m, 4H), 1.84-1.88 (m, 4H), 4.05 (dt, J = 2.4 Hz, 6.6 Hz, 4H), 6.92 (s, 1H), 6.96 (s, 1H), 7.82 (s, 1H), 7.84 (s, 1H) ppm; ^{13}C NMR ($CDCl_3$, 100 MHz) δ −0.1, 14.0, 22.6, 25.7, 28.9, 28.9, 31.5, 68.8, 97.9, 103.9, 106.3, 107.0, 119.6, 120.1, 127.5, 129.0, 130.0, 131.8, 150.1, 150.9 ppm. HRMS (APCI) calcd. for $C_{27}H_{40}BrO_2Si$ $[M+H]^+$: 503.1975, found: 503.1967. Elemental analysis calcd. for $C_{27}H_{39}BrO_2Si$: C 64.40 H 7.81 Br 15.87, found: C 64.31 H 7.92 Br 15.88.

Synthesis of 3. A solution of *n*-BuLi (1.65 M in hexane, 1.45 mL, 2.32 mmol) was slowly added to a solution of **2** (1.06 g, 2.11 mmol) in THF (40 mL) at –78 °C under Ar atmosphere. After 30 min, a solution of iodine (0.80 g, 3.16 mmol) in THF (10 mL) was added, and the mixture was stirred for 28 h at –78 °C to room temperature. The reaction mixture was quenched by the addition of aqueous $NaHSO_3$ solution, and the organic layer was extracted three times with hexane. The combined organic layer was washed with brine and dried over $MgSO_4$. $MgSO_4$ was removed by filtration, and the solvent was evaporated. The residue was purified by column chromatography on SiO_2 ($CHCl_3$/hexane = 1/2 v/v as

an eluent) to afford **3** (848 mg, 1.54 mmol, 73%) as a yellow oil. R_f = 0.42 ($CHCl_3$/hexane = 1/2 v/v). ^{1}H NMR ($CDCl_3$, 400 MHz) δ 0.30 (s, 9H), 0.91-0.93 (m, 6H), 1.35-1.36 (m, 8H), 1.51 (m, 4H), 1.88 (m, 4H), 4.11 (dt, J = 2.4 Hz, 6.6 Hz, 4H), 6.92 (s, 1H), 6.95 (s, 1H), 7.81 (s, 1H), 8.13 (s, 1H) ppm; ^{13}C NMR ($CDCl_3$, 100 MHz) δ 0.2, 14.1, 22.7, 25.8, 29.0, 29.0, 31.6, 31.7, 69.0, 94.5, 106.2, 107.2, 107.3, 123.9, 128.2, 130.5, 130.9, 136.1, 150.4, 150.8 ppm. HRMS (APCI) calcd. for $C_{27}H_{40}IO_2Si$ $[M+H]^+$: 551.1837, found: 551.1829. Elemental analysis calcd. for $C_{27}H_{39}IO_2Si$: C 58.90 H 7.14 I 23.05, found: C 58.69 H 7.31 I 22.89.

Synthesis of 6. A mixture of 2,5-*n*-dibutylfuran (**5**) (5.91 g, 15.0 mmol) and 1,2,4,5-tetrabromobenzene (**4**) (3.23 g, 18 mmol) was placed in a round-bottom flask equipped with a magnetic stirring bar. After degassing several times, *n*-BuLi (11.3mL, 1.60 M in hexane, 18.0 mmol) was added dropwise over the course of 30 min. The solution was stirred at 0 °C for 2 h, allowed to warm to room temperature, stirred for 3.5 h. It was quenched by the careful addition of 5 mL MeOH and water. The organic layer was extracted with toluene and washed with water. The combined organic layer was washed with brine and dried over $MgSO_4$. $MgSO_4$ was removed by filtration, and the solvent was evaporated. The product was purified by column chromatography on SiO_2 ($CHCl_3$/hexane = 1/5 v/v as an eluent) to afford **6** (4.39 g, 10.6 mmol, 71%) as a light yellow viscous oil. R_f = 0.40 ($CHCl_3$/hexane = 1/5 v/v). ^{1}H NMR ($CDCl_3$, 400MHz) δ 0.96 (t, J = 7.1 Hz, 6H), 1.30-1.66 (m, 8H), 2.07-2.31 (m, 4H), 6.73 (s, 2H), 7.30 (s, 2H) ppm; ^{13}C NMR ($CDCl_3$, 100MHz) δ 13.9, 23.1, 26.8, 28.9, 91.7, 120.3, 124.2, 145.5, 154.1 ppm. HRMS (APCI) calcd. for $C_{18}H_{23}Br_2O$ $[M+H]^+$: 413.0110, found: 413.0097. Elemental analysis calcd. for $C_{18}H_{22}Br_2O$: C 52.20 H 5.35 Br 38.58, found: C 52.32 H 5.37 Br 38.35.

Synthesis of 7. A suspension of **6** (4.15 g, 10 mmol) and dry NaI (4.50 g, 30 mmol) in acetonitrile (100 mL) was placed in a round-bottom flask equipped with a magnetic stirring bar. After degassing several times, TMS-Cl (3.8 mL, 30 mmol) was added dropwise. The solution turned from red to brown during the addition and was stirred at room temperature for 11 h. The mixture was quenched by addition of aqueous $NaHSO_3$ solution and the product was extracted with CH_2Cl_2. The combined organic layer was washed with brine and dried over $MgSO_4$. $MgSO_4$ was removed by filtration, and the solvent was evaporated. The product was purified by column chromatography on SiO_2 ($CHCl_3$/hexane = 1/5 v/v as an eluent) to afford **7** (3.31 g, 8.31 mmol, 83%) as a light yellow oil. R_f = 0.70 ($CHCl_3$/hexane = 1/5 v/v). ^{1}H NMR ($CDCl_3$, 400MHz) δ 0.97 (t, J = 7.3 Hz, 6H), 1.38-1.49 (m, 4H), 1.64-1.73 (m, 4H), 2.95 (t, J = 7.8 Hz, 4H), 7.24 (s, 2H), 8.30 (s, 2H) ppm; ^{13}C NMR($CDCl_3$, 100MHz) δ 13.9, 22.7, 32.4, 32.8, 120.5, 126.9, 129.4, 132.4, 136.3 ppm. HRMS (APCI) calcd. for $C_{18}H_{23}Br_2$ $[M+H]^+$: 396.0083, found:

396.0080. Elemental analysis calcd. for $C_{18}H_{22}Br_2$: C 54.30 H 5.57 Br 40.13, found: C 54.55 H 5.47 Br 40.11.

Synthesis of 8. A mixture of **7** (2.99 g, 7.5 mmol), $Pd_2(dba)_3$ (0.172 g, 0.188 mmol), dppf (0.208 g, 0.376 mmol), CuI (0.0716 g, 0.376 mmol), THF (25 mL) and Et_3N (25 mL) was placed in a round-bottom flask equipped with a magnetic stirring bar. After degassing the reaction mixture several times, TMS-acetylene (1.04 mL, 7.52 mmol) was added to the mixture via a syringe. The reaction was carried out at 70 °C for 8 h with stirring. After the reaction mixture was cooled to room temperature, precipitates were removed by filtration, and the solvent was removed with a rotary evaporator. The crude residue was purified by column chromatography on SiO_2 (hexane as an eluent) to afford **8** (2.10 g, 5.1 mmol, 67%) as a colorless oil. R_f = 0.38 (hexane only). ^{1}H NMR ($CDCl_3$, 400 MHz) δ 0.33 (s, 9H), 0.95 (t, J = 7.3 Hz, 6H), 1.33-1.49 (m, 4H), 1.57-1.73 (m, 4H), 2.94-3.00 (m, 4H), 7.17 (s, 2H), 8.18 (s, 1H), 8.22 (s, 1H) ppm; ^{13}C NMR ($CDCl_3$, 100 MHz) δ −0.1, 13.9, 22.7, 32.4, 32.8, 32.9, 98.9, 104.1, 121.7, 126.4, 127.4, 127.9, 130.3, 130.7, 133.0, 136.0, 137.0 ppm. HRMS (APCI) calcd. for $C_{23}H_{32}BrSi$ $[M+H]^+$: 414.1373, found: 414.1361. Elemental analysis calcd. for $C_{23}H_{31}BrSi$: C 66.49 H 7.52 Br 19.23, found: C 66.50 H 7.63 Br 19.46.

Synthesis of 9. A solution of *n*-BuLi (1.60 M in hexane, 3.15 mL, 5.04 mmol) was slowly added to a solution of **8** (1.90 g, 4.58 mmol) in THF (30 mL) at –78 °C under Ar atmosphere. After 15 min, a solution of iodine (1.74 g, 6.87 mmol) in THF (10 mL) was added, and the mixture was stirred for 16 h at –78 °C to room temperature. The reaction mixture was quenched by the addition of aqueous $NaHSO_3$ solution, and the organic layer was extracted three times with $CHCl_3$. The combined organic layer was washed with brine and dried over $MgSO_4$. $MgSO_4$ was removed by filtration, and the solvent was evaporated. The residue was purified by column chromatography on SiO_2 (hexane as an eluent) to afford **9** (1.71 g, 3.69 mmol, 81%) as a colorless crystal. R_f = 0.70 (hexane only). ^{1}H NMR ($CDCl_3$, 400 MHz) δ 0.34 (s, 9H), 0.94 (dt, J = 3.2 Hz, 7.3 Hz 6H), 1.30-1.49 (m, 4H), 1.55-1.74 (m, 4H), 2.80-3.00 (m, 4H), 7.14 (s, 2H), 8.14 (s, 1H), 8.49 (s, 1H) ppm; ^{13}C NMR ($CDCl_3$, 100 MHz) δ −0.1, 14.0, 22.7, 32.2, 32.7, 32.8, 97.1, 98.0, 107.5, 125.2, 126.5, 127.1, 129.1, 131.1, 133.2, 135.0, 135.7, 136.9 ppm. HRMS (APCI) calcd. for $C_{23}H_{32}ISi$ $[M+H]^+$:462.1234, found: 462.1223. Elemental analysis calcd. for $C_{23}H_{31}ISi$: C 59.73 H 6.76 I 27.44, found: C 59.66 H 6.71 I 27.34.

Synthesis of Np-TMS. A mixture of (R_p)-**Cp** (20.0 mg, 0.0657 mmol), **3** (160 mg, 0.289 mmol), $Pd_2(dba)_3$ (6.3 mg, 0.0066 mmol), dppf (7.3 mg, 0.013 mmol), CuI (2.5 mg, 0.013 mmol), THF (2.0 mL) and Et_3N (2.0 mL) was placed in a round-bottom flask equipped with a magnetic stirring bar. After

degassing the reaction mixture several times, the reaction was carried out at 50 °C for 16 h with stirring. After the reaction mixture was cooled to room temperature, precipitates were removed by filtration, and the solvent was removed with a rotary evaporator. The residue was purified by column chromatography on SiO_2 ($CHCl_3$/hexane = 1/2 v/v as an eluent). Further purification was carried out by HPLC and reprecipitation with $CHCl_3$ and MeOH (good and poor solvent, respectively) to afford (R_p)-**Np-TMS** (79.6 mg, 0.0399 mmol, 61%) as a light yellow solid. R_f = 0.50 ($CHCl_3$/hexane = 1/2 v/v). ^{1}H NMR ($CDCl_3$, 400 MHz) δ 0.21 (s, 36H), 0.91-0.95 (m, 24H), 1.34-1.42 (m, 32H), 1.45-1.59 (m, 16H), 1.80-1.94 (m, 16H), 3.17-3.32 (m, 4H), 3.74-3.84 (m, 4H), 3.86-3.97 (m, 8H), 4.09 (t, J = 6.4 Hz, 8H), 6.89 (s, 4H), 7.02 (s, 4H), 7.39 (s, 4H), 7.89 (s, 4H), 8.00 (s, 4H) ppm; ^{13}C NMR ($CDCl_3$, 100 MHz) δ 0.1, 14.0, 22.6, 22.6, 25.7, 25.8, 29.0, 31.6, 31.6, 32.7, 68.7, 68.9, 92.2, 93.9, 97.1, 104.5, 107.0, 107.1, 120.0, 121.0, 125.7, 128.3, 128.7, 130.9, 130.9, 135.3, 141.7, 150.5, 150.6 ppm. HRMS (APCI) calcd. for $C_{132}H_{169}O_8Si_4$ $[M+H]^+$: 1994.1889, found: 1994.1941. Elemental analysis calcd. for $C_{132}H_{168}O_8Si_4$: C 79.47 H 8.49, found: C 79.57 H 8.59. (S_p)-**Np-TMS** and *rac*-**Np-TMS** were obtained by the same procedure in 68% and 54% isolated yields, respectively. (R_p)-**Np-TMS**: $[\alpha]^{23}_D$ = −41.2 (*c* 0.1, $CHCl_3$). (S_p)-**Np-TMS**: $[\alpha]^{23}_D$ = +49.6 (*c* 0.1, $CHCl_3$).

Synthesis of NpC. (R_p)-**Np-TMS** (60.0 mg, 0.0301 mmol) in THF (5.0 mL) was placed in a round-bottom flask equipped with a magnetic stirring bar. After degassing several times, NBu_4F (1 M in THF, 0.3 mL, 0.3 mmol) was added to the solution at room temperature for 15 min with stirring. The mixture was quenched by the addition of H_2O, and the organic layer was extracted three times with $CHCl_3$. The combined organic layer was washed with brine and dried over $MgSO_4$. $MgSO_4$ was removed by filtration, and the solvent was evaporated. The product was purified by column chromatography on SiO_2 ($CHCl_3$ as an eluent). To this product in a round-bottom flask equipped with a magnetic stirring bar, $PdCl_2(PPh_3)_2$ (211 mg, 0.301 mmol), CuI (57.3 mg, 0.301 mmol), THF (300 mL) and Et_3N (50 mL) were added. The mixture was heated at reflux temperature for 16 h under air. After the reaction mixture was cooled to room temperature, the solvent was evaporated. The residue was purified by column chromatography on SiO_2 ($CHCl_3$/hexane = 2/1 v/v as an eluent). Further purification was carried out by HPLC to afford (R_p)-**NpC** (14.6 mg, 0.0086 mmol, 29%) as a light yellow solid. R_f = 0.45 ($CHCl_3$/hexane = 2/3 v/v). ^{1}H NMR ($CDCl_3$, 400 MHz) δ 0.90-0.94 (m, 24H), 1.34-1.38 (m, 32H), 1.51-1.55 (m, 16H), 1.85-1.90 (m, 16H), 3.16-3.32 (m, 4H), 3.59-3.75 (m, 4H), 4.03-4.17 (m, 16H), 7.00 (d, J = 4.4 Hz, 8H), 7.26 (s, 4H), 7.80 (s, 4H), 7.84 (s, 4H) ppm; ^{13}C NMR ($CDCl_3$, 100 MHz) δ 14.0, 14.0, 22.6, 22.6, 25.7, 25.7, 29.0, 29.0, 31.6, 31.6, 33.3, 68.9, 68.9, 77.9, 82.3, 92.1, 93.7, 107.2, 107.3, 118.7,

122.3, 124.6, 128.2, 129.0, 129.6, 130.7, 134.0, 143.0, 150.6, 150.9 ppm. HRMS (APCI) calcd. for $C_{120}H_{133}O_8$ $[M+H]^+$:1701.9995, found: 1702.0000. (S_p)-**NpC** and *rac*-**NpC** were obtained by the same procedure in 29% and 14% isolated yields, respectively. (R_p)-**NpC**: $[\alpha]^{23}_D$ = +789.4 (*c* 0.1, $CHCl_3$). (S_p)-**NpC**: $[\alpha]^{23}_D$ = –781.2 (*c* 0.1, $CHCl_3$).

Synthesis of Ph-TMS. A mixture of (R_p)-**Cp** (20.0 mg, 0.0657 mmol), **10** (145 mg, 0.289 mmol), $Pd_2(dba)_3$ (6.0 mg, 0.0066 mmol), cataCXium® A (9.4 mg, 0.026 mmol), CuI (2.5 mg, 0.013 mmol), THF (5.0 mL) and Et_3N (5.0 mL) was placed in a round-bottom flask equipped with a magnetic stirring bar. After degassing the reaction mixture several times, the reaction was carried out at 50 °C for 16 h with stirring. After the reaction mixture was cooled to room temperature, precipitates were removed by filtration, and the solvent was removed with a rotary evaporator. The crude residue was purified by column chromatography on SiO_2 ($CHCl_3$/hexane = 1/3 v/v as an eluent). Further purification was carried out by HPLC to afford (R_p)-**Ph-TMS** (26.3 mg, 0.0145 mmol, 22%) as a yellow solid. R_f = 0.53 ($CHCl_3$/hexane = 1/2 v/v). ^{1}H NMR ($CDCl_3$, 400 MHz) δ 0.21 (s, 36H), 0.86-0.97 (m, 28H), 1.28-1.39 (m, 32H), 1.40-1.53 (m, 16H), 1.71-1.89 (m, 20H), 3.15 (s, 4H), 3.67 (s, 4H), 3.89 (t, *J* = 6.1 Hz, 8H), 4.00 (t, *J* = 6.6 Hz, 8H), 6.95 (s, 4H), 6.89 (s, 4H), 7.27 (s, 4H) ppm; ^{13}C NMR ($CDCl_3$, 100 MHz) δ 0.1, 14.0, 14.0, 22.6, 25.7, 25.7, 29.2, 29.2, 31.6, 31.6, 32.7, 69.1, 69.4, 91.8, 93.4, 96.5, 104.3, 116.4, 117.1, 118.0, 119.5, 125.5, 135.1, 141.7, 149.1, 149.6 ppm. HRMS (APCI) calcd. for $C_{132}H_{169}O_8Si_4$ $[M+H]^+$: 1794.1263, found: 1794.1250. (S_p)-**Ph-TMS** and *rac*-**Ph-TMS** were obtained by the same procedure in 22% and 25% isolated yields, respectively. (R_p)-**Ph-TMS**: $[\alpha]^{23}_D$ = −17.9 (*c* 0.1, $CHCl_3$). (S_p)-**Ph-TMS**: $[\alpha]^{23}_D$ = +16.3 (*c* 0.1, $CHCl_3$).

Synthesis of PhC. (R_p)-**Ph-TMS** (33.1 mg, 0.0185 mmol) in THF (5.0 mL) was placed in a round-bottom flask equipped with a magnetic stirring bar. After degassing several times, NBu_4F (1 M in THF, 0.2 mL, 0.2 mmol) was added to the solution at room temperature for 15 min with stirring. The mixture was quenched by the addition of H_2O, and the organic layer was extracted three times with $CHCl_3$. The combined organic layer was washed with brine and dried over $MgSO_4$. $MgSO_4$ was removed by filtration, and the solvent was evaporated. The product was purified by column chromatography on SiO_2 ($CHCl_3$ as an eluent). To this product in a round-bottom flask equipped with a magnetic stirring bar, $PdCl_2(PPh_3)_2$ (130 mg, 0.185 mmol), CuI (35.2 mg, 0.185 mmol), THF (300 mL) and Et_3N (50 mL) were added. The mixture was heated at reflux temperature for 16 h under air. After the reaction mixture was cooled to room temperature, the solvent was evaporated. The residue was purified by column chromatography on SiO_2 ($CHCl_3$/hexane = 2/1 v/v as an eluent). Further purification was carried out by

HPLC to afford (R_p)-**PhC** (5.5 mg, 0.0037 mmol, 20%) as a light yellow solid. R_f = 0.63 ($CHCl_3$/hexane = 2/1 v/v). ^{1}H NMR ($CDCl_3$, 400 MHz) δ 0.86-0.97(m, 24H), 1.29-1.40 (m, 32H), 1.43-1.54 (m, 16H), 1.78-1.89 (m, 16H), 3.07-3.19 (m, 4H), 3.47-3.58 (m, 4H), 3.98-4.08 (m, 16H), 6.96 (d, J = 3.4 Hz, 8H), 7.19 (s, 4H) ppm; ^{13}C NMR ($CDCl_3$, 100 MHz) δ 14.0, 14.0, 22.6, 22.6, 25.7, 25.7, 29.0, 29.0, 31.6, 31.6, 33.3, 68.9, 68.9, 77.9, 82.3, 92.1, 93.7, 107.2. 107.3, 118.7, 122.3, 124.6, 128.2, 129.0, 129.6, 130.7, 134.0, 143.0, 150.6, 150.9 ppm. HRMS (APCI) calcd. for $C_{104}H_{125}O_8$ $[M+H]^+$:1501.9369, found: 1501.9383. (S_p)-**PhC** and *rac*-**PhC** were obtained by the same procedure in 19% and 76% isolated yields, respectively. (R_p)-**PhC**: $[\alpha]^{23}_D$ = +1086.4 (*c* 0.1, $CHCl_3$). (S_p)-**PhC**: $[\alpha]^{23}_D$ = −1082.6 (*c* 0.1, $CHCl_3$).

Synthesis of NpBu$_2$-TMS. A mixture of (R_p)-**Cp** (23.0 mg, 0.0756 mmol), **9** (154 mg, 0.332 mmol), $Pd_2(dba)_3$ (6.9 mg, 0.0076 mmol), cataCXium® A (10.8 mg, 0.030 mmol), CuI (2.9 mg, 0.015 mmol), THF (5.0 mL) and Et_3N (5.0 mL) was placed in a round-bottom flask equipped with a magnetic stirring bar. After degassing the reaction mixture several times, the reaction was carried out at 50 °C for 12 h with stirring. After the reaction mixture was cooled to room temperature, precipitates were removed by filtration, and the solvent was removed with a rotary evaporator. The crude residue was purified by column chromatography on SiO_2 ($CHCl_3$/hexane = 1/3 v/v as an eluent). Further purification was carried out by HPLC to afford (R_p)-**NpBu$_2$-TMS** (74 mg, 0.0451 mmol, 60%) as a yellow solid. R_f = 0.50 ($CHCl_3$/hexane = 1/3 v/v). ^{1}H NMR ($CDCl_3$, 400 MHz) δ 0.23 (s, 36H), 0.79 (t, J = 7.3 Hz, 12H), 1.01 (t, J = 7.3 Hz, 12H), 1.15-1.23 (m, 8H), 1.44-1.58 (m, 16H), 1.69-1.80 (m, 8H), 2.69-2.89 (m, 8H), 2.98-3.08 (m, 8H), 3.27-3.37 (m, 4H), 3.80-3.90 (m, 4H), 7.18 (d, J = 7.3 Hz, 4H), 7.24 (d, J = 7.3 Hz, 4H), 7.44 (s, 4H) , 8.25 (s, 4H) , 8.28 (s, 4H) ppm; ^{13}C NMR ($CDCl_3$, 100 MHz) δ 0.1, 13.9, 14.0, 22.5, 22.8, 32.2, 32.4, 32.6, 32.9, 92.3, 94.0, 97.5, 104.6, 121.1, 121.8, 125.6, 126.8, 126.9, 129.2, 129.9, 131.3, 131.6, 135.3, 136.8, 136.9, 142.1 ppm. HRMS (APCI) calcd. for $C_{116}H_{137}Si_4$ $[M+H]^+$: 1641.9792, found: 1641.9803. Elemental analysis calcd. for $C_{116}H_{136}Si_4$: C 84.82 H 8.35, found: C 84.76 H 8.20. (S_p)-**NpBu$_2$-TMS** and *rac*-**NpBu$_2$-TMS** were obtained by the same procedure in 43% and 39% isolated yields, respectively. (R_p)-**NpBu$_2$-TMS**: $[\alpha]^{23}_D$ = −183.7 (*c* 0.1, $CHCl_3$). (S_p)-**NpBu$_2$-TMS**: $[\alpha]^{23}_D$ = +174.2 (*c* 0.1, $CHCl_3$).

Synthesis of NpBu$_2$C. (R_p)-**NpBu$_2$-TMS** (54 mg, 0.0329 mmol) in THF (5.0 mL) was placed in a round-bottom flask equipped with a magnetic stirring bar. After degassing several times, NBu_4F (1 M in THF, 0.33 mL, 0.33 mmol) was added to the solution at room temperature for 15 min with stirring. The mixture was quenched by the addition of H_2O, and the organic layer was extracted three times with

$CHCl_3$. The combined organic layer was washed with brine and dried over $MgSO_4$. $MgSO_4$ was removed by filtration, and the solvent was evaporated. The product was purified by column chromatography on SiO_2 ($CHCl_3$ as an eluent). To this product in a round-bottom flask equipped with a magnetic stirring bar, $PdCl_2(PPh_3)_2$ (230 mg, 0.329 mmol), CuI (63 mg, 0.329 mmol), THF (300 mL) and Et_3N (50 mL) were added. The mixture was heated at reflux temperature for 16 h under air. After the reaction mixture was cooled to room temperature, the solvent was evaporated. The residue was purified by column chromatography on SiO_2 ($CHCl_3$/hexane = 1/3 v/v as an eluent). Further purification was carried out by HPLC to afford (R_p)-**PhC** (8.1 mg, 0.0060 mmol, 18%) as a light yellow solid. R_f = 0. 56 ($CHCl_3$/hexane = 1/3 v/v). ^{1}H NMR ($CDCl_3$, 400 MHz) δ 0.97 (t, J = 7.3 Hz, 12H), 1.02 (t, J = 7.3 Hz, 12H), 1.40-1.51 (m, 16H), 1.68-1.79 (m, 16H), 2.98-3.08 (m, 16H), 3.23-3.29 (m, 4H), 3.66-3.73 (m, 4H), 7.29 (s, 8H), 7.33 (s, 4H), 8.26 (s, 4H), 8.31 (s, 4H) ppm; ^{13}C NMR ($CDCl_3$, 100 MHz) δ 14.0, 22.7, 22.9, 32.4, 32.7, 32.9, 33.2, 33.4, 78.3, 82.6, 92.6, 93.7, 120.0, 123.3, 124.6, 127.4, 127.6, 128.7, 129.3, 131.3, 132.0, 134.3, 137.1, 137.3, 143.2 ppm. HRMS (APCI) calcd. for $C_{104}H_{101}$ $[M+H]^+$:1349.7898, found: 1349.7901. (S_p)-**NpBu$_2$C** and *rac*-**NpBu$_2$C** were obtained by the same procedure in 40% and 32% isolated yields. (R_p)-**NpBu$_2$C**: $[\alpha]^{23}_D$ = +1040.1 (c 0.1, $CHCl_3$). (S_p)-**NpBu$_2$C**: $[\alpha]^{23}_D$ = −1041.0 (c 0.1, $CHCl_3$).

References and Notes

(1) For example: (a) *Handbook of Conducting Polymers*; Skotheim, T. A., Elsenbaumer R. L., Reynolds J. R., Eds.; Marcel Dekker: New York, 3rd edn, 2006. (b) *Organic Light Emitting Devices: Synthesis, Properties and Application*; Müellen K., Scherf, U., Eds.; Wiley-VCH: Weinheim, 2006. (c) *Organic Field-Effect Transistors*; Groza, J. R., Locklin, J. J., Eds.; CRC Press Taylor & Francis Group: New York, 2007. (d) *Organic Photovoltaics: Materials, Device Physics, and Manufacturing Technologies*; Brabec, C., Dyakonov V., Scherf, U., Eds.; Wiley-VCH, Weinheim, 2008.

(2) (a) *Cyclophane Chemistry: Synthesis, Structures and Reactions*; Vögtle, F., Ed.; John Wiley & Sons: Chichester, 1993. (b) *Modern Cyclophane Chemistry*; Gleiter, R., Hopf, H., Eds.; Wiley-VCH: Weinheim, 2004.

(3) Brown, C. J.; Farthing, A. C. *Nature* **1949**, *164*, 915–916.

(4) Cram, D. J.; Steinberg, H. *J. Am. Chem. Soc.* **1951**, *73*, 5691–5704.

(5) Morisaki, Y.; Gon, M.; Sasamori, T.; Tokitoh N.; Chujo, Y. *J. Am. Chem. Soc.* **2014**, *136*, 3350–3353.

(6) Gon, M.; Morisaki, Y.; Chujo, Y. *J. Mater. Chem. C* **2015**, *3*, 521–529.

(7) Zapf, A.; Ehrentraut, A.; Beller, M. *Angew. Chem., Int. Ed.* **2000**, 39, 4153–4155.

(8) CD dissymmetry factor is defined as $g_{abs} = 2\Delta\varepsilon/\varepsilon$, where $\Delta\varepsilon$ indicates differences of absorbance between left- and right-handed circularly polarized light, respectively. CPL dissymmetry factor is defined as $g_{lum} = 2(I_{left} - I_{right})/(I_{left} + I_{right})$, where I_{left} and I_{right} indicate luminescence intensities of left- and right-handed CPL, respectively.

(9) Morisaki, Y.; Inoshita, K.; Chujo, Y. *Chem.–Eur. J.* **2014**, *20*, 8386–8390.

(10) Nakamura, K.; Furumi, S.; Takeuchi, M.; Shibuya, T.; Tanaka, K. *J. Am. Chem. Soc.* **2014**, *136*, 5555–5558.

(11) (a) Field, J. E.; Muller, G.; Riehl, J. P.; Venkataraman, D. *J. Am. Chem. Soc.* **2003**, *25*, 11808–11809. (b) Kaseyama, T.; Furumi, S.; Zhang, X.; Tanaka, K.; Takeuchi, M.; *Angew. Chem., Int. Ed.* **2011**, *50*, 3684–3687. (c) Maeda, H.; Bando, Y.; Shimomura, K.; Yamada, I.; Naito, M.; Nobusawa, K.; Tsumatori, H.; Kawai, T. *J. Am. Chem. Soc.* **2011**, *133*, 9266–9269. (d) Sawada, Y.; Furumi, S.; Takai, A.; Takeuchi, M.; Noguchi, K.; Tanaka, K. *J. Am. Chem. Soc.* **2012**, *134*, 4080–4083. (e) Haketa, Y.; Bando, Y.; Takaishi, K.; Uchiyama, M.; Muranaka, A.; Naito, M.; Shibaguchi, H.; Kawai, T.; Maeda, H. *Angew. Chem., Int. Ed.* **2012**, 51, 7967–7971. (f) Oyama, H.; Nakano, K.; Harada, T.; Kuroda, R.; Naito, M.; Nobusawa, K.; Nozaki, K. *Org. Lett.* **2013**, *15*, 2104–2107. (g) Sakai, H.; Shinto, S.; Kumar, J.; Araki, Y.; Sakanoue, T.; Takenobu, T.; Wada, T.; Kawai, T.; Hasobe, T. *J. Phys. Chem. C* **2015**, *119*, 13937–13947.

(12) (a) Maeda, H.; Bando, Y. *Pure Appl. Chem.* **2013**, *85*, 1967–1978. (b) CPL was observed from chiral orientation of flurophores. Based on axially chiral scaffolds: Kawai, T.; Kawamura, K.; Tsumatori, H.; Ishikawa, M.; Naito, M.; Fujiki, M.; Nakashima, T. *ChemPhysChem* **2007**, *8*, 1465–1468. (c) Tsumatori, H.; Nakashima, T.; Kawai, T.; *Org. Lett.* **2010**, *12*, 2362–2365. (d) Kimoto, T.; Tajima, N.; Fujiki, M.; Imai, Y.; *Chem.–Asian J.* **2012**, *7*, 2836–2841. (e) Amako, T.; Kimoto, T.; Tajima, N.; Fujiki, M.; Imai, Y. *RSC Adv.* **2013**, *3*, 6939–6944. (f) Amako, T.; Kimoto, T.; Tajima, N.; Fujiki, M.; Imai, Y. *Tetrahedron* **2013**, *69*, 2753–2757. (g) Kimoto, T.; Amako, T.; Tajima, N.; Kuroda, R.; Fujiki, M.; Imai, Y. *Asian J. Org. Chem.* **2013**, *2*, 404–410. (h) Kumar, J.; Nakashima, T.; Tsumatori, H.; Kawai, T. *J. Phys. Chem. Lett.* **2014**, *5*, 316–321. (i) Kitayama, Y.; Amako, T.; Suzuki, N.; Fujiki, M.; Imai, Y. *Org. Biomol. Chem.* **2014**,

12, 4342–4346. (j) Based on centrally chiral scaffold: Kumar, J.; Nakashima, T.; Tsumatori, H.; Mori, M.; Naito, M.; Kawai, T. *Chem.–Eur. J.* **2013**, *19*, 14090–14097. (k) Amako, T.; Nakabayashi, K.; Mori, T.; Inoue, Y.; Fujiki, M.; Imai, Y. *Chem. Commun.* **2014**, *50*, 12836–12839. (l) Kitayama, Y.; Nakabayashi, K.; Wakabayashi, T.; Tajima, N.; Fujiki, M.; Imai, Y. *RSC Adv.* **2015**, *5*, 410–415. (m) CPL from inherently achiral monochromophore systems is recently reported: Sánchez-Carnerero, E. M.; Moreno, F.; Maroto, B. L.; Agarrabeitia, A. R.; Ortiz, M. J.; Vo, B. G.; Muller, G.; de la Moya, S. *J. Am. Chem. Soc.* **2014**, *136*, 3346–3349. (n) Excimer complex: Inouye, M.; Hayashi, K.; Yonenaga, Y.; Itou, T.; Fujimoto, K.; Uchida, T.; Iwamura, M.; Nozaki, K. *Angew. Chem., Int. Ed.* **2014**, *53*, 14392–14396.

(13) Some optically active conjugated polymers exhibit CPL. For polymers emitting CPL in their film or aggregation states: (a) Peeters, E.; M. Christiaans, P. T.; Janssen, R. A. J.; Schoo, H. F. M.; Dekkers H. P. J. M.; Meijer, E. W. *J. Am. Chem. Soc.* **1997**, *119*, 9909–9910. (b) Satrijio, A.; Meskers, S. C. J.; Swager, T. M. *J. Am. Chem. Soc.*, **2006**, *128*, 9030–9031. (c) Wilson, J. N.; Steffen, W.; McKenzie, T. G.; Lieser, G.; Oda, M.; Neher, D.; Bunz, U. H. F.; *J. Am. Chem. Soc.* **2002**, *124*, 6830–6831. (d) Langeveld-Voss, B. M. W.; Janssen, R. A.; Christiaans, M. P. T.; Meskers, S. C. J.; Dekkers, H. P. J. M.; Meijer, E. W. *J. Am. Chem. Soc.* **1996**, *118*, 4908–4909. (e) Oda, M.; Nothofer, H.-G.; Lieser, G.; Scherf, U.; Meskers, S. C. J.; Neher, D. *Adv. Mater.* **2000**, *12*, 362–365. (f) Oda, M.; Nothofer, H.-G.; Scherf, U.; Šunjić, V.; Richter, D.; Regenstein, W.; Meskers, S. C. J.; Neher, D. *Macromolecules* **2002**, *35*, 6792–6798. (g) Goto, H.; Akagi, K. *Angew. Chem., Int. Ed.* **2005**, *44*, 4322–4328. (h) Hayasaka, H.; Miyashita, T.; Tamura, K.; Akagi, K. *Adv. Funct. Mater.* **2010**, *20*, 1243–1250. (i) Fukao S.; Fujiki, M. *Macromolecules* **2009**, *42*, 8062–8067. (j) Yu, J.-M.; Sakamoto, T.; Watanabe, K.; Furumi, S.; Tamaoki, N.; Chen, Y.; Nakano, T. *Chem. Commun.* **2011**, *47*, 3799–3801. (k) Watanabe, K.; Sakamoto, T.; Taguchi, M.; Fujiki, M.; and T. Nakano, *Chem. Commun.* **2011**, *47*, 10996–10998. (l) Hirahara, T.; Yoshizawa-Fujita, M.; Takeoka, Y.; Rikukawa, M. *Chem. Lett.* **2012**, *41*, 905–907. (m) Watanabe, K.; Koyama, Y.; Suzuki, N.; Fujiki, M.; Nakano, T. *Polym. Chem.* **2014**, *5*, 712–717. (n) For polymer aggregates in optically active solvents: Nakano, Y.; Liu, Y.; Fujiki, M. *Polym. Chem.* **2010**, *1*, 460–469. (o) Kawagoe, Y.; Fujiki, M.; Nakano, Y. *New J. Chem.* **2010**, *34*, 637–647. (p) For polymers emitting CPL in solution: Morisaki, Y.; Hifumi, R.; Lin, L.; Inoshita, K.; Chujo, Y. *Polym. Chem.* **2012**, *3*, 2727–2730. (q) Nagata, Y.; Nishikawa, T.; Suginome, M. *Chem. Commun.* **2014**, *50*, 9951–9953. (r) For CPL created by polymer-polymer complexation: Shiraki, T.; Tsuchiya, Y.; Noguchi, T.; Tamaru, S.; Suzuki, N.; Taguchi, M.; Fujiki, M.; Shinkai, S. *Chem.–Asian J.* **2014**, *9*, 218–222.

(14) Pangborn, A. B.; Giardello, M. A.; Grubbs, R. H.; Rosen, R. K.; Timmers, F. J. *Organometallics* **1996**, *15*, 1518–1520.

(15) Lynett, P. T.; Maley, K. E. *Org. Lett.*, **2009**, *11*, 3726–3729.

(16) Asta, C.; Conrad, J.; Mika, S.; Beifuss U. *Green Chem.* **2011**, *13*, 3066–3069.

(17) Balandina, T.; Tahara, K.; Sändig, N.; Blunt, M. O.; Adisoejoso, J.; Lei, S.; Zerbetto, F.; Tobe, Y.; De Feyter, S. *ACS Nano* **2012**, *6*, 8381–8389.

(18) Neese, F. *WIREs Comput. Mol. Sci.* **2012**, *2*, 73–78.

Chapter 6

Highly Emissive Optically Active Conjugated Dimers Consisting of Planar Chiral [2.2]Paracyclophane Showing Circularly Polarized Luminescence

Abstract

Optically active π-conjugated dimers based on a planar chiral 4,7,12,15-tetrasubstituted [2.2]paracyclophane were synthesized. The π-conjugated dimers were functionalized by aryl-ethynylene groups, such as benzene, naphthalene and anthracene. The strength of though-space conjugation was tuned by the π-surface. In the UV-vis and photoluminescence (PL) spectra, the absorption and emission maxima of the dimers exhibited bathochromic effect compared with those of the monomers. When the monomer had small π-surface unit, such as benzene and naphthalene, the dimer exhibited typical optical properties of the stacked molecule. On the other hand, when the monomer had large π-surface, such as anthracene, the dimer exhibited monomer-like optical properties. In the circular dichroism (CD) and circularly polarized luminescence (CPL) spectra, the functionalized optically active chromophores exhibited unique properties. These data are useful not only for understanding the properties of the planar chiral [2.2]paracyclophane but for the design of a new functional π-conjugation system.

Introduction

Aromatic compound-based π-conjugated systems are widely applied to luminescent materials, opto-electronic devices and organic thin film solar cell, and unique properties have been revealed.[1] Among various aromatic frameworks, [2.2]paracyclophanes have been received much attention for the possibility to stack two chromophores in the distance of 3Å.[2] [2.2]Paracyclophane frameworks can extend π-conjugation between two chromophores, which is called through-space conjugation.[3j] Bazan, Mukamel, and co-workers reported the unique optical properties of π-conjugated *pseudo-o*-disubstituted, *pseudo-p*-disubstituted and 4,7,12,15-tetrasubstituted [2.2]paracyclophane derivatives.[3] They revealed that the stacked position of the two chromophores affects the conjugation system in the ground and excited states mainly based on the phenylene-vinylene systems. In particular, in the case of 4,7,12,15-tetrasubstituted [2.2]paracyclophane, the two stacked π-conjugation systems exhibit strong through-space conjugation in addition to the common through-bond conjugation.[3b,d,e,i,j] Hopf, Haley, and co-workers synthesized a lot of multi-substituted [2.2]paracyclophane derivatives including three-dimensionally π-conjugated cyclic compounds.[4] The author's group reported functional oligomers[5] and polymers[6] using though-space conjugation based on [2.2]paracyclophane frameworks. It is possible to set two chromophores in an optically active position using planar chiral [2.2]paracyclophane frameworks. The author reported optical resolution methods of optically active [2.2]paracyclophane compounds and revealed that planar chiral π-conjugated [2.2]paracyclophane exhibited good chiroptical properties, especially circularly polarized luminescence (CPL).[7,8] In this chapter, the author designed optically active [2.2]paracyclophane-based π-conjugation systems functionalized by benzene, naphthalene and anthracene with ethynyl linkers. The author investigated optical and chiroptical properties of the planar chiral [2.2]paracyclophane compounds and the effect of ethynyl linkers and aromatic groups in detail.

Results and Discussion

Synthesis

The optical resolution of planar chiral 4,7,12,15-tetrasubstituted [2.2]paracyclophane was carried out using the diastereomer method developed in Chapter 3, and the obtained enantiopure compounds were converted to the corresponding (R_p)- and (S_p)-4,7,12,15-tetraethynyl[2.2]paracyclophanes.[8a] The synthetic routes to the target optically active dimers and monomeric model compounds are shown in Schemes 1 and 2. *n*-Butyl group in **3** was introduced to provide the target compounds with solubility in organic solvents, such as THF, $CHCl_3$, CH_2Cl_2 and toluene. Although the synthesis of **Cp-Ph** and **M-Ph** was already reported,[9] the author synthesized them by the different synthetic route to obtain an optically active compound.

Scheme 1 shows the syntheses of the target planar chiral dimers **Cp-Ph**, **Cp-Np** and **Cp-An**. In these Schemes, only the reactions of the (S_p)-isomers are shown; the (R_p)-isomers were synthesized under the same conditions from (R_p)-**Cp**. Sonogashira-Hagihara coupling reaction[10] of (S_p)-**Cp** was carried out with iodobenzene **1** in the catalytic system of $Pd_2(dba)_3$/CuI using XPhos[11] as a phosphine ligand to obtain compound (S_p)-**Cp-Ph** in 57% isolated yield. Using the same procedure, (S_p)-**Cp-Np** and (S_p)-**Cp-An** were obtained in 35% and 23% isolated yields, respectively. In the case of (S_p)-**Cp-An**, the reaction temperature was higher than that of the other systems because the brominated compound **3** is less reactive than the iodinated compounds **1** and **2**.

Scheme 2 shows the syntheses of the monomers, **M-Ph**, **M-Np** and **M-An**, as model compounds. These monomers are equivalent to the half units of the stacked dimers, **Cp-Ph**, **Cp-Np** and **Cp-An**, respectively. As shown in Scheme 2, these monomers were synthesized by the same procedure as that in Scheme 1, and **M-Ph**, **M-Np** and **M-An** were obtained in 78%, 68% and 70%, respectively. In the case of **M-Ph** and **M-Np**, PPh_3 was used as a phosphine

ligand because of the high reactivity. The structures of all new compounds in this study were confirmed by ^{1}H and ^{13}C NMR spectroscopy, high-resolution mass spectrometry (HRMS), and elemental analysis; the detailed synthetic procedures and NMR spectra data are shown in the experimental section.

Scheme 1. Synthesis of (S_p)-**Cp-Ph**, **Cp-Np** and **Cp-An**

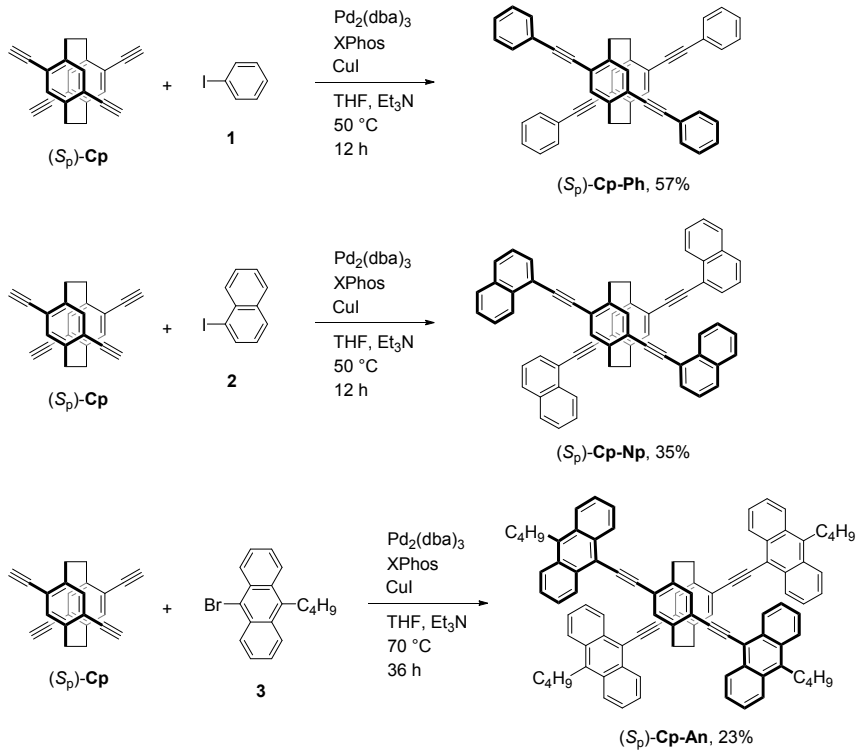

Scheme 2. Synthesis of model compounds **M-Ph**, **M-Np** and **M-An**

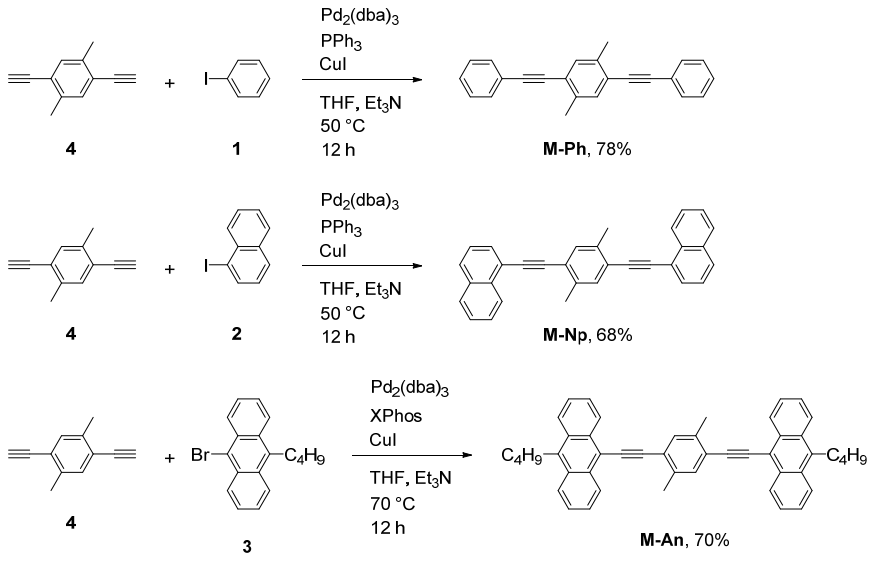

Optical Properties

The optical properties of both enantiomers of π-conjugated dimers with a planar chiral [2.2]paracyclophane, **Cp-Ph**, **Cp-Np**, and **Cp-An** as well as their monomers **M-Ph**, **Cp-Np** and **M-An** were evaluated. The optical and chiroptical data are summarized in Tables 1 and 2, respectively. Although the optical properties of **Cp-Ph** and **M-Ph** were already reported by Meijere in 1993,[9] the chiroptical data of **Cp-Ph** were the first report.

Table 1. Optical properties: Spectroscopic data of (S_p)-isomers

	$\lambda_{abs}{}^a$/nm (ε / 10^5 M^{-1} cm^{-1})	$\lambda_{lum}{}^b$/nm	τ^c/ns	χ^2	$\Phi_{lum}{}^d$
(S_p)-**Cp-Ph**	349 (0.63)	412	3.67	1.12	0.60
(S_p)-**Cp-Np**	380 (0.79)	421	1.89	1.16	0.78
(S_p)-**Cp-An**	268 (2.18), 459 (0.87)	503	2.09	1.03	0.42
M-Ph	328 (0.56)	355	0.78	1.11	0.52
M-Np	358 (0.58)	388	0.99	1.18	0.57
M-An	270 (1.38), 446 (0.49)	479	1.80	1.13	0.48

[a] In $CHCl_3$ (1.0×10^{-5} M). [b] In $CHCl_3$ (1.0×10^{-6} M), excited at absorption maxima. [c] Emission life time at λ_{lum}. [d] Absolute PL quantum efficiency.

Figures 1A, 1B and 1C show the UV-vis absorption spectra and photoluminescence (PL) spectra of dimers, **Cp-Ph**, **Cp-Np**, and **Cp-An** and the monomers, **M-Ph**, **M-Np** and **M-An** in the dilute $CHCl_3$ solutions (1.0×10^{-5} M for UV and 1.0×10^{-6} M for PL), respectively. Figure 1A shows a comparison of the spectra of **Cp-Ph** and **M-Ph**. The absorption maximum of **Cp-Ph** (349 nm) exhibited bathochromic effect compared with that of **M-Ph** (328 nm). This is because the three-dimensional extension of π-conjugation, which is called through-space conjugation, occurred via [2.2]paracyclophane unit. The same through-space conjugation was observed in the absorption spectra of **Cp-Np** and **M-Np** (380 nm and 358 nm, respectively). In the case of **Cp-An** and **M-An**, the same through-space conjugation was observed. The

absorption maxima of **Cp-An** and **M-An** were 459 nm and 446 nm, respectively. In the PL spectra, the emission maxima of dimers, **Cp-Ph** (412 nm), **Cp-Np** (421 nm), and **Cp-An** (503 nm) exhibited bathochromic effect compared with the monomers, **M-Ph** (355 nm), **M-Np** (388 nm) and **M-An** (479 nm). These results indicate that through-space conjugation occurred in the excited state. The shapes of UV-vis absorption and PL spectra were different in **Cp-Ph** and **M-Ph**, whereas those of UV-vis absorption and PL spectra were similar in **Cp-An** and **M-An**; the vibrational structure was clearly observed in the PL spectra of **Cp-An** and **M-An**. The difference of the wavelength at the emission maxima between dimers and monomers decreased as the π-surface increased; 57 nm (**Cp-Ph** and **M-Ph**), 33 nm (**Cp-Np** and **M-Np**) and 24 nm (**Cp-An** and **M-An**). These results indicate that the dimers exhibited monomer-like properties as the π-conjugation length of monomers increases. PL lifetime measurement supported these results. The difference of PL lifetime between dimers and monomers decreases as the π-conjugation length of monomers increases (PL lifetime (τ) and χ^2 parameters are summarized in Table 1). Thus, through-space conjugation was effectively in a short π-conjugation length system. Bazan, Mukamel and co-workers reported similar phenomena in the phenylene-vinylene systems.[3] An absolute PL quantum efficiency (Φ_{lum}) enhanced by the rigid structure of [2.2]paracyclophane unit. However, that of **Cp-An** decreased compared with **M-An** because anthracene has large π-surface to induce torsions in the structure of **Cp-An** (Table 1).

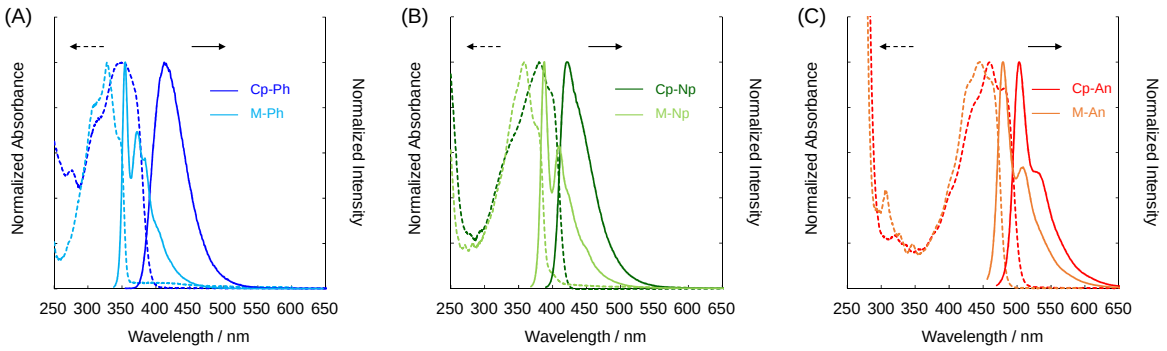

Figure 1. UV-vis absorption spectra in the dilute $CHCl_3$ (1.0×10^{-5} M) and PL spectra in the dilute $CHCl_3$ (1.0×10^{-6} M, excited at absorption maximum); (A) **Cp-Ph** and **M-Ph**, (B) **Cp-Np** and **M-Np**, (C) **Cp-An** and **M-An**.

Chiroptical Properties

The chiroptical properties in the ground and excited states of **Cp-Ph**, **Cp-Np**, and **Cp-An** were investigated by circular dichroism (CD) and CPL spectroscopy. Chiroptical data, CD and CPL dissymmetry factor[12] (g_{abs} and g_{lum}, respectively), are summarized in Table 2. Figures 2A, 2B and 2C show the CD and absorption spectra of both enantiomers of **Cp-Ph**, **Cp-Np**, and **Cp-An** in the dilute $CHCl_3$ (1.0×10^{-5} M). In all cases, mirror image Cotton effects were observed in the CD spectra, and the g_{abs} values of the first cotton effect were estimated to be $+1.6 \times 10^{-3}$ for (S_p)-**Cp-Ph**, $+1.7 \times 10^{-3}$ for (S_p)-**Cp-Ph** and $+0.85 \times 10^{-3}$ for (S_p)-**Cp-An**. The shape of the CD spectrum of (S_p)-**Cp-Ph** was similar to (S_p)-**Cp-Np**, but that of (S_p)-**Cp-An** was different from the others. The planar chirality of [2.2]paracyclophane induced anthracene chirality, and (S_p)-**Cp-An** exhibited minus sign in almost all region. The g_{abs} values of first Cotton effect of (S_p)-**Cp-An** were half of the others. These properties were derived from the anthracene unit, which were different from the benzene and naphthalene units.

The CPL spectra of both enantiomers of **Cp-Ph**, **Cp-Np**, and **Cp-An** in the dilute $CHCl_3$ (1.0×10^{-5} M) are shown in Figures 3A, 3B and 3C, respectively. Mirror image CPL spectra were observed for the enantiomers; a plus and minus CPL sign was observed in **Cp-Ph** (g_{lum} = $+1.1 \times 10^{-3}$ and -0.42×10^{-3} for (S_p)-**Cp-Ph**). Intense CPL was observed in **Cp-Np** (g_{lum} = $+1.6 \times 10^{-3}$ for (S_p)-**Cp-Np**), and weak CPL signal was observed in **Cp-An** (g_{lum} = $+0.45 \times 10^{-3}$ for (S_p)-**Cp-An**). In the case of **Cp-Ph**, the split sign was caused by the same level of the intensity of plus and minus signal, on the other hand, in the case of **Cp-Np**, the intensity of plus signal was larger than that of minus signal. In the case of **Cp-An**, induction of chirality to anthracene units was effective as can be seen in the CD spectrum. In the present stage, it is difficult to explain the chiroptical behaviors in the excited state.

Table 2. Chiroptical properties: Spectroscopic data of (S_p)-isomers and (R_p)-isomers

	g_{abs} / 10^{-3} at λ_{abs}[a]	g_{lum} / 10^{-3} at $\lambda_{lum,\,max}$[b]
(S_p)-**Cp-Ph**	+1.6	+1.1, −0.42
(S_p)-**Cp-Np**	+1.7	+1.6
(S_p)-**Cp-An**	+0.85	+0.45
(R_p)-**Cp-Ph**	−1.7	−1.2. +0.44
(R_p)-**Cp-Np**	−1.6	−1.7
(R_p)-**Cp-An**	−0.86	−0.41

[a] $g_{abs} = 2\Delta\varepsilon/\varepsilon$, where $\Delta\varepsilon$ indicates differences of absorbance between left- and right-handed circularly polarized light, respectively. The g_{abs} value of the first peak top was estimated. [b] $g_{lum} = 2(I_{left} - I_{right})/(I_{left} + I_{right})$, where I_{left} and I_{right} indicate luminescence intensities of left- and right-handed CPL, respectively.

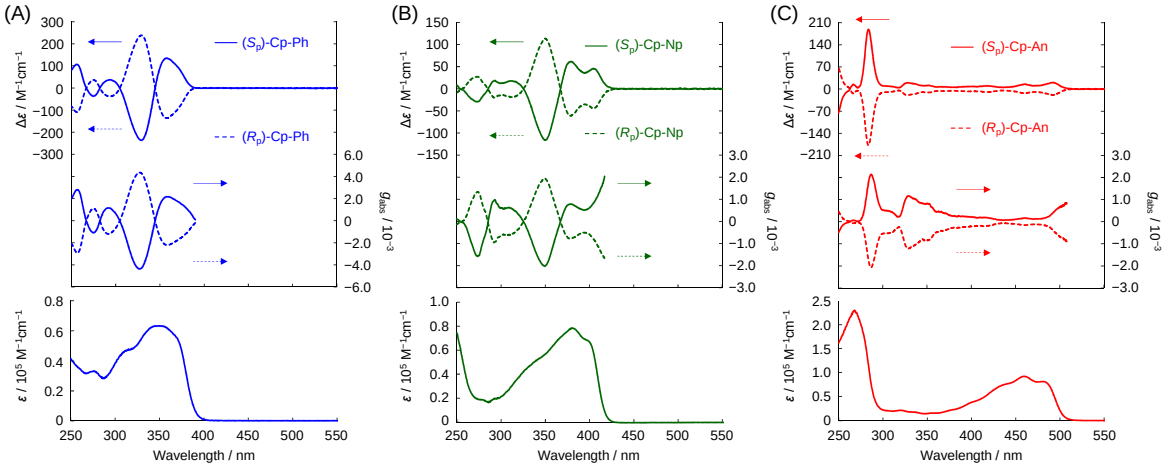

Figure 2. CD (top), g_{abs} (middle), and UV-vis absorption (bottom) spectra in the dilute $CHCl_3$ (1.0×10^{-5} M); (A) **Cp-Ph**, (B) **Cp-Np** and (C) **Cp-An**.

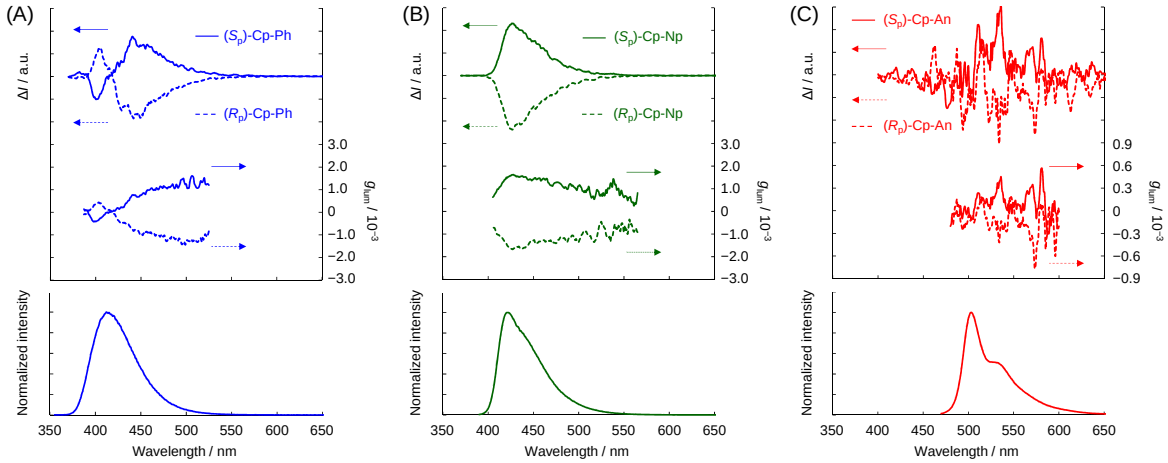

Figure 3. CPL (top), g_{lum} (middle), and PL (bottom) spectra of in the dilute $CHCl_3$ (1.0×10^{-5} M for CPL and 1.0×10^{-6} M for PL); (A) **Cp-Ph**, (B) **Cp-Np** and (C) **Cp-An**; excitation wavelength was 300 nm, 300 nm and 350 nm, respectively.

Conclusions

In summary, optically active π-conjugated dimers functionalized by aryl-ethynylene groups with a planar chiral [2.2]paracyclophane were synthesized. The strength of though-space conjugation was tuned by conjugation length of the monomer unit. In the UV-vis and PL spectra, the absorption and emission maxima of the dimers, **Cp-Ph**, **Cp-Np**, and **Cp-An** exhibited bathochromic effect compared with those of the monomers, **M-Ph**, **M-Np** and **M-An**. In addition, the difference of the shape and top wavelength of UV-vis and PL spectra between the dimers and the monomers decreased as the π-conjugation length of the monomer units increased. This result indicates through-space conjugation was effective in a short π-conjugation length system. Similar CD spectra were observed in the **Cp-Ph** and **Cp-Np** systems, while the **Cp-An** exhibited unique CD signals. Three different types of CPL spectra were obtained from **Cp-Ph**, **Cp-Np** and **Cp-An**. These results are useful not only for understanding one of the relationships between the planar chiral [2.2]paracyclophane and the attached chromophores but for the design of a new functional π-conjugation system.

Experimental Section

General. ^{1}H and ^{13}C NMR spectra were recorded on JEOL EX400 and AL400 instruments at 400 and 100 MHz, respectively. Samples were analyzed in $CDCl_3$ and CD_2Cl_2. In the case of $CDCl_3$, chemical shift values were expressed relative to Me_4Si as an internal standard. Analytical thin layer chromatography (TLC) was performed with silica gel 60 Merck F254 plates. Column chromatography was performed with Wakogel C-300 silica gel. High-resolution mass (HRMS) spectrometry was performed at the Technical Support Office (Department of Synthetic Chemistry and Biological Chemistry, Graduate School of Engineering, Kyoto University), and the HRMS spectra were obtained on a Thermo Fisher Scientific orbitrapXL spectrometer for matrix assisted laser desorption/ionization (MALDI). UV-vis spectra were recorded on a SHIMADZU UV-3600 spectrophotometer, and samples were analyzed in $CHCl_3$ at room temperature. Fluorescence emission spectra were recorded on a HORIBA JOBIN YVON Fluoromax-4 spectrofluorometer, and samples were analyzed in $CHCl_3$ at room temperature. The PL lifetime measurement was performed on a Horiba FluoroCube spectrofluorometer system; excitation was carried out using a UV diode laser (NanoLED 292 nm and 375 nm). Specific rotations ($[\alpha]^{t}_{D}$) were measured with a HORIBA SEPA-500 polarimeter. Circular dichroism (CD) spectra were recorded on a JASCO J-820 spectropolarimeter with $CHCl_3$ as a solvent at room temperature. Circularly polarized luminescence (CPL) spectra were recorded on a JASCO CPL-200S with $CHCl_3$ as a solvent at room temperature. Elemental analyses were performed at the Microanalytical Center of Kyoto University.

Materials. Commercially available compounds used without purification: (Tokyo Chemical Industry Co, Ltd.) Iodobenzene (**1**), 1-iodonaphthalene (**2**), $Pd_2(dba)_3$ (dba = dibenzylideneacetone); (Wako Pure Chemical Industries, Ltd.) PPh_3, CuI; (Sigma-Aldrich Co. LLC.) 2-dicyclohexylphosphino-2′,4′,6′-triisopropylbiphenyl (XPhos). Commercially available solvents: THF (Wako Pure Chemical Industries, Ltd.) and Et_3N (Kanto Chemical Co., Inc.), purified by passage through solvent purification columns under Ar pressure.[14] Compounds prepared as described in the literatures: 9-Bromo-10-butylanthracene (**3**)[15], 2,5-diethynyl-*p*-xylene (**4**)[16], (R_p)- and (S_p)-4,7,12,15-tetraethynyl[2.2]paracyclophane ((R_p)- and (S_p)-**Cp**).[8a]

Synthesis of Cp-Ph. A mixture of (S_p)-**Cp** (50 mg, 0.164 mmol), iodobenzene (**1**) (80.4 μL, 0.722 mmol), $Pd_2(dba)_3$ (30.1 mg, 0.0329 mmol), XPhos (62.5 mg, 0.131 mmol), CuI (12.5 mg, 0.0657 mmol), THF (5 mL) and Et_3N (5 mL) was placed in a round-bottom flask equipped with a magnetic stirring bar. After degassing the reaction mixture several times, the reaction was carried out at 50 °C for 12 h with

stirring. After the reaction mixture was cooled to room temperature, precipitates were removed by filtration, and the solvent was removed with a rotary evaporator. The residue was purified by column chromatography on SiO_2 ($CHCl_3$/hexane = 1/2 v/v as an eluent) and recrystallization from hexane to afford (S_p)-**Cp-Ph** (56.7 mg, 0.0931 mmol, 57%) as a colorless needle crystal. R_f = 0.16 ($CHCl_3$/hexane = 1/4 v/v). ^{1}H NMR ($CDCl_3$, 400 MHz) δ 3.07-3.15 (m, 4H), 3.54-3.61 (m, 4H), 7.17, (s, 4H), 7.35-7.43 (m, 12H), 7.58-7.61 (m, 8H) ppm; ^{13}C NMR ($CDCl_3$, 100 MHz) δ 32.7, 89.2, 94.5, 123.7, 125.2, 128.3, 128.5, 131.6, 134.7, 141.9 ppm. HRMS (MALDI) calcd. for $C_{48}H_{32}$ $[M]^+$: 608.24985, found: 608.25171. Elemental analysis calcd. for $C_{48}H_{32}$: C 94.70 H 5.30, found: C 94.82 H 5.17. (R_p)-**Cp-Ph** was obtained by the same procedure in 42% isolated yield. (S_p)-**Cp-Ph**: $[\alpha]^{23}_D$ = −77.4 (*c* 0.1, $CHCl_3$). (R_p)-**Cp-Ph**: $[\alpha]^{23}_D$ = +72.9 (*c* 0.1, $CHCl_3$).

Synthesis of Cp-Np. A mixture of (S_p)-**Cp** (30 mg, 0.0986 mmol), 1-iodonaphthalene (**2**) (63.4 μL, 0.434 mmol), $Pd_2(dba)_3$ (18.0 mg, 0.0197 mmol), XPhos (37.6 mg, 0.0789 mmol), CuI (7.5 mg, 0.0394 mmol), THF (5 mL) and Et_3N (5 mL) was placed in a round-bottom flask equipped with a magnetic stirring bar. After degassing the reaction mixture several times, the reaction was carried out at 50 °C for 12 h with stirring. After the reaction mixture was cooled to room temperature, precipitates were removed by filtration, and the solvent was removed with a rotary evaporator. The residue was purified by column chromatography on SiO_2 ($CHCl_3$/hexane = 1/2 v/v as an eluent) and recrystallization from hexane and $CHCl_3$ (poor solvent and good solvent, respectively) to afford (S_p)-**Cp-Np** (27.9 mg, 0.0345 mmol, 35%) as a yellow plate crystal. R_f = 0.46 ($CHCl_3$/hexane = 1/2 v/v). ^{1}H NMR ($CDCl_3$, 400 MHz) δ 3.29-3.37 (m, 4H), 3.78-3.86 (m, 4H), 7.34, (dt, *J* = 0.96, 6.8 Hz, 4H), 7.44 (s, 4H), 7.47-7.51 (m, 8H), 7.84 (dd, *J* = 0.96, 7.1 Hz, 8H), 7.90 (d, *J* = 8.3 Hz, 4H), 8.53 (d, *J* = 8.3 Hz, 4H) ppm; ^{13}C NMR ($CDCl_3$, 100 MHz) δ 33.0, 93.0, 94.1, 121.2, 125.4, 125.5, 126.2, 126.5, 127.1, 128.3, 128.9, 130.7, 133.3, 133.3, 135.0, 142.1 ppm. HRMS (MALDI) calcd. for $C_{64}H_{40}$ $[M]^+$: 808.31245, found: 808.31519. Elemental analysis calcd. for $C_{64}H_{40}$: C 95.02 H 4.98, found: C 94.81 H 4.85. (R_p)-**Cp-Np** was obtained by the same procedure in 64% isolated yield. (S_p)-**Cp-Np**: $[\alpha]^{23}_D$ = +209.1 (*c* 0.1, $CHCl_3$). (R_p)-**Cp-Np**: $[\alpha]^{23}_D$ = −203.8 (*c* 0.1, $CHCl_3$).

Synthesis of Cp-An. A mixture of (S_p)-**Cp** (40 mg, 0.131 mmol), 9-bromo-10-butylanthracene (**3**) (180.5 mg, 0.576 mmol), $Pd_2(dba)_3$ (24.0 mg, 0.0262 mmol), XPhos (50.0 mg, 0.105 mmol), CuI (10.0 mg, 0.0524 mmol), THF (5 mL) and Et_3N (5 mL) was placed in a round-bottom flask equipped with a magnetic stirring bar. After degassing the reaction mixture several times, the reaction was carried out at 70 °C for 36 h with stirring. After the reaction mixture was cooled to room temperature, precipitates

were removed by filtration, and the solvent was removed with a rotary evaporator. The residue was purified by column chromatography on SiO_2 ($CHCl_3$/hexane = 1/2 v/v as an eluent) and recrystallization from hexane, MeOH and $CHCl_3$ (poor and good solvent, respectively) to afford (S_p)-**Cp-An** (37.4 mg, 0.0303 mmol, 23%) as a light brown crystal. R_f = 0.58 ($CHCl_3$/hexane = 1/2 v/v). ^{1}H NMR (CD_2Cl_2, 400 MHz) δ 1.10 (t, J = 7.4 Hz, 12H), 1.67 (sext, J = 7.6 Hz, 8H), 1.84-1.92 (m, 8H), 3.60-3.71 (m, 12H), 4.08-4.16 (m, 4H), 7.06-7.10, (m, 8H), 7.38-7.42 (m, 8H), 7.71 (s, 4H), 8.32 (d, J = 8.8 Hz, 8H), 8.73 (d, J = 8.3 Hz, 8H) ppm; ^{13}C NMR (CD_2Cl_2, 100 MHz) δ 14.3, 23.8, 28.5, 33.7, 34.1, 92.9, 101.0, 116.5, 125.2, 126.1, 126.3, 126.7, 127.7, 129.7, 133.0, 135.5, 138.1, 142.3 ppm. HRMS (MALDI) calcd. for $C_{96}H_{80}$ $[M]^+$: 1232.62545, found: 1232.62964 Elemental analysis calcd. for $C_{96}H_{80}$: C 93.46 H 6.54, found: C 93.25 H 6.38. (R_p)-**Cp-An** was obtained by the same procedure in 20% isolated yield. (S_p)-**Cp-An**: $[\alpha]^{23}_D$ = +875.4 (c 0.1, $CHCl_3$). (R_p)-**Cp-An**: $[\alpha]^{23}_D$ = −873.3 (c 0.1, $CHCl_3$).

Synthesis of M-Ph. A mixture of 2,5-diethynyl-*p*-xylene (**4**) (100 mg, 0.648 mmol), iodobenzene (**1**) (0.18 mL, 1.62 mmol), $Pd_2(dba)_3$ (29.7 mg, 0.0324 mmol), PPh_3 (34.0 mg, 0.130 mmol), CuI (12.4 mg, 0.0648 mmol), THF (5 mL) and Et_3N (5 mL) was placed in a round-bottom flask equipped with a magnetic stirring bar. After degassing the reaction mixture several times, the reaction was carried out at 50 °C for 12 h with stirring. After the reaction mixture was cooled to room temperature, precipitates were removed by filtration, and the solvent was removed with a rotary evaporator. The residue was purified by column chromatography on SiO_2 (hexane as an eluent) and recrystallization from hexane to afford **M-Ph** (154.4 mg, 0.504 mmol, 78%) as a colorless plate crystal. R_f = 0.16 (hexane). ^{1}H NMR ($CDCl_3$, 400 MHz) δ 2.47 (s, 6H), 7.33-7.37, (m, 8H), 7.52-7.54 (m, 4H) ppm; ^{13}C NMR ($CDCl_3$, 100 MHz) δ 20.0, 88.3, 94.5, 123.0, 123.4, 128.3, 128.4, 131.5, 132.6, 137.3 ppm. HRMS (MALDI) calcd. for $C_{24}H_{18}$ $[M]^+$: 306.14030, found: 304.14056. Elemental analysis calcd. for $C_{24}H_{18}$: C 94.08 H 5.92, found: C 94.03 H 5.86.

Synthesis of M-Np. A mixture of 2,5-diethynyl-*p*-xylene (**4**) (100 mg, 0.648 mmol), 1-iodonaphthalene (**2**) (2.37 mL, 1.62 mmol), $Pd_2(dba)_3$ (29.7 mg, 0.0324 mmol), PPh_3 (34.0 mg, 0.130 mmol), CuI (12.4 mg, 0.0648 mmol), THF (5 mL) and Et_3N (5 mL) was placed in a round-bottom flask equipped with a magnetic stirring bar. After degassing the reaction mixture several times, the reaction was carried out at 50 °C for 12 h with stirring. After the reaction mixture was cooled to room temperature, precipitates were removed by filtration, and the solvent was removed with a rotary evaporator. The residue was purified by column chromatography on SiO_2 ($CHCl_3$/hexane = 1/9 v/v as an eluent) and recrystallization from hexane and toluene (poor and good solvent, respectively) to afford **M-Np** (179.6 mg, 0.442 mmol,

68%) as a light yellow crystal. R_f = 0.20 ($CHCl_3$/hexane = 1/9 v/v). ^{1}H NMR ($CDCl_3$, 400 MHz) δ 2.63 (s, 6H), 7.46-7.50, (m, 2H), 7.53-7.57 (m, 4H), 7.60-7.64 (m, 2H), 7.79 (dd, J = 1.4, 7.1 Hz, 2H), 7.85-7.89 (m, 4H), 8.47 (d, J = 8.3 Hz, 2H) ppm; ^{13}C NMR ($CDCl_3$, 100 MHz) δ 20.4, 92.9, 93.3, 121.2, 123.4, 125.3, 126.3, 126.5, 126.9, 128.4, 128.8, 130.5, 133.0, 133.3, 133.4, 137.3 ppm. HRMS (MALDI) calcd. for $C_{32}H_{22}$ $[M]^+$: 406.17160, found: 406.17014. Elemental analysis calcd. for $C_{32}H_{22}$: C 94.55 H 5.45, found: C 94.56 H 5.47.

Synthesis of M-An. A mixture of 2,5-diethynyl-*p*-xylene (**4**) (50 mg, 0.324 mmol), 9-bromo-10-butylanthracene (**3**) (213 mg, 0.681 mmol), $Pd_2(dba)_3$ (14.8 mg, 0.0162 mmol), XPhos (30.9 mg, 0.648 mmol), CuI (6.2 mg, 0.0324 mmol), THF (5 mL) and Et_3N (5 mL) was placed in a round-bottom flask equipped with a magnetic stirring bar. After degassing the reaction mixture several times, the reaction was carried out at 70 °C for 12 h with stirring. After the reaction mixture was cooled to room temperature, precipitates were removed by filtration, and the solvent was removed with a rotary evaporator. The residue was purified by column chromatography on SiO_2 ($CHCl_3$/hexane = 1/4 v/v as an eluent) and recrystallization from hexane and toluene (poor and good solvent, respectively) to afford **M-An** (140.8 mg, 0.228 mmol, 70%) as a yellow crystal. R_f = 0.38 ($CHCl_3$/hexane = 1/4 v/v). ^{1}H NMR ($CDCl_3$, 400 MHz) δ 1.05 (t, J = 7.6 Hz, 6H), 1.62 (sext, J = 7.3 Hz, 4H), 1.79-1.87 (m, 4H), 2.77 (s, 6H), 3.62-3.66 (m, 4H), 7.55-7.65 (m, 8H), 7.70 (s, 2H), 8.32 (d, J = 8.6 Hz, 4H), 8.76-8.78 (m, 4H) ppm; ^{13}C NMR ($CDCl_3$, 100 MHz) δ 14.1, 20.9, 23.5, 28.2, 33.7, 92.1, 99.7, 116.3, 123.6, 124.9, 125.6, 126.1, 127.6, 129.2, 132.4, 132.9, 137.1, 137.4 ppm. HRMS (MALDI) calcd. for $C_{48}H_{42}$ $[M]^+$: 618.32810, found: 618.32677. Elemental analysis calcd. for $C_{48}H_{42}$: C 93.16 H 6.84, found: C 93.13 H 6.86.

References and Notes

(1) For example: (a) *Handbook of Conducting Polymers*; Skotheim, T. A., Elsenbaumer R. L., Reynolds J. R., Eds.; Marcel Dekker: New York, 3rd edn, 2006. (b) *Organic Light Emitting Devices: Synthesis, Properties and Application*; Müellen K., Scherf, U., Eds.; Wiley-VCH: Weinheim, 2006. (c) *Organic Field-Effect Transistors*; Groza J. R., Locklin, J. J., Eds.; CRC Press Taylor & Francis Group: New York, 2007. (d) *Organic Photovoltaics: Materials, Device Physics, and Manufacturing Technologies*; Brabec, C., Dyakonov V., Scherf, U., Eds.; Wiley-VCH, Weinheim, 2008.

(2) (a) *Cyclophane Chemistry: Synthesis, Structures and Reactions*; Vögtle, F., Ed.; John Wiley & Sons: Chichester, 1993. (b) *Modern Cyclophane Chemistry*; Gleiter, R., Hopf, H., Eds.; Wiley-VCH: Weinheim, 2004.

(3) (a) Bazan,G. C.; Oldham Jr, W. J.; Lachicotte,R. J.; Tretiak, S.; Chernyak, V.; Mukamel, S. *J. Am. Chem. Soc.* **1998**, *120*, 9188–9204. (b) Wang, S.; Bazan, G. C.; Tretiak, S.; Mukamel, S. *J. Am. Chem. Soc.* **2000**, *122*, 1289–1297. (c) Zyss, J.; Ledoux, I.; Volkov, S.; Chernyak, V.; Mukamel, S.; Bartholomew, G. P.; Bazan, G. C. *J. Am. Chem. Soc.* **2000**, *122*, 11956–11962. (d) Bartholomew, G. P.; Bazan, G. C. *Acc. Chem. Res.* **2001**, *34*, 30–39. (e) Bartholomew G. P.; Bazan, G. C. *Synthesis* **2002**, 1245–1255. (f) Bartholomew G. P.; Bazan, G. C.; *J. Am. Chem. Soc.* **2002**, *124*, 5183–5196. (g) Seferos, D. S.; Banach, D. A.; Alcantar, N. A.; Israelachvili, J. N.; Bazan, G. C. *J. Org. Chem.* **2004**, *69*, 1110–1119. (h) Bartholomew, G. P.; Rumi, M.; Pond, S. J. K.; Perry, J. W.; Tretiak, S.; Bazan, G. C. *J. Am. Chem. Soc.* **2004**, *126*, 11529–11542. (i) Hong, J. W.; Woo H. Y.; Bazan, G. C. *J. Am. Chem. Soc.* **2005**, *127*, 7435–7443. (j) Bazan, G. C. *J. Org. Chem.*, **2007**, *72*, 8615–8635.

(4) (a) Bondarenko, L.; Dix, I.; Hinrichs, H.; Hopf, H. *Synthesis* **2004**, *16*, 2751–2759. (b) Hinrichs, H. A.; Boydston, J.; Jones, P. G.; Hess, K.; Herges, R.; Haley; M. M.; Hopf, H. *Chem.–Eur. J.* **2006**, *12*, 7103–7115. (c) Hopf, H. *Angew. Chem., Int. Ed.* **2008**, *47*, 9808−9812.

(5) Morisaki, Y.; Kawakami, N.; Shibata, S.; Chujo, Y. *Chem.–Asian J.* **2014**, *9*, 2891–2895.

(6) For example: (a) Morisaki, Y.; Chujo, Y. *Angew. Chem., Int. Ed.* **2006**, *45*, 6430–6437. (b) Morisaki, Y.; Chujo, Y. *Polym. Chem.* **2011**, *2*, 1249–1257. (c) Morisaki, Y.; Chujo, Y. *Chem. Lett.* **2012**, *41*, 840–846. (d) Morisaki, Y.; Ueno, S.; Saeki, A.; Asano, A.; Seki, S.; Chujo, Y.; *Chem.–Eur. J.* **2012**, *18*, 4216–4224.

(7) (a) Morisaki, Y.; Hifumi, R.; Lin, L.; Inoshita, K.; Chujo Y. *Chem. Lett.* **2012**, *41*, 990–992. (b) Morisaki, Y.; Hifumi, R.; Lin, L.; Inoshita, K.; Chujo Y. *Polym. Chem.* **2012**, *3*, 2727–2730. (c) Morisaki, Y.; Inoshita, K.; Chujo Y. *Chem.–Eur. J.* **2014**, *20*, 8386–8390.

(8) (a) Morisaki, Y.; Gon, M.; Sasamori, T.; Tokitoh N.; Chujo, Y. *J. Am. Chem. Soc.* **2014**, *136*, 3350–3353. (b) Gon, M.; Morisaki, Y.; Chujo, Y. *J. Mater. Chem. C* **2015**, *3*, 521–529.

(9) Konig, B.; Knieriem, B.; Meijere A. *Chem. Ber.* **1993**, *126*, 1643–1650.

(10) (a) Tohda, Y.; Sonogashira, K.; Hagihara, N. *Tetrahedron Lett.* **1975**, *16*, 4467–4470. (b) Sonogashira, K. In *Handbook of Organopalladium Chemistry for Organic Synthesis*; Negishi, E., Ed.; Wiley-Interscience: New York, 2002; pp 493−529.

(11) Billingsley, K.; Buchwald, S. L. *J. Am. Chem. Soc.* **2007**, *129*, 3358−3366.

(12) CD dissymmetry factor is defined as $g_{abs} = 2\Delta\varepsilon/\varepsilon$, where $\Delta\varepsilon$ indicates differences of absorbance between left- and right-handed circularly polarized light, respectively. CPL dissymmetry factor is defined as $g_{lum} = 2(I_{left}$

– I_{right})/(I_{left} + I_{right}), where I_{left} and I_{right} indicate luminescence intensities of left- and right-handed CPL, respectively.

(13) Pangborn, A. B.; Giardello, M. A.; Grubbs, R. H.; Rosen, R. K.; Timmers, F. J. *Organometallics* **1996**, *15*, 1518–1520.

(14) Keg, P.; Dell'Aquila, A.; Marinelli, F.; Kapitanchuk, O. L.; Fichou, D.; Mastrorilli, P.; Romanazzi, G.; Suranna, G. P.; Torsi, L.; Lam, Y. M.; Mhaisalkar, S. G. *J. Mater*. *Chem.* **2010**, *20*, 2448–2456.

(15) Takahashi, S.; Kuroyama, Y.; Sonogashira, K.; Hagihara, N. *Synthesis* **1980**, *8*, 627–630.

Chapter 7

Enhancement of Circularly Polarized Luminescence Based on a Planar Chiral Tetrasubstituted [2.2]Paracyclophane Framework in Dilute Solution and Aggregation

Abstract

Optically active π-conjugated oligo(phenylene-ethynylene) dimers with a planar chiral 4,7,12,15-tetrasubstituted [2.2]paracyclophane were synthesized. The author investigated the optical and chiroptical properties of the racemic and optically active compounds by UV-vis, photoluminescence (PL), circular dichroism (CD) and circularly polarized luminescence (CPL) measurements in the ground and excited states. Aggregates were prepared by the self-assembly in the mixed $CHCl_3$/MeOH solution, a spin-coated film, a drop-cast film and the annealed films. In the dilute solution, the dimers exhibited good chiroptical properties, such as 10^{-3} order dissymmetry factors (g_{abs} and g_{lum}). In the aggregation state, one of dimers formed J-aggregates and the others formed parallel H-aggregates or inclined H-aggregates as kinetically stable self-assemblies. These differences were caused by the length of π-conjugation and the strength of the intermolecular π-π interaction. The spin-coated films and drop-cast films exhibited opposite CPL signal and 10^{-2} order dissymmetry factors. Annealing of the films provided the thermodynamically stable forms. The g_{lum} values of the drop-cast thick films were drastically enhanced after annealing, and the g_{lum} values reached 10^{-1} order.

Introduction

Self-assembly of π-conjugated compounds is widely known to exhibit different properties from the isolated molecule.[1] For example, J-aggregates and H-aggregates are representative self-assembled aggregates and they have specific optical properties.[2] In the case of the optically active π-conjugated compounds, their aggregates have a potential to be circular dichroism (CD) active. The theory of intermolecular interaction between chiral chromophores based on exciton coupling is studied in detail, and it is possible to predict the direction of chirality, such as right- or left-handed helicate, using the sign of the Cotton effect in the CD spectrum.[3] It is reported that regularly high-ordered chiral structures, such as helicate, enhance the chiroptical properties of self-assembly in the ground state.[4] Recently, it was focused that the optically active chromophores exhibit circularly polarized luminescence (CPL) property. Various molecules have been designed to obtain good chiroptical properties, such as dissymmetry factor (g_{lum}) and photoluminescence quantum yield (Φ_{lum}).[5-7] The CPL properties can be enhanced by regularly high-ordered chiral structures based on low molecular weight compounds[8] and polymers[6] in the excited state. Chirality inversion sometimes occurs in the self-assembly between kinetically and thermodynamically stable aggregates.[9] The CD and CPL active π-conjugated compounds are the candidates for chiroptical sensors[10] and circularly polarized light emitters. Recently, the author reported the planar chiral 4,7,12,15-tetrasubstituted [2.2]paracyclophane framework[11] to stack two chromophores in the chiral position.[5h,k] The framework also has good planarity and symmetrical structure, which is suitable for the investigation of the behavior of self-assembly. In this chapter, the author used oligo(phenylene-ethynylene) units as rigid and planar chromophores which were easy to interact intermolecularly. Dodecyloxy groups were introduced to oligo(phenylene-ethynylene) unit to support intermolecular interaction. The chromophores are stacked in an X-shaped form which induces torsions in the self-assembly. Therefore, it is expected to exhibit different properties from racemic and chiral compounds in

their aggregation states. The author investigated the optical and chiroptical properties of the racemic and optically active oligo(phenylene-ethynylene) dimers with the planar chiral [2.2]paracyclophane framework using UV-vis, PL, CD and CPL measurements. Self-assembled aggregates were prepared in the mixed $CHCl_3$/MeOH solutions, the spin-coated, drop-cast and annealed films. The author succeeded in the observation of chirality inversion of self-assembled aggregates of the spin-coated and drop-cast films with 10^{-2} order dissymmetry factor of luminescence (g_{lum}). In addition, annealing process enhanced the g_{lum} values up to the 10^{-1} order regardless of the film preparation methods.

Results and Discussion

Synthesis

The optical resolution of planar chiral 4,7,12,15-tetrasubstituted [2.2]paracyclophane was carried out using the diastereomer method described in Chapter 3, and the obtained enantiopure compounds were converted to the corresponding (R_p)- and (S_p)-4,7,12,15-tetraethynyl[2.2]paracyclophanes.[8h] The synthetic routes to the target optically active cyclic compounds are shown in Schemes 1 and 2. Dodecyloxy groups in **CP3** and **CP5** were introduced to form self-assembled aggregates. 2-Ethylhexyl groups in **M3** and **M5** were introduced to provide the target compounds with solubility in organic solvents, such as THF, $CHCl_3$, CH_2Cl_2 and toluene because **M3** and **M5** containing dodecyloxy groups had poor solubility in organic solvents.

Scheme 1 shows the synthesis of the target planar chiral dimers **CP3** and **CP5**. In this scheme, only the reactions of the (R_p)-isomers are shown; the (S_p)-isomers were synthesized under similar conditions from (R_p)-**CP1**. Sonogashira-Hagihara coupling reaction[11] of (R_p)-**CP1** was carried out with 1-(dodecyloxy)-4-iodobenzene **1** in the catalytic system of $Pd_2(dba)_3$/CuI using dppf as a phosphine ligand to obtain compound (R_p)-**CP3** in 49% isolated

yield. Iodide of 1-bromo-4-iodobenzene **3** was reacted chemoselectively with 1-(dodecyloxy)-4-ethynylbenzene **2** to afford compound **4** in 90% isolated yield. With the same procedure as (R_p)-**CP3**, Sonogashira-Hagihara coupling of (R_p)-**CP1** with **4** was carried out to obtain (R_p)-**CP5** in 24% isolated yield.

Schemes 2 shows the synthesis of the monomeric model compounds, **M3** and **M5**. 2,5-diethynyl-*p*-xylene **5** was used as a starting compound, and **M3** and **M5** were prepared with the same procedure as the synthesis of (R_p)-**CP3** and (R_p)-**CP5**. Isolated yields were 88% for **M3** and 61% for **M5**, respectively. The structures of all new compounds in this chapter were confirmed by ^{1}H and ^{13}C NMR spectroscopy, high-resolution mass spectrometry (HRMS), and elemental analysis; the detailed synthetic procedures and NMR data are shown in the experimental section.

Scheme 1. Synthesis of (R_p)-**CP3** and (R_p)-**CP5**

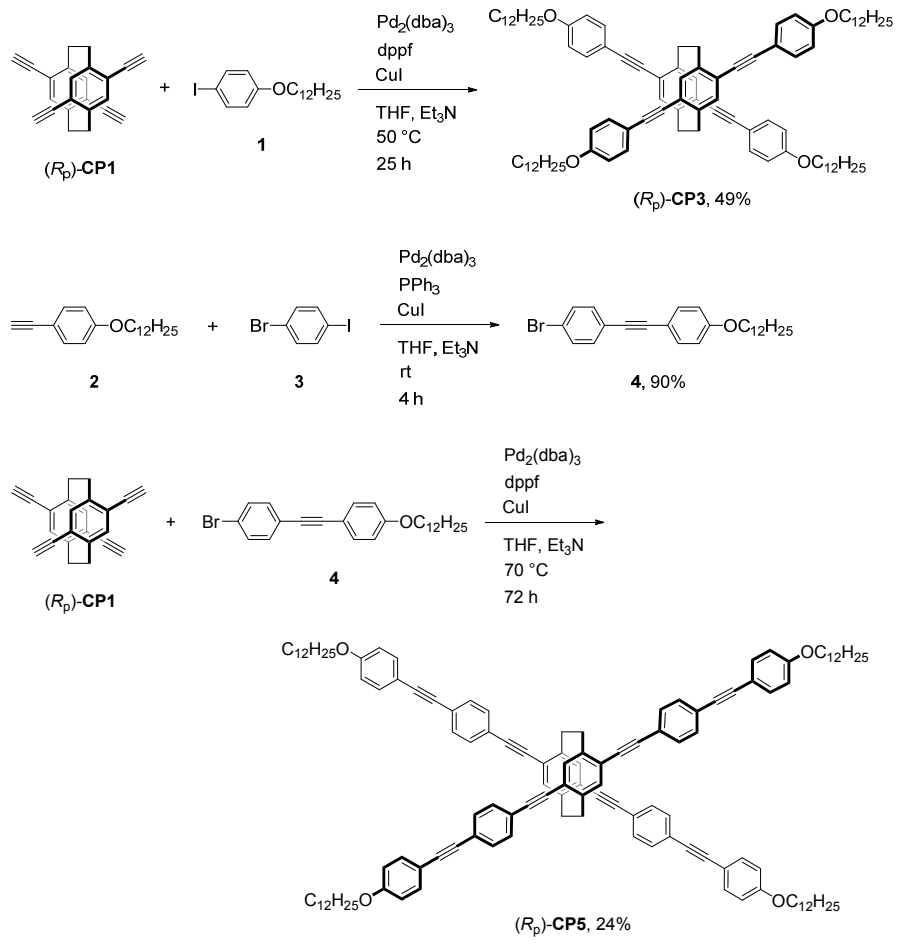

Scheme 2. Synthesis of model compounds **M3** and **M5**

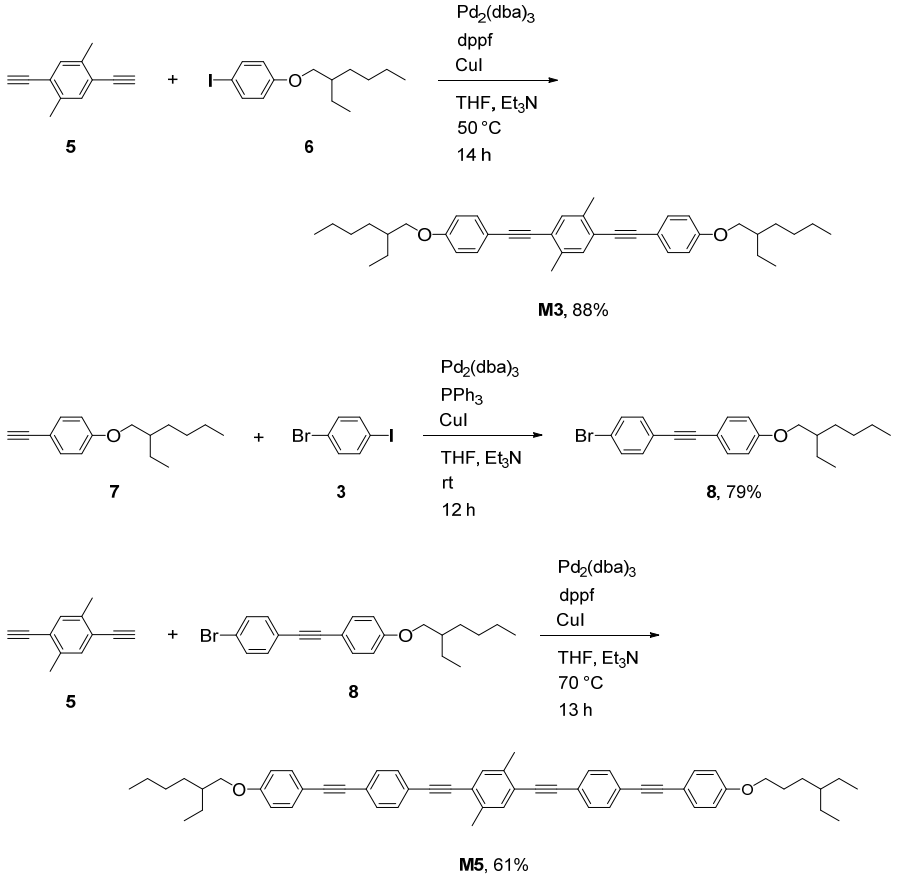

Optical Properties in the Dilute Solution

The optical properties of both enantiomers of **CP3** and **CP5** as well as their monomers **M3** and **M5** were evaluated. The optical and chiroptical data are summarized in Tables 1 and 2, respectively.

Table 1. Optical properties: Spectroscopic data of (R_p)-isomers

	λ_{abs}[a]/nm (ε / 10^5 M^{-1} cm^{-1})	λ_{lum}[b]/nm	τ[c]/ns (χ^2)	Φ_{lum}[d]
CP3	366 (0.73)	415	2.05 (1.13)	0.60
CP5	386 (1.39)	425	0.88 (1.01)	0.78
M3	338 (0.54), 363 (0.97)	368	0.77 (1.00)	0.42
M5	363 (0.97)	399	0.61 (1.11)	0.52

[a] In $CHCl_3$ (1.0×10^{-5} M). [b] In $CHCl_3$ (1.0×10^{-6} M), excited at absorption maxima. [c] Emission life time at λ_{lum}. [d] Absolute PL quantum efficiency.

Figures 1A and 1B show the UV-vis absorption spectra and photoluminescence (PL) spectra of dimers (**CP3** and **CP5**) and the monomers (**M3** and **M5**) in the dilute $CHCl_3$ solutions (1.0×10^{-5} M for UV and 1.0×10^{-6} M for PL). As shown in Figure 1A, the absorption maximum of **CP3** (366 nm) exhibited bathochromic shift compared with that of **M3** (338 nm). This effect was caused by the through-space conjugation via the [2.2]paracyclophane framework in the ground state.[11c] In PL spectra, the same bathochromic effect was observed between **CP3** (415 nm) and **M3** (368 nm). This indicates through-space conjugation occurred in the excited state. Figure 1B shows the comparison of the spectra of **CP5** and **M5**. Although the bathochromic effect was observed in the UV-vis (**CP5**: 386 nm, **M5**: 363 nm) and PL (**CP5**: 425 nm, **M5**: 399 nm) spectra, as can be seen in **CP3** and **M3**, the shorter bathochromic shift and monomer-like spectra were obtained. When the monomer conjugation length of the dimer extends, the property becomes similar to the monomeric compound. This effect was previously reported in the literature on the oligo(phenylene-vinylene) systems.[11c] PL lifetime measurement supported these results. The PL lifetime (τ) of **CP3** (τ = 2.05 ns) was far longer than that of **M3** (τ = 0.77 ns), whereas the τ of **CP5** (τ = 0.88 ns) was similar to that of **M5** (τ = 0.61 ns). An absolute PL quantum efficiency (Φ_{lum}) was enhanced by the rigid structure of [2.2]paracyclophane unit, and **CP5** exhibited high absolute PL quantum efficiency (Φ_{lum} = 0.87).

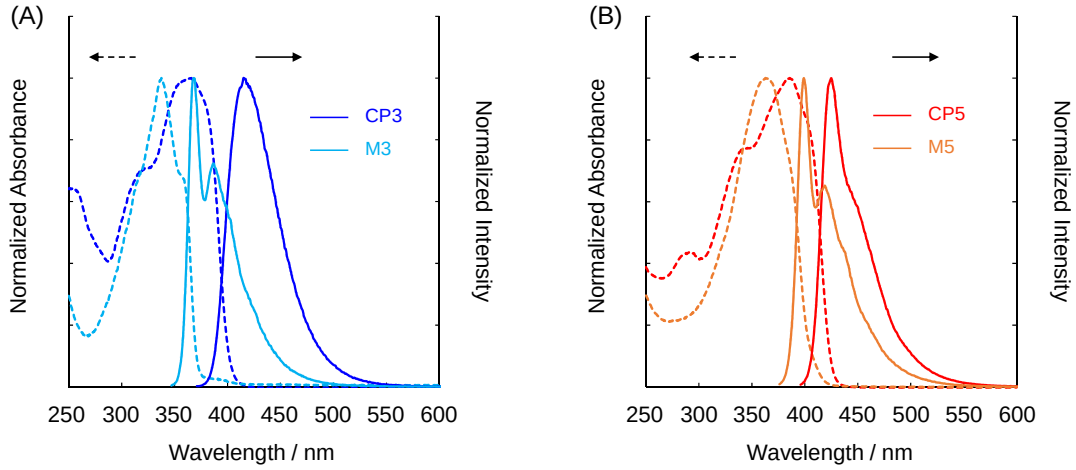

Figure 1. UV-vis absorption spectra in the dilute $CHCl_3$ (1.0×10^{-5} M) and PL spectra in the dilute $CHCl_3$ (1.0×10^{-6} M, excited at absorption maximum); (A) **CP3** and **M3**, (B) **CP5** and **M5**.

Chiroptical Properties in the Dilute Solution

The chiroptical properties in the ground and excited states of **CP3** and **CP5** were investigated by circular dichroism (CD) and CPL spectroscopy, respectively. The chiroptical data including CD and CPL dissymmetry factor[13] (g_{abs} and g_{lum}, respectively) are summarized in Table 2. Although the only properties of (R_p)-isomers are discussed here, (S_p)-isomers exhibited the same properties as (R_p)-isomers. However, the inverse signal was obtained between (R_p)-isomers and (S_p)-isomers. Figure 2 shows the CD and absorption spectra of both enantiomers of **CP3** and **CP5** in the dilute $CHCl_3$ (1.0×10^{-5} M). Mirror image Cotton effects were observed in both of CD spectra, and the g_{abs} values of the first cotton effect were estimated to be -1.2×10^{-3} for (R_p)-**CP3** and -1.1×10^{-3} for (R_p)-**CP5**, respectively. The g_{abs} values of (R_p)-**CP3** and (R_p)-**CP5** were similar in the ground state. The CPL spectra of both enantiomers of **CP3** and **CP5** in the dilute $CHCl_3$ (1.0×10^{-5} M) are shown in Figure 3. Intense mirror image CPL spectra were obtained. The g_{abs} values were estimated to be -1.7×10^{-3} for (R_p)-**CP3** and -1.2×10^{-3} for (R_p)-**CP5**, respectively. In addition, **CP5** exhibits excellent absolute PL quantum efficiency ($\Phi_{lum} = 0.87$); thus, **CP5** is a promising candidate for a CPL emitter.

Table 2. Chiroptical properties: Spectroscopic data of (S_p)-isomers and (R_p)-isomers

	g_{abs} / 10^{-3} at λ_{abs}[a]	g_{lum} / 10^{-3} at $\lambda_{lum,\,max}$[b]
(R_p)-**CP3**	−1.2	−1.7
(S_p)-**CP3**	+1.3	+1.6
(R_p)-**CP5**	−1.1	−1.2
(S_p)-**CP5**	+1.1	+1.1

[a] $g_{abs} = 2\Delta\varepsilon/\varepsilon$, where $\Delta\varepsilon$ indicates differences of absorbance between left- and right-handed circularly polarized light, respectively. The g_{abs} value of the first peak top was estimated. [b] $g_{lum} = 2(I_{left} - I_{right})/(I_{left} + I_{right})$, where I_{left} and I_{right} indicate luminescence intensities of left- and right-handed CPL, respectively.

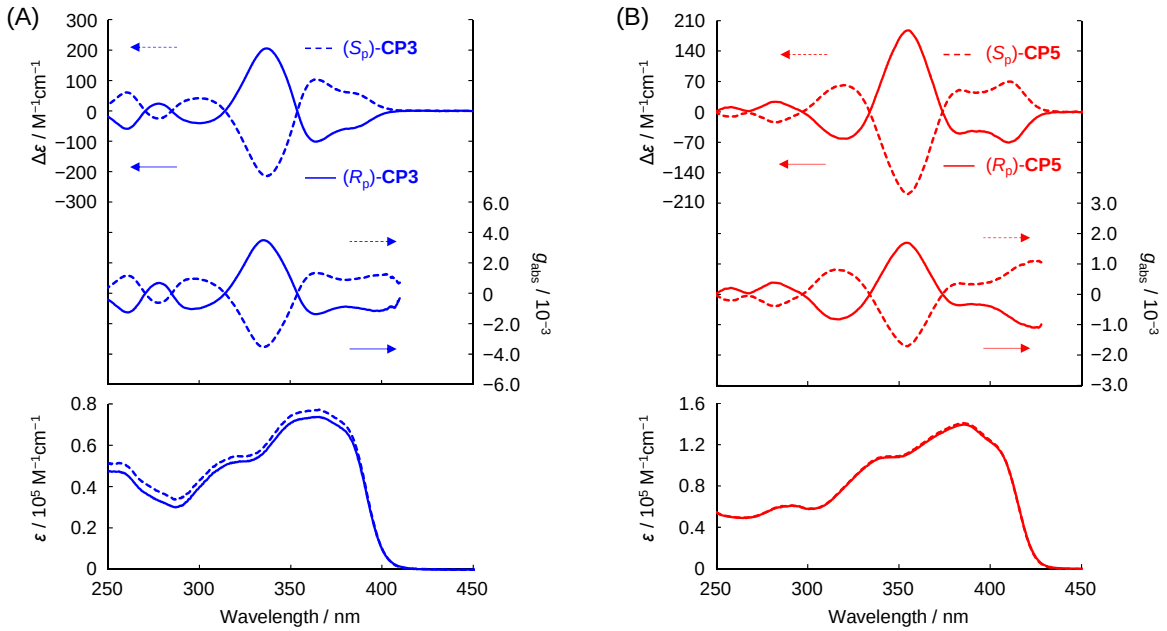

Figure 2. CD (top), g_{abs} (middle), and UV-vis absorption (bottom) spectra in the dilute $CHCl_3$ (1.0×10^{-5} M); (A) **CP3** and (B) **CP5**.

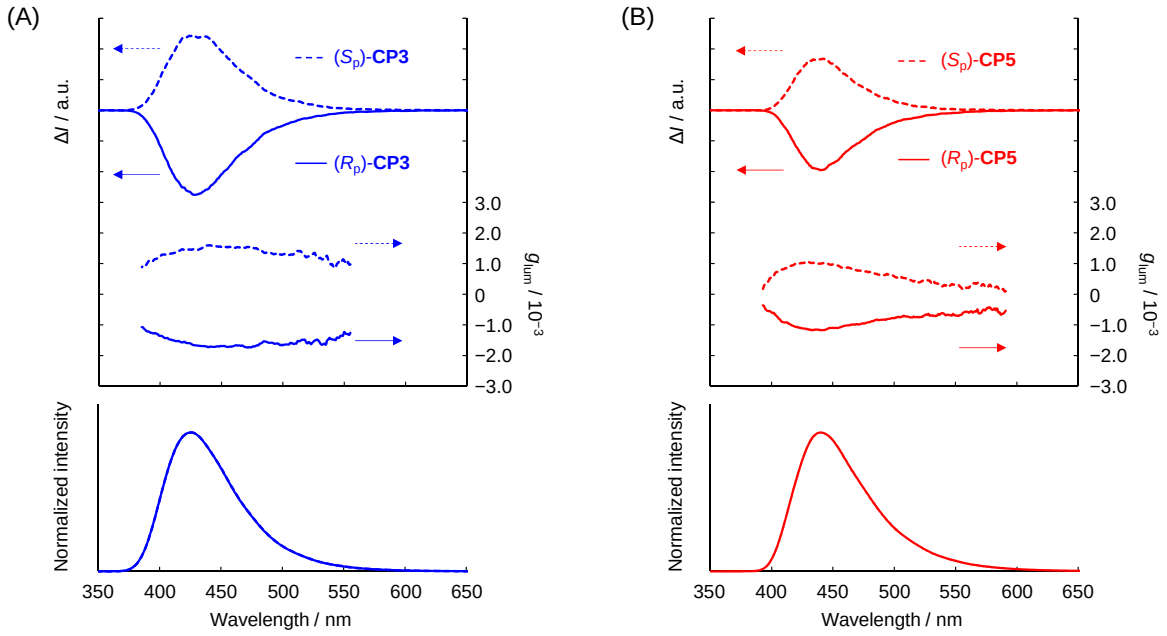

Figure 3. CPL (top), g_{lum} (middle), and PL (bottom) spectra of in the dilute $CHCl_3$ (1.0×10^{-5} M); (A) **CP3** and (B) **CP5**, excited at 300 nm.

Optical Properties in the Aggregation State

Planar π-conjugated compounds containing long alkyl chains often make self-assembly due to the π-π staking and Van der Waals interactions. Chirality are sometimes enhanced by making high-ordered structure with self-assembly. In this section, the chirality of **CP3** and **CP5** in the aggregation state was investigated by optical (UV-vis and PL) and chiroptical (CD and CPL) measurements. The spectroscopic data are summarized in Tables 3-6. Preparation methods of films are shown in the experimental section.

Figures 4 and 5 show the UV-vis absorption spectra and PL spectra of **CP3** and **CP5** in the mixed $CHCl_3$/MeOH solutions (1.0×10^{-5} M) and in the spin-coated films. The spectroscopic data are summarized in Tables 3 and 4. As shown in Figures 4A and 4B, the absorbance clearly decreased in the $CHCl_3$/MeOH = 20/80 v/v solution both in *rac*-**CP3** and in (R_p)-**CP3**. This indicates that aggregation occurred from this ratio of the mixed $CHCl_3$/MeOH solution. In the spin-coated films, the specific peaks of J-aggregates[2] were observed at 398 nm for *rac*-**CP3** and 400 nm for (R_p)-**CP3**. Figures 4C and 4D show the PL spectra of *rac*-**CP3** and (R_p)-**CP3**. The peak tops were gradually bathochromic-shifted because of the π-π interaction in the aggregates in the excited state, and relatively sharp spectra were obtained in the spin-coated films of *rac*-**CP3** and (R_p)-**CP3**. These results also indicate the formation of J-aggregates. Considering the results of UV-vis and PL spectra, (R_p)-**CP3** formed J-aggregates clearly. Figures 5A and 5B show the UV-vis absorption spectra of *rac*-**CP5** and (R_p)-**CP5**. In the case of *rac*-**CP5**, by increasing the ratio of MeOH in the mixed $CHCl_3$/MeOH solution, the absorbance from 300 nm to 430 nm decreased, and the absorbance from 250 nm to 300 nm increased. These results indicate that the formation of H-aggregates,[2] and the spin-coated films exhibited almost the same behavior. On the other hand, (R_p)-**CP5** did not show the same behavior. The absorbance of (R_p)-**CP5** aggregates decreased due to the intermolecular π-π interaction of the aggregates (vide infra). In the PL spectra (Figures 5C and 5D), the peak tops

were gradually bathochromic-shifted because of the intermolecular π-π interaction in the excited state. Larger bathochromic shift was observed in **CP5** than in **CP3** because the π-π interaction of five benzene rings of **CP5** was stronger than that of three benzene rings of **CP3**. In addition, the larger bathochromic effect indicates the existence of H-aggregation.[2a]

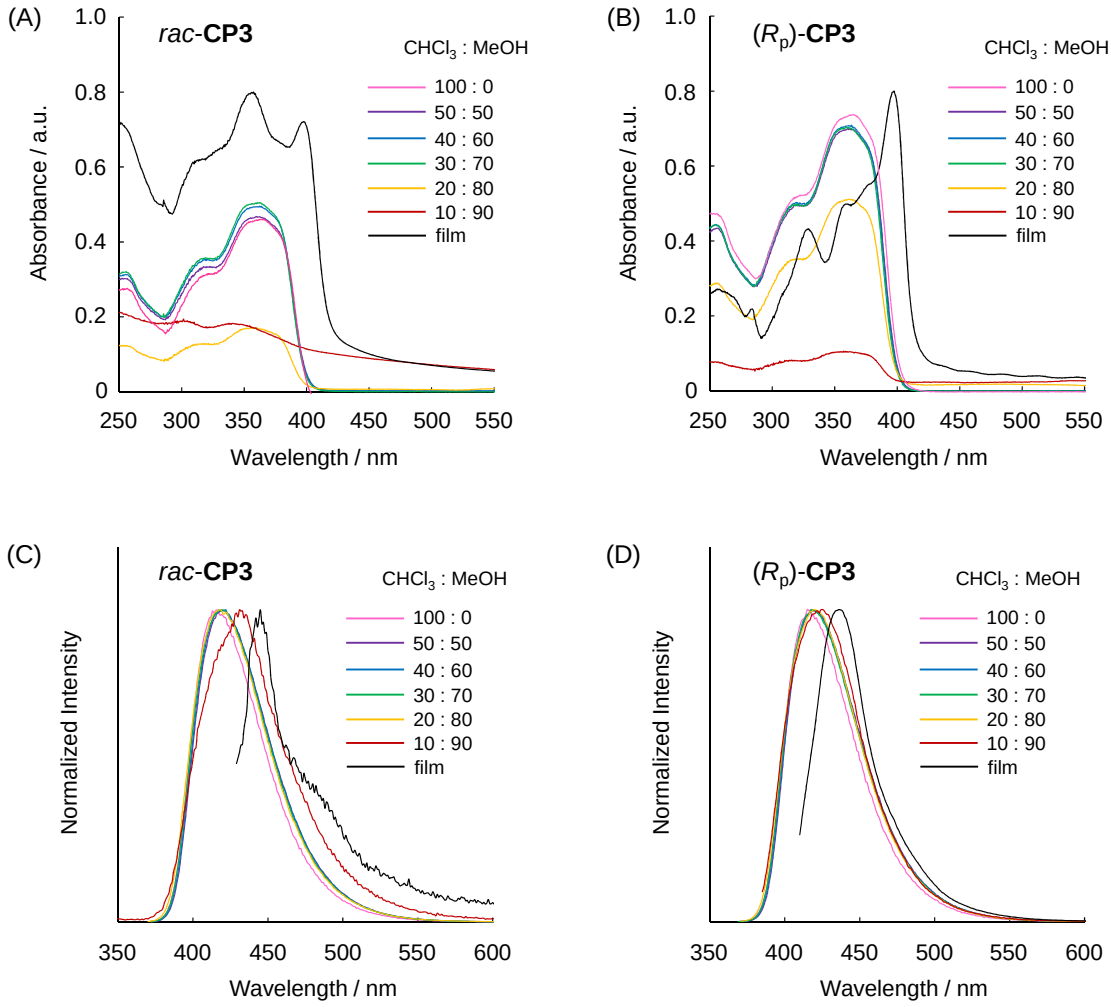

Figure 4. UV-vis absorption and PL spectra in $CHCl_3$/MeOH = 100/0, 50/50, 40/60, 30/70, 20/80, 10/90 v/v (1.0×10^{-5} M) and a spin-coated film prepared from $CHCl_3$ (3.4×10^{-3} M); (A) UV-vis absorption spectra of *rac*-**CP3** and (B) (R_p)-**CP3**. The absorbance of the spin-coated film was normalized at a base line of the absorbance of aggregation in $CHCl_3$/MeOH = 10/90 v/v. (C) PL spectra of *rac*-**CP3** and (D) (R_p)-**CP3**, excited at absorption maximum.

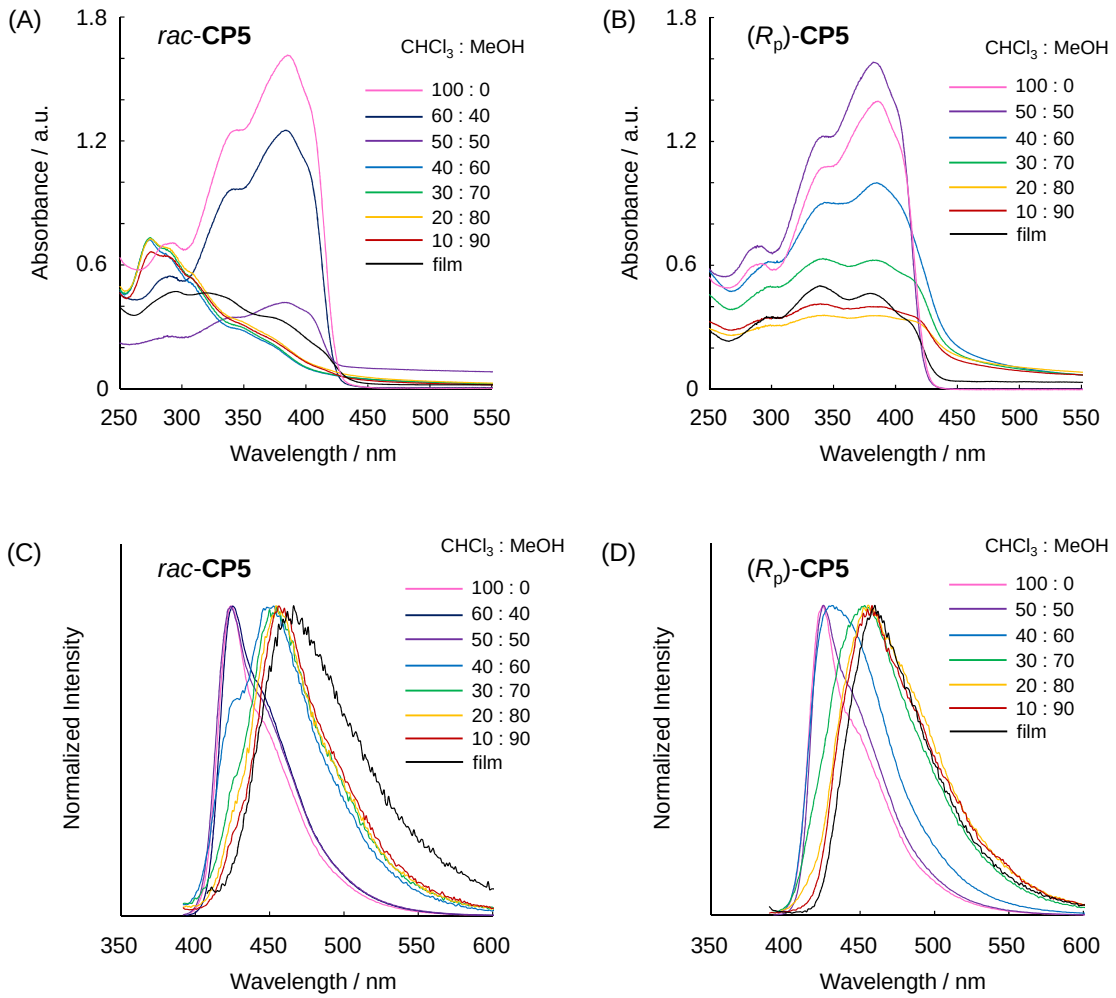

Figure 5. UV-vis absorption and PL spectra in $CHCl_3$/MeOH = 100/0, 60/40, 50/50, 40/60, 30/70, 20/80, 10/90 v/v (1.0×10^{-5} M) and a spin-coated film prepared from $CHCl_3$ (3.4×10^{-3} M); (A) UV-vis absorption spectra of *rac*-**CP5** and (B) (R_p)-**CP5**. The absorbance of the spin-coated film was normalized at a base line of the absorbance of aggregation in $CHCl_3$/MeOH = 10/90 v/v. (C) PL spectra of *rac*-**CP5** and (D) (R_p)-**CP5**, excited at absorption maximum.

Chiroptical Properties in the Aggregation State

The chiroptical properties of **CP3** and **CP5** in the aggregation states were also investigated by circular dichroism (CD) and CPL spectroscopy. Chiroptical data are summarized in Tables 3-6. Figures 6A and 6B show the CD and UV-vis absorption spectra of both enantiomers of **CP3** in the mixed $CHCl_3$/MeOH solutions (1.0×10^{-5} M) and in the spin-coated films. Figures

6A and 6B show the spectra of (R_p)-**CP3** and (S_p)-**CP3**, respectively. In both CD spectra, mirror image Cotton effects were observed. As shown in Figure 6, by increasing the ratio of MeOH, the g_{abs} values decreased. On the other hand, the largest g_{abs} values were observed at the specific peak of J-aggregates in the spin-coated films, and the g_{abs} values were estimated to be -9.8×10^{-3} for (R_p)-**CP3** and $+9.6 \times 10^{-3}$ for (S_p)-**CP3**, respectively. They were 8.2 times and 7.4 times larger than those in the dilute solution, respectively. The enhancement of the g_{abs} values were caused by chiral J-aggregates of **CP3** in the ground state. The CPL spectra of both enantiomers of **CP3** in the mixed $CHCl_3$/MeOH solutions (1.0×10^{-5} M) and in the spin-coated films are shown in Figures 6C and 6D. Intense mirror image CPL spectra were obtained for the enantiomers. As shown in the CD spectra, the largest g_{lum} values were obtained in the spin-coated films, and they were estimated to be -7.9×10^{-3} for (R_p)-**CP3** and $+11 \times 10^{-3}$ for (S_p)-**CP3**, respectively. They were 4.6 times and 6.9 times larger than those in the dilute solution, respectively. This enhancement of the chirality in the spin-coated films was caused by J-aggregates formation in the excited state.

Figures 7A and 7B show the CD and absorption spectra of both enantiomers of **CP5** in the mixed $CHCl_3$/MeOH solutions (1.0×10^{-5} M) and in the spin-coated films. In both CD spectra, mirror image Cotton effects were observed. Unlike the case of **CP3**, by increasing the ratio of MeOH, signal inversion of the g_{abs} values occurred at the first Cotton effect. This effect was caused by the exciton couplings of the intermolecular π-π interaction and the details are discussed in the mechanism section. The largest g_{abs} value was observed in the mixed solution $CHCl_3$/MeOH = 40/60 v/v. They were estimated to be $+6.5 \times 10^{-3}$ for (R_p)-**CP5** and -7.4×10^{-3} for (S_p)-**CP5**, which were 5.9 times and 6.7 times larger than in the dilute solution, respectively. The CPL spectra of both enantiomers of **CP5** in the mixed $CHCl_3$/MeOH solutions (1.0×10^{-5} M) and in the spin-coated films are shown in Figures 7C and 7D. As can be seen in the CD spectra, signal inversion was observed in the CPL spectra. The largest g_{lum}

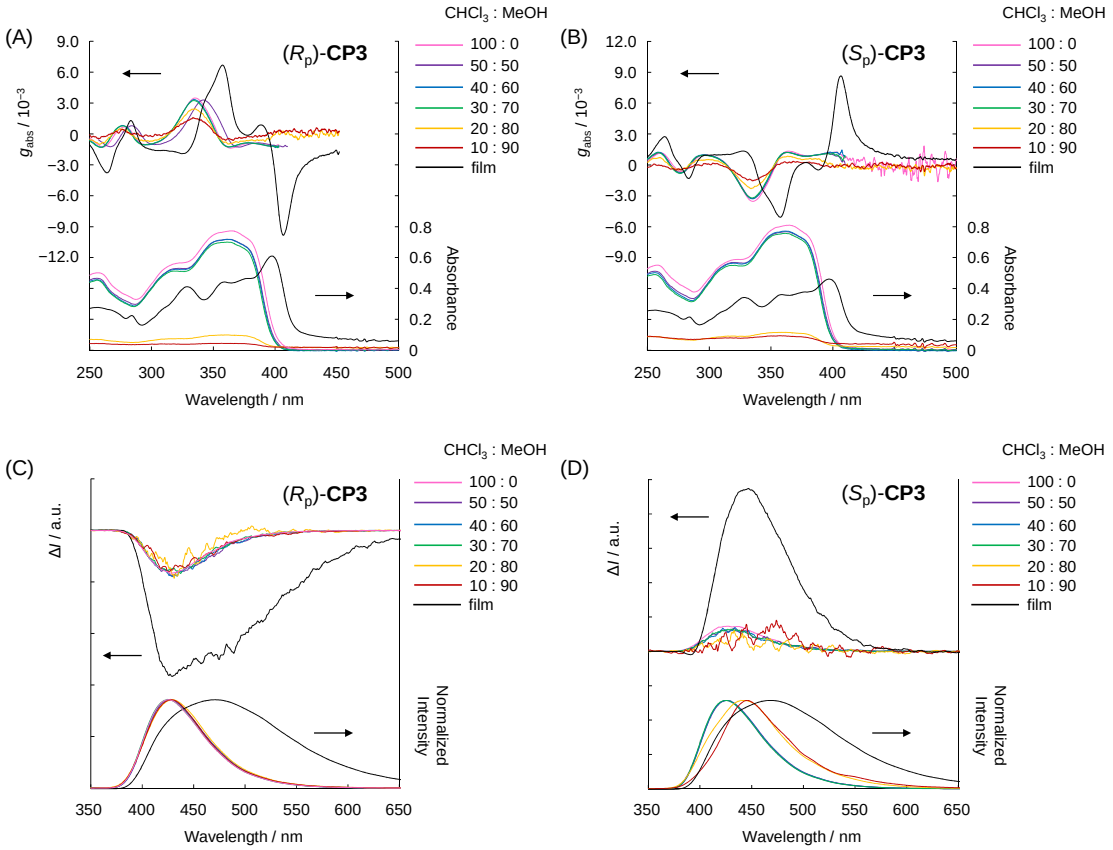

Figure 6. CD and CPL spectra in $CHCl_3$/MeOH = 100/0-10/90 v/v (1.0×10^{-5} M) and a spin-coated film prepared from $CHCl_3$ (3.4×10^{-3} M); (A) CD spectra of (R_p)-**CP3** and (B) (S_p)-**CP3**; (C) PL spectra of (R_p)-**CP3** and (D) (S_p)-**CP3**, excited at 300 nm.

Table 3. Optical and chiroptical spectroscopic data of (R_p)-**CP3** in the aggregation state or the film state

$CHCl_3$:MeOH or film	10:0	5:5	4:6	3:7	2:8	1:9	film[a]
λ_{abs} / nm	365	360	363	359	361	357	400
λ_{lum} / nm	415	418	418	418	419	425	436
Φ_{lum}[b]	0.65	0.86	0.86	0.72	0.28	0.19	0.22
g_{abs}[c] / 10^{-3}	−1.2	−1.3	−1.3	−1.7	−1.0	−0.63	−9.8
g_{lum}[d] / 10^{-3}	−1.7	−1.8	−1.9	−1.9	−1.9	−1.6	−7.9

[a] Spin-coated film prepared from $CHCl_3$ solution (3.4×10^{-3} M). [b] Absolute PL quantum efficiency. [c] $g_{abs} = 2\Delta\varepsilon/\varepsilon$, where $\Delta\varepsilon$ indicates differences of absorbance between left- and right-handed circularly polarized light, respectively. The g_{abs} value of the first peak top was estimated. [d] $g_{lum} = 2(I_{left} - I_{right})/(I_{left} + I_{right})$, where I_{left} and I_{right} indicate luminescence intensities of left- and right-handed CPL, respectively.

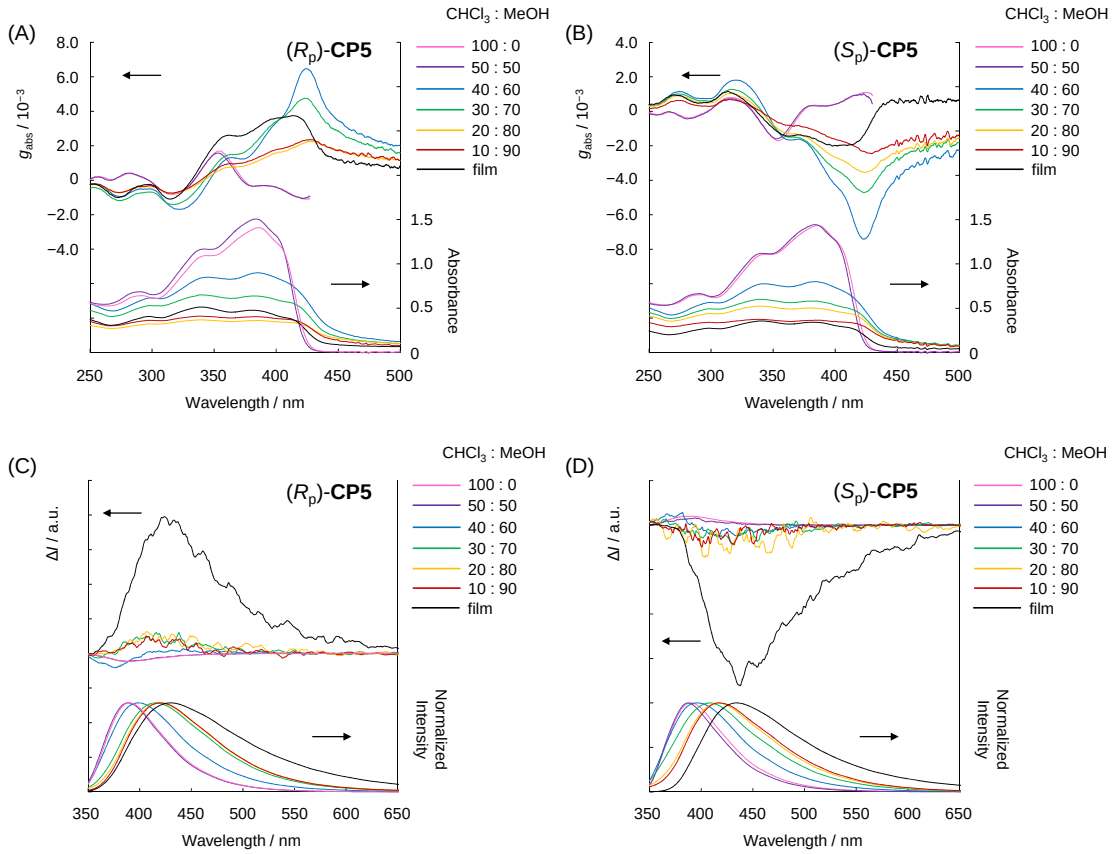

Figure 7. CD and CPL spectra in $CHCl_3$/MeOH = 100/0-10/90 v/v (1.0×10^{-5} M) and a spin-coated film prepared from $CHCl_3$ (3.4×10^{-3} M); (A) CD spectra of (R_p)-**CP5** and (B) (S_p)-**CP5**; (C) PL spectra of (R_p)-**CP5** and (D) (S_p)-**CP5**, excited at 300 nm.

Table 4. Optical and chiroptical spectroscopic data of (R_p)-**CP5** in the aggregation state or the film state

$CHCl_3$:MeOH or film	10:0	5:5	4:6	3:7	2:8	1:9	film[a]
λ_{abs} / nm	386	382	387	379	381	385	339
λ_{lum} / nm	425	425	431	453	455	458	462
Φ_{lum}[b]	0.82	0.89	0.43	0.20	0.13	0.13	0.19
g_{abs}[c] / 10^{-3}	−1.1	−1.1	+6.4	+5.7	+2.2	+2.4	+3.7
g_{lum}[d] / 10^{-3}	−1.2	−1.1	+1.1	+3.4	+3.3	+2.7	+20

[a] Spin-coated film prepared from $CHCl_3$ solution (3.4×10^{-3} M). [b] Absolute PL quantum efficiency. [c] $g_{abs} = 2\Delta\varepsilon/\varepsilon$, where $\Delta\varepsilon$ indicates differences of absorbance between left- and right-handed circularly polarized light, respectively. The g_{abs} value of the first peak top was estimated. [d] $g_{lum} = 2(I_{left} - I_{right})/(I_{left} + I_{right})$, where I_{left} and I_{right} indicate luminescence intensities of left- and right-handed CPL, respectively.

value was obtained in the spin-coated films instead of the $CHCl_3$/MeOH = 40/60 v/v solution. They were estimated to be $+2.0 \times 10^{-2}$ for (R_p)-**CP5** and -1.3×10^{-2} for (S_p)-**CP5**, which were 17 times and 12 times larger than those in the dilute solution, respectively. This enhancement of the chirality in the spin-coated films was also caused by exciton couplings in the excited state.

Properties of Annealing Films

Three types of films, spin-coated film, drop-cast thin film and drop-cast thick film were prepared to investigate the chirality of the self-assembly. The details of the film preparation methods are shown in the experimental section. CD and CPL measurements were carried out, and the spectroscopic data are summarized in Tables 5 and 6.

Table 5. $g_{abs} \times 10^2$ values of (R_p)-, (S_p)-**CP3** and **CP5** in film states

film state	spin-coated film[a]		drop-cast thin film[a]	
	before annealing	after annealing[b]	before annealing	after annealing[b]
(R_p)-**CP3**	−0.97	−0.76	−3.9	−0.36
(S_p)-**CP3**	+0.96	+1.2	+3.4	+0.32
(R_p)-**CP5**	−0.035	−5.2	−0.12	−10
(S_p)-**CP5**	+0.086	+5.3	+0.039	+10

[a] Films prepared from $CHCl_3$ solution (3.4×10^{-3} M). [b] **CP3**: Annealing at 65 ˚C for 3 h, **CP5**: Annealing at 90 ˚C for 5 h.

Table 6. $g_{lum} \times 10^2$ values of (R_p)-, (S_p)-**CP3** and **CP5** in film states

film state	spin-coated film[a]		drop-cast thin film[a]		drop-cast thick film[a]	
	before annealing	after annealing[b]	before annealing	after annealing[b]	before annealing	after annealing[b]
(R_p)-**CP3**	−0.61	−0.87	−1.2	−2.6	−7.5	−0.43
(S_p)-**CP3**	+0.56	+1.0	+0.96	+3.4	+5.6	+0.15
(R_p)-**CP5**	+2.1	−12	−0.86	−17	−3.0	−25
(S_p)-**CP5**	−1.4	+13	+1.6	+13	+1.1	+27

[a] Films prepared from $CHCl_3$ solution (3.4×10^{-3} M). [b] **CP3**: Annealing at 65 ˚C for 3 h, **CP5**: Annealing at 90 ˚C for 5 h.

Figures 8A and 8B show the CD spectra of (R_p)-**CP3** and (S_p)-**CP3**, respectively. The spectra of the drop-cast thick films were not included in the Figure because the absorbance was too large to measure. The spin-coated films and the annealing films exhibited almost same profiles. However, the g_{abs} value of the drop-cast thin films decreased after annealing. The largest g_{abs} values in the ground state were obtained in the drop-cast thin films before annealing, and the g_{abs} values were estimated to be -3.9×10^{-2} for (R_p)-**CP3** and $+3.4 \times 10^{-2}$ for (S_p)-**CP3**, respectively. The absorption band was too weak to be observed in the UV-vis absorption spectra because it was attributed to the intermolecular π-π interaction. On the other hand, in the CPL spectra (Figures 8C and 8D), the g_{lum} values of the drop-cast thin films were enhanced after annealing. This is caused by the difference of the ground state and the excited state. The

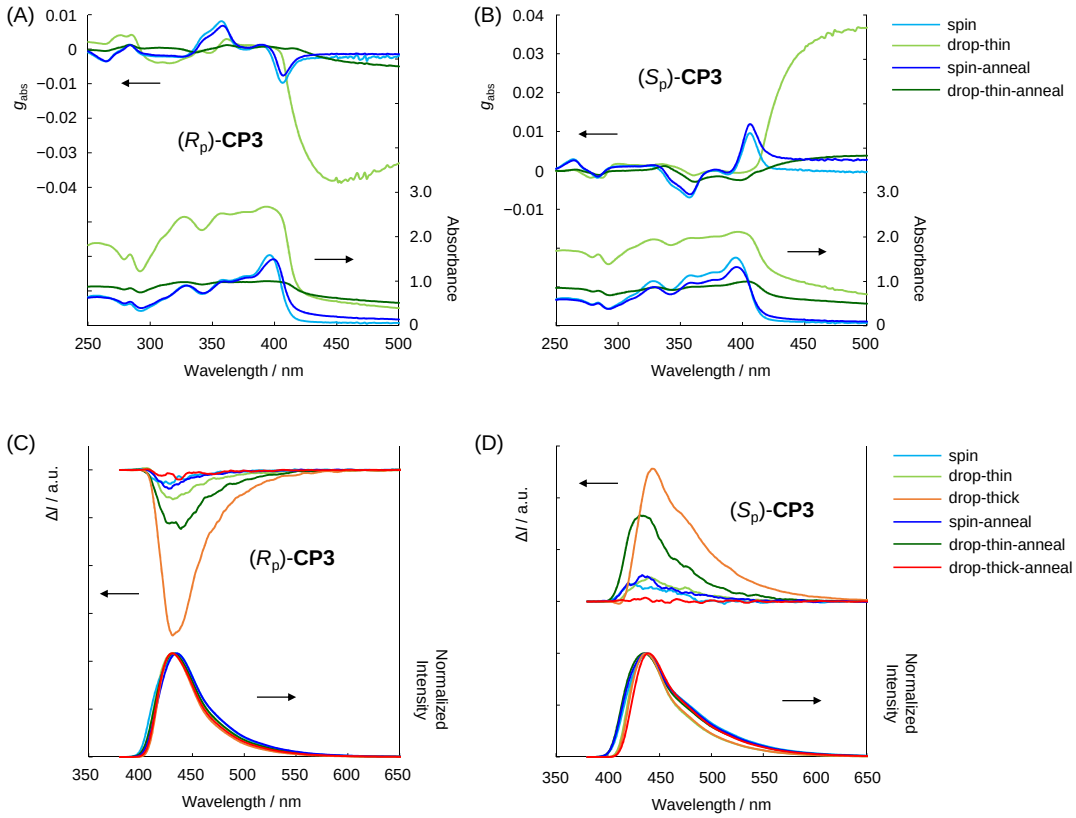

Figure 8. CD and CPL spectra in the spin-coated film and the drop-cast film. The spin-coated film prepared from $CHCl_3$ (3.4×10^{-3} M), drop-cast thin film prepared from $CHCl_3$ (3.4×10^{-3} M, 30 μL × 5 times) and drop-cast thick film prepared from $CHCl_3$ (3.4×10^{-3} M, 30 μL × 15 times). (A) CD spectra of (R_p)-**CP3** and (B) (S_p)-**CP3**; (C) CPL spectra of (R_p)-**CP3** and (D) (S_p)-**CP3**, excited at 350 nm.

largest g_{lum} values were observed in the drop-cast thick films before annealing, and they were estimated to be -7.5×10^{-2} for (R_p)-**CP3** and $+5.6 \times 10^{-2}$ for (S_p)-**CP3**, respectively. In the case of the drop-cast thick films, the g_{lum} values decreased after annealing because chiral self-assembly was disordered by heating.

Figures 9A and 9B show the CD spectra of (R_p)-**CP5** and (S_p)-**CP5**, respectively. The g_{abs} values of the spin-coated films and the drop-cast thin films were enhanced at the weak absorption band at the longest wavelength after annealing. This behavior was not seen in the **CP3** systems. The signal was inverse compared with the aggregates in the spin-coated films before annealing or mixed $CHCl_3$/MeOH solution systems. These results indicate that the different aggregation formed in the spin-coated and drop-cast films before annealing.

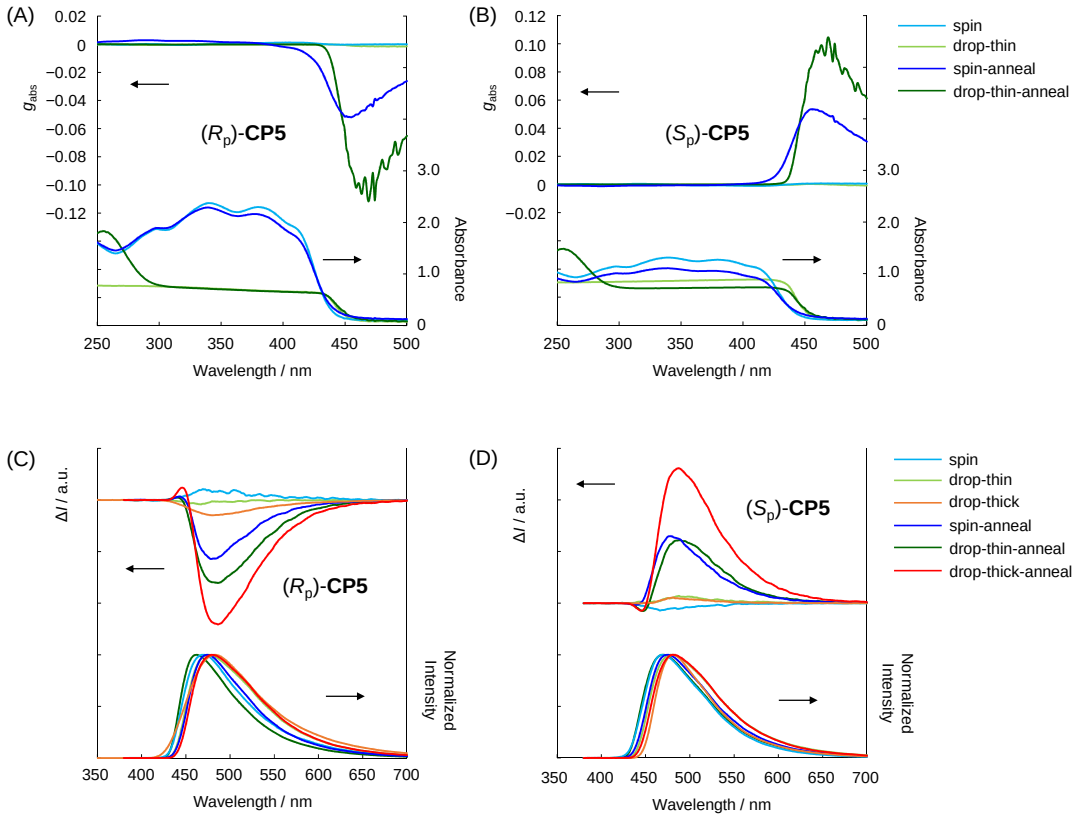

Figure 9. CD and CPL spectra in the spin-coated film and the drop-cast film. The spin-coated film prepared from $CHCl_3$ (3.4×10^{-3} M), drop-cast thin film prepared from $CHCl_3$ (3.4×10^{-3} M, 30 μL × 5 times) and drop-cast thick film prepared from $CHCl_3$ (3.4×10^{-3} M, 30 μL × 15 times). (A) CD spectra of (R_p)-**CP5** and (B) (S_p)-**CP5**; (C) CPL spectra of (R_p)-**CP5** and (D) (S_p)-**CP5**, excited at 350 nm.

Annealing formed the stable aggregation regardless of the film preparation methods. The largest g_{abs} values in the ground state were obtained in the drop-cast thin films after annealing, and the g_{abs} values were estimated to be −0.1 for (R_p)-**CP5** and +0.1 for (S_p)-**CP5**, respectively. In the CPL spectra (Figures 9C and 9D), largest g_{abs} values in the excited state were observed in the drop-cast thick films after annealing, and the g_{lum} values were estimated to be −0.25 for (R_p)-**CP5** and +0.27 for (S_p)-**CP5**, respectively. In the case of **CP5**, the chirality was enhanced by annealing. This is one of the largest g_{lum} values in the self-assembled organic compounds.[6c,e,f,k,l] Absolute PL quantum efficiency was calculated; however, absorptions of these films were too large to obtain correct values. The calculated absolute PL quantum efficiencies are summarized in Table 7.

Table 7. Absolute quantum efficiency of prepared films[a]

film state	spin-coated film[b]		drop-cast thin film[b]	
	before annealing	after annealing[c]	before annealing	after annealing[c]
(R_p)-**CP3**	0.36	0.38	0.39	0.39
(S_p)-**CP3**	0.31	0.32	0.34	0.34
(R_p)-**CP5**	0.09	0.06	0.53	0.09
(S_p)-**CP5**	0.13	0.05	0.58	0.09

[a] Absorption rate was approximately 60%-90% and thick film was removed because the absorption maximum was saturated. [b] Films prepared from $CHCl_3$ solution (3.4×10^{-3} M). [c] **CP3**: Annealing at 65 ˚C for 3 h, **CP5**: Annealing at 90 ˚C for 5 h.

Mechanism

The mechanism of the self-assembly and chirality is discussed here. A spin-coated method formed a kinetically stable film. A drop-cast method formed a thermodynamically stable film. Annealing method moved the films to more stable forms. The transition dipole moment was estimated by time-dependent density functional theory (TD-DFT) at the B3LYP/6-31G(d,p)//B3LYP/6-31G(d,p) levels.

Figure 10 shows the proposal mechanism of self-assembly of **CP3**. The reason of decrease of chirality of **CP3** in the drop-cast thick films is that the interaction of dodecyloxy groups was very large and **CP3** made random aggregates. Dodecyloxy chains of the thin films did not move drastically than those of the thick films; therefore, the chirality was slightly enhanced by forming rigid aggregates. UV-vis absorption spectra of thin films of **CP3** before and after annealing (Figure 8A) support this proposal. The shape of the spectra was almost similar, but the molar extinction coefficient decreased because of the strong intermolecular interaction. In the case of the spin-coated films, the spectra remained before and after annealing because the J-aggregates were stable at 65 ˚C.

Figure 11 shows the proposal mechanism of the self-assembly of **CP5**. As shown in Figure 5, *rac*-**CP5** formed H-aggregates, while (R_p)-**CP5** did not form it. These were spin-coated films, and the aggregates made kinetically stable form. The main interaction was π-π interaction of five benzene rings. Figure 11 shows the intermolecular π-π interaction of *rac*-**CP5** and (R_p)-**CP5**. As shown clearly in the structure, the arrangement of transition dipole moment was different between *rac*-**CP5** and (R_p)-**CP5**. *Rac*-**CP5** exhibited parallel H-aggregates but (R_p)-**CP5** exhibited inclined H-aggregates.[14] When the inclined H-aggregates arrange the transition moment in approximately 60˚ described in Figure 11, positive Cotton effect was observed due to exciton coupling. Therefore, CD and CPL signal in the aggregation state was inverse compared with in the dilute solution (Figure 7). The drop-cast and annealing methods moved the films to thermodynamically stable forms. The main interaction is not π-π interaction and the inclined H-aggregates were slightly changed to overlap the dodecyloxy chain. As a result, exciton coupling was inverse compared with the kinetically stable form (Figure 9), although the regular form was not clear (the angle was $0^\circ < x < 90^\circ$). In addition, annealing process made the interaction stronger and the chirality was enhanced drastically.

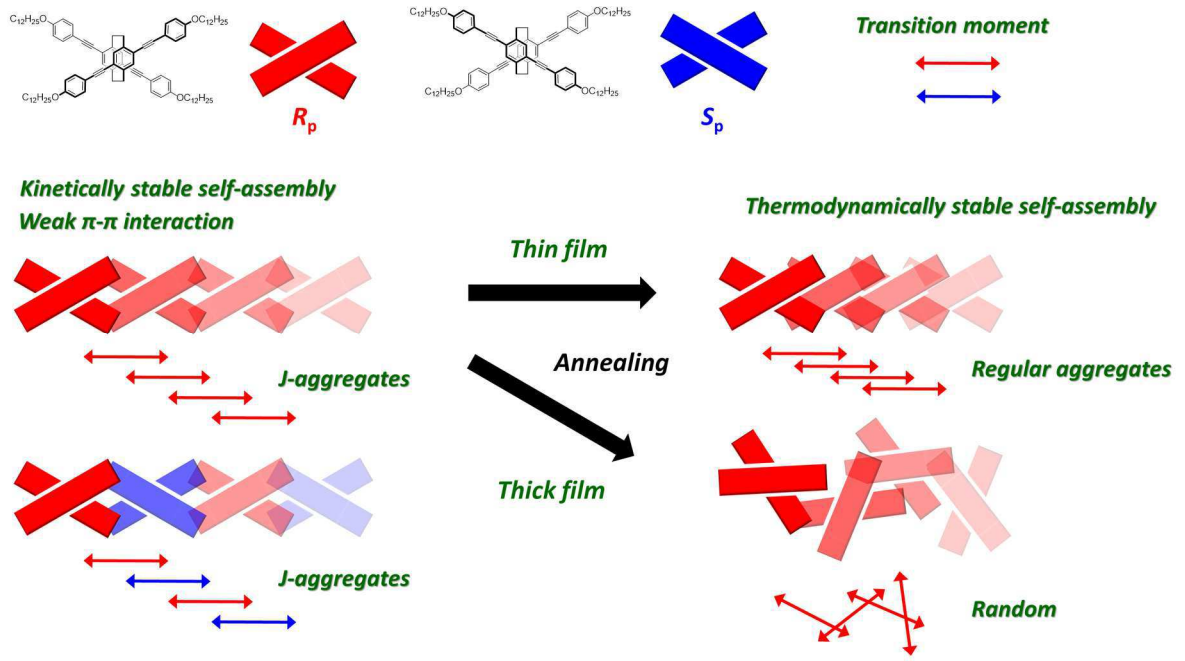

Figure 10. Proposal mechanism of Self-assembly of **CP3**.

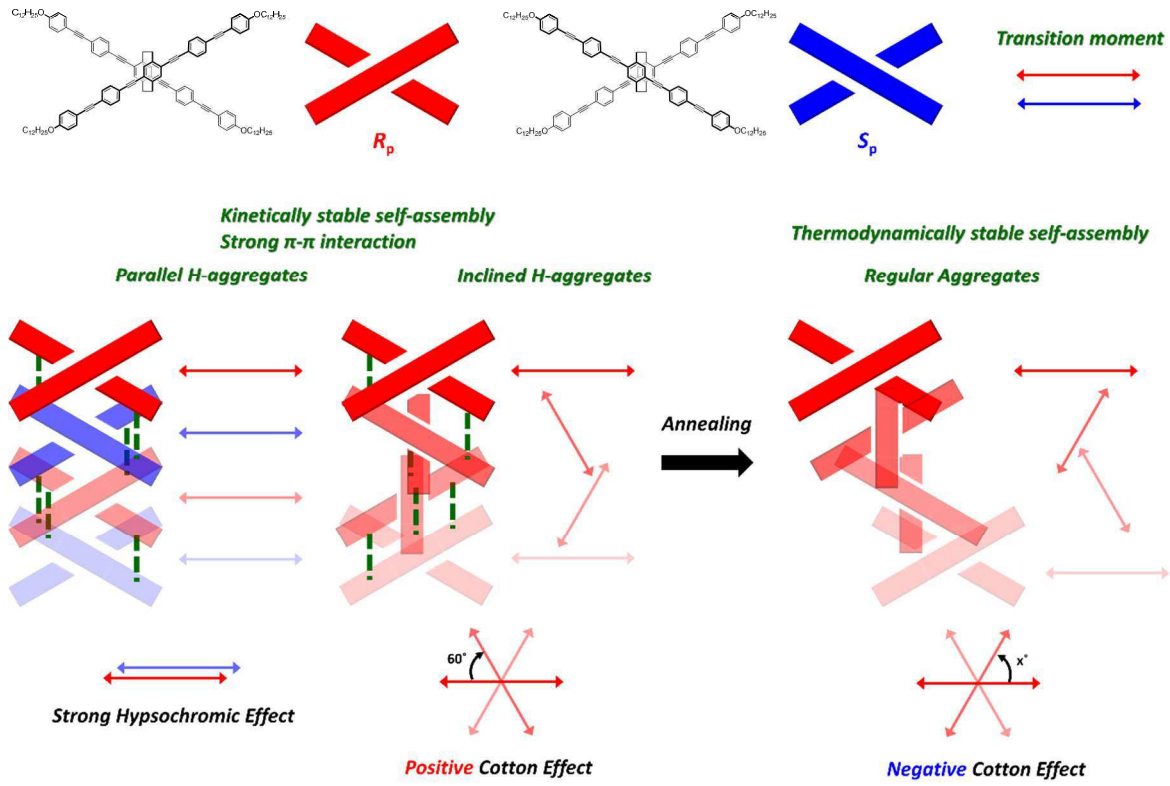

Figure 11. Proposal mechanism of self-assembly of **CP5**. The direction of transition dipole moment was estimated by TD-DFT (B3LYP/6-31G(d,p)//B3LYP/6-31G(d,p)).

Conclusions

In summary, optically active π-conjugated oligo(phenylene-ethynylene) dimers with a planar chiral [2.2]paracyclophane were synthesized. In the dilute solution, **CP3** and **CP5** exhibited good chiroptical properties, 10^{-3} order g_{abs} and g_{lum} values. Especially, **CP5** exhibited excellent CPL profiles (ε_{abs} = 13,900, Φ_{lum} = 0.87, and $|g_{lum}| = 1.2 \times 10^{-3}$). The properties of the aggregates of **CP3** and **CP5** were investigated. Under the kinetically stable condition, racemic and optically active **CP3** formed J-aggregates, whereas, *rac*-**CP5** formed parallel H-aggregates and optically active **CP5** formed inclined H-aggregates because of the difference of the strength of the intermolecular π-π interaction. **CP5** exhibited unique chiroptical properties, for example, signal inversion depending on the aggregates. The g_{lum} values reached 10^{-2} order in the opposite signal between the spin-coated films and the drop-cast films. Annealing method moved the films to the thermodynamically stable forms. The g_{lum} values of the drop-cast thick films of **CP5** were drastically enhanced after annealing, and the g_{lum} values reached 10^{-1} order ($|g_{lum}| = 0.27$) regardless of the film preparation methods. This is one of the largest g_{lum} values in the self-assembled organic compounds. These properties are attributed to the unique chirality of the planar chiral 4,7,12,15-tetrasubstituted [2.2]paracyclophane framework. This is the first report realizing 10^{-1} order g_{lum} using the self-assembled system thanks to the planar chirality as the only chiral source.

Experimental Section

General. ^{1}H and ^{13}C NMR spectra were recorded on JEOL EX400 and AL400 instruments at 400 and 100 MHz, respectively. Samples were analyzed in $CDCl_3$, and the chemical shift values were expressed relative to Me_4Si as an internal standard. Analytical thin layer chromatography (TLC) was performed with silica gel 60 Merck F254 plates. Column chromatography was performed with Wakogel C-300 silica gel. High-resolution mass (HRMS) spectrometry was performed at the Technical Support Office (Department of Synthetic Chemistry and Biological Chemistry, Graduate School of Engineering, Kyoto University), and the HRMS spectra were obtained on a Thermo Fisher Scientific orbitrapXL spectrometer for matrix assisted laser desorption/ionization (MALDI) and a Thermo Fisher Scientific EXACTIVE spectrometer for atmospheric pressure chemical ionization (APCI). Recyclable preparative high-performance liquid chromatography (HPLC) was carried out on a Japan Analytical Industry Co. Ltd., Model LC918R (JAIGEL-1H and 2H columns) and LC9204 (JAIGEL-2.5H and 3H columns) using $CHCl_3$ as an eluent. UV-vis spectra were recorded on a SHIMADZU UV-3600 spectrophotometer, and samples were analyzed in $CHCl_3$ at room temperature. Fluorescence emission spectra were recorded on a HORIBA JOBIN YVON Fluoromax-4 spectrofluorometer, and samples were analyzed in $CHCl_3$ at room temperature. The PL lifetime measurement was performed on a Horiba FluoroCube spectrofluorometer system; excitation was carried out using a UV diode laser (NanoLED 292 nm and 375 nm). Specific rotations ($[\alpha]^{t}_{D}$) were measured with a HORIBA SEPA-500 polarimeter. Circular dichroism (CD) spectra were recorded on a JASCO J-820 spectropolarimeter with $CHCl_3$ as a solvent at room temperature. Circularly polarized luminescence (CPL) spectra were recorded on a JASCO CPL-200S with $CHCl_3$ as a solvent at room temperature. Elemental analyses were performed at the Microanalytical Center of Kyoto University.

Materials. Commercially available compounds used without purification: (Tokyo Chemical Industry Co, Ltd.) $PdCl_2(PPh_3)_2$, $Pd_2(dba)_3$ (dba = dibenzylideneacetone), 1,1'-bis(diphenylphosphino)ferrocene (dppf); (Wako Pure Chemical Industries, Ltd.) 1-bromo-4-iodobenzene (**3**), PPh_3, CuI. Commercially available solvents: MeOH (Wako Pure Chemical Industries, Ltd.), used without further purification. THF (Wako Pure Chemical Industries, Ltd.) and Et_3N (Kanto Chemical Co., Inc.), purified by passage through solvent purification columns under Ar pressure.[15] Compounds prepared as described in the literatures: 1-(Dodecyloxy)-4-iodobenzene (**1**)[16], 1-(dodecyloxy)-4-ethynylbenzene (**2**)[17], 2,5-diethynyl-*p*-xylene (**5**)[18], 1-[(2-ethylhexyl)oxy]-4-iodobenzene (**6**)[19], 1-[(2-ethylhexyl)oxy]-4-

ethynylbenzene (**7**)[19], *rac*-4,7,12,15-tetraethynyl[2.2]paracyclophane (*rac*-**CP1**)[20], (R_p)- and (S_p)-4,7,12,15-tetraethynyl[2.2]paracyclophane ((R_p)- and (S_p)-**CP1**).[5h]

Preparation of Films. CP3: A spin-coated film: 30 μL of the $CHCl_3$ solution (3.4×10^{-3} M) was put on a Quartz plate and rotated at 200 rpm (10 sec.). After the rotation, the solvent was evaporated at 500 rpm (10 sec.). A spin-coated film was prepared by repeating this manipulation 15 times on the same Quartz plate. A drop-cast thin film: 30 μL of the $CHCl_3$ solution (3.4×10^{-3} M) was put on a Quartz plate and leave it in the fume hood until all the solvent was evaporated. A drop-cast thin film was prepared by repeating this manipulation 5 times on the same Quartz plate. A drop-cast thick film: 30 μL of the $CHCl_3$ solution (3.4×10^{-3} M) was put on a Quartz plate and leave it in the fume hood until all the solvent was evaporated. A drop-cast thick film was prepared by repeating this manipulation 15 times on the same Quartz plate. These films were annealed at 65 ˚C for 3 h. This temperature was selected to prevent melting and crystallization. **CP5**: A spin-coated film, a drop-cast thin film and a drop-cast thick film were prepared by the same way as **CP3**. These films were annealed at 90 ˚C for 5 h. This temperature was selected to prevent melting and crystallization.

Computational Details. The Gaussian 09 program package[21] was used for computation. The structures of **CP5** were optimized in the ground S_0 states and their electric structures were calculated. The density functional theory (DFT) was applied for the optimization of the structures in the S_0 states at the B3LYP/6-31G(d,p) levels. The electric states and transitions from S_0 to S_1 states of the **CP5** with the optimized geometries in the S_0 states were calculated by time-dependent DFT (TD-DFT) at the B3LYP/6-31G(d,p) levels. The transition moment was estimated in the transitions from S_0 to S_1 states.

Synthesis of CP3. A mixture of (R_p)-**CP1** (20.0 mg, 0.0657 mmol), 1-(dodecyloxy)-4-iodobenzene (**4**) (112.3 mg, 0.289 mmol), $Pd_2(dba)_3$ (6.3 mg, 0.0066 mmol), dppf (7.3 mg, 0.013 mmol), CuI (2.5 mg, 0.013 mmol), THF (1.5 mL) and Et_3N (1.5 mL) was placed in a round-bottom flask equipped with a magnetic stirring bar. After degassing the reaction mixture several times, the reaction was carried out at 50 °C for 25 h with stirring. After the reaction mixture was cooled to room temperature, precipitates were removed by filtration, and the solvent was removed with a rotary evaporator. The crude residue was purified by column chromatography on SiO_2 ($CHCl_3$/hexane = 2/3 v/v as an eluent). Further purification was carried out by HPLC ($CHCl_3$ as an eluent) and reprecipitation with $CHCl_3$ and MeOH (good and poor solvent, respectively) to afford (R_p)-**CP3** (43.3 mg, 0.0322 mmol, 49%) as a light yellow solid. R_f = 0.30 ($CHCl_3$/hexane = 2/3 v/v). ^{1}H NMR ($CDCl_3$, 400 MHz) δ 0.89 (t, J = 6.7 Hz, 12H), 1.22-1.42 (m, 64H), 1.42-1.51 (m, 8H), 1.78-1.86 (m, 8H), 3.02-3.12 (m, 4H), 3.46-3.58 (m, 4H), 4.00

(t, J = 6.5 Hz, 8H), 6.91 (d, J = 8.5 Hz, 8H), 7.11 (s, 4H), 7.51 (d, J = 8.8 Hz, 8H) ppm; ^{13}C NMR ($CDCl_3$, 100 MHz) δ 14.1, 22.7, 26.0, 29.2, 29.3, 29.4, 29.6, 29.6, 29.6, 29.7, 31.9, 32.6, 68.2, 88.1, 94.5, 114.6, 115.7, 125.1, 132.9, 134.4, 141.6, 159.3 ppm. HRMS (MALDI) calcd. for $C_{96}H_{128}O_4$ $[M]^+$: 1345.98071, found: 1344.97867. Elemental analysis calcd. for $C_{96}H_{128}O_4$: C 85.66 H 9.59, found: C 84.96 H 9.67. (S_p)-**CP3** and *rac*-**CP3** were obtained by the same procedure in 30% and 46% isolated yields, respectively. (R_p)-**CP3**: $[\alpha]^{23}_D$ = +51.7 (*c* 0.1, $CHCl_3$). (S_p)-**CP3**: $[\alpha]^{23}_D$ = −42.6 (*c* 0.1, $CHCl_3$).

Synthesis of 4. A mixture of **2** (2.67 g, 9.35 mmol), 1-bromo-4-iodobenzene (**3**) (2.78 g, 9.82 mmol), $Pd_2(dba)_3$ (219 mg, 0.234 mmol), PPh_3 (251 mg, 0.935 mmol), CuI (92.2 mg, 0.468 mmol), THF (80 mL) and Et_3N (20 mL) was placed in a round-bottom flask equipped with a magnetic stirring bar. After degassing the reaction mixture several times, the reaction was carried out at room temperature for 4 h with stirring. After the reaction, precipitates were removed by filtration, and the solvent was removed with a rotary evaporator. The residue was purified by column chromatography on SiO_2 ($CHCl_3$/hexane = 1/1 v/v as an eluent). Further purification was carried out by recrystallization with $CHCl_3$ and MeOH (good and poor solvent, respectively) to afford **4** (3.72 g, 8.42 mmol, 90%) as a light brown solid. R_f = 0.88 ($CHCl_3$/hexane = 1/1 v/v). ^{1}H NMR ($CDCl_3$, 400 MHz) δ 0.88 (t, J = 6.8 Hz, 3H), 1.22-1.39 (m, 16H), 1.39-1.49 (m, 2H), 1.74-1.82 (m, 2H), 3.96 (t, J = 6.6 Hz, 2H), 6.88 (d, J = 9.0 Hz, 2H), 7.35 (d, J = 8.5 Hz, 2H), 7.45 (s, 2H), 7.45 (s, 2H) ppm; ^{13}C NMR ($CDCl_3$, 100 MHz) δ 14.1, 22.7, 26.0, 29.2, 29.3, 29.4, 29.6, 29.6, 29.6, 29.7, 31.9, 68.1, 86.9, 90.7 114.6, 114.7, 122.0, 122.7, 131.5, 132.8, 133.0, 159.4 ppm. HRMS (APCI) calcd. for $C_{26}H_{34}BrO$ $[M+H]^+$: 441.1788, found: 441.1778. Elemental analysis calcd. for $C_{26}H_{33}BrO$: C 70.74 H 7.54 Br 18.10, found: C 70.80 H 7.68 Br 18.33.

Synthesis of CP5. A mixture of (R_p)-**CP1** (10.0 mg, 0.0329 mmol), **4** (63.8 mg, 0.645 mmol), $Pd_2(dba)_3$ (3.0 mg, 0.0033 mmol), dppf (3.6 mg, 0.0066 mmol), CuI (1.3 mg, 0.0066 mmol), THF (1.5 mL) and Et_3N (1.5 mL) was placed in a round-bottom flask equipped with a magnetic stirring bar. After degassing the reaction mixture several times, the reaction was carried out at 70 °C for 72 h with stirring. After the reaction mixture was cooled to room temperature, precipitates were removed by filtration, and the solvent was removed with a rotary evaporator. The residue was purified by column chromatography on SiO_2 ($CHCl_3$/hexane = 2/3 v/v as an eluent). Further purification was carried out by HPLC ($CHCl_3$ as an eluent) and reprecipitation with $CHCl_3$ and MeOH (good and poor solvent, respectively) to afford (R_p)-**CP5** (14.1 mg, 0.00873 mmol, 24%) as a light yellow solid. R_f = 0.18 ($CHCl_3$/hexane = 2/3 v/v). ^{1}H NMR ($CDCl_3$, 400 MHz) δ 0.89 (t, J = 6.8 Hz, 12H), 1.22-1.41 (m, 64H), 1.41-1.51 (m, 8H), 1.75-1.83 (m, 8H), 3.04-3.17 (m, 4H), 3.51-3.61 (m, 4H), 3.98 (t, J = 6.6 Hz, 8H), 6.88 (d, J = 9.0 Hz, 8H),

7.15 (s, 4H), 7.48 (d, J = 8.8 Hz, 8H), 7.54 (s, 8H), 7.54 (s, 8H) ppm; ^{13}C NMR ($CDCl_3$, 100 MHz) δ 14.1, 22.7, 26.0, 29.2, 29.3, 29.4, 29.6, 29.6, 29.6, 29.7, 31.9, 32.7, 68.1, 87.9, 90.9, 91.7, 94.6, 114.6, 114.9, 122.9, 123.8, 125.2, 131.4, 131.5, 133.1, 134.8, 141.9, 159.5 ppm. HRMS (MALDI) calcd. for $C_{128}H_{144}O_4$ $[M]^+$: 1745.10591, found: 1745.10742. Elemental analysis calcd. for $C_{128}H_{144}O_4$: C 88.03 H 8.31, found: C 86.99 H 8.30. (S_p)-**CP5** and *rac*-**CP5** were obtained by the same procedure in 12% and 11% isolated yields, respectively. (R_p)-**CP5**: $[\alpha]^{23}_D$ = +8.2 (c 0.1, $CHCl_3$). (S_p)-**CP5**: $[\alpha]^{23}_D$ = −7.3 (c 0.1, $CHCl_3$).

Synthesis of M3. A mixture of **5** (100 mg, 0.648 mmol), **6** (519 mg, 1.43 mmol), $Pd_2(dba)_3$ (29.7 mg, 0.0324 mmol), dppf (35.9 mg, 0.0648 mmol), CuI (12.4 mg, 0.0648 mmol), THF (5 mL) and Et_3N (5 mL) was placed in a round-bottom flask equipped with a magnetic stirring bar. After degassing the reaction mixture several times, the reaction was carried out at 50 °C for 14 h with stirring. After the reaction mixture was cooled to room temperature, precipitates were removed by filtration, and the solvent was removed with a rotary evaporator. The residue was purified by column chromatography on SiO_2 ($CHCl_3$/hexane = 1/1 v/v as an eluent). Further purification was carried out by recrystallization with $CHCl_3$ and MeOH (good and poor solvent, respectively) to afford **M3** (320.5 mg, 0.569 mmol, 88%) as a yellow solid. R_f = 0.78 ($CHCl_3$/hexane = 1/1 v/v). ^{1}H NMR ($CDCl_3$, 400 MHz) δ 0.88-0.97 (m, 12H), 1.28-1.36 (m, 8H), 1.36-1.56 (m, 8H) 1.68-1.77 (m, 2H), 2.44 (s, 6H), 3.82-3.89 (m, 4H), 6.87 (d, J = 9.0 Hz, 4H), 7.33 (s, 2H), 7.44 (d, J = 9.0 Hz, 4H) ppm; ^{13}C NMR ($CDCl_3$, 100 MHz) δ 11.1, 14.0, 20.0, 23.1, 14.0, 29.1, 30.6, 39.5, 70.8, 87.1, 94.6, 114.7, 115.4, 123.1, 132.4, 132.9, 137.0, 159.6 ppm. HRMS (APCI) calcd. for $C_{40}H_{51}O_2$ $[M+H]^+$: 563.3884, found: 563.3877. Elemental analysis calcd. for $C_{40}H_{50}O_2$: C 85.36 H 8.95 found: C 85.28 H 8.86.

Synthesis of 8. A mixture of **7** (5.94 g, 25.8 mmol), 1-bromo-4-iodobenzene (**3**) (7.30 g, 25.8 mmol), $Pd_2(dba)_3$ (591 mg, 0.645 mmol), PPh_3 (677 mg, 2.58 mmol), CuI (245.7 mg, 1.29 mmol), THF (80 mL) and Et_3N (20 mL) was placed in a round-bottom flask equipped with a magnetic stirring bar. After degassing the reaction mixture several times, the reaction was carried out at room temperature for 12 h with stirring. Then, precipitates were removed by filtration, and the solvent was removed with a rotary evaporator. The residue was purified by column chromatography on SiO_2 ($CHCl_3$/hexane = 1/9 v/v as an eluent). Further purification was carried out by recrystallization with $CHCl_3$ and MeOH (good and poor solvent, respectively) to afford **8** (7.81 g, 20.3 mmol, 79%) as a light brown crystal. R_f = 0.38 ($CHCl_3$/hexane = 1/9 v/v). ^{1}H NMR ($CDCl_3$, 400 MHz) δ 0.86-0.98 (m, 6H), 1.25-1.56 (m, 8H), 1.68-1.78 (m, 1H), 3.80-3.90 (d, J = 6.0 Hz, 2H), 6.86 (d, J = 8.7 Hz, 2H), 7.32-7.39 (m, 2H), 7.40-7.56 (m,

4H) ppm; ^{13}C NMR ($CDCl_3$, 100 MHz) δ 11.2, 14.2, 23.1, 23.9, 29.2, 30.6, 39.4, 70.7, 86.9, 90.7, 114.6, 114.6, 121.9, 122.6, 131.5, 132.8, 132.9, 159.6 ppm. HRMS (APCI) calcd. for $C_{22}H_{26}BrO$ $[M+H]^+$: 385.1162, found: 385.1154. Elemental analysis calcd. for $C_{22}H_{25}BrO$: C 68.57 H 6.54 Br 20.74, found: C 68.33 H 6.52 Br 20.88.

Synthesis of M5. A mixture of **5** (100 mg, 0.648 mmol), **8** (550 mg, 1.43 mmol), $Pd_2(dba)_3$ (29.7 mg, 0.0324 mmol), dppf (35.9 mg, 0.0648 mmol), CuI (12.4 mg, 0.0648 mmol), THF (5 mL) and Et_3N (5 mL) was placed in a round-bottom flask equipped with a magnetic stirring bar. After degassing the reaction mixture several times, the reaction was carried out at 70 °C for 13 h with stirring. After the reaction mixture was cooled to room temperature, precipitates were removed by filtration, and the solvent was removed with a rotary evaporator. The residue was purified by column chromatography on SiO_2 ($CHCl_3$/hexane = 1/1 v/v as an eluent). Further purification was carried out by recrystallization with $CHCl_3$ and MeOH (good and poor solvent, respectively) to afford **M5** (299.3 mg, 0.392 mmol, 61%) as a yellow solid. R_f = 0.82 ($CHCl_3$/hexane = 1/1 v/v). ^{1}H NMR ($CDCl_3$, 400 MHz) δ 0.89-0.95 (m, 12H), 1.28-1.36 (m, 8H), 1.36-1.53 (m, 8H) 1.68-1.78 (m, 2H), 2.47 (s, 6H), 3.81-3.90 (m, 4H), 6.87 (d, J = 8.8 Hz, 4H), 7.34 (s, 2H), 7.45 (d, J = 8.8 Hz, 4H), 7.48 (s, 8H) ppm; ^{13}C NMR ($CDCl_3$, 100 MHz) δ 11.1, 14.0, 20.0, 23.0, 24.0, 29.1, 30.6, 39.5, 70.8, 87.8, 90.1, 91.7, 94.5, 114.7, 114.9, 122.8, 123.1, 123.8, 131.4, 131.4, 132.7, 133.1, 137.4, 159.8 ppm. HRMS (MALDI) calcd. for $C_{56}H_{58}O_2$ $[M]^+$: 762.44313, found: 762.44222. Elemental analysis calcd. for $C_{56}H_{58}O_2$: C 88.15 H 7.66 found: C 88.23. H 7.58.

References and Notes

(1) (a) Hoeben, F. J. M.; Jonkheijm, P.; Meijer, E. W.; Schenning, A. P. H. J. *Chem. Rev.* **2005**, *105*, 1491–1546. (b) Zang, L.; Che, Y.; Moore, J. S. *Acc. Chem. Res.* **2008**, *41*, 1596–1608. (c) Frauenrath, H.; Jahnke, E. *Chem.–Eur. J.* **2008**, *14*, 2942–2955. (d) Vogelsang, J.; Adachi, T.; Brazard, J.; Vanden Bout, D. A.; Barbara, P. F. *Nat. Mater.* **2011**, *10*, 942–946. (e) Ortony, J. H.; Chatterjee, T.; Garner, L. E.; Chworos, A.; Mikhailovsky, A.; Kramer, E. J.; Bazan, G. C. *J. Am. Chem. Soc.* **2011**, *133*, 8380–8387. (f) Cabanetos, C.; El Labban, A.; Bartelt, J. A.; Douglas, J. D.; Mateker, W. R.; Fréchet, J. M. J.; McGehee, M. D.; Beaujuge, P. M. *J. Am. Chem. Soc.* **2013**, *135*, 4656–4659.

(2) (a) Spano, F. C. *Acc. Chem. Res.* **2010**, *43*, 429–439. (b) Würthner, F.; Kaiser, T. E.; Saha-Möller, C. R. *Angew. Chem., Int. Ed.* **2011**, *50*, 3376–3410.

(3) (a) Person, R. V.; Monde, K.; Humpf, H.; Berova, N.; Nakanishi, K. *Chirality* **1995**, *7*, 128–135. (b) Freedman, T. B.; Cao, X.; Dukor, R. K.; Nafie, L. A. *Chirality* **2003**, *15*, 743–758. (c) Berova, N.; Bari, L. D.; Pescitelli, G. *Chem. Soc. Rev.* **2007**, *36*, 914–931. (d) van Dijk, L.; Bobbert, P. A.; Spano, F. C. *J. Phys. Chem. B* **2010**, *114*, 817–825.

(4) (a) Koe, J. R.; Fujiki, M.; Motonaga, M.; Nakashima, H. *Macromolecules* **2001**, *34*, 1082–1089. (b) Schenning, A. P. H. J.; Jonkheijm, P.; Peeters, E.; Meijer, E. W. *J. Am. Chem. Soc.* **2001**, *123*, 409–416. (c) George, S. J.; Ajayaghosh, A.; Jonkheijm, P.; Schenning, A. P. H. J.; Meijer, E. W. *Angew. Chem., Int. Ed.* **2004**, *43*, 3422–3425. (d) Ajayaghosh, A.; Varghese, R.; George, S. J.; Vijayakumar, C. *Angew. Chem., Int. Ed.* **2006**, *45*, 1141–1144. (e) Ajayaghosh, A.; Varghese, R.; Mahesh, S.; Praveen, V. K. *Angew. Chem., Int. Ed.* **2006**, *45*, 7729–7732. (f) Cardolaccia, T.; Li, Y.; Schanze, K. S. *J. Am. Chem. Soc.* **2008**, *130*, 2535–2545. (g) Nowacki, B.; Oh, H.; Zanlorenzi, C.; Jee, H.; Baev, A.; Prasad, P. N.; Akcelrud, L. *Macromolecules* **2013**, *46*, 7158–7165.

(5) (a) Field, J. E.; Muller, G.; Riehl, J. P.; Venkataraman, D. *J. Am. Chem. Soc.* **2003**, *25*, 11808–11809. (b) Kawai, T.; Kawamura, K.; Tsumatori, H.; Ishikawa, M.; Naito, M.; Fujiki, M.; Nakashima, T. *ChemPhysChem* **2007**, *8*, 1465–1468. (c) Kaseyama, T.; Furumi, S.; Zhang, X.; Tanaka, K.; Takeuchi, M.; *Angew. Chem., Int. Ed.* **2011**, *50*, 3684–3687. (d) Maeda, H.; Bando, Y.; Shimomura, K.; Yamada, I.; Naito, M.; Nobusawa, K.; Tsumatori, H.; Kawai, T. *J. Am. Chem. Soc.* **2011**, *133*, 9266–9269. (e) Sawada, Y.; Furumi, S.; Takai, A.; Takeuchi, M.; Noguchi, K.; Tanaka, K. *J. Am. Chem. Soc.* **2012**, *134*, 4080–4083. (f) Haketa, Y.; Bando, Y.; Takaishi, K.; Uchiyama, M.; Muranaka, A.; Naito, M.; Shibaguchi, H.; Kawai, T.; Maeda, H. *Angew. Chem., Int. Ed.* **2012**, 51, 7967–7971. (g) Oyama, H.; Nakano, K.; Harada, T.; Kuroda, R.; Naito, M.; Nobusawa, K.; Nozaki, K. *Org. Lett.* **2013**, *15*, 2104–2107. (h) Morisaki, Y.; Gon, M.; Sasamori, T.; Tokitoh N.; Chujo, Y. *J. Am. Chem. Soc.* **2014**, *136*, 3350–3353. (i) Nakamura, K.; Furumi, S.; Takeuchi, M.; Shibuya, T.; Tanaka, K. *J. Am. Chem. Soc.* **2014**, *136*, 5555–5558. (j) Morisaki, Y.; Inoshita, K.; Chujo, Y. *Chem.–Eur. J.* **2014**, *20*, 8386–8390. (k) Gon, M.; Morisaki, Y.; Chujo, Y. *J. Mater. Chem. C* **2015**, *3*, 521–529. (l) Sakai, H.; Shinto, S.; Kumar, J.; Araki, Y.; Sakanoue, T.; Takenobu, T.; Wada, T.; Kawai, T.; Hasobe, T. *J. Phys. Chem. C* **2015**, *119*, 13937–13947.

(6) (a) Peeters, E.; M. Christiaans, P. T.; Janssen, R. A. J.; Schoo, H. F. M.; Dekkers H. P. J. M.; Meijer, E. W. *J. Am. Chem. Soc.* **1997**, *119*, 9909–9910. (b) Satrijio, A.; Meskers, S. C. J.; Swager, T. M. *J. Am. Chem. Soc.* **2006**, *128*, 9030–9031. (c) Wilson, J. N.; Steffen, W.; McKenzie, T. G.; Lieser, G.; Oda, M.; Neher, D.; Bunz, U. H. F.; *J. Am. Chem. Soc.* **2002**, *124*, 6830–6831. (d) Langeveld-Voss, B. M. W.;

Janssen, R. A.; Christiaans, M. P. T.; Meskers, S. C. J.; Dekkers, H. P. J. M.; Meijer, E. W. *J. Am. Chem. Soc.* **1996**, *118*, 4908–4909. (e) Oda, M.; Nothofer, H.-G.; Lieser, G.; Scherf, U.; Meskers, S. C. J.; Neher, D. *Adv. Mater.* **2000**, *12*, 362–365. (f) Oda, M.; Nothofer, H.-G.; Scherf, U.; Šunjić, V.; Richter, D.; Regenstein, W.; Meskers, S. C. J.; Neher, D. *Macromolecules* **2002**, *35*, 6792–6798. (g) Goto, H.; Akagi, K. *Angew. Chem., Int. Ed.* **2005**, *44*, 4322–4328. (h) Hayasaka, H.; Miyashita, T.; Tamura, K.; Akagi, K. *Adv. Funct. Mater.* **2010**, *20*, 1243–1250. (i) Fukao S.; Fujiki, M. *Macromolecules* **2009**, *42*, 8062–8067. (j) Yu, J.-M.; Sakamoto, T.; Watanabe, K.; Furumi, S.; Tamaoki, N.; Chen, Y.; Nakano, T. *Chem. Commun.* **2011**, *47*, 3799–3801. (k) Watanabe, K.; Sakamoto, T.; Taguchi, M.; Fujiki, M.; and T. Nakano, *Chem. Commun.* **2011**, *47*, 10996–10998. (l) Hirahara, T.; Yoshizawa-Fujita, M.; Takeoka, Y.; Rikukawa, M. *Chem. Lett.* **2012**, *41*, 905–907. (m) Watanabe, K.; Koyama, Y.; Suzuki, N.; Fujiki, M.; Nakano, T. *Polym. Chem.* **2014**, *5*, 712–717. (n) For polymer aggregates in optically active solvents: Nakano, Y.; Liu, Y.; Fujiki, M. *Polym. Chem.* **2010**, *1*, 460–469. (o) Kawagoe, Y.; Fujiki, M.; Nakano, Y. *New J. Chem.* **2010**, *34*, 637–647. (p) For polymers emitting CPL in solution: Morisaki, Y.; Hifumi, R.; Lin, L.; Inoshita, K.; Chujo, Y. *Polym. Chem.* **2012**, *3*, 2727–2730. (q) Nagata, Y.; Nishikawa, T.; Suginome, M. *Chem. Commun.* **2014**, *50*, 9951–9953. (r) For CPL created by polymer-polymer complexation: Shiraki, T.; Tsuchiya, Y.; Noguchi, T.; Tamaru, S.; Suzuki, N.; Taguchi, M.; Fujiki, M.; Shinkai, S. *Chem.–Asian J.* **2014**, *9*, 218–222.

(7) Review: Maeda, H.; Bando, Y. *Pure Appl. Chem.* **2013**, *85*, 1967–1978.

(8) (a) Imai, Y.; Kawaguchi, K.; Harada, T.; Sato, T.; Ishikawa, M.; Fujiki, M.; Kuroda, R.; Matsubara, Y. *Tetrahedron Lett.* **2007**, *48*, 2927–2930. (b) Imai, Y.; Murata, K.; Asano, N.; Nakano, Y.; Kawaguchi, K.; Harada, T.; Sato, T.; Fujiki, M.; Kuroda, R.; Matsubara, Y. *Cryst. Growth & Des.* **2008**, *8*, 3376–3379. (c) Tsumatori, H.; Nakashima, T.; Kawai, T.; *Org. Lett.* **2010**, *12*, 2362–2365. (d) Liu, J.; Su, H.; Meng, L.; Zhao, Y.; Deng, C.; Ng, J. C. Y.; Lu, P.; Faisal, M.; Lam, J. W. Y.; Huang, X.; Wu, H.; Wong, K. S.; Tang, B. Z. *Chem. Sci.* **2012**, *3*, 2737–2747. (e) Ng, J. C. Y.; Liu, J.; Su, H.; Hong, Y.; Li, H.; Lam, J. W. Y.; Wong, K. S.; Tang, B. Z. *J. Mater. Chem. C* **2014**, *2*, 78–83. (f) Kumar, J.; Nakashima, T.; Tsumatori, H.; Kawai, T. *J. Phys. Chem. Lett.* **2014**, *5*, 316–321. (g) Kumar, J.; Nakashima, T.; Kawai, T. *Langmuir* **2014**, *30*, 6030–6037. (h) Ng, J. C. Y.; Li, H.; Yuan, Q.; Liu, J.; Liu, C.; Fan, X.; Li, B. S.; Tang, B. Z. *J. Mater. Chem. C* **2014**, *2*, 4615–4621. (i) Ikeda, T.; Takayama, M.; Kumar, J.; Kawai, T.; Haino, T. *Dalton Trans.* **2015**, *44*, 13156–13162.

(9) Lohr, A.; Lysetska, M.; Würthner, F. *Angew. Chem., Int. Ed.* **2005**, *44*, 5071–5074.

(10) (a) Hembury, G. A.; Borovkov, V. V.; Inoue, Y. *Chem. Rev.* **2008**, *108*, 1–73. (b) Liu, M.; Zhang, L.; Wang, T. *Chem. Rev.* **2015**, *115*, 7304–7397.

(11) (a) *Cyclophane Chemistry: Synthesis, Structures and Reactions*; Vögtle, F., Ed.; John Wiley & Sons: Chichester, 1993. (b) *Modern Cyclophane Chemistry*; Gleiter, R., Hopf, H., Eds.; Wiley-VCH: Weinheim, 2004. (c) Bazan, G. C. *J. Org. Chem.* **2007**, *72*, 8615–8635.

(12) (a) Tohda, Y.; Sonogashira, K.; Hagihara, N. *Tetrahedron Lett.* **1975**, *16*, 4467–4470. (b) Sonogashira, K. In *Handbook of Organopalladium Chemistry for Organic Synthesis*; Negishi, E., Ed.; Wiley-Interscience: New York, 2002; pp 493−529.

(13) CD dissymmetry factor is defined as $g_{abs} = 2\Delta\varepsilon/\varepsilon$, where $\Delta\varepsilon$ indicates differences of absorbance between left- and right-handed circularly polarized light, respectively. CPL dissymmetry factor is defined as g_{lum} =

$2(I_{left} - I_{right})/(I_{left} + I_{right})$, where I_{left} and I_{right} indicate luminescence intensities of left- and right-handed CPL, respectively.

(14) Peyratout, C.; Daehne, L. *Phys. Chem. Chem. Phys.* **2002**, *4*, 3032−3039.

(15) Pangborn, A. B.; Giardello, M. A.; Grubbs, R. H.; Rosen, R. K.; Timmers, F. J. *Organometallics* **1996**, *15*, 1518–1520.

(16) Weiss, K.; Beernink, G.; Dötz, F.; Berliner, A.; Müllen, K.; Wöll, G. H. *Angew. Chem., Int. Ed.* **1999**, *38*, 3748–3752.

(17) Lee, S. J.; Park, C. R.; Chang, J. Y. *Langmuir* **2004**, *20*, 9513–9519.

(18) Takahashi, S.; Kuroyama, Y.; Sonogashira, K.; Hagihara, N. *Synthesis* **1980**, *8*, 627–630.

(19) Varshney, S. K.; Takezoe, H.; Rao, D. S. S. *Bull. Chem. Soc. J.* **2008**, *81*, 163–167.

(20) (a) Bondarenko, L.; Dix, I.; Hinrichs, H.; Hopf, H. *Synthesis* **2004**, 2751–2759. (b) Chow, H.-F.; Low, K.-H.; Wong, K. Y. *Synlett* **2005**, 2130–2134.

(21) Gaussian 09, Revision D.01, Frisch, M. J.; Trucks, G. W.; Schlegel, H. B.; Scuseria, G. E.; Robb, M. A.; Cheeseman, J. R.; Scalmani, G.; Barone, V.; Mennucci, B.; Petersson, G. A.; Nakatsuji, H.; Caricato, M.; Li, X.; Hratchian, H. P.; Izmaylov, A. F.; Bloino, J.; Zheng, G.; Sonnenberg, J. L.; Hada, M.; Ehara, M.; Toyota, K.; Fukuda, R.; Hasegawa, J.; Ishida, M.; Nakajima, T.; Honda, Y.; Kitao, O.; Nakai, H.; Vreven, T.; Montgomery, J. A., Jr.; Peralta, J. E.; Ogliaro, F.; Bearpark, M.; Heyd, J. J.; Brothers, E.; Kudin, K. N.; Staroverov, V. N.; Kobayashi, R.; Normand, J.; Raghavachari, K.; Rendell, A.; Burant, J. C.; Iyengar, S. S.; Tomasi, J.; Cossi, M.; Rega, N.; Millam, J. M.; Klene, M.; Knox, J. E.; Cross, J. B.; Bakken, V.; Adamo, C.; Jaramillo, J.; Gomperts, R.; Stratmann, R. E.; Yazyev, O.; Austin, A. J.; Cammi, R.; Pomelli, C.; Ochterski, J. W.; Martin, R. L.; Morokuma, K.; Zakrzewski, V. G.; Voth, G. A.; Salvador, P.; Dannenberg, J. J.; Dapprich, S.; Daniels, A. D.; Farkas, Ö.; Foresman, J. B.; Ortiz, J. V.; Cioslowski, J.; Fox, D. J. Gaussian, Inc., Wallingford CT, 2009.

Chapter 8

Optically Active Phenylethene Dimers Based on Planar Chiral Tetrasubstituted [2.2]Paracyclophane

Abstract

Optically active phenylethene dimers based on a planar chiral 4,7,12,15-tetrasubstituted [2.2]paracyclophane were synthesized. Intense photoluminescence (PL) both in the dilute solution and in the aggregation state was observed by attached an aggregation-induced emission (AIE) unit monomer to the [2.2]paracyclophane framework. The PL property in the dilute solution was obtained because the molecular motion of the AIE active monomers was restricted by the rigid [2.2]paracyclophane framework. The planar chiral [2.2]paracyclophane provided the circular dichroism (CD) and circularly polarized luminescence (CPL) property to the chromophores. The obtained diphenylethene dimer and monophenylethene dimer exhibited good CPL properties in the dilute solution and the aggregation state. The optical and chiroptical properties varied drastically with the only attaching phenyl groups to the ethene moiety. These strategy are useful to obtain optically active PL materials.

Introduction

The molecular design of π-conjugated systems is very important for the application in photoluminescent (PL) materials, opto-electronic devices and organic thin film solar cell.[1] Considering the application in photoluminescent materials, decrease of PL efficiency by aggregation-caused quenching (ACQ)[2] is a serious problem. Common π-conjugated systems have high planarity, and the aggregates cause energy loss by radiation-less deactivation due to the formation of delocalized exciton or excimer.[3] In order to obtain good PL property in the aggregation state, the molecules exhibiting aggregation-induced emission (AIE) property have received much attention. The AIE molecule does not emit PL in the dilute solution by radiation-less deactivation derived from the molecular motion. However, the molecule exhibits good PL property in the aggregation state by suspension of the molecular motion.[4] Common AIE molecules have distorted π-conjugation systems, which inhibit ACQ by steric hindrance. This switching property of AIE molecules is widely applied to optical sensors.[5] However, considering their application to PL materials, it is important to design the molecular structure having good PL property both in the dilute solution and the aggregation state.[6] Therefore, the author focused on a [2.2]paracyclophane framework.[7] The [2.2]paracyclophane framework has a potential to suppress molecular motion effectively because it can stack two chromophores in close proximity. In other words, using AIE molecules as the stacked chromophores, it is possible to synthesize the molecule exhibiting good PL property both in the dilute solution and the aggregation state. In addition, [2.2]paracyclophanes with substituents provide planar chirality to the stacked chromophores. Thus, the molecule exhibits circularly polarized luminescence (CPL) property by the planar chiral [2.2]paracyclophane framework.[8] In Chapter 3, the author reported that a planar chiral 4,7,12,15-tetrasubstiruted [2.2]paracyclophane was a chiral building block to give CPL property to the chromophores.[8d,e] In this chapter, the author

synthesized the compound containing two AIE active molecules stacked by the planar chiral [2.2]paracyclophane and investigated the optical and chiroptical properties in detail.

Results and Discussion

Synthesis

The optical resolution of planar chiral 4,7,12,15-tetrasubstituted [2.2]paracyclophane was carried out using the diastereomer method developed in Chapter 3, and the obtained enantiopure compounds were converted to the corresponding (S_p)- and (R_p)-4,7,12-tribromo-15-(trifluoromethanesulfonate)[2.2]paracyclophanes ((S_p)-**CpOTf**, (R_p)-**CpOTf**).[8d] The synthetic routes to the target optically active cyclic compounds are shown in Schemes 1 and 2. Although the synthesis of **DPh1** and **MPh1** has already reported,[9] the author modified the synthetic route to obtain optically active compounds.

At first, a bromide of compounds **1**[10] was converted to boronate ester group to obtain compound **2** in 97% isolated yield. Compound **2** was readily used for the Suzuki-Miyaura coupling reaction[11] (Scheme 1).

Scheme 2 shows the synthesis of the target planar chiral dimers **DPh1** and **DPh2**. In this Scheme, only the reactions of the (S_p)-isomers are shown; the (R_p)-isomers were synthesized under identical conditions from (R_p)-**CpOTf**. Suzuki-Miyaura coupling reaction of (S_p)-**CpOTf** was carried out with *trans*-2-(4,4,5,5-tetramethyl-1,3,2-dioxaborolan-2-yl)styrene (**3**) in the catalytic system of $Pd_2(dba)_3$/PPh_3 using $CsCO_3$ as a base to obtain compound (S_p)-**DPh1** in 54% isolated yield. Using the same procedure, (S_p)-**DPh2** was obtained in 67% isolated yield. In the case of (S_p)-**DPh2**, unreacted OTf groups were converted to OH groups to remove by-products by silica gel column chromatography. The details are shown in the experimental section.

Schemes 3 shows the synthesis of the monomeric model compounds, **MPh1** and **MPh2**. These compounds are the half units of the dimers, **DPh1** and **DPh2**, respectively. As shown in Scheme 3, the same procedure as Scheme 1 was available for **MPh1** and **MPh2**, and they were obtained in 74% and 46%, respectively. The structures of all new compounds in this chapter were confirmed by ^{1}H and ^{13}C NMR spectroscopy, high-resolution mass spectrometry (HRMS), and elemental analysis; the detailed synthetic procedures and NMR data are shown in the experimental section.

Scheme 1. Synthesis of Compound **2**

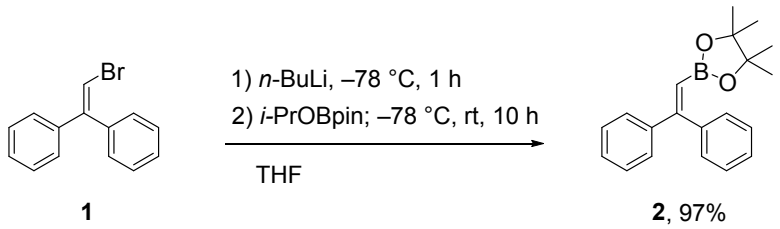

Scheme 2. Synthesis of planar chiral dimers (S_p)-**DPh1** and **DPh2**

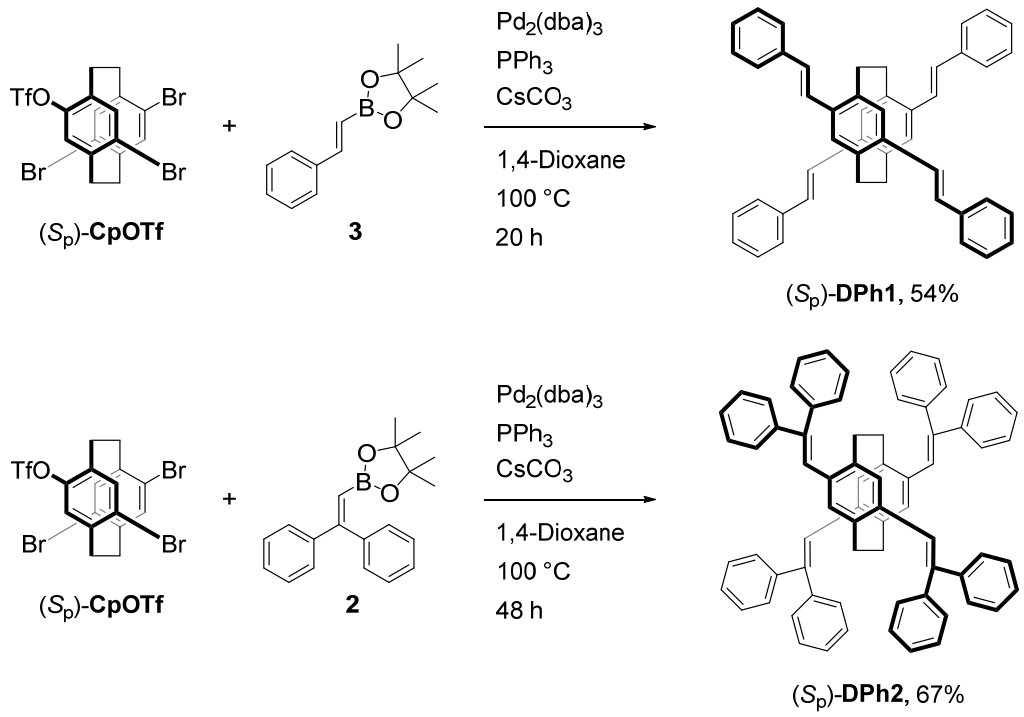

Scheme 3. Synthesis of model compounds **MPh1** and **MPh2**

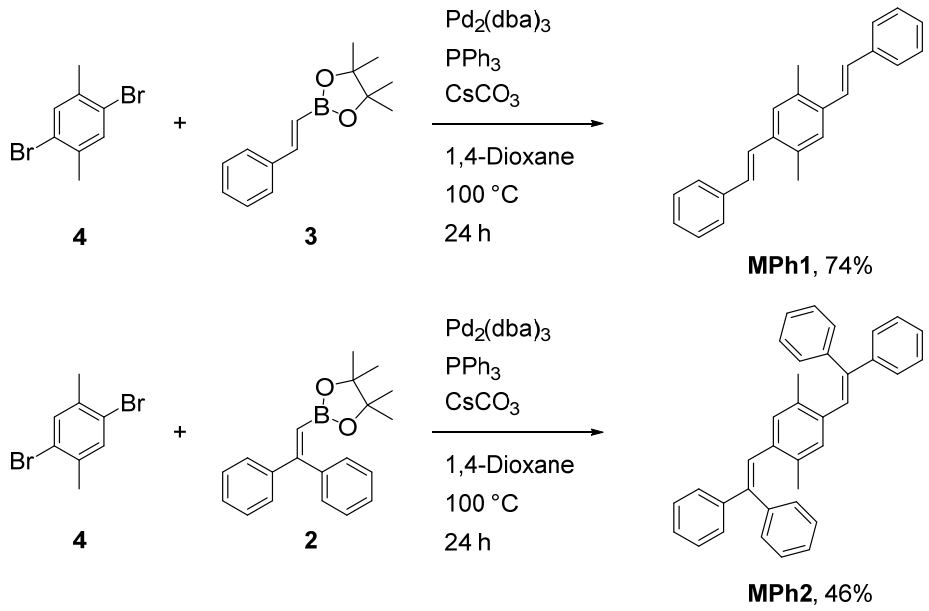

Optical Properties

The optical properties of both enantiomers of π-conjugated dimers, **DPh1** and **DPh2** as well as their monomeric model compounds **MPh1** and **MPh2** were evaluated. The optical and chiroptical data are summarized in Tables 1 and 2, respectively. Although the optical properties of **MPh1** and *rac*-**DPh1** have been already reported by Meijere in 1993,[9] the author shows the original data.

Table 1. Optical properties: Spectroscopic data

	λ_{abs}[c]/nm	λ_{lum}[c,d]/nm	τ[e]/ns	χ^2	Φ_{lum}[f]
DPh1[a]	395	455	3.28	1.02	0.78
DPh1-agg[b]	394	470	0.24 (80.9%), 1.59 (19.1%)	1.58	0.03
MPh1[a]	353	401, 424	1.40	1.09	0.87
MPh1-agg[b]	344	443	0.24 (80.6%), 0.88 (19.4%)	1.44	0.13
DPh2[a]	403	494	2.60	1.17	0.58
DPh2-agg[b]	403	503	1.40	1.13	0.24
MPh2[a]	337	468	0.19	1.19	0.04
MPh2-agg[b]	341	473	2.30	1.07	0.56

[a] In 1,4-dioxane. [b] In 1,4-dioxane/H_2O = 1/99 v/v. [c] 1.0×10^{-5} M. [d] Excited at absorption maxima. [e] Emission lifetime at λ_{lum}. [f] Absolute PL quantum efficiency.

Figure 1 shows the UV-vis absorption spectra of dimers, **DPh1** and **DPh2**, and the monomers, **MPh1** and **MPh2** in the dilute solution (1,4-dioxane, 1.0×10^{-5} M) and the aggregation state (1,4-dioxane/H_2O = 1/99 v/v, 1.0×10^{-5} M). Molar extinction coefficiencies of **DPh1** and **MPh1** in the dilute solution were less than those in the aggregation state. In addition, absorption edge exhibited bathochromic shift in the aggregation state. These results show the existence of intermolecular interaction in the aggregation state. In the cases of **DPh2** and **MPh2**, those effects were weak compared with the case of **DPh1** and **MPh1** because of steric hindrance of distorted phenyl groups. The peak top wavelengths of [2.2]paracyclophane-stacked dimers were longer than those of monomers due to through-space conjugation via the [2.2]paracyclophane framework.[12] The difference of the absorption maxima between **DPh2** and **MPh2** was larger than between **DPh1** and **MPh1**. Planarity of **DPh2** was the additional effect of bathochromic shift because phenyl groups in **DPh2** were congested much more than those in others. Figure 2 shows the PL spectra of dimers, **DPh1** and **DPh2**, and the monomers, **MPh1** and **MPh2** in the dilute solution (1,4-dioxane, 1.0×10^{-5} M) and the aggregation state (1,4-dioxane/H_2O = 1/99 v/v, 1.0×10^{-5} M). ACQ was clearly observed in the aggregation state of **DPh1** and **MPh1** because of π-π interaction by the high planarity of **DPh1** and **MPh1**. On the other hand, **MPh2** exhibited AIE property[13] because of the restricted molecular motion in the aggregation state; molecular motion of distorted phenyl groups cause radiation-less deactivation. However, **DPh2** exhibited good PL property both in the dilute solution and the aggregation state. This is because congested structure could suppress the molecular motion in the dilute solution; therefore, **DPh2** did not exhibit AIE property. Absolute quantum efficiency of **DPh2** decreased in the aggregation state due to the ACQ. PL lifetime measurement supported the formation of the aggregation in 1,4-dioxane/H_2O = 1/99 v/v. Table 1 includes the PL decay data (PL lifetime (τ) and χ^2 parameters) for all compounds. PL lifetimes depended

on the state of compounds, showing different PL lifetimes in the dilute solution and the aggregation state.

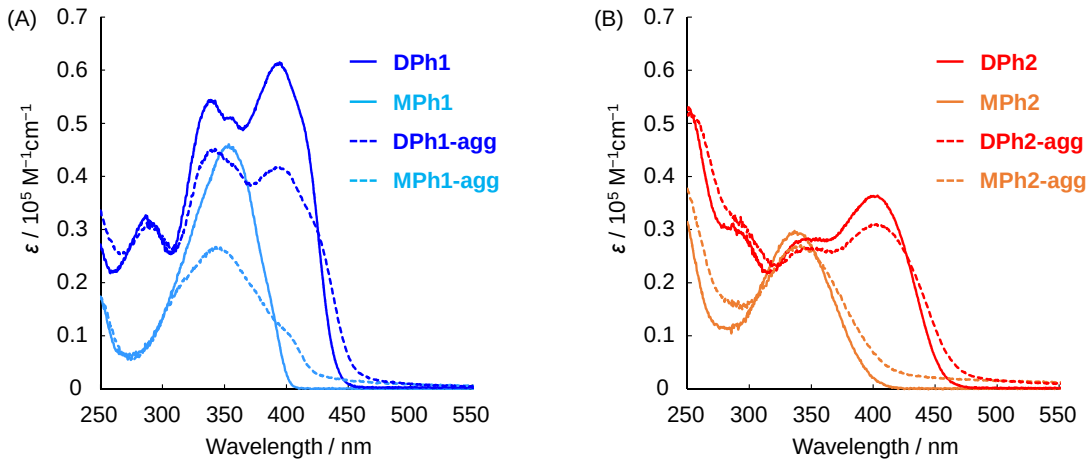

Figure 1. UV-vis absorption spectra in 1,4-dioxane (solid line) and 1,4-dioxane/H_2O = 1/99 v/v (dotted line) (1.0×10^{-5} M); (A) **DPh1** and **MPh1**; (B) **DPh2** and **MPh2**.

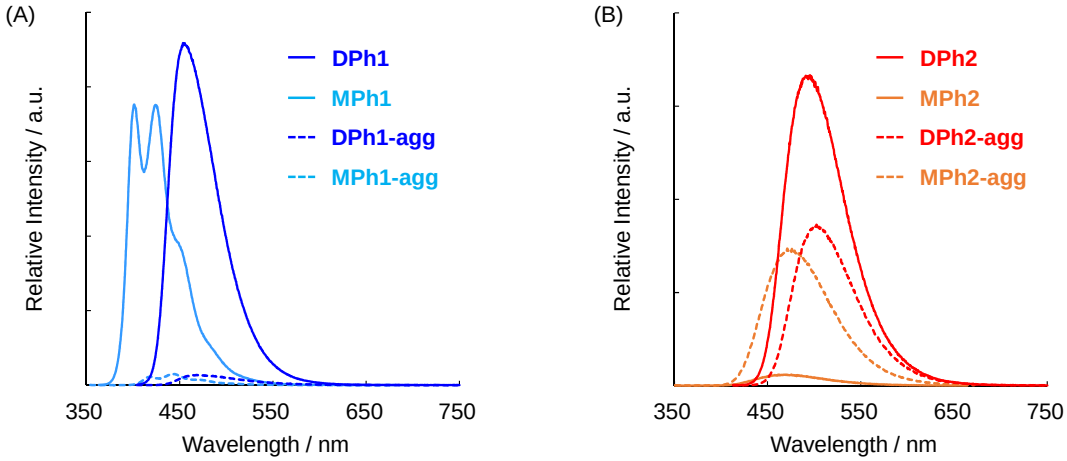

Figure 2. PL spectra in 1,4-dioxane (solid line) and 1,4-dioxane/H_2O = 1/99 v/v (dotted line) (1.0×10^{-5} M); (A) **DPh1** and **MPh1**; (B) **DPh2** and **MPh2**.

Chiroptical Properties

The chiroptical properties of the ground and excited states of **DPh1** and **DPh2** were investigated by circular dichroism (CD) and CPL spectroscopy, respectively. Chiroptical data,

such as CD and CPL dissymmetry factor[14] (g_{abs} and g_{lum}, respectively), are summarized in Table 2. Figure 3 shows the CD and absorption spectra of both enantiomers of **DPh1** and **DPh2** in the dilute solution (1,4-dioxane, 1.0×10^{-5} M) and the aggregation state (1,4-dioxane/H_2O = 1/99 v/v, 1.0×10^{-5} M). In both enantiomers, mirror image Cotton effects were observed clearly in the CD spectra. In the dilute solution, the g_{abs} values of the first Cotton effect were estimated to be $+3.5 \times 10^{-3}$ for (S_p)-**DPh1** and $+1.0 \times 10^{-3}$ for (S_p)-**DPh2**, respectively. In the aggregation state, the g_{abs} values of the first Cotton effect were estimated to be $+3.0 \times 10^{-3}$ for (S_p)-**DPh1** and $+0.87 \times 10^{-3}$ for (S_p)-**DPh2**, respectively. When these compounds formed the aggregates, the g_{abs} value for (S_p)- and (R_p)-**DPh1** decreased in all region, whereas those for (S_p)- and (R_p)-**DPh2** remained in almost all region. This result also indicates the existence of strong intermolecular interaction of **DPh1** and weak intermolecular interaction of **DPh2**.

The CPL spectra of both enantiomers of **DPh1** and **DPh2** in the dilute solution (1,4-dioxane, 1.0×10^{-5} M) and the aggregation state (1,4-dioxane/H_2O = 1/99 v/v, 1.0×10^{-5} M) are shown in Figure 4. Mirror image CPL spectra were observed for the enantiomers. The g_{lum} values were estimated to be $+3.7 \times 10^{-3}$ for (S_p)-**DPh1** and $+0.73 \times 10^{-3}$ for (S_p)-**DPh2** in the dilute solution, and $+4.3 \times 10^{-3}$ for (S_p)-**DPh1** and $+0.90 \times 10^{-3}$ for (S_p)-**DPh2** in the aggregation state. In the

Table 2. Chiroptical properties: Spectroscopic data of (S_p)-isomers

	g_{abs} / 10^{-3} at λ_{abs}[c]	g_{lum} / 10^{-3} at $\lambda_{lum,\,max}$[d]
(S_p)-**DPh1**[a]	+3.5	+3.7
(S_p)-**DPh1-agg**[b]	+3.0	+4.3
(S_p)-**DPh2**[a]	+1.0	+0.73
(S_p)-**DPh2-agg**[b]	+0.87	+0.90

[a] In 1,4-dioxane. [b] In 1,4-dioxane/H_2O = 1/99 v/v. [c] $g_{abs} = 2\Delta\varepsilon/\varepsilon$, where $\Delta\varepsilon$ indicates differences of absorbance between left- and right-handed circularly polarized light, respectively. The g_{abs} value of the first peak top was estimated. [d] $g_{lum} = 2(I_{left} - I_{right})/(I_{left} + I_{right})$, where I_{left} and I_{right} indicate luminescence intensities of left- and right-handed CPL, respectively.

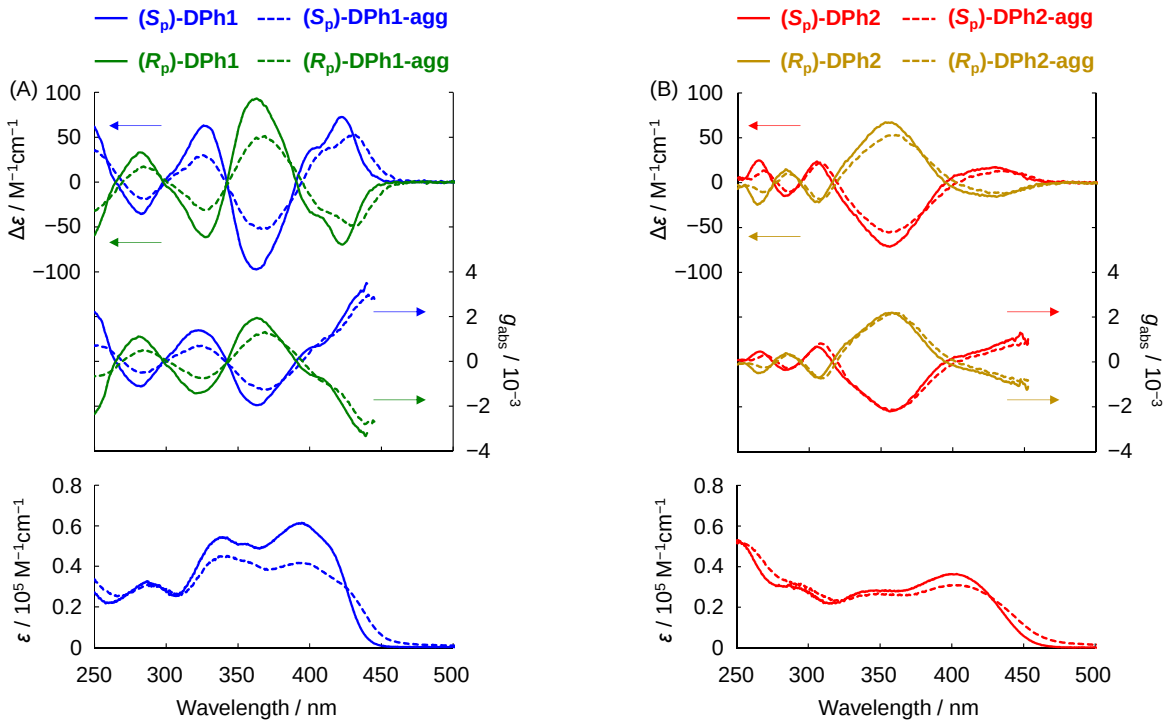

Figure 3. CD spectra in 1,4-dioxane (solid line) and in 1,4-dioxane/H_2O = 1/99 v/v (dotted line) (1.0 × 10^{-5} M); (A) (S_p)- and (R_p)-**DPh1**; (B) (S_p)- and (R_p)-**DPh2**.

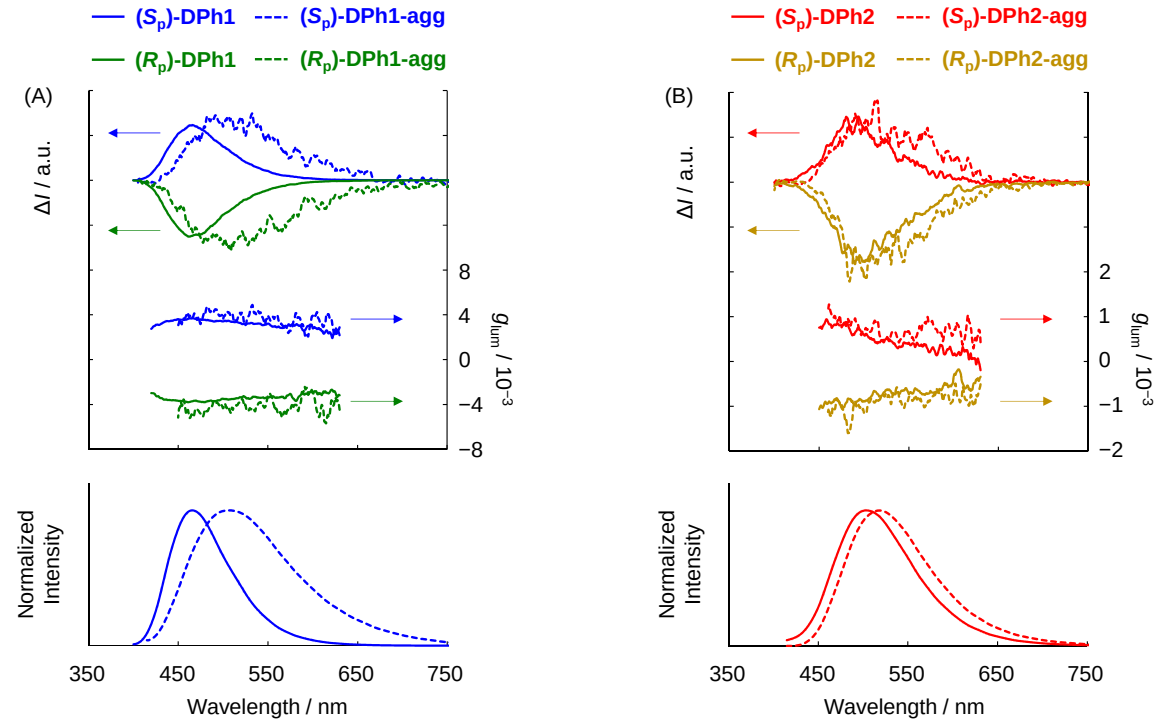

Figure 4. CPL spectra in 1,4-dioxane (solid line) and 1,4-dioxane/H_2O = 1/99 v/v (dotted line) (1.0 × 10^{-5} M); (A) (S_p)- and (R_p)-**DPh1**; (B) (S_p)- and (R_p)-**DPh2**. Excitation wavelength: 350 nm.

aggregation system of (S_p)- and (R_p)-**DPh1**, CPL peak tops were bathochromically shifted, and the g_{lum} values clearly increased because of stronger intermolecular interaction in the excited state. On the other hand, small changes were observed in the CPL peak top and g_{lum} values of (S_p)-**DPh2** because of weaker intermolecular interaction in the excited state. In the dilute solution, **DPh1** exhibited good optical and chiroptical properties as luminescence materials (Φ_{lum} = 0.78 and g_{lum} = +3.7 × 10^{-3} for (S_p)-**DPh1**). On the other hand, in the aggregation state, **DPh2** exhibited good optical and chiroptical property as luminescence materials (Φ_{lum} = 0.24 and g_{lum} = +0.90 × 10^{-3} for (S_p)-**DPh2**).

Variable Temperature PL Measurement

Variable temperature UV-vis and PL measurements were carried out to obtain further information on the suppression of the molecular motion by the [2.2]paracyclophane framework. These spectra were obtained in the dilute toluene solution (1.0 × 10^{-5} M for UV-vis and 1.0 × 10^{-6} M for PL) at 20, 40, 60 and 80 ˚C. Relative PL quantum efficiency was calculated from the absolute PL quantum efficiency in 1,4-dioxane at 25 ˚C as a standard (Table 3). In the UV-vis absorption spectra (Figures 5A and 5B), by increasing the temperature, the molar extinction coefficients of **DPh1** and **DPh2** decreased and the absorption maxima exhibited hypsochromic shift. This is because the effective conjugation length became shorter by the molecular motion of the phenyl groups. In the PL spectra (Figures 5C and 5D), the PL intensity of **DPh2** drastically decreased by increasing the temperature. The relative PL quantum efficiency was estimated to be 0.70 at 20 ˚C, 0.68 at 40 ˚C, 0.65 at 60 ˚C, 0.63 at 80 ˚C for **DPh1** and 0.51 at 20 ˚C, 0.44 at 40 ˚C, 0.39 at 60 ˚C, 0.29 at 80 ˚C for **DPh2**. In summary, 9.0% decrease for **DPh1** and 43.3% for **DPh2** decrease were observed by increasing the temperature from 20 ˚C to 80 ˚C. The PL intensity was recovered by cooling the temperature. This result shows that the molecular motion of the phenyl groups of **DPh2** was suppressed by the [2.2]paracyclophane framework at room temperature and that it was activated by increasing the temperature. Usually,

PL of AIE molecules decreased by the molecular motion at room temperature and the formation of aggregate or cooling the temperature provide the good PL property. On the other hand, good PL property was obtained by introducing [2.2]paracyclophane skeleton into with only staking two AIE-active units in the dilute solution. This is interesting feature of the rigid [2.2]paracyclophane framework.

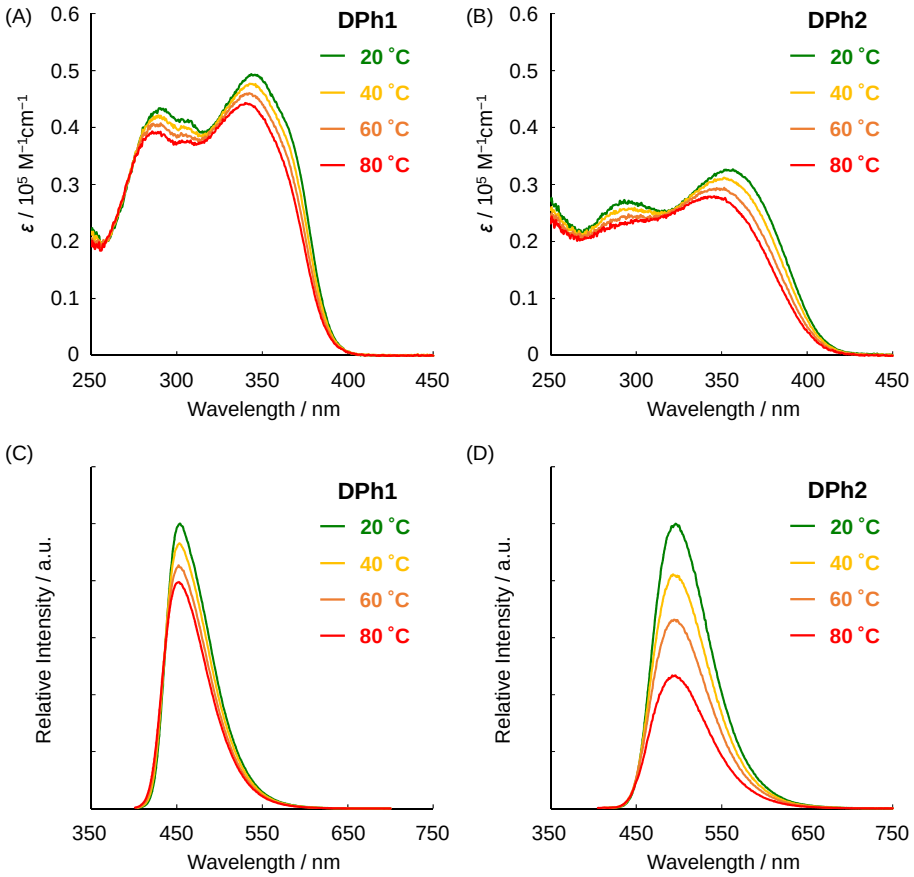

Figure 5. UV-vis and PL variable temperature spectra in toluene (1.0×10^{-5} M for UV-vis and 1.0×10^{-6} M for PL, excited at absorption maximum) at 20 ˚C, 40 ˚C, 60 ˚C, 80 ˚C; (A) UV-vis spectra of **DPh1**; (B) UV-vis spectra of **DPh2**; PL spectra of **DPh1**; PL spectra of **DPh2**.

Table 3. Relative PL quantum efficiencies[a,b]

	20 ˚C	40 ˚C	60 ˚C	80 ˚C
DPh1	0.70	0.68	0.65	0.63
DPh2	0.51	0.44	0.39	0.29

[a] In toluene (1.0×10^{-6} M excited at absorption maximum). [b] Relative PL quantum efficiencies were calculated from absolute PL quantum efficiencies of **DPh1** and **DPh2** in 1,4-dioxane (Table 1), respectively.

Dispersion of the Dimers in Polystyrene Film

To investigate the effect of ACQ and molecular motion, **DPh1** or **DPh2** were dispersed in polystyrene (M_n = 80,000, PDI = 2.6) films. The films including 1-100 wt% of **DPh1** or **DPh2** in polystyrene were prepared with a spin-coat method from 40 μL $CHCl_3$ solution (1.0×10^{-3} M of **DPh1** or **DPh2** in polystyrene). The results are summarized in Figure 6 and Table 4. **DPh1** and **DPh2** exhibited high absolute PL quantum efficiency in the 1 wt% films (Φ_{lum} = 0.86 and 0.80, respectively). The Φ_{lum} of the 1 wt% film of **DPh2** was much higher than that in the dilute solution (Φ_{lum} = 0.58). The result shows that molecular motion slightly decreased the PL property at room temperature. As shown in Figure 6, Φ_{lum} of **DPh1** dropped drastically in the 20 wt% film (Φ_{lum} = 0.26) by ACQ. The 40-100 wt% films exhibited the low Φ_{lum} (= 0.09-0.04). On the other hand, the decrease of Φ_{lum} of **DPh2** films was moderate, and the Φ_{lum} of the 100 wt% film was estimated to be 0.27, which was identical to the aggregate (Φ_{lum} = 0.24). Therefore, the decrease of Φ_{lum} in the aggregate of **DPh2** was caused by ACQ. The **DPh2** films exhibited good Φ_{lum} at 60 wt% film (Φ_{lum} = 0.44), and the results can be advantage for obtaining high brightness films.

Molecular Model

To obtain further information about molecular motion, density functional theory (DFT) was carried out. The structures of **MPh2** and **DPh2** were optimized at BLYP/def2-TZVPP level. The results are shown in Figure 7. The optimized structure of **MPh2** was highly twisted, whereas that of **DPh2** was relatively planar because of the intramolecular interaction of the stacked chromophores. The two chromophores were located at the distance of 4-6 Å, which was sufficient to inhibit the free molecular motion. The restriction of the molecular motion was the main reason of high PL intensity of **DPh2** in the dilute solution. In addition, the relatively planar structure caused ACQ and the difference of Φ_{lum} between **MPh2** (Φ_{lum} = 0.56) and **DPh2** (Φ_{lum} = 0.24) in the aggregation state.

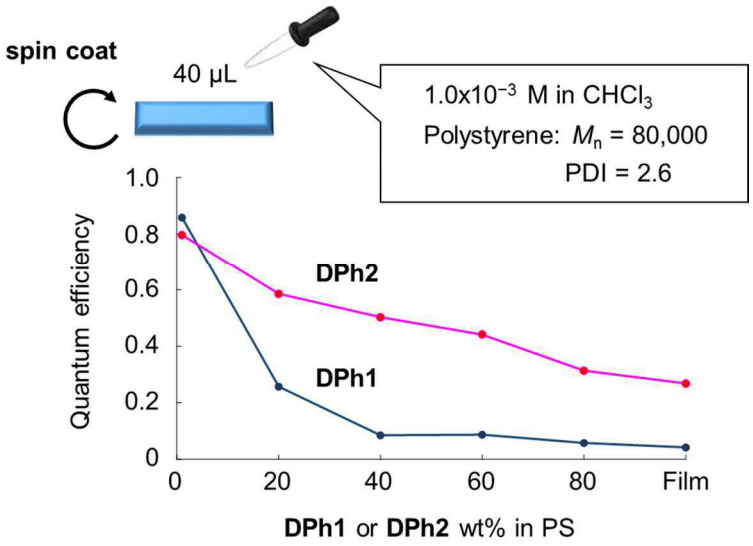

Figure 6. Absolute PL quantum efficiency of the films of 1-100 wt% **DPh1** or **DPh2** in polystyrene. The films were prepared by a spin-coat method from $CHCl_3$ solution (1.0×10^{-3} M of **DPh1** or **DPh2** in polystyrene).

Table 4. Absolute PL quantum efficiencies of the films

	1 wt%	20 wt%	40 wt%	60 wt%	80 wt%	100 wt% (Film)
DPh1	0.86	0.26	0.09	0.09	0.06	0.04
DPh2	0.80	0.59	0.50	0.44	0.31	0.27

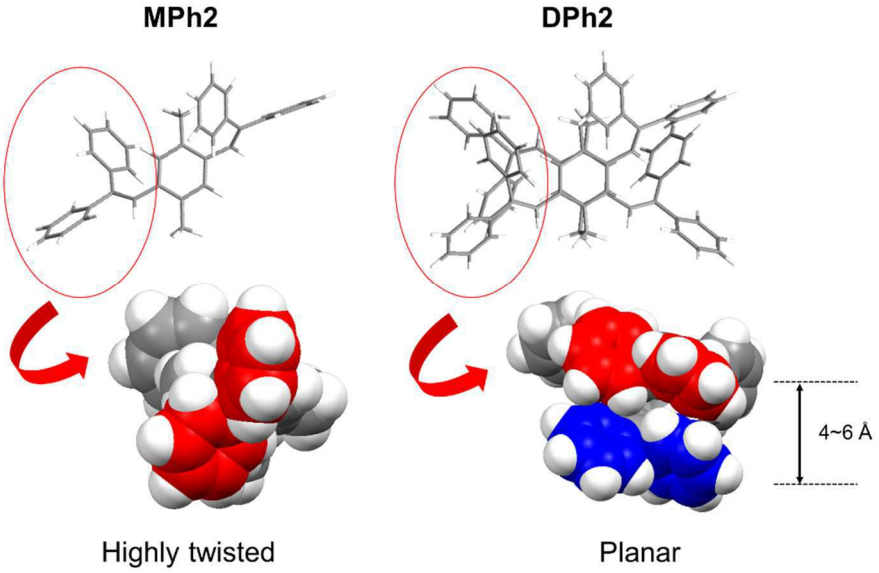

Figure 7. Molecular models of **MPh2** and **DPh2**. The structure was optimized by DFT at BLYP/def2-TZVPP levels.

Conclusions

Optically active phenylethene dimers, **DPh1** and **DPh2**, with a planar chiral 4,7,12,15-tetrasubstituted [2.2]paracyclophane were synthesized. Dimer **DPh1** and the monomer **MPh1** exhibited ACQ because of high planarity of the stacked π-electron system. On the other hand, **DPh2** exhibited good PL properties both in the dilute solution and in the aggregation state in spite of the fact that monomer **MPh2** did not exhibit PL in the dilute solution. Therefore, the rigid [2.2]paracyclophane framework has a potential to suppress the molecular motion by staking two chromophores. In addition, by increasing temperature, PL property of **DPh2** decreased much more sensitively than that of **DPh1**. The PL properties were recovered by cooling the temperature. **DPh1** and **DPh2** exhibited good chiroptical properties and the *g* values on the order of approximately 10^{-3}. In the dilute solution, **DPh1** had good CPL properties (Φ_{lum} = 0.78 and g_{lum} = $+3.7 \times 10^{-3}$), and in the aggregation state, **DPh2** had good CPL properties (Φ_{lum} = 0.24 and g_{lum} = $+0.90 \times 10^{-3}$). The optical and chiroptical properties varied drastically by only attaching phenyl groups to the ethene units.

Experimental Section

General. ^{1}H and ^{13}C NMR spectra were recorded on JEOL EX400 and AL400 instruments at 400 and 100 MHz, respectively. Samples were analyzed in $CDCl_3$, and the chemical shift values were expressed relative to Me_4Si as an internal standard. Analytical thin layer chromatography (TLC) was performed with silica gel 60 Merck F254 plates. Column chromatography was performed with Wakogel C-300 silica gel. High-resolution mass (HRMS) spectrometry was performed at the Technical Support Office (Department of Synthetic Chemistry and Biological Chemistry, Graduate School of Engineering, Kyoto University), and the HRMS spectra were obtained on a Thermo Fisher Scientific EXACTIVE spectrometer for atmospheric pressure chemical ionization (APCI). UV-vis spectra were recorded on a SHIMADZU UV-3600 spectrophotometer, and samples were analyzed in $CHCl_3$ at room temperature. Fluorescence emission spectra were recorded on a HORIBA JOBIN YVON Fluoromax-4 spectrofluorometer, and samples were analyzed in $CHCl_3$ at room temperature. The PL lifetime measurement was performed on a Horiba FluoroCube spectrofluorometer system; excitation was carried out using a UV diode laser (NanoLED 292 nm and 375 nm). Circular dichroism (CD) spectra were recorded on a JASCO J-820 spectropolarimeter with $CHCl_3$ as a solvent at room temperature. Circularly polarized luminescence (CPL) spectra were recorded on a JASCO CPL-200S with $CHCl_3$ as a solvent at room temperature. Elemental analyses were performed at the Microanalytical Center of Kyoto University.

Materials. Commercially available compounds used without purification: (Tokyo Chemical Industry Co, Ltd.) 2,5-Dibromo-*p*-xylene (**4**), 2-isopropoxy-4,4,5,5-tetramethyl-1,3,2-dioxaborolane (*i*-PrOBpin), $Pd_2(dba)_3$ (dba = dibenzylideneacetone); (Wako Pure Chemical Industries, Ltd.) *trans*-2-(4,4,5,5-tetramethyl-1,3,2-dioxaborolan-2-yl)styrene (**3**), PPh_3, $CsCO_3$; (Kanto Chemical Co., Inc.) *n*-butyllitium (*n*-BuLi, 1.6 M in hexane). Commercially available solvents: 1,4-Dioxane (deoxygenated grade, Wako Pure Chemical Industries, Ltd.), used without purification. THF (Wako Pure Chemical Industries, Ltd.), purified by passage through solvent purification columns under Ar pressure.[15] Compounds prepared as described in the literatures: 2-Bromo-1,1-diphenylethylene (**1**)[16], (S_p)- and (R_p)-4,7,12-tribromo-15-(trifluoromethanesulfonate)-[2.2]paracyclophane ((R_p)- and (S_p)-**CpOTf**).[8d]

Computational Details. The Orca program package[17] was used for computation. The author optimized the structures of **MPh2** and **DPh2** in the ground states. The density functional theory (DFT) was applied for the optimization of the structures at the BLYP/def2-TZVPP levels in the ground state.

Synthesis of 2. A solution of *n*-BuLi (1.60 M in hexane, 17.9 mL, 28.7 mmol) was slowly added to a solution of 2-bromo-1,1-diphenylethylene (**1**) (6.77 g, 26.1 mmol) in THF (80 mL) at –78 °C under Ar atmosphere. After 1 h, *i*-PrOBpin (15.8 mL, 78.3 mmol) was added, and the mixture was stirred for 10 h at –78 °C to room temperature. The reaction mixture was quenched by the addition of aqueous NH_4Cl solution, and the organic layer was extracted three times with CH_2Cl_2. The combined organic layer was washed with brine and dried over Na_2SO_4. Na_2SO_4 was removed by filtration, and the solvent was evaporated. The residue was purified by column chromatography on SiO_2 (EtOAc/hexane = 1/10 v/v as an eluent) to afford **2** (7.72 g, 25.2 mmol, 97%) as a light yellow oil. Further purification with HPLC was carried out to obtain characterization data. R_f = 0.48 (EtOAc/hexane = 1/10 v/v). ^{1}H NMR ($CDCl_3$, 400 MHz) δ 1.13 (s, 12H), 6.00 (s, 1H), 7.22-7.27 (m, 10H) ppm; ^{13}C NMR ($CDCl_3$, 100 MHz) δ 24.5, 82.9, 117.7, 127.4, 127.4, 127.8, 127.8, 129.7, 141.7, 142.9, 159.7 ppm. HRMS (APCI) calcd. for $C_{20}H_{24}BO_2$ $[M+H]^+$: 307.1864, found: 307.1855. Elemental analysis calcd. for $C_{20}H_{23}BO_2$: C 78.45 H 7.57, found: C 78.23 H 7.39.

Synthesis of DPh1. A mixture of (S_p)-**CpOTf** (50.0 mg, 0.0843 mmol), **3** (194.0 mg, 0.843 mmol), $Pd_2(dba)_3$ (7.7 mg, 0.00843 mmol), PPh_3 (8.8 mg, 0.0337 mmol), $CsCO_3$ (549.3 mg, 1.69 mmol) and 1,4-dioxane (5.0 mL) was placed in a round-bottom flask equipped with a magnetic stirring bar. After degassing the reaction mixture several times, the reaction was carried out at 100 °C for 20 h with stirring. After the reaction mixture was cooled to room temperature, precipitates were removed by filtration, and the solvent was removed with a rotary evaporator. The residue was purified by column chromatography on SiO_2 ($CHCl_3$/hexane = 1/2 v/v as an eluent). Further purification was carried out by HPLC to afford (S_p)-**DPh1** (28.3 mg, 0.0459 mmol, 54%) as a light yellow crystal. R_f = 0.39 ($CHCl_3$/hexane = 1/2 v/v). ^{1}H NMR ($CDCl_3$, 400 MHz) δ 2.85-2.93 (m, 4H), 3.54-3.62 (m, 4H), 6.92, (d, J = 16.1 Hz, 4H), 7.00 (s, 4H), 7.21 (d, J = 16.1 Hz, 4H), 7.29 (t, J = 7.3 Hz, 4H), 7.38 (t, J = 7.3 Hz, 8H), 7.47 (d, J = 7.6 Hz, 8H) ppm; ^{13}C NMR ($CDCl_3$, 100 MHz) δ 33.1, 125.3, 126.6, 127.6, 128.2, 128.7, 128.7, 136.7, 137.7, 137.8 ppm. HRMS (APCI) calcd. for $C_{48}H_{41}$ $[M+H]^+$: 617.3203, found: 617.3205. Elemental analysis calcd. for $C_{48}H_{40}$: C 93.46 H 6.54, found: C 93.53 H 6.30. (R_p)-**DPh1** was obtained by the same procedure in 50% isolated yield.

Synthesis of DPh2. A mixture of (S_p)-**CpOTf** (50.0 mg, 0.0843 mmol), **2** (258.1 mg, 0.843 mmol), $Pd_2(dba)_3$ (7.7 mg, 0.00843 mmol), PPh_3 (8.8 mg, 0.0337 mmol), $CsCO_3$ (549.3 mg, 1.69 mmol) and 1,4-dioxane (5.0 mL) was placed in a round-bottom flask equipped with a magnetic stirring bar. After degassing the reaction mixture several times, the reaction was carried out at 100 °C for 48 h with stirring.

After the reaction mixture was cooled to room temperature, precipitates were removed by filtration, and the solvent was removed with a rotary evaporator. The residue was added to KOH (250 mg, 4.46 mmol) in H_2O (1 mL) and dissolved in EtOH (40 mL). The mixture was stirred with a magnetic stirring bar and heated to 60 °C for 12 h to convert unreacted OTf groups completely to OH groups, which were easily removed by silica gel column chromatography. After the reaction, the organic layer was extracted three times with $CHCl_3$ and the combined organic layer was washed with brine and dried over $MgSO_4$. $MgSO_4$ was removed by filtration, and the solvent was evaporated. The residue was purified by column chromatography on SiO_2 (EtOAc/hexane = 1/19 v/v as an eluent). Further purification was carried out by HPLC to afford (S_p)-**DPh2** (51.7 mg, 0.0561 mmol, 67%) as a light yellow crystal. R_f = 0.33 (EtOAc/hexane = 1/19 v/v). ^{1}H NMR ($CDCl_3$, 400 MHz) δ 2.35-2.43 (m, 4H), 2.98-3.06 (m, 4H), 6.24, (s, 4H), 6.65 (s, 4H), 7.06-7.09 (m, 8H), 7.21-7.32 (m, 32H) ppm; ^{13}C NMR ($CDCl_3$, 100 MHz) δ 32.5 126.7, 127.3, 127.4, 128.1, 128.1, 128.1, 130.7, 133.8, 125.9, 137.6, 140.6, 142.1, 144.1 ppm. HRMS (APCI) calcd. for $C_{72}H_{57}$ $[M+H]^+$: 921.4455, found: 921.4438. Elemental analysis calcd. for $C_{72}H_{56}$: C 93.87 H 6.13, found: C 93.95 H 6.11. (R_p)-**DPh2** was obtained by the same procedure in 51% isolated yield.

Synthesis of MPh1. A mixture of 2,5-dibromo-*p*-xylene (**4**) (132.0 mg, 0.500 mmol), **3** (241.6 mg, 1.05 mmol), $Pd_2(dba)_3$ (22.9 mg, 0.0250 mmol), PPh_3 (26.2 mg, 0.100 mmol), $CsCO_3$ (684.2 mg, 2.10 mmol) and 1,4-dioxane (15.0 mL) was placed in a round-bottom flask equipped with a magnetic stirring bar. After degassing the reaction mixture several times, the reaction was carried out at 100 °C for 24 h with stirring. After the reaction mixture was cooled to room temperature, precipitates were removed by filtration, and the solvent was removed with a rotary evaporator. The residue was purified by column chromatography on SiO_2 ($CHCl_3$/hexane = 1/3 v/v as an eluent) and recrystallization from $CHCl_3$ and MeOH (good and poor solvent, respectively) to afford **MPh1** (115.1 mg, 0.371 mmol, 74%) as a colorless crystal. R_f = 0.51 ($CHCl_3$/hexane = 1/3 v/v). ^{1}H NMR ($CDCl_3$, 400 MHz) δ 2.44 (s, 6H), 7.03, (d, J = 16.1 Hz, 2H), 7.26 (t, J = 7.1 Hz, 2H), 7.31, (d, J = 16.1 Hz, 2H), 7.37 (t, J = 7.3 Hz, 4H), 7.44 (s, 2H), 7.53, (d, J = 7.3 Hz, 4H) ppm; ^{13}C NMR ($CDCl_3$, 100 MHz) δ 19.5, 126.3, 126.6, 127.3, 127.5, 128.7, 129.6, 133.6, 135.6, 137.9 ppm. HRMS (APCI) calcd. for $C_{24}H_{23}$ $[M+H]^+$: 311.1794, found: 311.1788. Elemental analysis calcd. for $C_{24}H_{22}$: C 92.86 H 7.14, found: C 92.72 H 7.21.

Synthesis of MPh2. A mixture of 2,5-dibromo-*p*-xylene (**4**) (132.0 mg, 0.500 mmol), **2** (321.5 mg, 1.05 mmol), $Pd_2(dba)_3$ (22.9 mg, 0.0250 mmol), PPh_3 (26.2 mg, 0.100 mmol), $CsCO_3$ (684.2 mg, 2.10 mmol) and 1,4-dioxane (15.0 mL) was placed in a round-bottom flask equipped with a magnetic stirring bar.

After degassing the reaction mixture several times, the reaction was carried out at 100 °C for 24 h with stirring. After the reaction mixture was cooled to room temperature, precipitates were removed by filtration, and the solvent was removed with a rotary evaporator. The residue was purified by column chromatography on SiO_2 ($CHCl_3$/hexane = 1/4 v/v as an eluent) and recrystallization from $CHCl_3$ and MeOH (good and poor solvent, respectively) to afford **MPh2** (105.6 mg, 0.228 mmol, 46%) as a colorless crystal. R_f = 0.39 ($CHCl_3$/hexane = 1/4 v/v). ^{1}H NMR ($CDCl_3$, 400 MHz) δ 1.96 (s, 6H), 6.56, (s, 2H), 6.88 (s, 2H), 7.07-7.10 (m, 4H), 7.21-7.25 (m, 6H), 7.26-7.34 (m, 10H) ppm; ^{13}C NMR ($CDCl_3$, 100 MHz) δ 19.5, 127.0, 127.1, 127.4, 128.0, 128.0, 128.1, 130.6, 131.0, 133.5, 135.4, 140.4, 143.0, 143.7 ppm. HRMS (APCI) calcd. for $C_{36}H_{31}$ $[M+H]^+$: 463.2420, found: 463.2414. Elemental analysis calcd. for $C_{36}H_{30}$: C 93.46 H 6.54, found: C 93.46 H 6.62.

References and Notes

(1) For example: (a) *Handbook of Conducting Polymers*; Skotheim, T. A., Elsenbaumer R. L., Reynolds J. R., Eds.; Marcel Dekker: New York, 3rd edn, 2006. (b) *Organic Light Emitting Devices: Synthesis, Properties and Application*; Müellen K., Scherf, U., Eds.; Wiley-VCH: Weinheim, 2006. (c) *Organic Field-Effect Transistors*; Groza J. R., Locklin, J. J., Eds.; CRC Press Taylor & Francis Group: New York, 2007. (d) *Organic Photovoltaics: Materials, Device Physics, and Manufacturing Technologies*; Brabec, C., Dyakonov V., Scherf, U., Eds.; Wiley-VCH, Weinheim, 2008.

(2) Thomas, S. W.; Joly, G. D.; Swager, T. M. *Chem. Rev.* **2007**, *107*, 1339–1386.

(3) Jenekhe, S. A.; Osaheni, J. A. *Science* **1994**, *265*, 765–768.

(4) (a) *Aggregation-induced emission: Fundamentals*; Qin, A., Tang B. Z., Eds.; Wiley, New York, 2013. (b) *Aggregation-induced emission: Applications*; Qin, A., Tang B. Z., Eds.; Wiley, New York, 2013; (c) Luo, J.; Xie, Z.; Lam, J. W. Y.; Cheng, L.; Chen, H.; Qiu, C.; Kwok, H. S.; Zhan, X.; Liu, Y.; Zhu, D.; (d) Tang, B. Z. *Chem. Commun.* **2001**, 1740–1741. (e) Hong, Y.; Lam, J. W. Y.; Tang, B. Z. *Chem. Soc. Rev.* **2011**, *40*, 5361–5388.

(5) Wu, J.; Liu, W.; Ge, J.; Zhang, H.; Wang, P. *Chem. Soc. Rev.* **2011**, *40*, 3483–3495.

(6) (a) Sato, T.; Jiang, D.-L.; Aida, T. *J. Am. Chem. Soc.* **1999**, *121*, 10658–10659. (b) Zhao, C.-H.; Wakamiya, A.; Inukai, Y.; Yamaguchi, S. *J. Am. Chem. Soc.* **2006**, *128*, 15934–15935. (c) Wakamiya, A.; Mori, K.; Yamaguchi, S. *Angew. Chem., Int. Ed.* **2007**, *46*, 4273–4276. (d) Zhao, C.-H.; Wakamiya, A.; Yamaguchi, S. *Macromolecules* **2007**, *40*, 3898–3900. (e) Shimizu, M.; Takeda, Y.; Higashi, M.; Hiyama, T. *Angew. Chem., Int. Ed.* **2009**, *48*, 3653–3656. (f) Zhao, C.-H.; Sakuda, E.; Wakamiya, A.; Yamaguchi, S. *Chem.–Eur. J.* **2009**, *15*, 10603–10612. (g) Iida, A.; Yamaguchi, S. *Chem. Commun.* **2009**, 3002–3004. (h) Kim, E.; Park, S. B. *Chem.–Asian J.* **2009**, *4*, 1646–1658. (i) Shimizu, M.; Hiyama, T. *Chem.–Asian J.* **2010**, *5*, 1516–1531.

(7) (a) *Cyclophane Chemistry: Synthesis, Structures and Reactions*; Vögtle, F., Ed.; John Wiley & Sons: Chichester, 1993. (b) *Modern Cyclophane Chemistry*; Gleiter, R., Hopf, H., Eds.; Wiley-VCH: Weinheim, 2004.

(8) (a) Morisaki, Y.; Hifumi, R.; Lin, L.; Inoshita, K.; Chujo, Y. *Chem. Lett.* **2012**, *41*, 990–992. (b) Morisaki, Y.; Hifumi, R.; Lin, L.; Inoshita, K.; Chujo, Y. *Polym. Chem.* **2012**, *3*, 2727–2730. (c) Morisaki, Y.; Inoshita, K.; Chujo Y. *Chem.–Eur. J.* **2014**, *20*, 8386–8390. (d) Morisaki, Y.; Gon, M.; Sasamori, T.; Tokitoh N.; Chujo, Y. *J. Am. Chem. Soc.* **2014**, *136*, 3350–3353. (e) Gon, M.; Morisaki, Y.; Chujo, Y. *J. Mater. Chem. C* **2015**, *3*, 521–529.

(9) Konig, B.; Knieriem, B.; Meijere A. *Chem. Ber.* **1993**, *126*, 1643–1650.

(10) Annunziata, A.; Galli, C.; Gentili, P.; Guarnieri, A.; Beit-Yannai, M.; Rappoport, Z. *Eur. J. Org. Chem.* **2002**, *13*, 2136–2143.

(11) Miyaura, N.; Yamada, K.; Suzuki, A. *Tetrahedron Lett.* **1979**, *20*, 3437–3440.

(12) Bazan, G. C. *J. Org. Chem.* **2007**, *72*, 8615–8635.

(13) The AIE property of derivatives was already reported: Itami, K.; Ohashi, Y.; Yoshida, J. *J. Org. Chem.* **2005**, *70*, 2778–2792.

(14) CD dissymmetry factor is defined as $g_{abs} = 2\Delta\varepsilon/\varepsilon$, where $\Delta\varepsilon$ indicates differences of absorbance between left- and right-handed circularly polarized light, respectively. CPL dissymmetry factor is defined as g_{lum} =

$2(I_{left} - I_{right})/(I_{left} + I_{right})$, where I_{left} and I_{right} indicate luminescence intensities of left- and right-handed CPL, respectively.

(15) Pangborn, A. B.; Giardello, M. A.; Grubbs, R. H.; Rosen, R. K.; Timmers, F. J. *Organometallics* **1996**, *15*, 1518–1520.

(16) Annunziata, A.; Galli, C.; Gentili, P.; Guarnieri, A.; Beit-Yannai, M.; Rappoport, Z. *Eur. J. Org. Chem.* **2002**, *13*, 2136–2143.

(17) Neese, F. *WIREs Comput. Mol. Sci.* **2012**, *2*, 73–78.

Part III

Optically Active Materials

Based on Planar Chiral [2.2]Paracyclophanes

Chapter 9

Control of Optical and Chiroptical Properties with Metal-Induced Higher-Ordered Structure Based on Planar Chiral Tetrasubstituted [2.2]Paracyclophane

Abstract

Optically active *meta*-arylene-ethynylene dimers with pyridine groups based on a planar chiral 4,7,12,15-tetrasubstituted [2.2]paracyclophane were synthesized. The enantiopure higher-ordered structures were controlled by pyridine-Ag(I) coordination or formation of excimer. Their optical and chiroptical properties before and after Ag(I) coordination were investigated by UV-vis, photoluminescence (PL), circular dichroism (CD) and circularly polarized luminescence (CPL) spectra. Although all compounds exhibited no specific interactions in the ground state before Ag(I) coordination, the compound having the pyrene units constructed higher-ordered structure derived from the excimer, which enhanced chiroptical property. After Ag(I) coordination, the structural change was observed. The intramolecular interaction of the pyrene units was observed in the ground state, and static excimer properties were observed because of the π-π interaction in the excited state. Titration of Ag(I) revealed that the difference coordination number of the compounds from two to four Ag(I) ions. Optical and chiroptical properties suggested the existence of intramolecular Ag(I)-π interaction. The chirality was enhanced by the rigid higher-ordered structure in the ground state. These unique and unprecedented properties were attributed to the rigid planar chiral [2.2]paracyclophane framework.

Introduction

Stimuli-responsive materials have a potential for various applications to photochemistry[1], biochemistry[2], shape memory polymers[3] and supramolecular molecular assembly.[4] Especially, stimuli-responsive optically active compounds are received much attention for next-generation materials with advanced technique based on chirality.[5] The chiral properties are informative and sensitive to structural change. In addition, they are often enhanced by forming the optically active higher-ordered structure.[6] Cozzi, Siegel and co-workers suggested the novel direction for the design of double-helical structure with the chiral scaffold and metal ion coordination method.[7] Otera and coworkers constructed the double-helical structure based on rigid arylene-ethynylene groups with the pyridine-Ag(I) coordination strategy.[8] They used an enantiopure binaphthyl group as the chiral scaffold and investigated the construction of the double-helical structure with CD spectra. It is possible to obtain the enantiopure higher-ordered structure with the chiral scaffold. As a new chiral scaffold, the author focused on a planar chiral [2.2]paracyclophane framework.[9] Recently, our research group reported optical resolution methods of the planar chiral [2.2]paracyclophanes and revealed their unique chiroptical properties, especially in circularly polarized luminescence (CPL) property.[10] The planar chiral [2.2]paracyclophane framework can be used as a rigid chiral source and received much attention for new chiral building block.[11] In this chapter, the author designed *meta*-arylene-ethynylene system containing pyridinyl groups using a planar chiral 4,7,12,15-tetasubstituted [2.2]paracyclophane[10c,d] as the chiral scaffold. The [2.2]paracyclophane unit is located at the center of the molecule, and the molecule has a highly symmetrical structure, which makes structural analysis clear. Pyrene groups are introduced in the terminal units to investigate intramolecular interaction and the structural change based on the excimer formation.[12,13] As a result, the author observed unique chiroptical properties and interesting intramolecular interaction with stimuli-responsive system.

Results and Discussion

Synthesis

The optical resolution of planar chiral 4,7,12,15-tetrasubstituted [2.2]paracyclophane was carried out using the diastereomer method in Chapter 3, and the obtained enantiopure compounds were converted to the corresponding (R_p)- and (S_p)-4,7,12,15-tetraethynyl[2.2]paracyclophanes.[10c] Schemes 1 and 2 show the synthetic routes to the target optically active compounds. *n*-Butyl groups in **N-Py** were introduced to provide solubility to the target compounds in organic solvents such as CH_2Cl_2 and $CHCl_3$.

As shown in Scheme 1, one of bromides of 4,9-dibromo-1,2,3,6,7,8-hexahydropyrene **1** was converted to *n*-butyl group with 1-bromobutane to afford compound **2**. The 1,2,3,6,7,8-hexahydropyrene ring of compound **2** was oxidized to the pyrene ring with *o*-chloranil to obtain compound **3** in 42% isolated yield from **1**. Sonogashira-Hagihara coupling reaction[14] of compound **3** was carried out with TMS-acetylene in the catalytic system of $Pd_2(dba)_3$/CuI using dppf as a phosphine ligand to obtain compound **4**. The TMS group of compound **4** was deprotected to afford compound **5** in 58% isolated yield from **3**. Iodide of compound **5** was reacted chemoselectively with 2-bromo-6-iodopyridine **6** to obtain compound **7** in 78% isolated yield. Compound **3** was reacted in the presence of a catalytic amount of $Pd_2(dba)_3$ to obtain compound **2** in 26% isolated yield.

Scheme 2 shows the synthesis of the target planar chiral compounds **N**, **N-Ph** and **N-Py**, respectively. In this scheme, only the reactions of the (S_p)-isomers are shown; the (R_p)-isomers were synthesized under the same conditions as that for (R_p)-**Cp**. Sonogashira-Hagihara coupling reaction of (S_p)-**Cp** was carried out with 2-iodopyridine **1** in the catalytic system of $Pd_2(dba)_3$/CuI using dppf as a phosphine ligand to obtain compound (S_p)-**N** in 64% isolated yield. Using the same procedure, (S_p)-**N-Ph** and (S_p)-**N-Py** were obtained in 15% and 62%

isolated yields, respectively. The reaction was carried out at 80 ˚C because the reactivity of bromide in compounds **7** and **9** was less than that of iodide in compound **8**.

Scheme 3 shows the synthesis and predicted structure of Ag(I) coordinated complexes (S_p)-**N**, (S_p)-**N-Ph** and (S_p)-**N-Py**. Ag(I) coordination reactions were carried out in the presence of excess of AgOTf to obtain (S_p)-**N-Ag**, (S_p)-**N-Ph-Ag** and (S_p)-**N-Py-Ag**. The structures of all new compounds in this study were confirmed by ^{1}H and ^{13}C NMR spectroscopy, high-resolution mass spectrometry (HRMS), and elemental analysis; the detailed synthetic procedures and NMR data are shown in the experimental section.

Ag(I) Coordinated Compounds

Ag(I) coordination was confirmed by ^{1}H NMR spectra. Figure 1 shows the ^{1}H NMR spectra of (S_p)-**N** (S_p)-**N-Ag**, (S_p)-**N-Ph** and (S_p)-**N-Ph-Ag**. The ^{1}H NMR spectrum of (S_p)-**N-Ag** indicated downfield shift of H_a, H_b, H_c and H_d relative to those of (S_p)-**N**. The ^{1}H NMR spectrum of (S_p)-**N-Ph-Ag** indicated that the hydrogens of pyridine units, H_a, H_b, and H_c, were downfield-shifted relative to those of (S_p)-**N-Ph**. On the other hand, H_d and H_e exhibited clear upfield shift. This is because of the shield effect of the benzene rings located at the other side.

Scheme 1. Synthesis of compound **7**

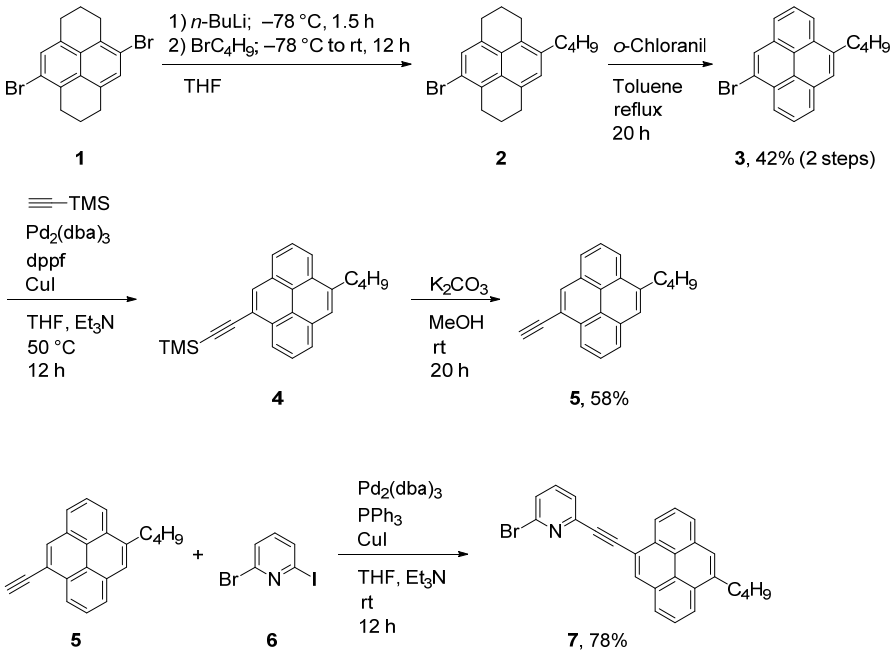

Scheme 2. Synthesis of (S_p)-**N**, **N-Ph** and **N-Py**

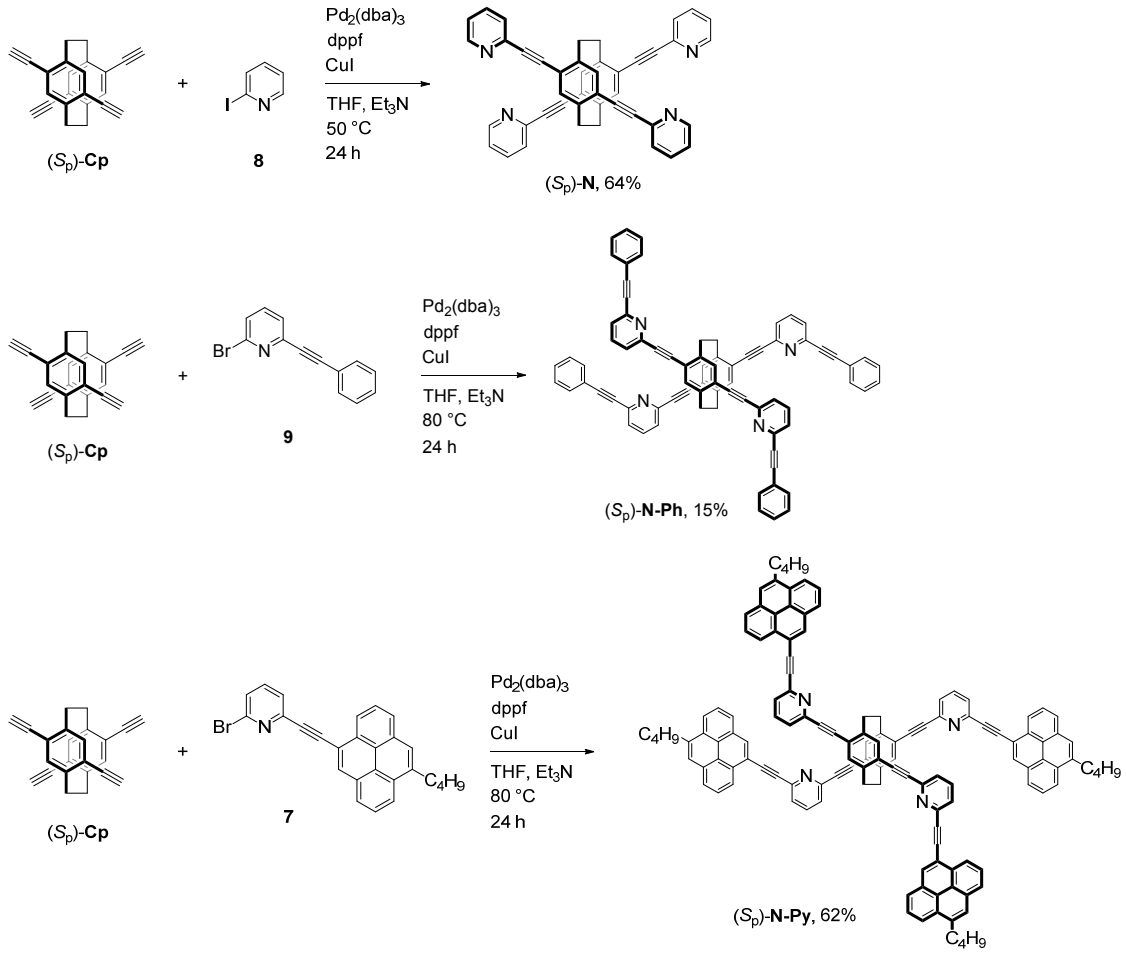

Scheme 3. Synthesis and predicted structures of (S_p)-**N-Ag**, **N-Ph-Ag** and **N-Py-Ag**

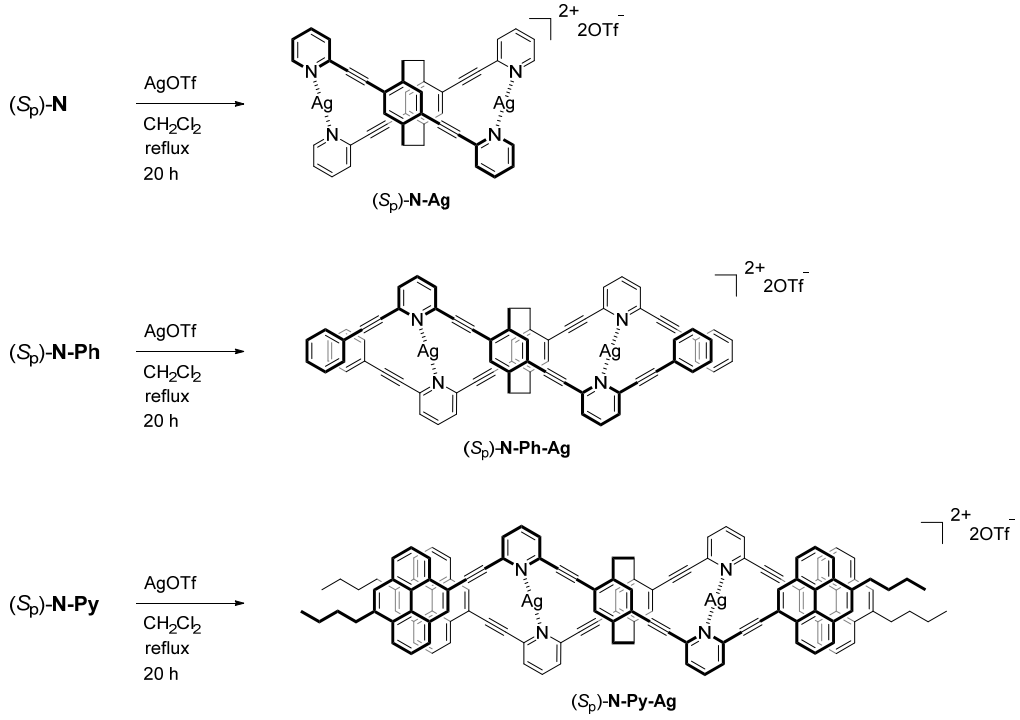

H_f exhibited almost the same chemical shift because downfield shift by Ag(I) ions and upfield shift by benzene rings were balanced. Difference of solubility between before and after Ag(I) addition indicates the Ag(I) coordination. (S_p)-**N-Ag** was dissolved in CH_3CN, while (S_p)-**N** was not dissolved in CH_3CN. (S_p)-**N-Ph-Ag** was dissolved in MeOH, while (S_p)-**N-Ph** was not dissolved in MeOH. (S_p)-**N-Py-Ag** was dissolved in CH_3CN, while (S_p)-**N-Py** was not dissolved in CH_3CN. However, once (S_p)-**N-Py-Ag** was dissolved in CH_3CN, Ag(I) ion was removed from (S_p)-**N-Py-Ag** and (S_p)-**N-Py**. In this case, AgOTf was more stable in CH_3CN than in the (S_p)-**N-Py-Ag** complex. MS spectra could detect the Ag(I)-coordinated species, however, the only mono-coordinated compounds were detected.[8] (R_p)-Isomers exhibited the same properties as those of (S_p)-isomers.

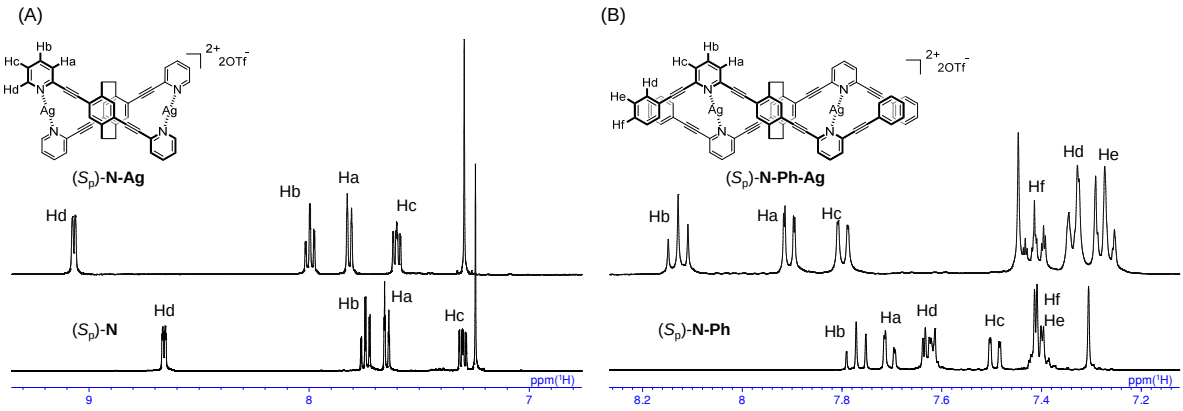

Figure 1. ^{1}H NMR spectra of (A) (S_p)-**N** and (S_p)-**N-Ag** (B) (S_p)-**N-Ph** and (S_p)-**N-Ag-Ph** in CD_2Cl_2.

The structure of *rac*-**N-Ag** was confirmed by X-ray single crystal analysis. Figure 2 shows the structures of *rac*-**N** and *rac*-**N-Ag** obtained by X-ray single crystal analysis. Four nitrogen atoms of *rac*-**N** directed outside of the structure, whereas the nitrogen atoms of *rac*-**N-Ag** directed inside of the structure; Ag(I) ion was sandwiched by two nitrogen atoms of pyridine

groups at the *trans* position. The angle of N(1)−Ag(1)−N(2) (174.6˚) was almost planar, whereas that of N(3)−Ag(2)−N(4) (161.6˚) was not planar because one of oxygen atoms of the OTf group combined with the Ag(I) atom (bond length of O(1)−Ag(2) was 2.640 Å, which was shorter than the sum of van der Waals radii, 3.27 Å). As a result, the structure of *rac*-**N-Ag** was formed by two Ag(I) ion combined with *rac*-**N**. Although X-ray single crystal structures of (S_p)-**N-Ag**, (S_p)-**N-Ph-Ag** and (S_p)-**N-Py-Ag** were not obtained, it was predicted that they formed the same complexes as *rac*-**N-Ag**.

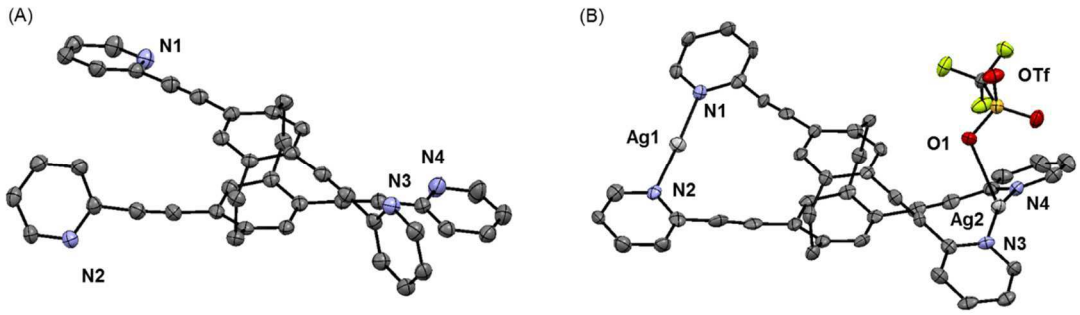

Figure 2. ORTEP drawings of (A) *rac*-**N** and (B) *rac*-**N-Ag** (50% probability for thermal ellipsoids). Hydrogen atoms and one of OTf groups are omitted to clarify.

Optical Properties

The optical properties of both enantiomers with a planar chiral 4,7,12,15-tetrasubstituted [2.2]paracyclophane **N**, **N-Ph**, and **N-Py** as well as their Ag(I)-coordinated complexes **N-Ag**, **N-Ph-Ag**, and **N-Py-Ag** were evaluated. The optical and chiroptical data are summarized in Tables 1 and 2, respectively. The UV-vis absorption spectra and the PL spectra were obtained in the dilute CH_2Cl_2 solutions (1.0×10^{-5} M for **N**, **N-Ph**, **N-Ag** and **N-Ph-Ag**; 5.0×10^{-6} M for **N-Py** and **N-Py-Ag**).

Figure 3 shows the UV-vis absorption spectra of **N**, **N-Ph**, and **N-Py** and the Ag(I) complexes **N-Ag**, **N-Ph-Ag**, and **N-Py-Ag**. All of the absorption spectra changed after Ag(I)

coordination. The absorption spectra of Ag(I) complexes exhibited bathochromic shift compared with those of non-coordination compounds due to the increase of planarity (Figure 2). Especially in the **N-Py** and **N-Py-Ag**, the vibration bands of pyrene from 350 nm to 400 nm disappeared, and absorption edge exhibited bathochromic shift drastically. This is because of intramolecular π-π interaction of the pyrene units by conformation change due to Ag(I) coordination in the ground state. Figure 4 shows the PL spectra of **N**, **N-Ph**, and **N-Py** and the Ag(I) complexes **N-Ag**, **N-Ph-Ag**, and **N-Py-Ag**. There were few changes before and after Ag(I) coordination of **N** because of the identical planarity of the structures in the excited state. **N-Ph** exhibited almost the same properties of **N**. **N-Py** exhibited the two peaks attributed to the same structure of **N** or pyrene emission (419 nm, τ = 1.18 ns) and pyrenes excimer emission (491 nm, τ = 7.79 ns). On the other hand, **N-Py-Ag** exhibited the only one peak top at 535 nm. According to the PL lifetime measurement, the long PL lifetime derived from the excimer was not observed. This indicates that the pyrene units of **N-Py-Ag** were interacted more strongly both in the ground state and in the excited state.

Table 1. Optical properties: Spectroscopic data

	λ_{abs}[a]/nm (ε / 10^5 $M^{-1}cm^{-1}$)	λ_{lum}[a]/nm	τ[c]/ns	χ^2	Φ_{lum}[d]
(S_p)-**N**	342 (0.63)	421	6.05	1.02	0.59
(S_p)-**N-Ag**	378 (0.66)	427	2.42	1.07	0.24
(S_p)-**N-Ph**	276 (1.05), 356 (0.91)	417	3.96	1.04	0.56
(S_p)-**N-Ph-Ag**	285 (0.79), 393 (1.14)	424	1.27	1.06	0.35
(S_p)-**N-Py**	361 (1.77), 379 (1.69)[b]	419, 491[b]	1.18 (76.2%)[e] 7.79 (23.8%)[e]	1.23	0.50
(S_p)-**N-Py-Ag**	389 (1.34)[b]	538[b]	0.69 (51.5%) 1.64 (48.5%)	1.23	0.04

[a] In CH_2Cl_2 (1.0×10^{-5} M); excited at absorption maxima for PL. [b] In CH_2Cl_2 (5.0×10^{-6} M). [c] Emission lifetime at λ_{lum}. [d] Absolute PL quantum efficiency. [e] Detected at 491 nm.

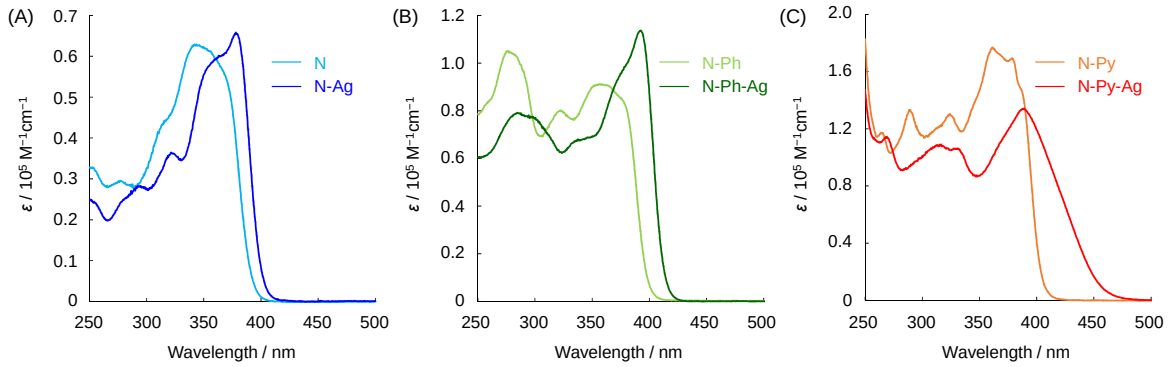

Figure 3. UV-vis absorption spectra of (A) **N** and **N-Ag** in the dilute CH_2Cl_2 (1.0×10^{-5} M), (B) **N-Ph** and **N-Ph-Ag** in the dilute CH_2Cl_2 (1.0×10^{-5} M), (C) **N-Py** and **N-Py-Ag** in the dilute CH_2Cl_2 (5.0×10^{-6} M).

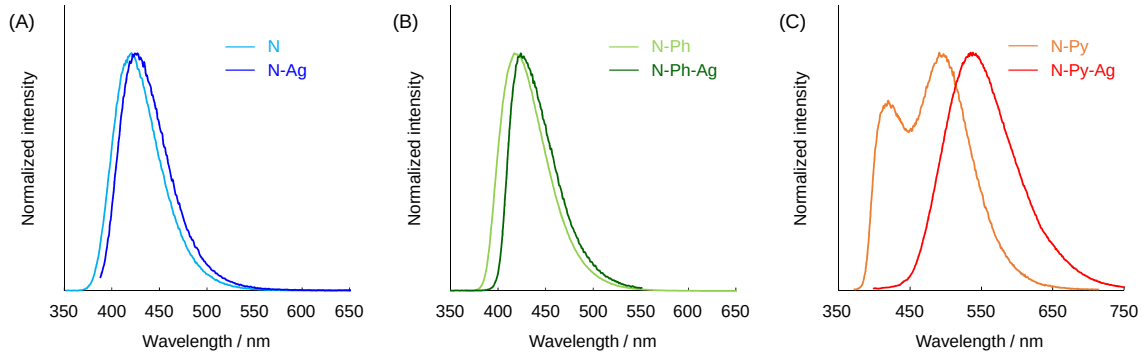

Figure 4. PL spectra of (A) **N** and **N-Ag** in the dilute CH_2Cl_2 (1.0×10^{-5} M), (B) **N-Ph** and **N-Ph-Ag** in the dilute CH_2Cl_2 (1.0×10^{-5} M), (C) **N-Py** and **N-Py-Ag** in the dilute CH_2Cl_2 (5.0×10^{-6} M).

Chiroptical Properties

The chiroptical properties of the ground and excited states of (S_p)- and (R_p)-**N**, **N-Ph**, and **N-Py** and the Ag(I) complexes (S_p)- and (R_p)-**N-Ag**, **N-Ph-Ag**, and **N-Py-Ag** were investigated by CD and CPL spectroscopy. The spectra were obtained in the dilute CH_2Cl_2 solutions (1.0×10^{-5} M for **N**, **N-Ph**, **N-Ag** and **N-Ph-Ag**; 5.0×10^{-6} M for **N-Py** and **N-Py-Ag**). Chiroptical data, such as CD and CPL dissymmetry factor[15] (g_{abs} and g_{lum}, respectively) are summarized in Table 2.

Table 2. Chiroptical properties: Spectroscopic data of (S_p)-isomers

	$\lvert g_{abs,\,max}\rvert^a$ / 10^{-3}	$g_{abs}{}^b$ / 10^{-3}	g_{lum} / 10^{-3} at $\lambda_{lum,\,max}{}^c$
(S_p)-**N**	4.1	−1.8	−2.8
(S_p)-**N-Ag**	4.6	−2.8	−2.5
(S_p)-**N-Ph**	2.5	−0.74	−1.2, +0.25
(S_p)-**N-Ph-Ag**	7.0	+2.6	+0.29
(S_p)-**N-Py**	1.2	+0.6	+6.7
(S_p)-**N-Py-Ag**	3.1	+2.3	+1.5

[a] $g_{abs} = 2\Delta\varepsilon/\varepsilon$, where $\Delta\varepsilon$ indicates differences of absorbance between left- and right-handed circularly polarized light, respectively. The maximum g_{abs} value of the CD spectra was estimated. [b] The g_{abs} value of the first peak top was estimated. [c] $g_{lum} = 2(I_{left} - I_{right})/(I_{left} + I_{right})$, where I_{left} and I_{right} indicate luminescence intensities of left- and right-handed CPL, respectively.

Figure 5 shows the CD and absorption spectra of (S_p)- and (R_p)-**N**, **N-Ph**, and **N-Py** and the Ag(I) complexes (S_p)- and (R_p)-**N-Ag**, **N-Ph-Ag**, and **N-Py-Ag**. In all cases, mirror image Cotton effects were observed in the CD spectra. The shape of the spectra of (S_p)- and (R_p)-**N** and **N-Ag** were similar, whereas the maximum g_{abs} values of **N-Ph** and **N-Py** were enhanced after Ag(I) coordination. The maximum g_{abs} values were estimated to be 4.1×10^{-3} for (S_p)-**N**, 4.6×10^{-3} for (S_p)-**N-Ag**, 2.5×10^{-3} for (S_p)-**N-Ph**, 7.0×10^{-3} for (S_p)-**N-Ph-Ag**, 1.2×10^{-3} for (S_p)-**N-Py**, and 3.1×10^{-3} for (S_p)-**N-Py-Ag**, respectively, suggesting the major structural change between **N-Ph** and **N-Ph-Ag** or **N-Py** and **N-Py-Ag**. The higher-ordered structures of **N-Ph-Ag** and **N-Py-Ag** are discussed in the Ag(I) titration section.

Figure 6 shows the CPL and PL spectra of (S_p)- and (R_p)-**N**, **N-Ph**, and **N-Py** and the Ag(I) complexes (S_p)- and (R_p)-**N-Ag**, **N-Ph-Ag**, and **N-Py-Ag**. Mirror image CPL spectra were observed for the enantiomers. The shape of the CPL spectra of (S_p)- and (R_p)-**N** and **N-Ag** were similar with the same reason as the CD spectra. On the other hand, the CPL signal of the **N-Ph-Ag** was almost silent at the PL peak top, and the g_{lum} values of longer wavelength (around 530 nm) were identical with those of **N-Ph** ($g_{lum} = +0.25 \times 10^{-3}$ for **N-Ph** and $+0.29 \times 10^{-3}$ for

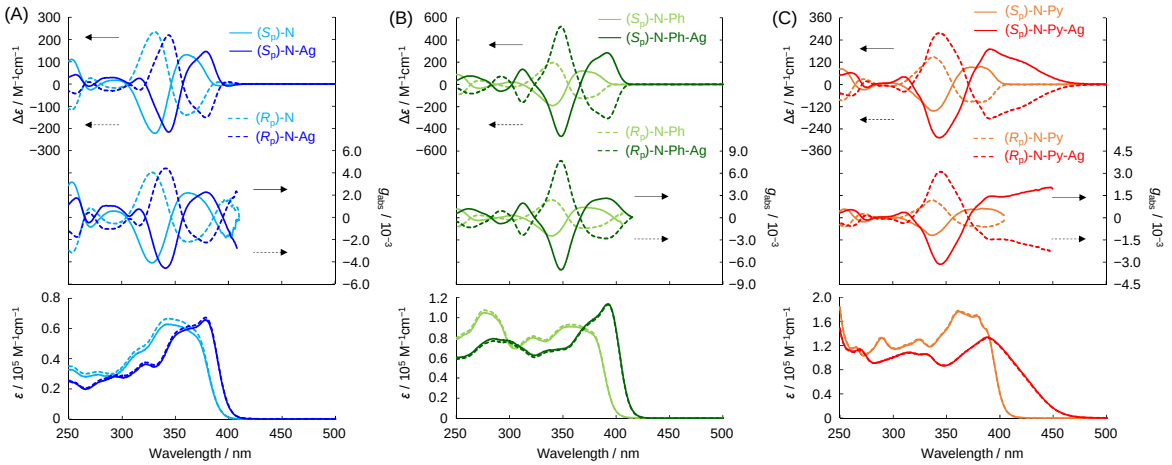

Figure 5. CD (top), g_{abs} (middle), and UV-vis absorption (bottom) spectra of (A) **N** and **N-Ag** in the dilute CH_2Cl_2 (1.0×10^{-5} M), (B) **N-Ph** and **N-Ph-Ag** in the dilute CH_2Cl_2 (1.0×10^{-5} M), (C) **N-Py** and **N-Py-Ag** in the dilute CH_2Cl_2 (5.0×10^{-6} M).

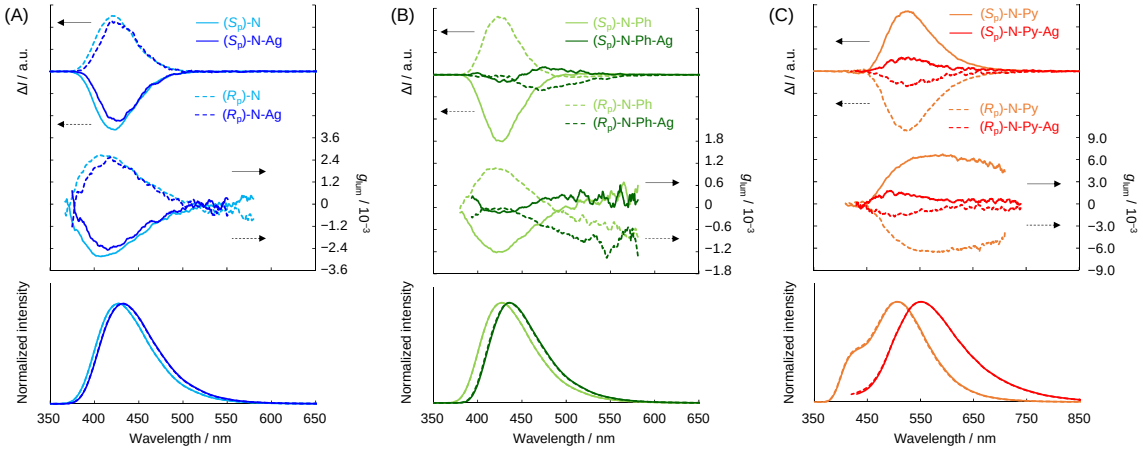

Figure 6. CPL (top), g_{lum} (middle), and PL (bottom) spectra of (A) **N** and **N-Ag** in the dilute CH_2Cl_2 (1.0×10^{-5} M), (B) **N-Ph** and **N-Ph-Ag** in the dilute CH_2Cl_2 (1.0×10^{-5} M), (C) **N-Py** and **N-Py-Ag** in the dilute CH_2Cl_2 (5.0×10^{-6} M). Excitation wavelength was 300 nm (**N**, **N-Ag**, **N-Ph**, **N-Ph-Ag** and **N-Py**) and 350 nm (**N-Py-Ag**).

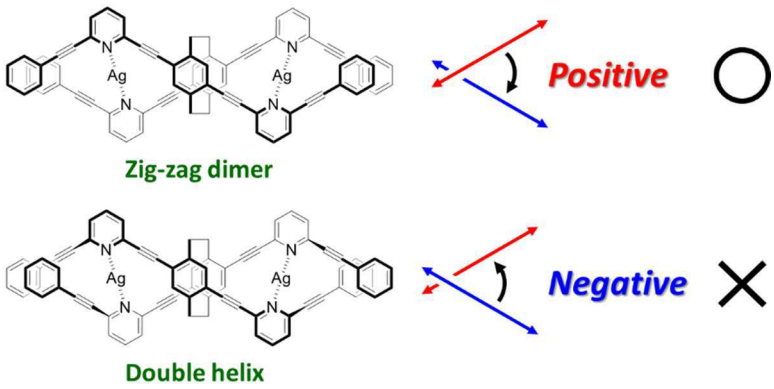

Figure 7. Predicted structures of the Ag(I) complex (S_p)-**N-Ph-Ag** by the exciton coupling.

N-Ph-Ag). It was considered that the PL at around 530 nm was derived from π-π interaction of terminal benzene rings. **N-Py** exhibited higher g_{lum} value ($g_{lum} = +6.7 \times 10^{-3}$) than g_{abs} value ($g_{abs} = +0.6 \times 10^{-3}$) because **N-Py** formed higher-ordered structure in the excited state with an excimer of the pyrene groups. On the other hand, **N-Py-Ag** did not exhibit such enhancement ($g_{lum} = +1.5 \times 10^{-3}$, $g_{abs} = +2.3 \times 10^{-3}$), indicating that **N-Py-Ag** formed almost similar structure both in the ground and excited states. Figure 7 shows the predicted Ag(I)-coordination structures with the exciton coupling theory from the CD and CPL spectra.[16] In the CD and CPL spectra, the first Cotton effect of (S_p)-**N-Ph-Ag** and (S_p)-**N-Py-Ag** exhibited positive signal. These results suggest the zig-zag dimer conformation. The excimer also formed the same structure in the excited state.

Ag(I) Titration Measurement

Titration of AgOTf to (R_p)-**N**, **N-Ph** and **N-Py** was carried out in the dilute mixed CH_2Cl_2/DMF = 95:5 v/v solution (1.0×10^{-5} M). DMF was used for the preparation of AgOTf solution because CH_2Cl_2 is not good solvent for AgOTf. Figures 8, 9 and 10 show the results of titration of (R_p)-**N**, **N-Ph** and **N-Py** monitored by the CD spectra, respectively. Black line exhibited the spectra of Ag(I) complexes (R_p)-**N-Ag**, **N-Ph-Ag** and **N-Py-Ag** in the dilute CH_2Cl_2 (1.0×10^{-5} M for (R_p)-**N-Ag** and **N-Ph-Ag**; 5.0×10^{-6} M for (R_p)-**N-Py**) discussed in the previous section. Figure 8A shows the total titration spectra of (R_p)-**N**, and Figure 8A is divided into Figures 8B and 8C to clarify. Spectral change was completed with 2.0 eq. of AgOTf, which is identified with the coordination number of (R_p)-**N**. On the other hand, as shown in Figure 9, the spectral change for (R_p)-**N-Ph** was not completed with 2.0 eq., and 4.0 eq. of AgOTf was required. The spectral change was similar to (R_p)-**N** from 0.0 to 2.0 eq., whereas the chirality was drastically enhanced from 2.0 to 4.0 eq. The property of (R_p)-**N-Ph-Ag** obtained from the reaction was similar to the result after the addition of 4.0 eq. of AgOTf. These results suggest that intramolecular Ag(I)-π interaction[18] occurred from 2.0 to 4.0 eq. and

that the interaction made the structure more rigid. The resulting structure enhanced the chirality in the ground state. Titration of AgOTf to (R_p)-**N-Py** (Figure 10) exhibited the almost same results as those of (R_p)-**N-Ph**. Figure 11 shows the titration results of AgOTf to (R_p)-**N** or (R_p)-**N-Ph** monitored by the CPL spectra. The g_{lum} value of (R_p)-**N-Ph** rapidly decreased at the 3.2

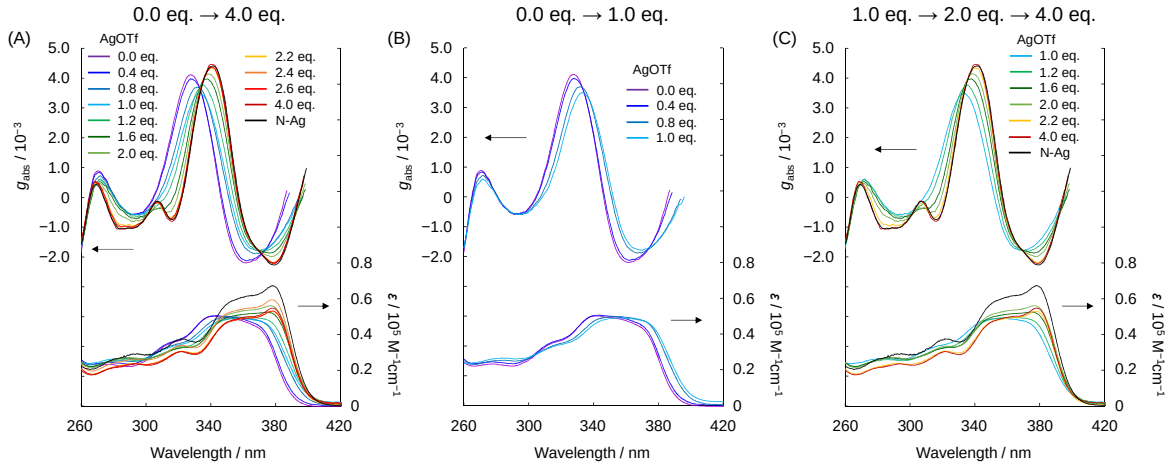

Figure 8. g_{abs} (top) and UV-vis absorption (bottom) spectra of AgOTf titration of (R_p)-**N** in the dilute CH_2Cl_2/DMF = 95/5 v/v solution (1.0×10^{-5} M). Black line shows the spectra of **N-Ag** in the dilute CH_2Cl_2 (1.0×10^{-5} M). (A) AgOTf titration from 0.0 eq. to 4.0 eq., (B) from 0.0 eq. to 1.0 eq., (C) from 1.0 eq. to 4.0 eq.

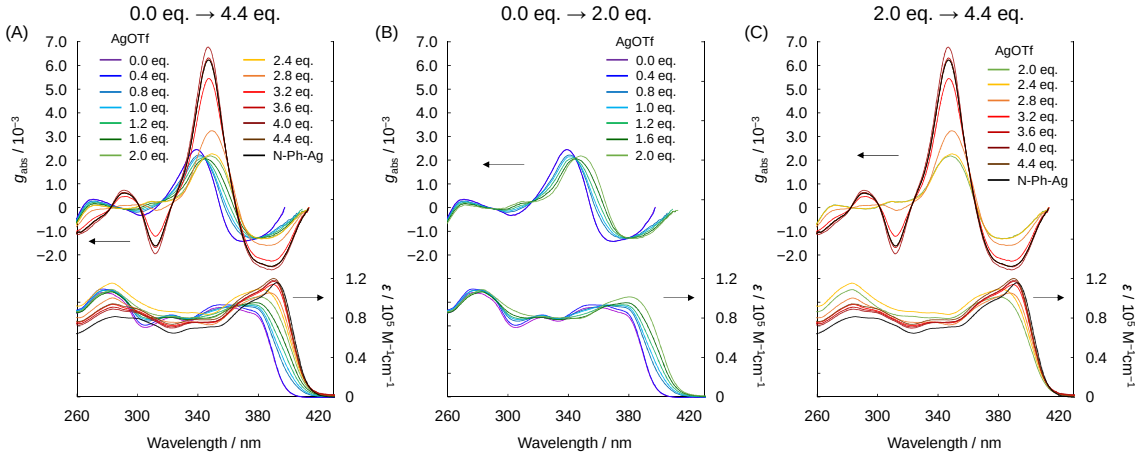

Figure 9. g_{abs} (top) and UV-vis absorption (bottom) spectra of AgOTf titration of (R_p)-**N-Ph** in the dilute CH_2Cl_2/DMF = 95/5 v/v solution (1.0×10^{-5} M). Black line shows the spectra of **N-Ph-Ag** in the dilute CH_2Cl_2 (1.0×10^{-5} M). (A) AgOTf titration from 0.0 eq. to 4.4 eq., (B) from 0.0 eq. to 2.0 eq., (C) from 2.0 eq. to 4.4 eq.

eq. of AgOTf (Figure 11B) whereas the g_{lum} value of (R_p)-**N** did not change from 2.2 eq. to **N-Ag** (and excess of AgOTf). Considering the fact that the g_{abs} value of (R_p)-**N-Ph** rapidly increased at 3.2 eq. of AgOTf, the intramolecular Ag(I)-π interaction was clearly observed at 3.2 eq. of AgOTf. The predicted conformational changes with various stimulation are summarized in Figure 12.

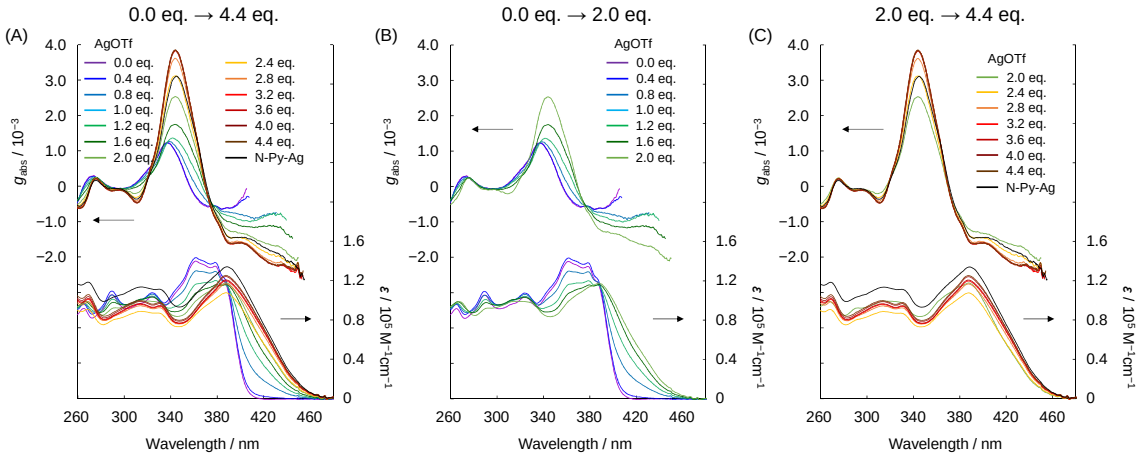

Figure 10. g_{abs} (top) and UV-vis absorption (bottom) spectra of AgOTf titration of (R_p)-**N-Py** in the dilute CH_2Cl_2/DMF = 95/5 v/v solution (1.0×10^{-5} M). Black line shows the spectra of **N-Ph-Ag** in the dilute CH_2Cl_2 (5.0×10^{-6} M). (A) AgOTf titration from 0.0 eq. to 4.4 eq., (B) from 0.0 eq. to 2.0 eq., (C) from 2.0 eq. to 4.4 eq.

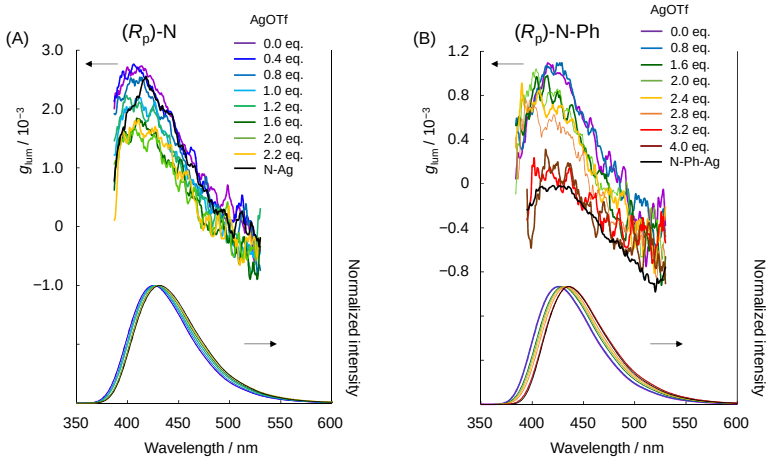

Figure 11. g_{lum} (top) and PL (bottom) spectra of AgOTf titration of (A) (R_p)-**N** and (B) (R_p)-**N-Ph** in the dilute CH_2Cl_2/DMF = 95/5 v/v solution (1.0×10^{-5} M). Black line shows the spectra of **N-Ag** and **N-Ph-Ag** in the dilute CH_2Cl_2 (1.0×10^{-5} M), respectively; excitation wavelength was 300 nm (**N**, **N-Ag**, **N-Ph**, **N-Ph-Ag** and **N-Py**) and 350 nm (**N-Py-Ag**).

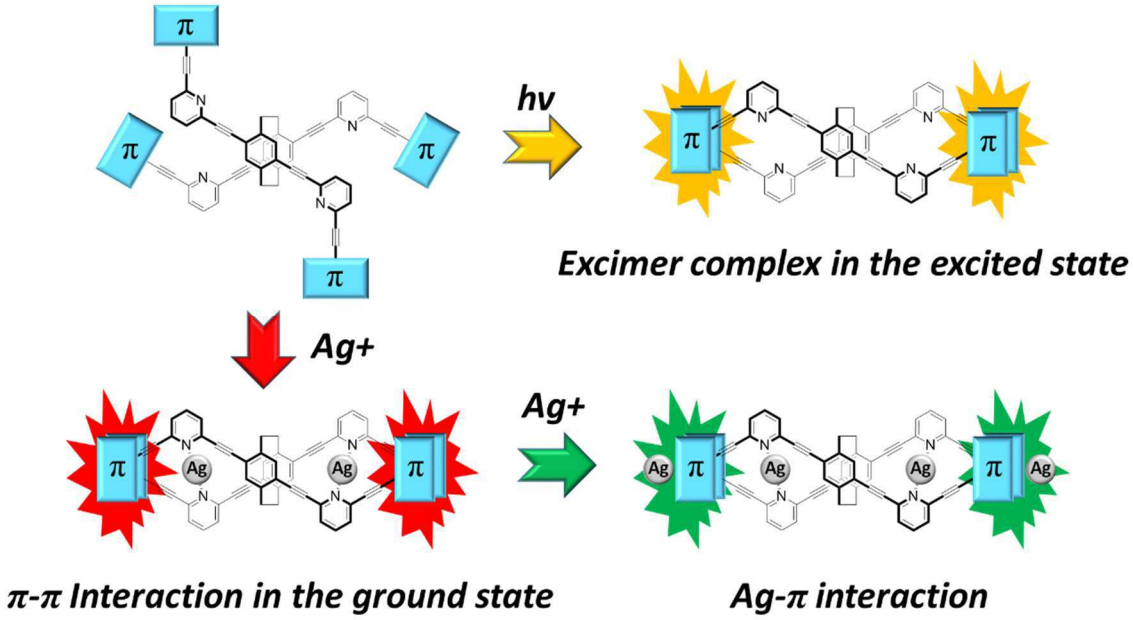

Figure 12. Mechanism of Ag(I)-coordination behaviors and excimer form.

Conclusions

Optically active *m*-phenylene-ethynylene dimers containing pyridine groups with a planar chiral 4,7,12,15-tetrasubstituted [2.2]paracyclophane were synthesized. Pyridine groups can form *trans*-coordination structure with Ag(I) ion. The optical and chiroptical properties before and after Ag(I) coordination were investigated by UV, PL, CD and CPL spectra. Before Ag(I) coordination, all compounds exhibited no specific interactions in the ground state. On the other hand, the pyrene of **N-Py** formed higher-ordered structure derived from the excimer. As a result, (S_p)-**N-Py** showed the enhanced g_{lum} values ($g_{lum} = +6.7 \times 10^{-3}$) in the excited state compared with the g_{abs} values ($g_{abs} = +0.6 \times 10^{-3}$) in the ground state. After Ag(I) coordination, UV-vis spectra of all compounds exhibited bathochromic shift due to increasing the planarity in the ground state. The intramolecular interaction of pyrene units of **N-Py-Ag** was observed in the ground state, and **N-Py-Ag** exhibited static excimer in the excited state. Titration of AgOTf revealed that two Ag(I) ions were coordinated to **N**, whereas four Ag(I) ions were coordinated to **N-Ph** and **N-Py**. The maximum g_{abs} values were drastically enhanced from 2.0 to 4.0 eq. AgOTf. Titration results and chiroptical properties suggested that the existence of Ag(I)-π interaction in the **N-Ph** and **N-Py** system and that the resulting higher-ordered structure enhanced maximum g_{abs} values. These metal coordination properties are unique and unprecedented, and the results are available for multi-mode (optical and chiroptical) metal sensing chemistry and stimuli-response CPL materials.

Experimental Section

General. ^{1}H and ^{13}C NMR spectra were recorded on JEOL EX400 and AL400 instruments at 400 and 100 MHz, respectively. Samples were analyzed in $CDCl_3$ and CD_2Cl_2. The chemical shift values were expressed relative to Me_4Si as an internal standard in $CDCl_3$. Analytical thin layer chromatography (TLC) was performed with silica gel 60 Merck F254 plates. Column chromatography was performed with Wakogel C-300 silica gel and aluminium oxide 90 active basic (0.063-0.200 mm, pH = 8.5-10.5). High-resolution mass (HRMS) spectrometry was performed at the Technical Support Office (Department of Synthetic Chemistry and Biological Chemistry, Graduate School of Engineering, Kyoto University), and the HRMS spectra were obtained on a Thermo Fisher Scientific EXACTIVE spectrometer for electrospray ionization (ESI), a Thermo Fisher Scientific EXACTIVE spectrometer for electron ionization (EI) and a Thermo Fisher Scientific EXACTIVE spectrometer for atmospheric pressure chemical ionization (APCI). Recyclable preparative high-performance liquid chromatography (HPLC) was carried out on a Japan Analytical Industry Co. Ltd., Model LC918R (JAIGEL-1H and 2H columns) and LC9204 (JAIGEL-2.5H and 3H columns) using $CHCl_3$ as an eluent. UV-vis spectra were recorded on a SHIMADZU UV-3600 spectrophotometer, and samples were analyzed in CH_2Cl_2 at room temperature. Fluorescence emission spectra were recorded on a HORIBA JOBIN YVON Fluoromax-4 spectrofluorometer, and samples were analyzed in CH_2Cl_2 at room temperature. The PL lifetime measurement was performed on a Horiba FluoroCube spectrofluorometer system; excitation was carried out using a UV diode laser (NanoLED 375 nm). Specific rotations ($[\alpha]^{t}_{D}$) were measured with a HORIBA SEPA-500 polarimeter. Circular dichroism (CD) spectra were recorded on a JASCO J-820 spectropolarimeter with CH_2Cl_2 as a solvent at room temperature. Circularly polarized luminescence (CPL) spectra were recorded on a JASCO CPL-200S with CH_2Cl_2 as a solvent at room temperature. Elemental analyses were performed at the Microanalytical Center of Kyoto University.

Materials. Commercially available compounds used without purification: (Tokyo Chemical Industry Co, Ltd.) 2-Iodo-pyridine (**8**), *o*-chloranil, trimethylsilylacetylene (TMS-acetylene), $Pd_2(dba)_3$ (dba = dibenzylideneacetone), 1,1'-bis(diphenylphosphino)ferrocene (dppf); (Wako Pure Chemical Industries, Ltd.) 1-bromobutane, CuI, K_2CO_3; (Kanto Chemical Co., Inc.) *n*-butyllithium (*n*-BuLi, 1.6 M in hexane); (Strem Chemicals Inc.) AgOTf (silver trifluoromethanesulfonate). Commercially available solvents: MeOH (Wako Pure Chemical Industries, Ltd.), toluene (deoxygenated grade, Wako Pure Chemical Industries, Ltd.) used without purification. THF (Wako Pure Chemical Industries, Ltd.) and Et_3N (Kanto Chemical Co., Inc.), purified by passage through solvent purification columns under Ar

pressure.[18] Compounds prepared as described in the literatures: 2,3-Dibromo-6,7-bis(hexyloxy)naphthalene (**1**)[19], 2,5-di-*n*-butylfuran (**5**)[20], 1,2-bis(hexyloxy)-4-iodo-5-[2-(trimethylsilyl)ethynyl]benzene (**10**)[21], (R_p)- and (S_p)-4,7,12,15-tetraethynyl[2.2]paracyclophane ((R_p)- and (S_p)-**Cp**).[10c]

Ag(I) Titration Measurement. Titration of AgOTf to (R_p)-**N**, **N-Ph** and **N-Py** was carried out in the dilute mixed CH_2Cl_2/DMF = 95:5 v/v solution (1.0×10^{-5} M). DMF was used for the preparation of AgOTf solution because CH_2Cl_2 is not good solvent for AgOTf. At first, (R_p)-**N**, **N-Ph**, **N-Py** and AgOTf in the dilute mixed CH_2Cl_2/DMF = 95:5 v/v solution (5.0×10^{-4} M) were prepared. Then, AgOTf solution (from 0 mL to 4.4 mL) was added to (R_p)-**N**, **N-Ph**, **N-Py** solution (0.10 mL) and adjust the total volume of 5.0 mL (1.0×10^{-5} M) by the CH_2Cl_2/DMF = 95:5 v/v mixed solvent.

Synthesis of 2. A solution of *n*-BuLi (1.65 M in hexane, 6.67 mL, 11.0 mmol) was slowly added to a solution of **1** (3.66 g, 10.0 mmol) in THF (100 mL) at –78 °C under Ar atmosphere. After 1.5 h, 1-bromobutane (2.25 mL, 21.0 mmol) was added, and the mixture was stirred for 12 h at –78 °C to room temperature. The reaction mixture was quenched by the addition of aqueous NH_4Cl solution, and the organic layer was extracted three times with $CHCl_3$. The combined organic layer was washed with brine and dried over Na_2SO_4. Na_2SO_4 was removed by filtration, and the solvent was evaporated. Compound **2** was obtained and used for the next reaction without further purification.

Synthesis of 3. A mixture of **2**, *o*-chloranil (7.38 g, 30.0 mmol) and toluene (90 mL) was placed in a round-bottom flask equipped with a magnetic stirring bar. After degassing the reaction mixture several times, the reaction was carried out at reflux temperature for 12 h. The residue was semi-purified by flash column chromatography on neutral Al_2O_3 (toluene as an eluent). After removing the solvent, the residue was purified by column chromatography on SiO_2 ($CHCl_3$/hexane = 1/9 v/v as an eluent) to afford **3** (1.78 g, 5.28 mmol, 53%) as a colorless solid. R_f = 0.63 ($CHCl_3$/hexane = 1/9 v/v). ^{1}H NMR ($CDCl_3$, 400 MHz) δ 1.03 (t, J = 7.3 Hz, 3H), 1.56 (sext, J = 7.6 Hz, 2H), 1.87-1.94 (m, 2H), 3.27 (t, J = 7.8 Hz, 2H), 7.93 (s, 1H), 8.01-8.08 (m, 2H), 8.11 (d, J = 7.1 Hz, 1H), 8.18 (d, J = 7.3 Hz, 1H), 8.39 (d, J = 7.3 Hz, 1H), 8.42 (s, 1H), 8.53 (d, J = 7.1 Hz, 1H) ppm; ^{13}C NMR ($CDCl_3$, 100 MHz) δ 14.0, 23.0, 32.4, 33.2, 122.0, 122.3, 124.2, 124.3, 124.5, 124.6, 125.7, 126.1, 126.1, 126.5, 129.5, 130.7, 130.9, 131.2, 131.8, 138.1 ppm. HRMS (EI) calcd. for $C_{20}H_{17}Br$ $[M]^+$: 336.0514, found: 336.0514. Elemental analysis calcd. for $C_{20}H_{17}Br$: C 71.23 H 5.08, found: C 71.47 H 5.25.

Synthesis of 4. A mixture of **3** (1.63 g, 4.82 mmol), $Pd_2(dba)_3$ (95.7 mg, 0.105 mmol), dppf (116 mg, 0.209 mmol), CuI (39.8 mg, 0.209 mmol), THF (25 mL) and Et_3N (25 mL) was placed in a round-

bottom flask equipped with a magnetic stirring bar. After degassing the reaction mixture several times, trimethylsilylacetylene (1.80 mL, 12.5 mmol) was added to the mixture via a syringe. The reaction was carried out at 50 °C for 12 h. After the reaction mixture was cooled to room temperature, precipitates were removed by filtration, and the solvent was evaporated. The residue was purified by column chromatography on SiO_2 ($CHCl_3$/hexane = 1/9 v/v as an eluent) to afford **4**. Compound **4** was used for the next reaction without further purification.

Synthesis of 5. K_2CO_3 (744 mg, 5.38 mmol) was added to a suspension of **4** in MeOH (40 mL). After the mixture was stirred for 20 h at room temperature, H_2O was added to the reaction mixture. The organic layer was extracted with $CHCl_3$ and washed with brine. The combined organic layer was dried over $MgSO_4$. $MgSO_4$ was removed by filtration, and the solvent was evaporated. The residue was purified by column chromatography on SiO_2 ($CHCl_3$/hexane = 1/4 v/v as an eluent) and recrystallization from $CHCl_3$ and MeOH (good and poor solvent, respectively) to afford **5** (787 mg, 2.79 mmol, 58%) as a light yellow crystal. R_f = 0.58 ($CHCl_3$/hexane = 1/4 v/v). ^{1}H NMR ($CDCl_3$, 400 MHz) δ 1.02 (t, J = 7.3 Hz, 3H), 1.56 (sext, J = 7.6 Hz, 2H), 1.86-1.94 (m, 2H), 3.26 (t, J = 7.6 Hz, 2H), 3.54 (s, 1H), 7.91 (s, 1H), 8.00-8.06 (m, 2H), 8.13-8.16 (m, 2H), 8.37-8.39 (m, 2H), 8.63 (d, J = 7.8 Hz, 1H) ppm; ^{13}C NMR ($CDCl_3$, 100 MHz) δ 14.0, 23.0, 32.4, 33.2, 81.6, 82.1, 119.0, 122.6, 123.0, 123.5, 124.9, 125.1, 125.3, 125.9, 126.3, 126.3, 130.1, 130.5, 130.6, 131.2, 133.4, 137.8 ppm. HRMS (APCI) calcd. for $C_{22}H_{19}$ $[M+H]^+$: 283.1481, found: 283.1474. Elemental analysis calcd. for $C_{22}H_{18}$: C 93.57 H 6.43, found: C 93.61 H 6.29.

Synthesis of 7. A mixture of **5** (400 mg, 1.42 mmol), 2-bromo-6-iodopyridine (**6**) (402 mg, 1.42 mmol), $Pd_2(dba)_3$ (32.5 mg, 0.0355 mmol), PPh_3 (37.2 mg, 0.142 mmol), CuI (13.5 mg, 0.071 mmol), THF (20 mL) and Et_3N (10 mL) was placed in a round-bottom flask equipped with a magnetic stirring bar. After degassing the reaction mixture several times, the reaction was carried out at room temperature for 12 h. After the reaction, precipitates were removed by filtration, and the solvent was evaporated. The residue was purified by column chromatography on SiO_2 ($CHCl_3$/hexane = 1/9 v/v as an eluent) and recrystallization from $CHCl_3$ and MeOH (good and poor solvent, respectively) to afford **7** (486 mg, 1.10 mmol, 78%) as a colorless crystal. R_f = 0.54 (CH_2Cl_2/hexane = 1/1 v/v). ^{1}H NMR ($CDCl_3$, 400 MHz) δ 1.03 (t, J = 7.3 Hz, 3H), 1.57 (sext, J = 7.4 Hz, 2H), 1.88-1.95 (m, 2H), 3.28 (t, J = 7.8 Hz, 2H), 7.50 (dd, J = 0.92, 8.0 Hz, 1H), 7.61 (t, J = 7.8 Hz, 1H), 7.67 (dd, J = 0.84, 7.6 Hz, 1H), 7.94 (s, 1H), 8.03-8.10 (m, 2H), 8.19 (dd, J = 2.3, 7.3 Hz, 2H), 8.41 (d, J = 7.8 Hz, 1H), 8.49 (s, 1H), 8.70 (d, J = 7.6 Hz, 1H) ppm; ^{13}C NMR ($CDCl_3$, 100 MHz) δ 14.0, 23.0, 32.4, 33.2, 89.5, 91.8, 118.7, 122.9, 123.1,

123.5, 125.0, 125.4, 125.4, 126.0, 126.3, 126.3, 126.3, 127.5, 129.8, 130.5, 130.6, 131.3, 133.9, 137.8, 138.3, 142.0, 144.1 ppm. HRMS (APCI) calcd. for $C_{27}H_{21}BrN$ $[M+H]^+$: 438.0852, found: 438.0843. Elemental analysis calcd. for $C_{27}H_{20}BrN$: C 73.98 H 4.60 N 3.20 Br 18.23, found: C 74.06 H 4.62 N 3.01 Br 18.09.

Synthesis of N. A mixture of (S_p)-**Cp** (20.0 mg, 0.0657 mmol), 2-iodopyridine (**8**) (59.3 mg, 0.289 mmol), $Pd_2(dba)_3$ (6.0 mg, 0.00657 mmol), dppf (7.3 mg, 0.0131 mmol), CuI (2.5 mg, 0.0131 mmol), THF (2 mL) and Et_3N (2 mL) was placed in a round-bottom flask equipped with a magnetic stirring bar. After degassing the reaction mixture several times, the reaction was carried out at room temperature for 24 h. After the reaction, precipitates were removed by filtration, and the solvent was evaporated. The residue was semi-purified by flash column chromatography on basic (pH = 8.5-10.5) Al_2O_3 (EtOAc as an eluent) and recrystallization from CH_2Cl_2 and hexane (good and poor solvent, respectively) to afford (S_p)-**N** (25.7 mg, 0.0419 mmol, 64%) as a colorless crystal. R_f = 0.23 (EtOAc/CH_2Cl_2 = 1/1 v/v). ^{1}H NMR (CD_2Cl_2, 400 MHz) δ 3.16-3.24 (m, 4H), 3.61-3.69 (m, 4H), 7.25 (s, 4H), 7.31 (ddd, J = 1.4, 4.8, 7.6 Hz, 4H), 7.65 (td, J = 1.2, 7.8 Hz, 4H), 7.75 (dt, J = 1.8, 7.7 Hz, 4H), 8.67 (ddd, J = 0.96, 1.7, 4.8 Hz, 4H) ppm; ^{13}C NMR (CD_2Cl_2, 100 MHz) δ 33.2, 88.5, 94.9, 123.4, 125.3, 128.0, 135.5, 136.6, 143.2, 143.9, 150.6 ppm. HRMS (ESI) calcd. for $C_{44}H_{29}N_4$ $[M+H]^+$: 613.2387, found: 613.2364. (R_p)-**N** was obtained by the same procedure in 86% isolated yield. (S_p)-**N**: $[\alpha]^{23}_D$ = −96.4 (c 0.1, CH_2Cl_2). (R_p)-**N**: $[\alpha]^{23}_D$ = +97.7 (c 0.1, CH_2Cl_2).

Synthesis of N-Ph. A mixture of (S_p)-**Cp** (30.0 mg, 0.0986 mmol), 2-bromo-6-(phenylethynyl)pyridine (**9**) (127 mg, 0.493 mmol), $Pd_2(dba)_3$ (9.0 mg, 0.00986 mmol), dppf (10.9 mg, 0.0197 mmol), CuI (3.8 mg, 0.0197 mmol), THF (3 mL) and Et_3N (3 mL) was placed in a round-bottom flask equipped with a magnetic stirring bar. After degassing the reaction mixture several times, the reaction was carried out at 80 ˚C for 24 h. After the reaction, precipitates were removed by filtration, and the solvent was evaporated. The residue was semi-purified by flash column chromatography on SiO_2 (CH_2Cl_2/EtOAc = 9/1 v/v as an eluent). Further purification was carried out by HPLC with $CHCl_3$ and flash column chromatography on basic (pH = 8.5-10.5) Al_2O_3 (CH_2Cl_2/EtOAc = 19/1 v/v as an eluent). The purified sample was collected by lyophilization with benzene to afford (S_p)-**N-Ph** (14.6 mg, 0.0144 mmol, 15%) as a colorless powder. R_f = 0.23 (CH_2Cl_2). ^{1}H NMR (CD_2Cl_2, 400 MHz) δ 3.21-3.29 (m, 4H), 3.66-3.74 (m, 4H), 7.32 (s, 4H), 7.39-7.44 (m, 12H), 7.51 (dd, J = 0.72, 7.6 Hz, 4H), 7.61-7.66 (m, 8H), 7.72 (dd, J = 0.72, 7.8 Hz, 4H), 7.78 (t, J = 7.8 Hz, 4H), ppm; ^{13}C NMR (CD_2Cl_2, 100 MHz) δ 33.0, 88.9, 88.9, 89.6, 94.6, 122.4, 125.4, 126.9, 127.4, 128.9, 129.6, 132.4, 135.8, 137.1, 143.2, 144.1, 144.2 ppm.

HRMS (ESI) calcd. for $C_{76}H_{45}N_4$ $[M+H]^+$: 1013.3639, found: 1013.3624. Elemental analysis calcd. for $C_{76}H_{44}N_4$: C 90.09 H 4.38 N 5.53, found: C 89.51 H 4.51 N 5.47. (R_p)-**N-Ph** was obtained by the same procedure in 21% isolated yield. (S_p)-**N-Ph**: $[\alpha]^{23}_D$ = +16.8 (*c* 0.1, CH_2Cl_2). (R_p)-**N-Ph**: $[\alpha]^{23}_D$ = −16.5 (*c* 0.1, CH_2Cl_2).

Synthesis of N-Py. A mixture of (S_p)-**Cp** (20.0 mg, 0.0657 mmol), **7** (118 mg, 0.270 mmol), $Pd_2(dba)_3$ (6.0 mg, 0.00657 mmol), dppf (7.2 mg, 0.00657 mmol), CuI (2.5 mg, 0.00657 mmol), THF (12 mL) and Et_3N (12 mL) was placed in a round-bottom flask equipped with a magnetic stirring bar. After degassing the reaction mixture several times, the reaction was carried out at 80 ˚C for 24 h. After the reaction, precipitates were removed by filtration, and the solvent was evaporated. The residue was semi-purified by flash column chromatography on SiO_2 ($CHCl_3$ as an eluent) and further purification was carried out by HPLC with $CHCl_3$ to afford (S_p)-**N-Py** (70.7 mg, 0.0408 mmol, 62%) as a light yellow powder. R_f = 0.68 ($CHCl_3$). ^{1}H NMR ($CDCl_3$, 400 MHz) δ 1.02 (t, *J* = 7.4 Hz, 12H), 1.56 (sext, *J* = 7.6 Hz, 8H), 1.85-1.93 (m, 8H), 3.24 (t, *J* = 7.8 Hz, 8H), 3.24-3.33 (m, 4H), 3.73-3.81 (m, 4H), 7.40 (s, 4H), 7.57 (dd, *J* = 2.4 6.5 Hz, 4H), 7.80-7.85 (m, 8H), 7.97 (t, *J* = 7.8 Hz, 4H), 8.02 (t, *J* = 7.7 Hz, 4H), 8.12 (d, *J* = 7.6 Hz, 8H), 8.34 (d, *J* = 7.6 Hz, 4H), 8.43 (s, 4H), 8.70 (dd, *J* = 0.84, 7.8 Hz, 4H) ppm; ^{13}C NMR ($CDCl_3$, 100 MHz) δ 14.0, 23.0, 32.4, 32.9, 33.2, 88.2, 89.3, 93.1, 94.3, 119.1, 122.7, 123.3, 123.6, 125.0, 125.2, 125.3, 125.4, 125.9, 126.3, 126.4, 126.7, 127.2, 129.9, 130.6, 131.3, 133.7, 135.7, 136.7, 137.7, 142.7, 144.1, 144.3 ppm. HRMS (APCI) calcd. for $C_{132}H_{93}N_4$ $[M+H]^+$: 1733.7395, found: 1733.7371. (R_p)-**N-Py** was obtained by the same procedure in 58% isolated yield.

Ag(I) Complexes. The preparation methods of the Ag(I)-coordinated compounds, (S_p)-**N-Ag**, (S_p)-**N-Ph-Ag** and (S_p)-**N-Py-Ag** are as follows. Ag(I) coordination was confirmed by NMR spectra. The difference of solubility between starting compounds and the obtained compounds supported the Ag(I) coordination. Although Ag(I) coordination was also confirmed by MS spectra, *trans*-*N*-*N*-Ag(I) coordinate compounds having two coordination sites were usually detected as mono-coordinate compounds by the MS spectra. Yields of (S_p)-**N-Ph-Ag** and (S_p)-**N-Py-Ag** are not described because the coordination number of the obtained compounds are not clarified.

Preparation of N-Ag. A mixture of (S_p)-**N** (10.0 mg, 0.0163 mmol) and AgOTf (16.8 mg, 0.0652 mmol) was placed in a round-bottom flask equipped with a magnetic stirring bar. After degassing the reaction mixture several times, CH_2Cl_2 (1.0 mL) was added to the mixture. The reaction was carried out at reflux temperature for 14 h. After the reaction, all CH_2Cl_2 was dried over in the same flask. The residue was dissolved in CH_2Cl_2 and filtered to remove excess AgOTf. After the solvent of filtrate was

evaporated, the residue was dissolved in CH_3CN and filtered to remove unreacted (S_p)-**N**. After the solvent of filtrate was evaporated, repreticipation with CH_2Cl_2 and hexane (good and poor solvent respectively) was carried out to afford (S_p)-**N-Ag** (16.1 mg, 0.0143 mmol, 88%) as a light yellow solid. (S_p)-**N** was not dissolved in CH_3CN, but (S_p)-**N-Ag** was dissolved in CH_3CN. ^{1}H NMR (CD_2Cl_2, 400 MHz) δ 3.05-3.14 (m, 4H), 3.49-3.57 (m, 4H), 7.30 (s, 4H), 7.60 (ddd, J = 7.6 5.5, 1.3 Hz, 4H), 7.82 (d, J = 7.6 Hz, 4H), 8.00 (dt, J = 7.8, 1.6 Hz, 4H), 9.07 (d, J = 4.7 Hz, 4H) ppm; ^{13}C NMR ($CDCl_3$, 100 MHz) δ 32.8, 91.9, 94.2, 119.5, 122.7, 125.1, 125.4. 129.2, 135.4, 139.7, 143.5. 143.8, 153.8 ppm (only two peaks of quartet CF_3 peaks of trifluoromethanesulfonate are detected). HRMS (ESI) calcd. for $C_{44}H_{28}N_4Ag$ [M-Ag(OTf)$_2$]$^+$: 719.1359, found: 719.1346. (S_p)-**N-Ag**: $[\alpha]^{23}_D$ = −33.4 (c 0.1, CH_2Cl_2). (R_p)-**N-Ag**: $[\alpha]^{23}_D$ = +36.2 (c 0.1, CH_2Cl_2).

Preparation of N-Ph-Ag. A mixture of (S_p)-**N-Ph** (10.0 mg, 0.00987 mmol) and AgOTf (25.4 mg, 0.0987 mmol) was placed in a round-bottom flask equipped with a magnetic stirring bar. After degassing the reaction mixture several times, CH_2Cl_2 (1.0 mL) was added to the mixture. The reaction was carried out at reflux temperature for 20 h. After the reaction, all CH_2Cl_2 was removed in vacuo. The residue was dissolved in CH_2Cl_2 and filtered to remove excess AgOTf. After the solvent of filtrate was evaporated, the residue was dissolved in MeOH and filtered to remove unreacted (S_p)-**N-Ph**. After the solvent of filtrate was evaporated, repreticipation with CH_2Cl_2 and hexane (good and poor solvent respectively) was carried out to afford (S_p)-**N-Ph-Ag** (13.7 mg, 0.00897 mmol) as a light yellow solid. (S_p)-**N-Ph** was not dissolved in CH_3OH, but (S_p)-**N-Ph-Ag** was dissolved in CH_3OH. ^{1}H NMR (CD_2Cl_2, 400 MHz) δ 3.12-3.20 (m, 4H), 3.56-3.64 (m, 4H), 7.25-7.29 (m, 8H), 7.32-7.35 (m, 8H), 7.39-7.44 (m, 4H), 7.45 (s, 4H), 7.80 (dd, J = 7.8, 0.96 Hz, 4H), 7.90 (dd, J = 7.8, 0.96 Hz, 4H), 8.13 (t, J = 7.8 Hz, 4H) ppm; ^{13}C NMR ($CDCl_3$, 100 MHz) δ 33.0, 87.3, 93.0, 93.7, 95.6, 120.4, 124.9, 128.4, 128.5, 128.7, 130.6, 132.6, 135.8, 140.7, 143.9, 144.3, 145.1 ppm (quartet CF_3 peaks of trifluoromethanesulfonate are not detected). HRMS (ESI) calcd. for $C_{76}H_{44}N_4Ag$ [M-Ag(OTf)$_2$]$^+$: 1119.2611, found: 1119.2607. (R_p)-**N-Ph-Ag** was obtained by the same procedure. (S_p)-**N-Ph-Ag**: $[\alpha]^{23}_D$ = +172.0 (c 0.1, CH_2Cl_2). (R_p)-**N-Ph-Ag**: $[\alpha]^{23}_D$ = −195.2 (c 0.1, CH_2Cl_2).

Preparation of N-Py-Ag. A mixture of (S_p)-**N-Py** (20.0 mg, 0.0115 mmol) and AgOTf (29.5 mg, 0.115 mmol) was placed in a round-bottom flask equipped with a magnetic stirring bar. After degassing the reaction mixture several times, CH_2Cl_2 (2.0 mL) was added to the mixture. The reaction was carried out at reflux temperature for 20 h. After the reaction, all CH_2Cl_2 was removed in vacuo. The residue was dissolved in $CHCl_3$ and filtered to remove excess AgOTf. After the solvent of filtrate was evaporated,

repreticipation with $CHCl_3$ and hexane (good and poor solvent respectively) was carried out to afford (S_p)-**N-Py-Ag** (19.9 mg, 0.00885 mmol) as a light yellow solid. (S_p)-**N-Py** was not dissolved in CH_3CN, but (S_p)-**N-Py-Ag** was dissolved in CH_3CN. However, when (S_p)-**N-Py-Ag** was dissolved in CH_3CN, insoluble compounds (S_p)-**N-Py** precipitate because the Ag coordination of (S_p)-**N-Py-Ag** was weak. HRMS (ESI) calcd. for $C_{132}H_{92}N_4Ag$ $[M\text{-}Ag(OTf)_2]^+$: 1839.6367, found: 1839.6388. (R_p)-**N-Py-Ag** was obtained by the same procedure.

References and Notes

(1) (a) Akita, M. *Organometallics* **2011**, *30*, 43–51. (b) Sagara, Y.; Kato, T. *Nat Chem.* **2009**, *1*, 605–610.

(2) Shigemitsu, H.; Hamachi, I. *Chem.–Asian J.* **2015**, *10*, 2026–2038.

(3) Meng, H.; Li, G. *Polymer* **2013**, *54*, 2199–2221.

(4) (a) McConnell, A. J.; Wood, C. S.; Neelakandan, P. P.; Nitschke, J. R. *Chem. Rev.* **2015**, *115*, 7729–7793. (b) Qi, Z.; Schalley, C. A. *Acc. Chem. Res.* **2014**, *47*, 2222–2233. (c) Yan, X.; Wang, F.; Zheng, B.; Huang, F. *Chem. Soc. Rev.* **2012**, *41*, 6042–6065.

(5) (a) Hembury, G. A.; Borovkov, V. V.; Inoue, Y. *Chem. Rev.* **2008**, *108*, 1–73. (b) Iwamura, M.; Kimura, Y.; Miyamoto, R.; Nozaki, K. *Inorg. Chem.* **2012**, *51*, 4094–4098. (c) Maeda, H.; Bando, Y. *Pure Appl. Chem.* **2013**, *85*, 1967–1978. (d) Liu, M.; Zhang, L.; Wang, T. *Chem. Rev.* **2015**, *115*, 7304–7397.

(6) (a) van Dijk, L.; Bobbert, P. A.; Spano, F. C. *J. Phys. Chem. B* **2010**, *114*, 817–825. (b) Tempelaar, R.; Stradomska, A.; Knoester, J.; Spano, F. C. *J. Phys. Chem. B* **2011**, *115*, 10592–10603.

(7) (a) Woods, C. R.; Benaglia, M.; Siegel, J. S.; Cozzi, F. *Angew. Chem., Int. Ed. Engl.* **1996**, *35*, 1830–1833. (b) Annunziata, R.; Benaglia, M.; Cinquini, M.; Cozzi, F.; Woods, C. R.; Siegel, J. S. *Eur. J. Org. Chem.* **2001**, *2001*, 173–180.

(8) Orita, A.; Nakano, T.; An, D. L.; Tanikawa, K.; Wakamatsu, K.; Otera, J. *J. Am. Chem. Soc.* **2004**, *126*, 10389–10396.

(9) (a) *Cyclophane Chemistry: Synthesis, Structures and Reactions*; Vögtle, F., Ed.; John Wiley & Sons: Chichester, 1993. (b) *Modern Cyclophane Chemistry*; Gleiter, R., Hopf, H., Eds.; Wiley-VCH: Weinheim, 2004.

(10) (a) Morisaki, Y.; Hifumi, R.; Lin, L.; Inoshita, K.; Chujo, Y. *Polym. Chem.*, **2012**, *3*, 2727–2730. (b) Morisaki, Y.; Inoshita, K.; Chujo, Y. *Chem.–Eur. J.*, **2014**, *20*, 8386–8390. (c) Morisaki, Y.; Gon, M.; Sasamori, T.; Tokitoh N.; Chujo, Y. *J. Am. Chem. Soc.*, **2014**, *136*, 3350–3353. (d) Gon, M.; Morisaki, Y.; Chujo, Y. *J. Mater. Chem. C* **2015**, *3*, 521–529. (e) Morisaki, Y.; Inoshita, K.; Shibata, S.; Chujo Y. *Polym. J.* **2015**, 47, 278–281.

(11) For example: Felix, R. J.; Weber, D.; Gutierrez, O.; Tantillo, D. J.; Gagné, M. R. *Nat. Chem.* **2012**, *4*, 405–409.

(12) Jenekhe, S. A.; Osaheni, J. A. *Science* **1994**, *265*, 765–768.

(13) Winnik, F. M. *Chem. Rev.* **1993**, *93*, 587–614.

(14) (a) Tohda, Y.; Sonogashira, K.; Hagihara, N. *Tetrahedron Lett.* **1975**, *16*, 4467–4470. (b) Sonogashira, K. In *Handbook of Organopalladium Chemistry for Organic Synthesis*; Negishi, E., Ed.; Wiley-Interscience: New York, 2002; pp 493−529.

(15) CD dissymmetry factor is defined as $g_{abs} = 2\Delta\varepsilon/\varepsilon$, where $\Delta\varepsilon$ indicates differences of absorbance between left- and right-handed circularly polarized light, respectively. CPL dissymmetry factor is defined as $g_{lum} = 2(I_{left} - I_{right})/(I_{left} + I_{right})$, where I_{left} and I_{right} indicate luminescence intensities of left- and right-handed CPL, respectively.

(16) Berova, N.; Bari, L. D.; Pescitelli, G. *Chem. Soc. Rev.* **2007**, *36*, 914–931.

(17) (a) Munakata, M.; Wu, L. P.; Ning, G. L. *Coord. Chem. Rev.* **2000**, *198*, 171–203. (b) Chebny, V. J.; Rathore, R. *J. Am. Chem. Soc.* **2007**, *129*, 8458–8465. (c) Maier, J. M.; Li, P.; Hwang, J.; Smith, M. D.; Shimizu, K. D. *J. Am. Chem. Soc.* **2015**, *137*, 8014–8017.

(18) Pangborn, A. B.; Giardello, M. A.; Grubbs, R. H.; Rosen, R. K.; Timmers, F. J. *Organometallics* **1996**, *15*, 1518–1520.

(19) González, A. Z.; Benitez, D.; Tkatchouk, E.; Goddard, W. A.; Toste, F. D. *J. Am. Chem. Soc.* **2011**, *133*, 5500–5507.

(20) Huo, J.; Hoberg, J. O. *Int. J. Org. Chem.*, **2011**, *1*, 33–36.

(21) Li, Q.; Huang, F.; Fan, Y.; Wang, Y.; Li, J.; He, Y.; Jiang, H. *Eur. J. Inorg. Chem.* **2014**, *20*, 3235–3244.

Chapter 10

Synthesis of Optically Active X-Shaped Conjugated Compounds and Dendrimers Based on Planar Chiral [2.2]Paracyclophane, Leading to Highly Emissive Circularly Polarized Luminescence Materials

Abstract

The author synthesized optically active dendrimers with a planar chiral 4,7,12,15-tetrasubstituted [2.2]paracyclophane as a core unit. Taking advantage of the rigid and stable chiral conformation of the [2.2]paracyclophane framework, each dendrimer exhibited the maximum circularly polarized luminescence property (CPL) derived form the core unit. In addition, light-harvesting effect and steric protection of dendritic structure enhanced the photoluminescence property both in the dilute solution and in the film state (dissymmetry factor: $g_{lum} \approx 0.002$, and absolute fluorescence quantum efficiency: $\Phi_{lum} \approx 0.60$).

Introduction

Circularly polarized light is widely studied as optically active light in biochemistry,[1] photo-induced enantioselective synthesis,[2-6] and 3D display application. Optically active luminescent materials have a potential to exhibit circularly polarized luminescence (CPL). Recently, many studies were carried out to explore optically active compounds having good CPL property.[7-12] CPL property is usually evaluated with dissymmetry factor (g_{lum}) and photoluminescence (PL) intensity, in addition to molar absorption coefficient (ε) and photoluminescence quantum efficiency (Φ_{lum}). However, the molecule exhibiting good g_{lum} and PL intensity is still limited in number. One of the reasons is that the property of CPL depends on the inherent feature of molecules. If it is possible to enhance CPL property by suitable surroundings, various CPL compounds have the opportunity to be used as practical materials.

Recently, our research group revealed that π-conjugated compounds based on a planar chiral [2.2]paracyclophane exhibited excellent CPL properties ($g_{lum} = 10^{-3}$-10^{-2}, $\varepsilon = 10^5$-10^6 $M^{-1}cm^{-1}$, Φ_{lum} = 0.40-0.90) in the dilute solution.[7,8,12p] Planar chiral [2.2]paracyclophanes provide CPL properties to emitters because of the rigid and stable chiral structure.[13] However, PL intensity of their solids decreased drastically due to the aggregation-caused quenching.

To design next generation CPL materials, the author focuses on the dendritic structure. Dendrimers are widely known as enhancing the core luminescence property by light-harvesting effect and isolating the core unit by steric protection.[14,15] These effects bring out inherent properties of the core, such as the luminescence property, regardless of environment. Thus, dendrimers are expected to enhance the CPL property both in the dilute solution and the aggregation state.

Chiral core dendrimer received much attention as the potential application for catalysts[16] and sensors.[17] On the other hand, there are no reports focusing on the CPL material. One of the reasons is that there have not been a suitable dendrimer core showing conformationally stable

chirality and good luminescence property so far. If the core is flexible, the congested dendrimer structure sometimes reduces its chirality.[18] Hence, planar chiral [2.2]paracyclophanes having the rigid and stable chirality are suitable for the luminescent chiral dendrimer core. In this chapter, the author designed dendrimers having a π-conjugated planar chiral tetrasubstituted [2.2]paracyclophane as a core unit and Fréchet-type phenyl ether dendron. The author synthesized **G0**-**G4** dendrimers and investigated chiroptical properties. This is the first trial synthesizing CPL dendrimers using a luminescent π-conjugated [2.2]paracyclophane as a chiral core.

Results and Discussion

Synthesis

The optical resolution of planar chiral 4,7,12,15-tetrasubstituted [2.2]paracyclophane was carried out using the diastereomer method developed in Chapter 3, and the obtained enantiopure compounds were converted to the corresponding (R_p)- and (S_p)-4,7,12,15-tetraethynyl[2.2]paracyclophanes.[7a] The synthetic routes to the target optically active dendrimers are shown in Schemes 1 and 2. Firstly, the author synthesized iodinated dendrons **D1-I**-**D4-I** using Williamson ether synthesis (Scheme 1), and the synthetic methods of **D1-I**-**D3-I** were already reported (see the experimental section). The author used Sonogashira-Hagihara coupling[19] method to obtain the target optically active dendrimers **G1**-**G4** (Scheme 2). In addition, as a model compound of these dendrimers, chiral core unit **G0** was synthesized in the same way. 3,5-Disubstituted benzyl aryl ether dendrons (Fréchet-type dendrons) were prepared according to the literature.[20,21]

A mixture of **D4-Br**, *p*-iodophenol, K_2CO_3, KI, and 18-crown-6 was refluxed to afford iodinated dendrons **D4-I** in 75% isolated yield (Scheme 1). In Scheme 2, only the reactions of the (S_p)-isomers are shown in these reactions; the (R_p)-isomers were prepared under the same

conditions for (R_p)-**1**. The treatment of (S_p)-4,7,12,15-tetraethynyl[2.2]paracyclophane (S_p)-**1** with iodinated dendrons **Dn-I** (n = 1-4) in the presence of the $Pd_2(dba)_3$/CuI catalytic system using 1,1'-bis(diphenylphosphino)ferrocene (dppf) as a phosphine ligand afforded chiral core dendrimers (S_p)-**Gn** (n = 1-4) in 88% (**G1**), 69% (**G2**), 47% (**G3**), and 55% (**G4**) isolated yields, respectively. In addition, the treatment of (S_p)-**1** with *p*-iodoanisole in the presence of the same catalytic system afforded chiral core unit (S_p)-**G0** in 68% isolated yield. Reaction solvent was selected depending on the solubility of dendrimers. Chiral dendrimer structures are shown in Scheme 3. All dendrimers and the core unit were pale light yellow solids. The structures of all new compounds in this study were confirmed by ^1H and ^{13}C NMR spectroscopy, high-resolution mass spectrometry (HRMS), and elemental analysis; the detailed synthetic procedures and NMR spectra are shown in the experimental section.

Scheme 1. Synthesis of dendrons **D1-I**-**D4-I**

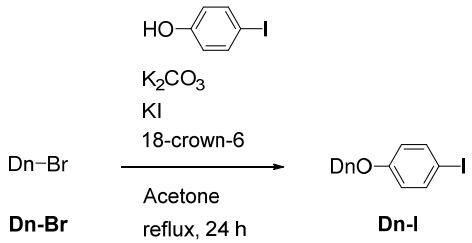

Scheme 2. Synthesis of chiral dendrimers (S_p)-**G0**-(S_p)-**G4**

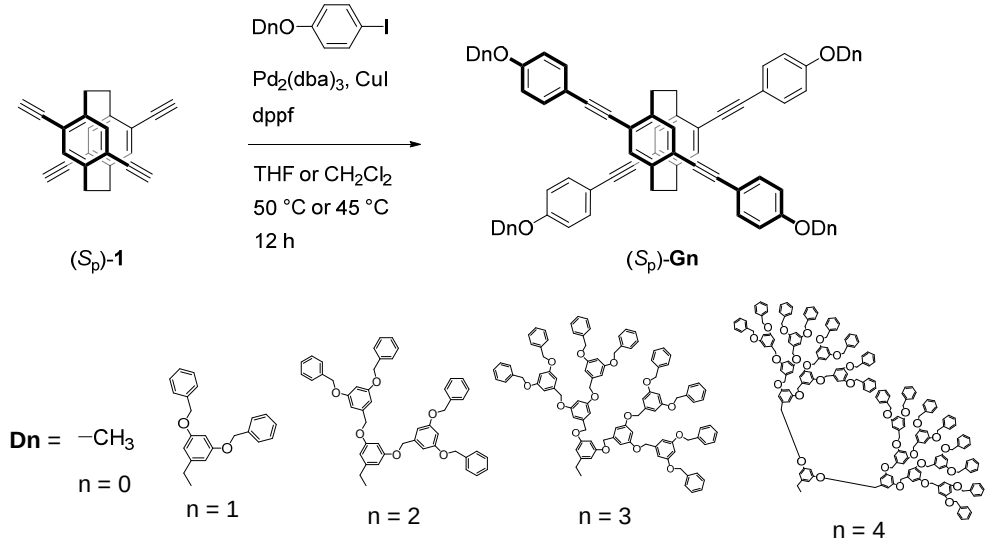

Scheme 3. Structure of chiral dendrimers (S_p)-**G0**-(S_p)-**G4**

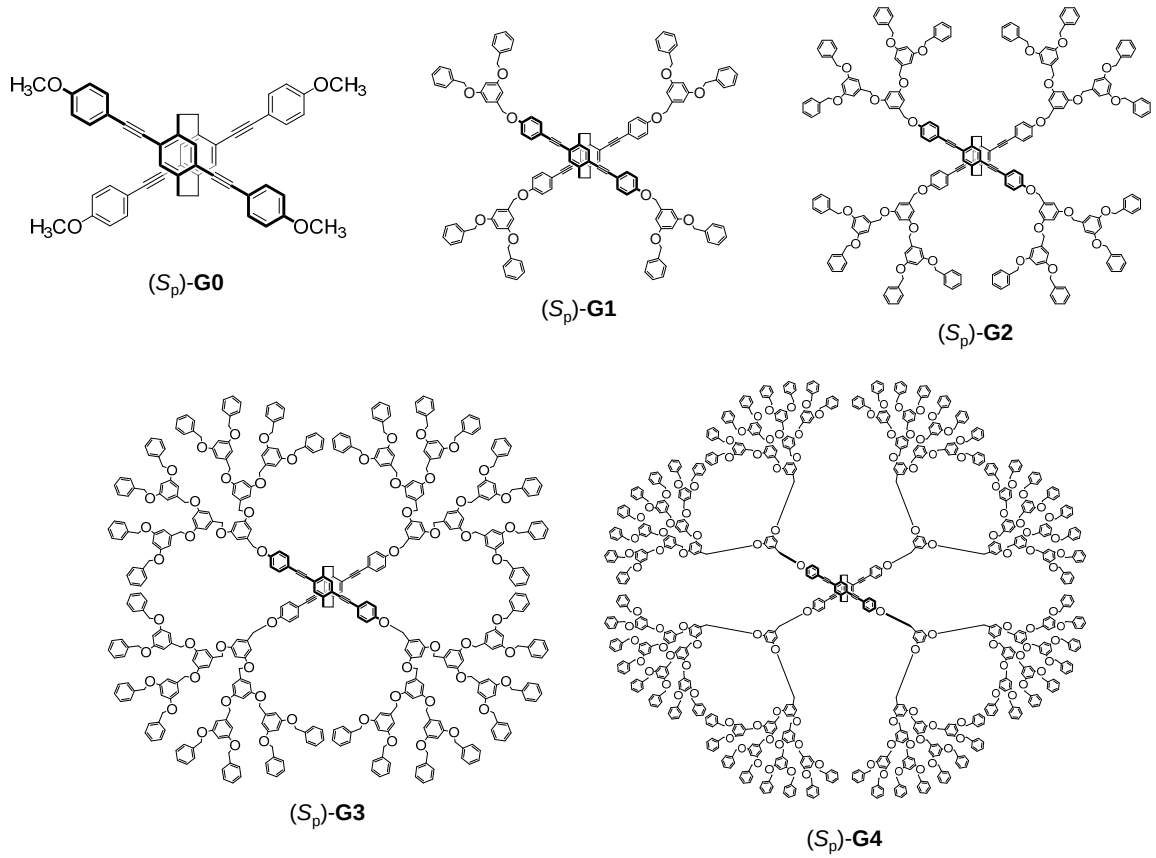

Optical Properties

The optical and chiroptical properties of both enantiomers of dendrimers **G0**-**G4** were evaluated. The data are summarized in Table 1. Optical properties were investigated both in the dilute $CHCl_3$ solution and in the film state (prepared from $CHCl_3$ solution). The film of each dendrimer was prepared by a spin-coated method.

Figures 1A and 1B show the UV-vis absorption spectra of dendrimers in the dilute $CHCl_3$ solution (1.0×10^{-5} M) and in the film state (prepared from $CHCl_3$ solution, 2.0×10^{-3} M), respectively. In the region from 300 to 400 nm, each dendrimer showed a similar absorption band. They are assigned to the absorption band of π-π* transition derived from the [2.2]paracyclophane core unit. This result shows all dendrimers exhibit the identical core properties regardless of the generation and concentration (the dilute solution or the film state) because the dendrons inhibit aggregation of the core units, especially in the film state. In

addition, the absorption at 279 nm increased as the generation increased. This area was identified with the absorption band of π-π* transition derived from benzene rings in the Fréchet-type dendrons.

Table 1. Optical properties: Spectroscopic data of (S_p)-isomers

	$\lambda_{abs}{}^{a}$/nm (ε / 10^5 $M^{-1}cm^{-1}$)	$\lambda_{abs}{}^{b}$/nm	$\lambda_{lum}{}^{c}$/nm	$\lambda_{lum}{}^{d}$/nm	$\Phi_{lum}{}^{e}$	$\Phi_{lum}{}^{f}$
(S_p)-**G0**	279 (0.30), 361 (0.68)	–	416	–	0.66	–
(S_p)-**G1**	279 (0.40), 363 (0.67)	368	415	425, 445	0.63	0.20
(S_p)-**G2**	279 (0.61), 364 (0.69)	278, 367	416	423, 435	0.66	0.54
(S_p)-**G3**	279 (1.00), 365 (0.68)	279, 369	417	421, 438	0.66	0.65
(S_p)-**G4**	279 (1.76), 363 (0.68)	283, 368	416	420, 435	0.67	0.58

[a] In $CHCl_3$ (1.0×10^{-5} M). [b] In film prepared by a spin-coated method from $CHCl_3$ (1.0×10^{-3} M). [c] In $CHCl_3$ (1.0×10^{-7} M), excited at 279 nm. [d] In $CHCl_3$ (1.0×10^{-7} M), excited at 279 nm. [e] Absolute PL quantum efficiency in $CHCl_3$ (1.0×10^{-6} M) excited at peak top of the core unit (365 nm). [f] Absolute PL quantum efficiency in film prepared by a spin-coated method from $CHCl_3$ (1.0×10^{-3} M), excited at peak top of the core unit (370 nm).

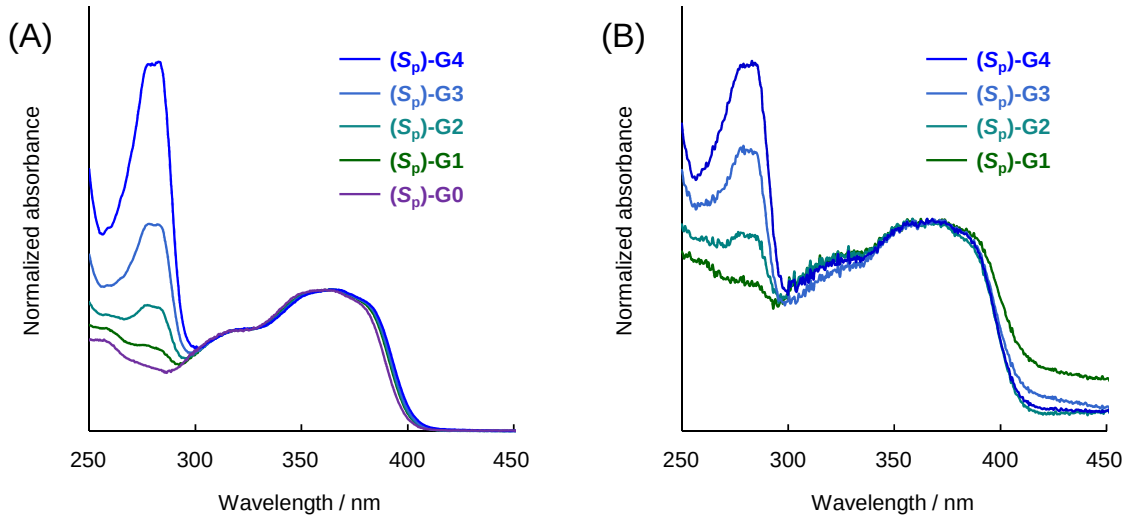

Figure 1. UV-vis absorption spectra of (S_p)-**G0**, **G1**, **G2**, **G3**, and **G4** (A) in the dilute $CHCl_3$ (1.0×10^{-5} M) and (B) in film prepared by a spin-coated method from $CHCl_3$ solution (2.0×10^{-3} M). The spectra were normalized at each peak top in the range from 360 to 370 nm.

Figures 2A and 2B show the photoluminescence (PL) spectra of dendrimers in the dilute $CHCl_3$ solution (1.0×10^{-7} M) and in the film state (prepared from $CHCl_3$ solution, 1.0×10^{-3} M), respectively. Dendrimers were excited at 279 nm, which is the absorption wavelength of benzene rings in the dendrons. Relative intensity was calculated by the excitation spectra, based on the intensity of [2.2]paracyclophane core unit (365 nm in the dilute solution and 325 nm in the film state) as a standard (Figure 3, see experimental section). The intensity of PL spectra increased clearly as the generation of dendrimers increased. This phenomenon was observed both in the dilute solution and in the film state. This clearly shows that dendron could transferred photo-excited energy to the [2.2]paracyclophane core unit and enhanced luminescence property. In the film state, the spectrum of **G1** was more bathochromically shifted than the other dendrimers. This result indicates that intermolecular interaction occurs between cores. That is, **G1** dendron is too small to inhibit intermolecular interaction, and **G2** dendrimer is necessary at least for inhibiting the aggregation-caused quenching.

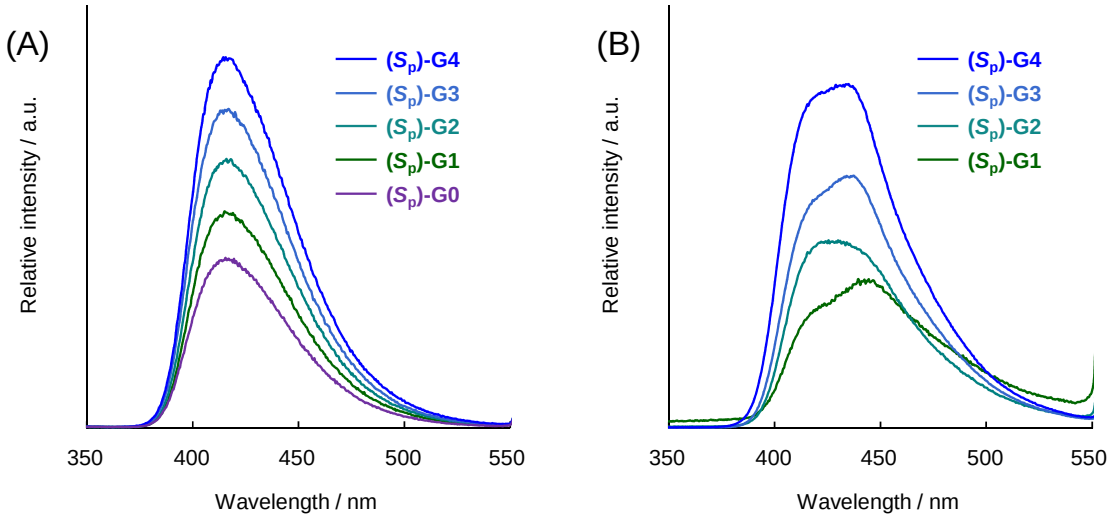

Figure 2. PL spectra of (S_p)-**G0**, **G1**, **G2**, **G3**, and **G4** (A) in the dilute $CHCl_3$ (1.0×10^{-7} M) and (B) in film prepared by a spin-coated method from $CHCl_3$ solution (1.0×10^{-3} M). Excitation wavelength: 279 nm.

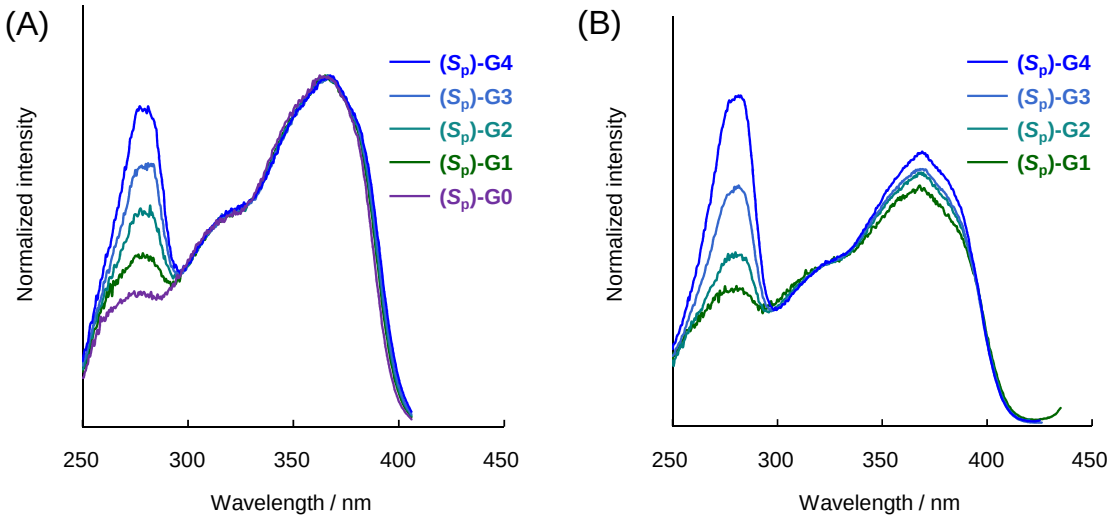

Figure 3. Excitation spectra of (S_p)-**G0**, **G1**, **G2**, **G3**, and **G4** (A) in the dilute $CHCl_3$ (1.0×10^{-5} M) and (B) in film prepared by a spin-coated method from $CHCl_3$ solution (1.0×10^{-3} M). The spectra were normalized at each peak top in the range from 360 to 370 nm in the dilute $CHCl_3$, and 325 nm in film.

Chiroptical Properties

The chiroptical properties of the ground and excited states of dendrimers were investigated by circular dichroism (CD) and CPL spectroscopy, respectively. The chiroptical data, *i.e.* CD and CPL dissymmetry factors (g_{abs} and g_{lum}) are summarized in Table 2.

Figures 3A and 3B show the CD and absorption spectra of both enantiomers of dendrimers in the dilute $CHCl_3$ (1.0×10^{-5} M) and in the film state (prepared from $CHCl_3$ solution, 5.0×10^{-3} M). In all cases, mirror image Cotton effects were observed in the CD spectra, and the g_{abs} values of the first Cotton effect were estimated to be $+1.3 \times 10^{-3}$-$+1.6 \times 10^{-3}$ in the dilute solution and $+1.5 \times 10^{-3}$-$+1.6 \times 10^{-3}$ in the film state, respectively. The spectral shapes of dendrimers in the dilute solution and the film state were similar. This result shows that chiroptical properties depend on the [2.2]paracyclophane core unit instead of the dendrons. In addition, constant chiroptical properties derived from the core were observed regardless of the generations and concentration. This is because of the steric protection of dendrons and the rigid as well as conformationally stable chirality of the [2.2]paracyclophane framework.

Table 2. Chiroptical properties: Spectroscopic data of (S_p)-isomers

	g_{abs}[a,b] / 10^{-3}	g_{abs}[b,c] / 10^{-3}	g_{lum}[a,d] / 10^{-3}	g_{lum}[b,d] / 10^{-3}
(S_p)-**G0**	+1.3	–	+1.4	–
(S_p)-**G1**	+1.3	+1.6	+1.4	+2.1
(S_p)-**G2**	+1.3	+1.6	+1.4	+2.0
(S_p)-**G3**	+1.6	+1.6	+1.4	+1.8
(S_p)-**G4**	+1.3	+1.5	+1.4	+2.0

[a] In $CHCl_3$ (1.0×10^{-5} M). [b] $g_{abs} = 2\Delta\varepsilon/\varepsilon$, where $\Delta\varepsilon$ indicates differences of absorbance between left- and right-handed circularly polarized light, respectively. The g_{abs} value of the first peak top was estimated. [c] In film prepared by a spin-coated method from $CHCl_3$ (5.0×10^{-3} M). [d] $g_{lum} = 2(I_{left} - I_{right})/(I_{left} + I_{right})$, where I_{left} and I_{right} indicate luminescence intensities of left- and right-handed CPL, respectively.

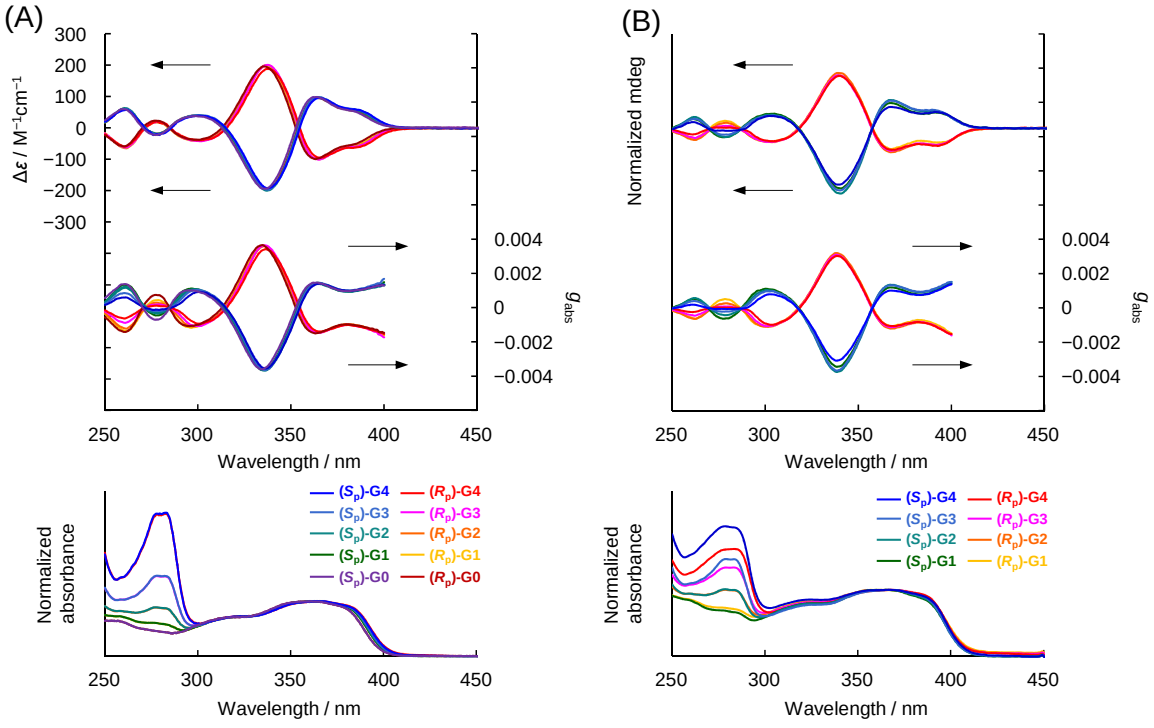

Figure 3. CD (top), g_{abs} (middle), and UV-vis (bottom) spectra of **G0**, **G1**, **G2**, **G3**, and **G4** (A) in the dilute $CHCl_3$ (1.0×10^{-5} M) and (B) in film prepared by a spin-coated method from $CHCl_3$ solution (5.0×10^{-3} M).

Figures 4A and 4B show CPL spectra of dendrimers in the dilute $CHCl_3$ solution (1.0×10^{-5} M) and in the film state (prepared from $CHCl_3$ solution, 5.0×10^{-3} M) excited at 279 nm. Intense and mirror image CPL signals were observed in the emission regions. All dendrimers exhibited very large and similar g_{lum} values of $+1.4 \times 10^{-3}$ in the dilute solution and $+1.8 \times 10^{-3}$-$+2.1 \times 10^{-3}$ in the film state, regardless of the generation and concentration. This result shows that dendrimers can enhance PL intensity keeping large g_{lum} value higher. Dendritic structure has a potential to improve the chiroptical properties.

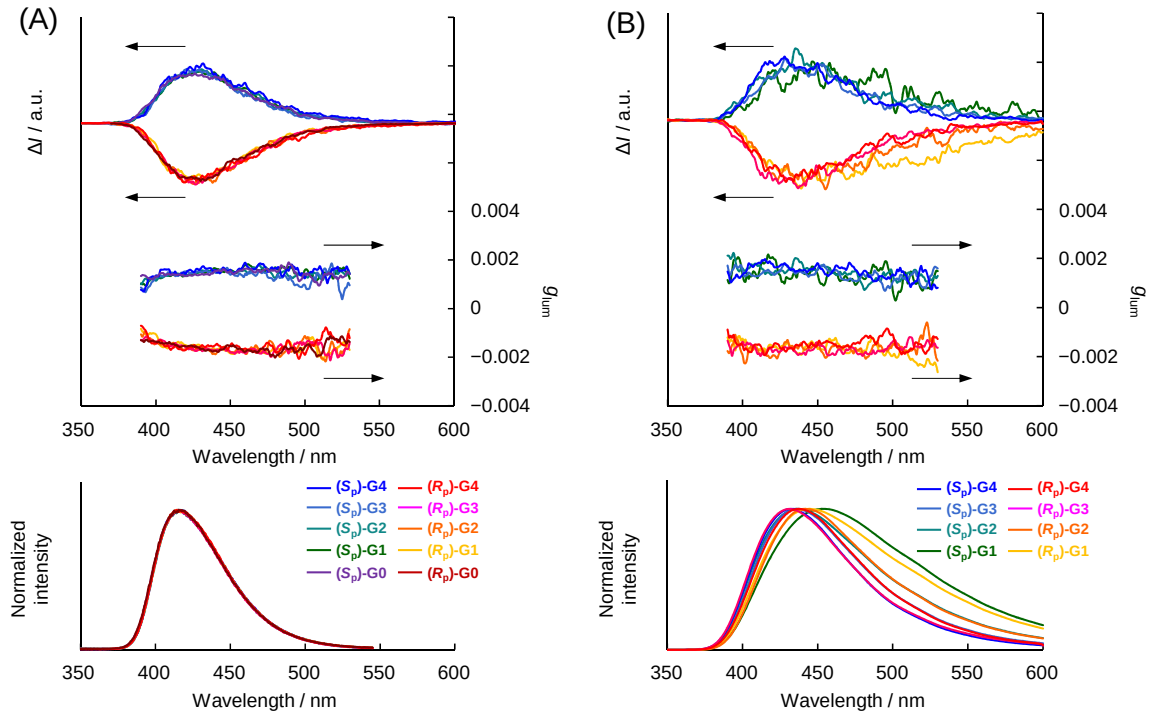

Figure 4. CPL (top), g_{abs} (middle), and PL (bottom) spectra of **G0**, **G1**, **G2**, **G3**, and **G4** (A) in the dilute $CHCl_3$ (1.0×10^{-5} M) and (B) in film prepared by a spin-coated method from $CHCl_3$ solution (5.0×10^{-3} M). Excitation wavelength: 279 nm.

Absolute PL Quantum Efficiency

In order to clarify the effect of steric protection of dendrimers, absolute fluorescence quantum efficiency (Φ_{lum}) was estimated. The [2.2]paracyclophane core unit was directly excited (excitation wavelength: 365 nm in the dilute solution and 370 nm in the film state) to

investigate whether the aggregation-caused quenching occurred or not. The data of Φ_{lum} were plotted, as shown in Figure 5. In the dilute solution, Φ_{lum} of all dendrimers, including core unit, was over 0.60, ((*S*p)-**G0**, 0.66; (*S*p)-**G1**, 0.63; (*S*p)-**G2**, 0.66; (*S*p)-**G3**, 0.66; (*S*p)-**G4**, 0.67). On the other hand, in the film state, Φ_{lum} was changed by the generations. The values were 0.20 ((*S*p)-**G1**), 0.54 ((*S*p)-**G2**), 0.65 ((*S*p)-**G3**), 0.58 ((*S*p)-**G4**). By increasing the generations, Φ_{lum} reached the value of the dilute solution. This is because steric protection of dendrons inhibited the aggregation-caused quenching. This result corresponds to the result of bathochromic shift in the PL spectra. In the case of **G4**, Φ_{lum} decreased slightly compared with **G3**. **G4** dendrons are congested, resulting in the conformational change of the π-conjugated [2.2]paracyclophane core.

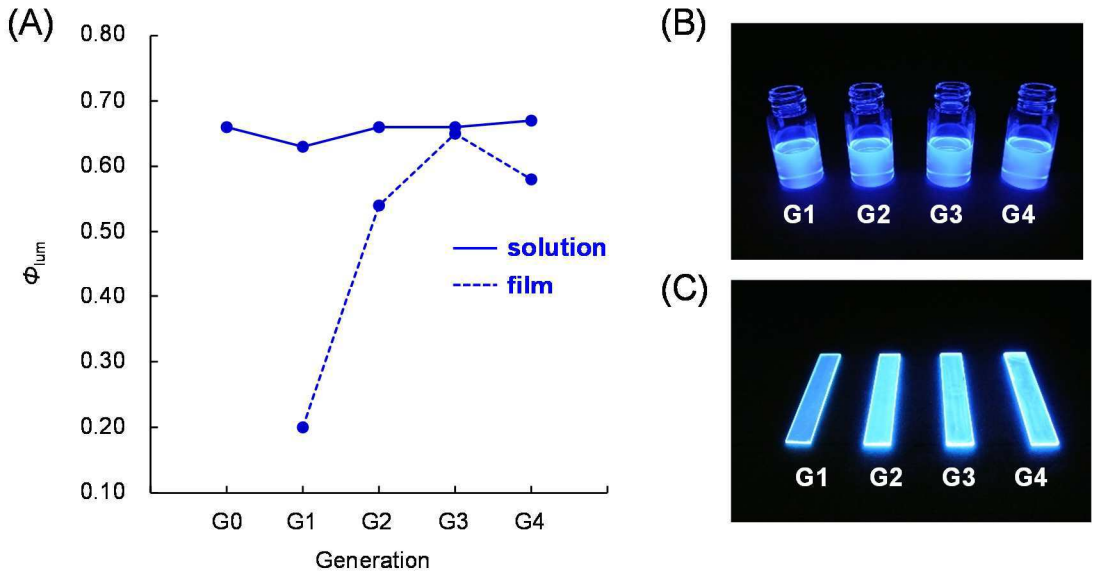

Figure 5. Absolute fluorescence quantum efficiency (Φ_{lum}) of (*S*p)-**G0**, **G1**, **G2**, **G3**, and **G4**. (A) Plot data of Φ_{lum}. (B) Photograph of (*S*p)-**G1**, **G2**, **G3**, and **G4** in $CHCl_3$, (C) Photograph of (*S*p)-**G1**, **G2**, **G3**, and **G4** in film, excited by long wave of UV lamp (365 nm).

Energy Transfer of Dendrons

To investigate the effect of energy transfer of Fréchet-type dendrons, PL intensity of (S_p)-**G0** dispersed in polystyrene, (S_p)-**G3**, and (S_p)-**G4** was investigated. Polystyrene (M_n = 80,000, PDI = 2.6) was used as a matrix to disperse **G0**. Polystyrene is commercially available polymer and can make benzene-rich environment in the same way as the Fréchet-type dendrons. Figures 6A and 6B show PL and excitation spectra of 5 wt% **G0** in polystyrene, 10 wt% **G0** in polystyrene, **G3**, and **G4**, respectively. The film of 5 wt% **G0** in polystyrene was the almost same composition of **G3** dendrimer and the film of 10 wt% **G0** in polystyrene was the almost same composition of **G4** dendrimer. PL spectra were normalized by excitation spectra; the intensity of 325 nm as a standard. (S_p)-**G0** dispersed in polystyrene was excited at 262 nm, which is the wavelength of polystyrene absorption. As shown in Figure 6A, PL intensity of dendrimers was apparently stronger than that of **G0** in polystyrene. According to the excitation spectra, energy transfer did not occur in the case of the dispersing system. The result indicates that the dendritic structure is essential for energy transfer from dendron to the core unit, *i.e.* light-harvesting effect.

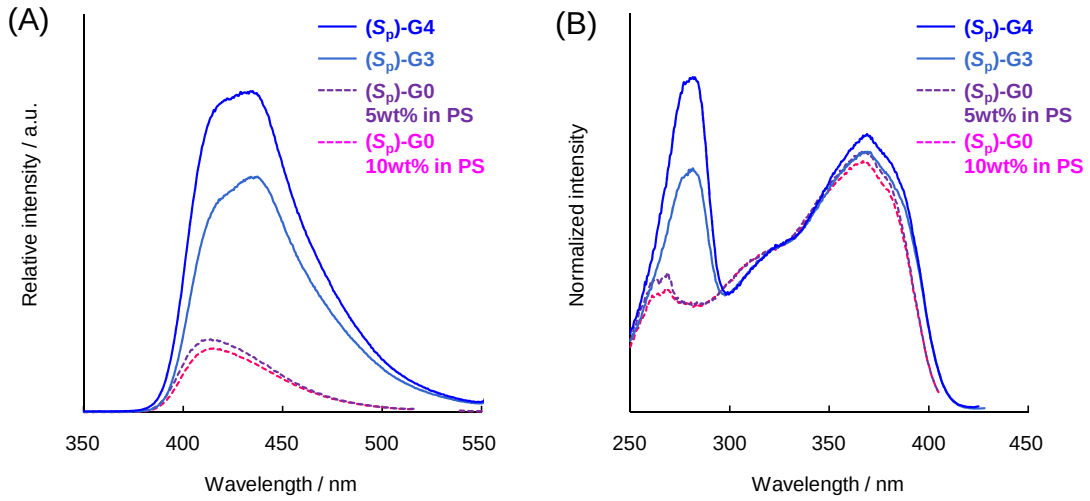

Figure 6. (A) PL spectra of 5 wt%, 10 wt% (S_p)-**G0** dispersed in polystyrene, **G3**, and **G4** in film prepared by a spin-coated method from $CHCl_3$ solution (1.0×10^{-3} M). Excitation wavelength: 262 nm, (S_p)-**G0** dispersed in polystyrene, 279 nm, **G3**, and **G4**. (B) Excitation spectra of 5 wt%, 10 wt% (S_p)-**G0** dispersed in polystyrene, **G3**, and **G4**. The spectra were normalized at 328 nm.

Structures of Dendrimers

Figure 7 shows the dendrimers structures optimized by PM3[22] with MOPAC2012.[23] The structures are shown by a space-fill model. In the case of **G1** and **G2**, the steric protection of dendrons was not sufficient to isolate the core. However, in the case of **G3**, dendrons partially covered core unit, and in **G4** dendrons completely isolated the core. Practically, considering the intermolecular interaction and dendrimer mobility, **G2** dendrimer was sufficient to inhibit the aggregation-caused quenching as judged from the experimental data.

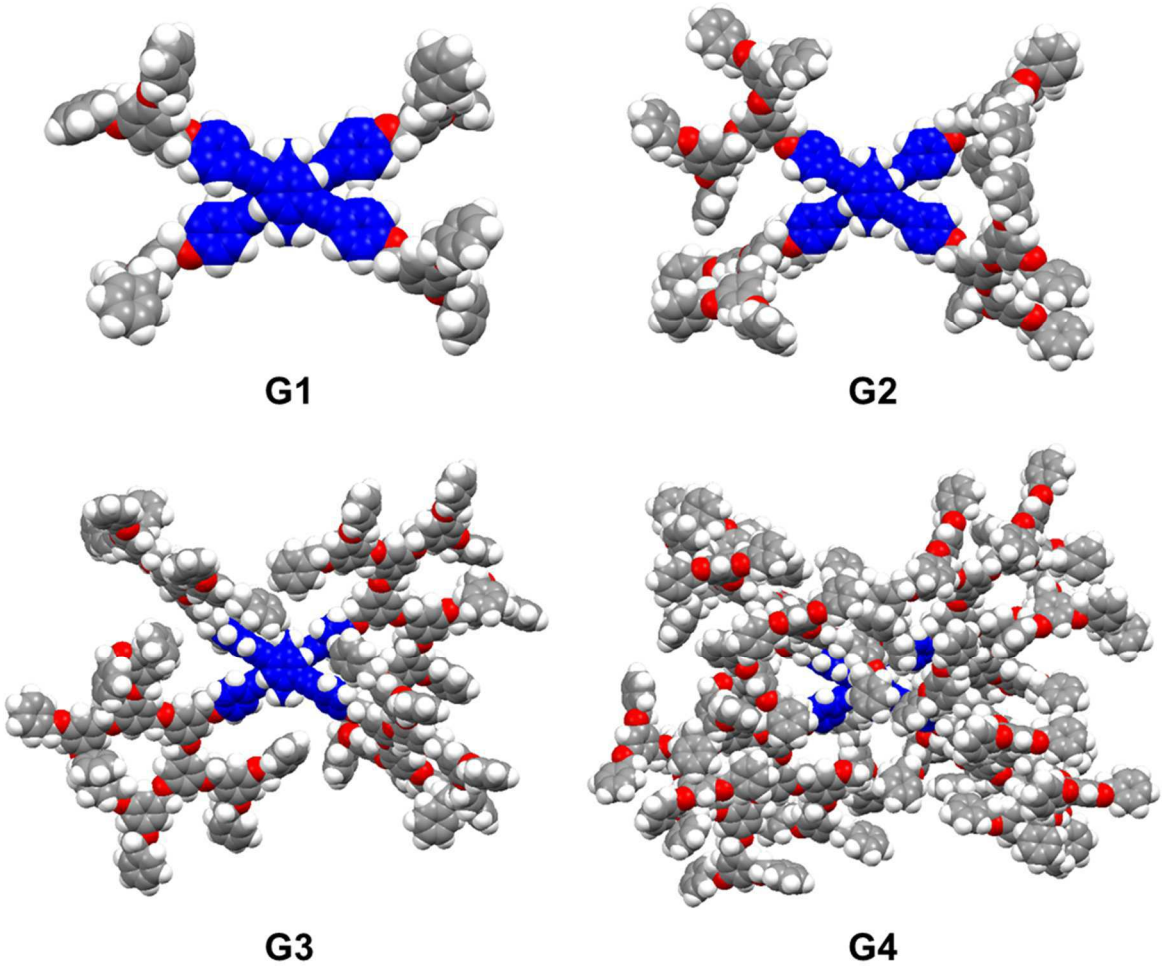

Figure 7. Space-fill model of dendrimers calculated by PM3. The π-conjugated [2.2]paracyclophane core unit is colored blue to clarify.

Conclusions

The author synthesized optically active dendrimers with planar chiral [2.2]paracyclophane as a core unit. In each dendrimer, the chiral core exhibited the inherent properties derived from the planar chiral [2.2]paracyclophane. This is because the planar chiral [2.2]paracyclophane has rigid and conformationally stable chiral structure. In addition, PL intensity was enhanced by light-harvesting effect of the dendritic structure, and intense PL was observed both in the dilute solution and in the film state because of steric protection of the dendrons. To best of the author's knowledge, this the first example of enhancing CPL property with making suitable surroundings. This result definitely leads to next generation CPL materials.

Experimental Section

General. ^{1}H and ^{13}C spectra were recorded on JEOL EX400 and AL400 instruments at 400 and 100 MHz, respectively. Samples were analyzed in $CDCl_3$, and the chemical shift values were expressed relative to Me_4Si as an internal standard. Analytical thin layer chromatography (TLC) was performed with silica gel 60 Merck F254 plates. Column chromatography was performed with Wakogel C-300 SiO_2. High-resolution mass (HRMS) spectrometry was performed at the Technical Support Office (Department of Synthetic Chemistry and Biological Chemistry, Graduate School of Engineering, Kyoto University), and the HRMS spectra were obtained on a Thermo Fisher Scientific EXACTIVE spectrometer for atmospheric pressure chemical ionization (APCI), and a Thermo Fisher Scientific orbitrapXL spectrometer for matrix assisted laser desorption/ionization (MALDI) using 1,8-dihydroxy-9,10-dihydroanthracen-9-one (DIT), α-cyano-4-hydroxycinnamic acid (CHCA), 2,5-dihydroxybenzoic acid (DHB), and 9-nitroanthracene (9-NA) as a matrix. Recyclable preparative high-performance liquid chromatography (HPLC) was carried out on a Japan Analytical Industry Model LC918R (JAIGEL-1H and 2H columns) using $CHCl_3$ as an eluent. UV-vis spectra were recorded on a SHIMADZU UV-3600 spectrophotometer, and samples were analyzed in $CHCl_3$ at room temperature. Photoluminescence (PL) spectra were recorded on a HORIBA JOBIN YVON Fluoromax-4 spectrofluorometer, and samples were analyzed in $CHCl_3$ at room temperature. Specific rotations ($[\alpha]^{t}_{D}$) were measured with a HORIBA SEPA-500 polarimeter. Circular dichroism (CD) spectra were recorded on a JASCO J-820 spectropolarimeter with $CHCl_3$ as a solvent at room temperature. Circularly polarized luminescence (CPL) spectra were recorded on a JASCO CPL-200S with $CHCl_3$ as a solvent at room temperature. Elemental analyses were performed at Organic Elemental Analysis Research Center, Kyoto University.

Materials. Commercially available compounds used without purification: (Tokyo Chemical Industry Co, Ltd.) 4-Iodophenol, $Pd_2(dba)_3$ (dba = dibenzylideneacetone), 1,1'-bis(diphenylphosphino)ferrocene (dppf); (Wako Pure Chemical Industries, Ltd.) *p*-iodoanisole, K_2CO_3 KI, 18-crown-6, CuI. Commercially available solvents and polymers: Acetone (super dehydrated grade, Wako Pure Chemical Industries, Ltd.) and CH_2Cl_2 (deoxygenated grade, Wako Pure Chemical Industries, Ltd.) used without purification. THF (Wako Pure Chemical Industries, Ltd.) and Et_3N (Kanto Chemical Co., Inc.), purified by passage through solvent purification columns under Ar pressure.[24] Polystyrene (degree of polymerization, n = 3,000) was purchased from Wako Pure Chemical Industries, Ltd. and purified with reprecipitation method with $CHCl_3$ and MeOH (good and poor solvent, respectively). The M_n (= 80,000) and PDI (= 2.6) were determined by gel permeation chromatography (GPC) with polystyrene standard.

Compounds prepared as described in the literatures: **Br-D1**, **Br-D2**, **Br-D3**, **Br-D4**[20] **I-D1**, **I-D2**, **I-D3**[21] (S_p)-4,7,12,15-Tetraethynyl[2.2]paracyclophane ((S_p)-**1**).[7a]

Modification Details about Excitation Spectra. PL intensity were normalized by excitation spectra. In the dilute solution, peak tops in the range from 360 to 370 nm was used as standard intensity because this area was derived from the π-conjugated [2.2]paracyclophane core. In the film state, the intensity at 325 nm was used as standard because in the case of the film state, the first peak around 370 nm decreased by π-π interaction between intermolecular cores. This influence was observed in the low generation dendrimers, especially.

Synthesis of D4-I. A mixture of **D4-Br** (1.68 g, 0.500 mmol), 4-iodophenol (110 mg, 0.500 mmol), K_2CO_3 (207 mg, 1.50 mmol), KI (83.0 mg, 0.500 mmol), and 18-crown-6 (6.6 mg, 0.025 mmol) was placed in a round-bottom flask equipped with a magnetic stirring bar. After degassing the reaction mixture several times, acetone (50 mL) was added via a syringe. The mixture was refluxed for 24 h. After the reaction, acetone was evaporated and the residue was washed with H_2O. The organic layer was extracted with CH_2Cl_2 and dried with brine and $MgSO_4$. After removing $MgSO_4$ by filtration, the solvent was evaporated. The residue was purified by column chromatography on SiO_2 (gradient; hexane/CH_2Cl_2 = 1:2-1:9 as an eluent) to afford **D4-I** (1.31 g, 0.375 mmol, 75%) as a colorless solid. R_f = 0.33 (hexane/CH_2Cl_2 = 1/3). ^{1}H NMR ($CDCl_3$, 400 MHz) δ 4.79-5.04 (m, 62H), 650-6.64 (m, 47H), 7.19-7.37, (m, 80H), 7.44 (d, J = 8.8 Hz, 2H) ppm; ^{13}C NMR ($CDCl_3$, 100 MHz) δ 69.7,69.8, 69.9, 70.0, 70.1, 83.1, 101.6, 101.6, 101.6, 101.6, 106.4, 106.4, 106.5, 106.5, 117.3, 127.5, 128.0, 128.5, 136.8, 138.2, 139.2, 139.2, 139.2, 139.2, 158.5, 160.0, 160.1, 160.1, 160.1 ppm. HRMS (CHCA) calcd. for $C_{223}H_{191}INaO_{31}$ $[M+Na]^+$: 3514.2312, found: 3514.2326. Elemental analysis calcd. for $C_{223}H_{191}IO_{31}$: C 76.66 H 5.51, found: C 75.95 H 5.49.

Synthesis of G1. A mixture of (S_p)-**1** (20.0 mg, 0.0657 mmol), **D1-I** (151.0 mg, 0.289 mmol), $Pd_2(dba)_3$ (6.0 mg, 0.0066 mmol), dppf (7.3 mg, 0.013 mmol), CuI (2.5 mg, 0.013 mmol), THF (2 mL) and Et_3N (2 mL) was placed in a round-bottom flask equipped with a magnetic stirring bar. After degassing the reaction mixture several times, the reaction was carried out at 45 °C for 12 h with stirring. After the reaction mixture was cooled to room temperature, precipitates were removed by filtration, and the solvent was removed with a rotary evaporator. The residue was purified by flash column chromatography on SiO_2 ($CHCl_3$ as an eluent). Further purification was carried out by HPLC to afford (S_p)-**G1** (123.4 mg, 0.0896 mmol, 88%) as a pale light yellow solid. ^{1}H NMR ($CDCl_3$, 400 MHz) δ 3.07, (m, 4H), 3.53 (m, 4H), 5.00 (br, 24H) 6.57 (t, J = 2.2 Hz, 4H) 6.67 (d, J = 2.2 Hz, 8H), 6.94 (d, J = 8.8

Hz, 8H), 7.13 (s, 4H), 7.27-7.39 (m, 40H), 7.50 (d, J = 8.8 Hz, 8H) ppm; ^{13}C NMR ($CDCl_3$, 100 MHz) δ 32.6, 69.9, 70.1, 88.2, 94.4, 101.6, 106.3, 115.0, 116.2, 125.1, 127.5, 128.0, 128.5, 132.9, 134.4, 136.7, 139.0, 141.6, 158.7, 160.2 ppm. HRMS (MALDI, DHB) calcd. for $C_{132}H_{104}O_{12}$ $[M]^+$: 1880.7528, found: 1880.7539. Elemental analysis calcd. for $C_{132}H_{104}O_{12}$: C 84.23 H 5.57, found: C 84.41 H 5.61. (R_p)-**G1** was obtained by the same procedure in 83% isolated yield. (S_p)-**G1**: $[\alpha]^{23}_D$ = −14.3 (c 0.1, $CHCl_3$). (R_p)-**G1**: $[\alpha]^{23}_D$ = +13.9 (c 0.1, $CHCl_3$).

Synthesis of G2. A mixture of (S_p)-**1** (10.0 mg, 0.0328 mmol), **D2-I** (155.3 mg, 0.164 mmol), $Pd_2(dba)_3$ (3.0 mg, 0.0033 mmol), dppf (3.6 mg, 0.0066 mmol), CuI (1.3 mg, 0.0066 mmol), CH_2Cl_2 (2 mL) and Et_3N (2 mL) was placed in a round-bottom flask equipped with a magnetic stirring bar. After degassing the reaction mixture several times, the reaction was carried out at 45 °C for 12 h with stirring. After the reaction mixture was cooled to room temperature, precipitates were removed by filtration, and the solvent was removed with a rotary evaporator. The residue was purified by flash column chromatography on SiO_2 ($CHCl_3$ as an eluent). Further purification was carried out by HPLC to afford (S_p)-**G2** (80.5 mg, 0.0225 mmol, 69%) as a pale light yellow solid. ^{1}H NMR ($CDCl_3$, 400 MHz) δ 3.05, (m, 4H), 3.52 (m, 4H), 4.78-5.08 (m, 56H), 6.38-6.66 (m, 36H), 6.95 (d, J = 8.3 Hz, 8H), 7.12 (s, 4H), 7.25-7.38 (m, 80H), 7.49 (d, J = 8.3 Hz, 8H) ppm; ^{13}C NMR ($CDCl_3$, 100 MHz) δ 32.6, 69.9, 70.0, 70.1, 88.3, 94.4, 101.6, 101.6, 106.3, 106.4, 115.0, 116.2, 125.1, 127.5, 127.9, 128.5, 133.0, 134.4, 136.7, 139.1, 139.2, 141.6, 158.7, 160.1, 160.1 ppm. HRMS (MALDI, DHB) calcd. for $C_{244}H_{200}NaO_{28}$ $[M+Na]^+$: 3600.4124, found: 3600.5067. Elemental analysis calcd. for $C_{244}H_{200}O_{28}$: C 81.86 H 5.63, found: C 81.65 H 5.55. (R_p)-**G2** was obtained by the same procedure in 49% isolated yield. (S_p)-**G2**: $[\alpha]^{23}_D$ = +2.9 (c 0.1, $CHCl_3$). (R_p)-**G2**: $[\alpha]^{23}_D$ = −2.7 (c 0.1, $CHCl_3$).

Synthesis of G3. A mixture of (S_p)-**1** (10.0 mg, 0.0329 mmol), **D3-I** (295.4 mg, 0.166 mmol), $Pd_2(dba)_3$ (3.0 mg, 0.0033 mmol), dppf (3.6 mg, 0.0066 mmol), CuI (1.3 mg, 0.0066 mmol), CH_2Cl_2 (3 mL) and Et_3N (3 mL) was placed in a round-bottom flask equipped with a magnetic stirring bar. After degassing the reaction mixture several times, the reaction was carried out at 45 °C for 12 h with stirring. After the reaction mixture was cooled to room temperature, precipitates were removed by filtration, and the solvent was removed with a rotary evaporator. The residue was purified by flash column chromatography on SiO_2 ($CHCl_3$ as an eluent). Further purification was carried out by HPLC to afford (S_p)-**G3** (108.6 mg, 0.0156 mmol, 47%) as a pale light yellow solid. ^{1}H NMR ($CDCl_3$, 400 MHz) δ 3.02, (m, 4H), 3.49 (m, 4H), 4.72-5.04 (m, 120H), 6.45-6.69 (m, 84H), 6.91 (d, J = 8.5 Hz, 8H), 7.09 (s, 4H), 7.20-7.36 (m, 160H), 7.46 (d, J = 8.5 Hz, 8H) ppm; ^{13}C NMR ($CDCl_3$, 100 MHz) δ 32.6, 69.9, 69.9,

70.0, 70.1, 88.3, 94.4, 101.6, 101.6, 101.7, 106.4, 106.5, 106.5, 115.1, 116.2, 125.1, 127.5, 127.9, 128.5, 133.0, 134.4, 136.8, 139.1, 139.2, 139.2, 141.6, 158.7, 160.1, 160.1, 160.2 ppm. HRMS (MALDI, CHCA) calcd. for $C_{468}H_{392}NaO_{60}$ $[M+Na]^+$: 6993.7521, found: 6994.2092. Elemental analysis calcd. for $C_{468}H_{392}O_{60}$: C 80.58 H 5.66, found: C 80.38 H 5.59. (R_p)-**G3** was obtained by the same procedure in 86% isolated yield. (S_p)-**G3**: $[\alpha]^{23}_D$ = +8.4 (*c* 0.1, $CHCl_3$). (R_p)-**G3**: $[\alpha]^{23}_D$ = −7.5 (*c* 0.1, $CHCl_3$).

Synthesis of G4. A mixture of (S_p)-**1** (5.0 mg, 0.016 mmol), **D4-I** (252.3 mg, 0.0722 mmol), $Pd_2(dba)_3$ (1.5 mg, 0.0016 mmol), dppf (1.8 mg, 0.0033 mmol), CuI (0.6 mg, 0.0033 mmol), CH_2Cl_2 (2.5 mL) and Et_3N (2.5 mL) was placed in a round-bottom flask equipped with a magnetic stirring bar. After degassing the reaction mixture several times, the reaction was carried out at 45 °C for 12 h with stirring. After the reaction mixture was cooled to room temperature, precipitates were removed by filtration, and the solvent was removed with a rotary evaporator. The residue was purified by flash column chromatography on SiO_2 ($CHCl_3$ as an eluent). Further purification was carried out by HPLC to afford (S_p)-**G4** (123.4 mg, 0.00896 mmol, 55%) as a pale light yellow solid. ^{1}H NMR ($CDCl_3$, 400 MHz) δ 2.99, (m, 4H), 3.47 (m, 4H), 4.67-4.98 (m, 248H), 6.35-6.60 (m, 180H), 6.87 (d, *J* = 8.3 Hz, 8H), 7.08 (s, 4H), 7.16-7.32 (m, 320H), 7.43 (d, *J* = 8.5 Hz, 8H) ppm; ^{13}C NMR ($CDCl_3$, 100 MHz) δ 32.6, 69.8, 69.8, 69.8, 69.8, 70.0, 88.3, 94.4, 101.5, 101.5, 101.6, 101.6, 106.3, 106.4, 106.4, 106.4, 114.9, 116.1, 125.0, 127.4, 127.9, 128.5, 132.9, 134.4, 136.7, 139.2, 139.2, 139.3, 139.3, 141.5, 158.7, 160.0, 160.0, 160.0, 160.1 ppm. HRMS (MALDI, Sample/9-NA/CH_3COONa = 1/10/1) calcd. for $C_{916}H_{776}NaO_{124}$ $[M+Na]^+$ (Average): 13790.9, found: 13791.7. Elemental analysis calcd. for $C_{916}H_{776}O_{124}$: C 79.91 H 5.68, found: C 78.70 H 5.48. (R_p)-**G4** was obtained by the same procedure in 16% isolated yield. (S_p)-**G4**: $[\alpha]^{23}_D$ = +9.8 (*c* 0.1, $CHCl_3$). (R_p)-**G4**: $[\alpha]^{23}_D$ = −9.0 (*c* 0.1, $CHCl_3$).

Synthesis of G0. A mixture of (S_p)-**1** (20.0 mg, 0.0657 mmol), *p*-iodoanisole (67.7 mg, 0.289 mmol), $Pd_2(dba)_3$ (6.0 mg, 0.0066 mmol), dppf (7.3 mg, 0.013 mmol), CuI (2.5 mg, 0.013 mmol), THF (2 mL) and Et_3N (2 mL) was placed in a round-bottom flask equipped with a magnetic stirring bar. After degassing the reaction mixture several times, the reaction was carried out at 50 °C for 12 h with stirring. After the reaction mixture was cooled to room temperature, precipitates were removed by filtration, and the solvent was removed with a rotary evaporator. The residue was purified by column chromatography on SiO_2 ($CHCl_3$/hexane = 4/1 v/v as an eluent). Further purification was carried out by HPLC to afford (S_p)-**G0** (32.8 mg, 0.0450 mmol, 68%) as a pale light yellow solid. R_f = 0.48 ($CHCl_3$/hexane = 4/1 v/v). ^{1}H NMR ($CDCl_3$, 400 MHz) δ 3.07, (m, 4H), 3.54 (m, 4H), 3.85 (s, 12H), 6.92 (d, *J* = 8.8 Hz, 8H),7.12 (s, 4H), 7.52 (d, *J* = 8.8 Hz, 8H) ppm; ^{13}C NMR ($CDCl_3$, 100 MHz) δ 32.7, 55.4, 88.2, 94.4, 114.2,

111.6, 125.1, 133.0, 134.4, 141.6, 159.7 ppm. HRMS (APCI) calcd. for $C_{52}H_{41}O_4$ $[M+H]^+$: 729.2999, found: 729.2983. Elemental analysis calcd. for $C_{52}H_{40}O_4$: C 85.69 H 5.53, found: C 85.45 H 5.48. (R_p)-**G0** was obtained by the same procedure in 69% isolated yield. (S_p)-**G0**: $[\alpha]^{23}_D$ = −82.1 (*c* 0.1, $CHCl_3$). (S_p)-**G0**: $[\alpha]^{23}_D$ = +84.5 (*c* 0.1, $CHCl_3$).

References and Notes

(1) (a) McLeod, G. C. *Limnol. Oceanogr.* **1957**, *2*, 360–362. (b) Steinberg, I. Z. *Ann. Rev. Biophys. Bioeng.* **1978**, *7*, 113–137. (c) Wynberg, H.; Meijer, E. W.; Hummelen, J. C.; Dekkers, H. P. J. M.; Schippers, P. H.; Carlson, A. D. *Nature* **1980**, *286*, 641–642. (d) Chiou, T.-H.; Kleinlogel, S.; Cronin, T.; Caldwell, R.; Loeffler, B.; Siddiqi, A.; Goldizen, A.; Marshall, J. *Curr. Biol.* **2008**, *18*, 429–434. (e) Sharma, V.; Crne, M.; Park, J. O.; Srinivasarao, M. *Science* **2009**, *325*, 449–451. (f) Shibayev, P. P.; Pergolizzi, R. G. *Int. J. Bot.* **2011**, *7*, 113–117.

(2) (a) Yang, G.; Han, L.; Jiang, H.; Zou, G.; Zhang, Q.; Zhang, D.; Wang, P.; Ming, H. *Chem. Commun.* **2014**, *50*, 2338–2340. (b) Jiang, H.; Pan, X.-J.; Lei, Z.-Y.; Zou, G.; Zhang, Q.-J.; Wang, K.-Y. *J. Mater. Chem.* **2011**, *21*, 4518–4522. (c) Zou, G.; Jiang, H.; Zhang, Q.; Kohn, H.; Manaka, T.; Iwamoto, M. *J. Mater. Chem.* **2010**, *20*, 285–291. (d) Zou, G.; Jiang, H.; Kohn, H.; Manaka, T.; Iwamoto, M. *Chem. Commun.* **2009**, 5627–5629. (e) Zou, G.; Kohn, H.; Ohshima, Y.; Manaka, T.; Iwamoto, M. *Chem. Phys. Lett.* **2007**, *442*, 97–100. (f) Choi, S.-W.; Kawauchi, S.; Ha, N. Y.; Takezoe, H. *Phys. Chem. Chem. Phys.* **2007**, *9*, 3671–3682. (g) Vera, F.; Tejedor, R. M.; Romero, P.; Barberá, J.; Ros, M. B.; Serrano, J. L.; Sierra, T. *Angew. Chem., Int. Ed.* **2007**, *46*, 1873–1877. (h) Choi, S.-W.; Izumi, T.; Hoshino, Y.; Takanishi, Y.; Ishikawa, K.; Watanabe, J.; Takezoe, H. *Angew. Chem., Int. Ed.* **2006**, *45*, 1382–1385. (i) Iftime, G.; Labarthet, F. L.; Natansohn, A.; Rochon, P. *J. Am. Chem. Soc.* **2000**, *122*, 12646–12650. (j) Fujiki, M.; Yoshida, K.; Suzuki, N.; Zhang, J.; Zhang, W.; Zhu, X. *RSC Adv.* **2013**, *3*, 5213–5219. (k) Tamaoki, N.; Wada, M. *J. Am. Chem. Soc.* **2006**, *128*, 6284–6285.

(3) (a) Meinert, C.; Hoffmann, S. V.; Cassam-Chenaï, P.; Evans, A. C.; Giri, C.; Nahon, L.; Meierhenrich, U. J. *Angew. Chem., Int. Ed.* **2014**, *53*, 210–214. (b) Noorduin, W. L.; Bode, A. A. C.; van der Meijden, M.; Meekes, H.; van Etteger, A. F.; van Enckevort, W. J. P.; Christianen, P. C. M.; Kaptein, B.; Kellogg, R. M.; Rasing, T.; Vlieg, E. *Nat. Chem.* **2009**, *1*, 729–732. (c) Nishino, H.; Kosaka, A.; Hembury, G. A.; Aoki, F.; Miyauchi, K.; Shitomi, H.; Onuki, H.; Inoue, Y. *J. Am. Chem. Soc.* **2002**, *124*, 11618–11627. (d) Shibata, T.; Yamamoto, J.; Matsumoto, N.; Yonekubo, S.; Osanai, S.; Soai, K. *J. Am. Chem. Soc.* **1998**, *120*, 12157–12158. (e) Tran, C. D.; Fendler, J. H. *J. Am. Chem. Soc.* **1979**, *101*, 1285–1288.

(4) (a) Wang, Y.; Sakamoto, T.; Nakano, T. *Chem. Commun.* **2012**, *48*, 1871–1873. (b) Huck, N. P. M.; Jager, W. F.; de Lange, B.; Feringa, B. L. *Science* **1996**, *273*, 1686–1688.

(5) (a) Wu, S.-T.; Cai, Z.-W.; Ye, Q.-Y.; Weng, C.-H.; Huang, X.-H.; Hu, X.-L.; Huang, C.-C.; Zhuang, N.-F. *Angew. Chem., Int. Ed.* **2014**, *53*, 12860–12864. (b) Li, J.; Schuster, G. B.; Cheon, K.-S.; Green, M. M.; Selinger, J. V. *J. Am. Chem. Soc.* **2000**, *122*, 2603–2612. (c) Burnham, K. S.; Schuster, G. B. *J. Am. Chem. Soc.* **1999**, *121*, 10245–10246.

(6) (a) Kawasaki, T.; Sato, M.; Ishiguro, S.; Saito, T.; Morishita, Y.; Sato, I.; Nishino, H.; Inoue, Y.; Soai, K. *J. Am. Chem. Soc.* **2005**, *127*, 3274–3275. (b) Stevenson, K. L. *J. Am. Chem. Soc.* **1972**, *94*, 6652–6654.

(7) (a) Morisaki, Y.; Gon, M.; Sasamori, T.; Tokitoh N.; Chujo, Y. *J. Am. Chem. Soc.* **2014**, *136*, 3350–3353. (b) Gon, M.; Morisaki, Y.; Chujo, Y. *J. Mater. Chem. C* **2015**, *3*, 521–529.

(8) Morisaki, Y.; Inoshita, K.; Chujo, Y. *Chem.–Eur. J.* **2014**, *20*, 8386–8390.

(9) Nakamura, K.; Furumi, S.; Takeuchi, M.; Shibuya, T.; Tanaka, K. *J. Am. Chem. Soc.* **2014**, *136*, 5555–5558.

(10) (a) Field, J. E.; Muller, G.; Riehl, J. P.; Venkataraman, D. *J. Am. Chem. Soc.* **2003**, *25*, 11808–11809. (b) Kaseyama, T.; Furumi, S.; Zhang, X.; Tanaka, K.; Takeuchi, M.; *Angew. Chem., Int. Ed.* **2011**, *50*, 3684–3687. (c) Maeda, H.; Bando, Y.; Shimomura, K.; Yamada, I.; Naito, M.; Nobusawa, K.; Tsumatori, H.; Kawai, T. *J. Am. Chem. Soc.* **2011**, *133*, 9266–9269. (d) Sawada, Y.; Furumi, S.; Takai, A.; Takeuchi, M.; Noguchi, K.; Tanaka, K. *J. Am. Chem. Soc.* **2012**, *134*, 4080–4083. (e) Haketa, Y.; Bando, Y.; Takaishi, K.; Uchiyama, M.; Muranaka, A.; Naito, M.; Shibaguchi, H.; Kawai, T.; Maeda, H. *Angew. Chem., Int. Ed.* **2012**, 51, 7967–7971. (f) Oyama, H.; Nakano, K.; Harada, T.; Kuroda, R.; Naito, M.; Nobusawa, K.; Nozaki, K. *Org. Lett.* **2013**, *15*, 2104–2107.

(11) (a) Maeda, H.; Bando, Y. *Pure Appl. Chem.* **2013**, *85*, 1967–1978. (b) CPL was observed from chiral orientation of flurophores. Based on axially chiral scaffolds: Kawai, T.; Kawamura, K.; Tsumatori, H.; Ishikawa, M.; Naito, M.; Fujiki, M.; Nakashima, T. *ChemPhysChem* **2007**, *8*, 1465–1468. (c) Tsumatori, H.; Nakashima, T.; Kawai, T.; *Org. Lett.* **2010**, *12*, 2362–2365. (d) Kimoto, T.; Tajima, N.; Fujiki, M.; Imai, Y.; *Chem.–Asian J.* **2012**, *7*, 2836–2841. (e) Amako, T.; Kimoto, T.; Tajima, N.; Fujiki, M.; Imai, Y. *RSC Adv.* **2013**, *3*, 6939–6944. (f) Amako, T.; Kimoto, T.; Tajima, N.; Fujiki, M.; Imai, Y. *Tetrahedron* **2013**, *69*, 2753–2757. (g) Kimoto, T.; Amako, T.; Tajima, N.; Kuroda, R.; Fujiki, M.; Imai, Y. *Asian J. Org. Chem.* **2013**, *2*, 404–410. (h) Kumar, J.; Nakashima, T.; Tsumatori, H.; Kawai, T. *J. Phys. Chem. Lett.* **2014**, *5*, 316–321. (i) Kitayama, Y.; Amako, T.; Suzuki, N.; Fujiki, M.; Imai, Y. *Org. Biomol. Chem.* **2014**, *12*, 4342–4346. (j) Based on centrally chiral scaffold: Kumar, J.; Nakashima, T.; Tsumatori, H.; Mori, M.; Naito, M.; Kawai, T. *Chem.–Eur. J.* **2013**, *19*, 14090–14097. (k) Amako, T.; Nakabayashi, K.; Mori, T.; Inoue, Y.; Fujiki, M.; Imai, Y. *Chem. Commun.* **2014**, *50*, 12836–12839. (l) Kitayama, Y.; Nakabayashi, K.; Wakabayashi, T.; Tajima, N.; Fujiki, M.; Imai, Y. *RSC Adv.* **2015**, *5*, 410–415. (m) CPL from inherently achiral monochromophore systems is recently reported: Sánchez-Carnerero, E. M.; Moreno, F.; Maroto, B. L.; Agarrabeitia, A. R.; Ortiz, M. J.; Vo, B. G.; Muller, G.; de la Moya, S. *J. Am. Chem. Soc.* **2014**, *136*, 3346–3349. (n) Excimer complex: nouye, M.; Hayashi, K.; Yonenaga, Y.; Itou, T.; Fujimoto, K.; Uchida, T.; Iwamura, M.; Nozaki, K. *Angew. Chem., Int. Ed.* **2014**, *53*, 14392–14396.

(12) Some optically active conjugated polymers exhibit CPL. For polymers emitting CPL in their film or the aggregation states: (a) Peeters, E.; M. Christiaans, P. T.; Janssen, R. A. J.; Schoo, H. F. M.; Dekkers H. P. J. M.; Meijer, E. W. *J. Am. Chem. Soc.* **1997**, *119*, 9909–9910. (b) Satrijio, A.; Meskers, S. C. J.; Swager, T. M. *J. Am. Chem. Soc.* **2006**, *128*, 9030–9031. (c) Wilson, J. N.; Steffen, W.; McKenzie, T. G.; Lieser, G.; Oda, M.; Neher, D.; Bunz, U. H. F.; *J. Am. Chem. Soc.* **2002**, *124*, 6830–6831. (d) Langeveld-Voss, B. M. W.; Janssen, R. A.; Christiaans, M. P. T.; Meskers, S. C. J.; Dekkers, H. P. J. M.; Meijer, E. W. *J. Am. Chem. Soc.* **1996**, *118*, 4908–4909. (e) Oda, M.; Nothofer, H.-G.; Lieser, G.; Scherf, U.; Meskers, S. C. J.; Neher, D. *Adv. Mater.* **2000**, *12*, 362–365. (f) Oda, M.; Nothofer, H.-G.; Scherf, U.; Šunjić, V.; Richter, D.; Regenstein, W.; Meskers, S. C. J.; Neher, D. *Macromolecules* **2002**, *35*, 6792–6798. (g) Goto, H.; Akagi, K. *Angew. Chem., Int. Ed.* **2005**, *44*, 4322–4328. (h) Hayasaka, H.; Miyashita, T.; Tamura, K.; Akagi, K. *Adv. Funct. Mater.* **2010**, *20*, 1243–1250. (i) Fukao S.; Fujiki, M. *Macromolecules* **2009**, *42*, 8062–8067. (j) Yu, J.-M.; Sakamoto, T.; Watanabe, K.; Furumi, S.; Tamaoki, N.; Chen, Y.; Nakano, T. *Chem. Commun.* **2011**, *47*, 3799–3801. (k) Watanabe, K.; Sakamoto, T.; Taguchi, M.; Fujiki, M.; and T. Nakano, *Chem. Commun.* **2011**, *47*, 10996–10998. (l) Hirahara, T.; Yoshizawa-Fujita, M.; Takeoka, Y.; Rikukawa, M. *Chem. Lett.* **2012**, *41*, 905–907. (m) Watanabe, K.; Koyama, Y.; Suzuki, N.; Fujiki, M.;

Nakano, T. *Polym. Chem.* **2014**, *5*, 712–717. (n) For polymer aggregates in optically active solvents: Nakano, Y.; Liu, Y.; Fujiki, M. *Polym. Chem.* **2010**, *1*, 460–469. (o) Kawagoe, Y.; Fujiki, M.; Nakano, Y. *New J. Chem.* **2010**, *34*, 637–647. (p) For polymers emitting CPL in solution: Morisaki, Y.; Hifumi, R.; Lin, L.; Inoshita, K.; Chujo, Y. *Polym. Chem.* **2012**, *3*, 2727–2730. (q) Nagata, Y.; Nishikawa, T.; Suginome, M. *Chem. Commun.* **2014**, *50*, 9951–9953. (r) For CPL created by polymer-polymer complexation: Shiraki, T.; Tsuchiya, Y.; Noguchi, T.; Tamaru, S.; Suzuki, N.; Taguchi, M.; Fujiki, M.; Shinkai, S. *Chem.–Asian J.* **2014**, *9*, 218–222.

(13) (a) Bazan, G. C.; Oldham Jr, W. J.; Lachicotte, R. J.; Tretiak,S.; Chernyak, V.; Mukamel, S. *J. Am. Chem. Soc.* **1998**, *120*, 9188–9204. (b) Wang, S.; Bazan, G. C.; Tretiak, S.; Mukamel, S. *J. Am. Chem. Soc.* **2000**, *122*, 1289–1297. (c) Zyss, J.; Ledoux, I.; Volkov, S.; Chernyak, V.; Mukamel, S.; Bartholomew, G. P.; Bazan, G. C. *J. Am. Chem. Soc.* **2000**, *122*, 11956–11962. (d) Bartholomew G. P.; Bazan, G. C.; *Acc. Chem. Res.* **2001**, *34*, 30–39. (e) Bartholomew G. P.; Bazan, G. C. *Synthesis* **2002**, 1245–1255. (f) Bartholomew G. P.; Bazan, G. C. *J. Am. Chem. Soc.* **2002**, *124*, 5183–5196. (g) Seferos, D. S.; Banach, D. A.; Alcantar, N. A.; Israelachvili, J. N.; Bazan, G. C. *J. Org. Chem.* **2004**, *69*, 1110–1119. (h) Bartholomew, G. P.; Rumi, M.; Pond, S. J. K.; Perry, J. W.; Tretiak, S.; Bazan, G. C. *J. Am. Chem. Soc.* **2004**, *126*, 11529– 11542. (i) Hong, J. W.; Woo, H. Y.; Bazan, G. C. *J. Am. Chem. Soc.* **2005**, *127*, 7435–7443. (j) Bazan, G. C. *J. Org. Chem.* **2007**, 72, 8615–8635.

(14) (a) Stewart, G. M.; Fox, M. A. *J. Am. Chem. Soc.* **1996**, *118*, 4354–4360. (b) Devadoss, C.; Bharathi, P.; Moore, J. S. *J. Am. Chem. Soc.* **1996**, *118*, 9635–9644. (c) Bar-Haim, A.; Klafter, J.; Kopelman, R. *J. Am. Chem. Soc.* **1997**, *119*, 6197–6198. (d) Shortreed, M. R.; Swallen, S. F.; Shi, S.-Y.; Tan, W.; Xu, Z.; Devadoss, C.; Moore, J. S.; Kopelman, R. *J. Phys. Chem. B* **1997**, *101*, 6318–6322. (e) Kawa, M.; Fréchet, J. M. *Chem. Mater.* **1998**, *10*, 286–296. (f) Jiang, D.-L.; Aida, T. *J. Am. Chem. Soc.* **1998**, *120*, 10895–10901. (g) Gilat, S. L.; Adronov, A.; Fréchet, J. M. J. *Angew. Chem., Int. Ed.* **1999**, *38*, 1422–1427. (h) Sato, T.; Jiang, D.-L.; Aida, T. *J. Am. Chem. Soc.* **1999**, *121*, 10658–10659. (i) Adronov, A.; Gilat, S. L.; Fréchet, J. M. J.; Ohta, K.; Neuwahl, F. V. R.; Fleming, G. R. *J. Am. Chem. Soc.* **2000**, *122*, 1175–1185. (j) Peng, Z.; Pan, Y.; Xu, B.; Zhang, J. *J. Am. Chem. Soc.* **2000**, *122*, 6619–6623. (k) Weil, T.; Reuther, E.; Müllen, K. *Angew. Chem., Int. Ed.* **2002**, *41*, 1900–1904. (l) Melinger, J. S.; Pan, Y.; Kleiman, V. D.; Peng, Z.; Davis, B. L.; McMorrow, D.; Lu, M. *J. Am. Chem. Soc.* **2002**, *124*, 12002–12012. (m) Cotlet, M.; Vosch, T.; Habuchi, S.; Weil, T.; Müllen, K.; Hofkens, J.; De Schryver, F. *J. Am. Chem. Soc.* **2005**, *127*, 9760–9768. (n) Wang, J.-L.; Yan, J.; Tang, Z.-M.; Xiao, Q.; Ma, Y.; Pei, J. *J. Am. Chem. Soc.* **2008**, *130*, 9952–9962.

(15) Reviews: (a) Adronov, A.; Frechet, J. M. J. *Chem. Commun.* **2000**, 1701–1710. (b) Liu, D.; Feyter, S. D.; Cotlet, M.; Stefan, A.; Wiesler, U.-M.; Herrmann, A.; Grebel-Koehler, D.; Qu, J.; Müllen, K.; De Schryver, F. C. *Macromolecules* **2003**, *36*, 5918–5925. (c) Ceroni, P.; Bergamini, G.; Marchioni, F.; Balzani, V. *Prog. Polym. Sci.* **2005**, *30*, 453–473. (d) Zeng, Y.; Li, Y.-Y.; Chen, J.; Yang, G.; Li, Y. *Chem.–Asian J.* **2010**, *5*, 992–1005. (e) Nantalaksakul, A.; Reddy, D. R.; Bardeen, C. J.; Thayumanavan, S. *Photosynth. Res.* **2006**, *87*, 133–150. (f) Balzani, V.; Bergamini, G.; Ceroni, P.; Marchi, E. *New J. Chem.* **2011**, *35*, 1944–1954.

(16) (a) Wang, Z.-J.; Deng, G.-J.; Li, Y.; He, Y.-M.; Tang, W.-J.; Fan, Q.-H. *Org. Lett.* **2007**, *9*, 1243–1246. (b) Zhang, F.; Li, Y.; Li, Z.-W.; He, Y.-M.; Zhu, S.-F.; Fan, Q.-H.; Zhou, Q.-L. *Chem. Commun.* **2008**,

6048–6050. (c) Caminade, A.-M.; Servin, P.; Laurent, R.; Majoral, J.-P. *Chem. Soc. Rev.* **2008**, *37*, 56–67. (d) Ma, B.; Ding, Z.; Liu, J.; He, Y.; Fan, Q.-H. *Chem.–Asian J.* **2013**, *8*, 1101–1104.

(17) (a) Pu, L. *Macromol. Rapid Commun*. **2000**, 21, 795–809. (b) Pugh, V. J.; Hu, Q.-S.; Pu, L. *Angew. Chem., Int. Ed.* **2000**, *39*, 3638–3641. (c) Gong, L.-Z.; Hu, Q.-S.; Pu, L. *J. Org. Chem.* **2001**, *66*, 2358–2367. (d) Pugh, V. J.; Hu, Q.-S.; Zuo, X.; Lewis, F. D.; Pu, L. *J. Org. Chem.* **2001**, *66*, 6136–6140.

(18) (a) Chaumette, J.-L.; Laufersweiler, M. J.; Parquette, J. R. *J. Org. Chem*. **1998**, *63*, 9399-9405. (b) Ma, L.; Lee, S. J.; Lin, W. *Macromolecule* **2002**, *35*, 6178–6184.

(19) (a) Tohda, Y.; Sonogashira K.; Hagihara, N. *Tetrahedron Lett.* **1975**, *16*, 4467–4470. (b) Sonogashira, K. In *Handbook of Organopalladium Chemistry for Organic Synthesis*; Negishi, E., Ed.; Wiley-Interscience: New York, 2002; pp 493−529.

(20) Hawker, C. J.; Fréchet, J. M. J. *J. Am. Chem. Soc.* **1990**, *112*, 7638–7647.

(21) Liu, H.; Du, D.-M. *Eur. J. Org. Chem.* **2010**, 2121–2131.

(22) Stewart, J. J. P. Optimization of Parameters for Semi-Empirical Methods I-Method. *J. Comput. Chem.* **1989**, *10*, 209–220.

(23) (a) Stewart, J. J. P. Stewart Computational Chemistry, Version 14.264W web: HTTP://OpenMOPAC.net (b) Maia, J. D. C., et al., *J. Chem. Theory Comput.* **2012**, *8*, 3072–3081.

(24) Pangborn, A. B.; Giardello, M. A.; Grubbs, R. H.; Rosen R. K.; Timmers, F. J. *Organometallics* **1996**, *15*, 1518–1520.

List of Publications

Part I: Conjugated Microporous Polymers Based on [2.2]Paracyclophanes

Chapter 1

Synthesis and Characterization of [2.2]Paracyclophane-Containing Conjugated Microporous Polymers

Morisaki, Y.; Gon, M.; Tsuji, Y.; Kajiwara, Y.; Chujo, Y.

Macromol. Chem. Phys. **2012**, *213*, 572−579.

Chapter 2

Conjugated Microporous Polymers Consisting of Tetrasubstituted [2.2]Paracyclophane Junctions

Morisaki, Y.; Gon, M.; Chujo, Y.

J. Polym. Sci. Part A: Polym. Chem. **2013**, *51*, 2311−2316.

Part II: π-Conjugated Compounds Based on Planar Chiral [2.2]Paracyclophanes

Chapter 3

Planar Chiral Tetrasubstituted [2.2]Paracyclophane: Optical Resolution and Functionalization

Morisaki, Y.; Gon, M.; Sasamori, T.; Tokitoh, N.; Chujo, Y.

J. Am. Chem. Soc. **2014**, *136*, 3350−3353.

Chapter 4

Optically Active Cyclic Compounds Based on Planar Chiral [2.2]Paracyclophane: Extension of the Conjugated Systems and Chiroptical Properties

Gon, M.; Morisaki, Y.; Chujo Y.

J. Mater. Chem. C **2015**, *3*, 521−529.

Chapter 5

Optically Active Cyclic Compounds Based on Planar Chiral [2.2]Paracyclophane: Extension of π-Surface with Naphthalene Units

Gon, M.; Kozuka, H.; Morisaki, Y.; Chujo, Y.

Submitted to Asian J. Org. Chem.

Chapter 6

Highly Emissive Optically Active Conjugated Dimers Consisting of Planar Chiral [2.2]Paracyclophane Showing Circularly Polarized Luminescence

Gon, M.; Morisaki, Y.; Chujo, Y.

Eur. J. Org. Chem. in press.

Chapter 7

Enhancement of Circularly Polarized Luminescence Based on a Planar Chiral Tetrasubstituted [2.2]Paracyclophane Framework in Dilute Solution and Aggregation

Gon, M.; Sawada, R.; Morisaki, Y.; Chujo, Y.

to be submitted

Chapter 8

Optically Active Phenylethene Dimers Based on Planar Chiral Tetrasubstituted [2.2]Paracyclophane

Gon, M.; Morisaki, Y.; Chujo Y.

Submitted for publication

Part III: Optically Active Materials Based on Planar Chiral [2.2]Paracyclophanes

Chapter 9

Control of Optical and Chiroptical Properties with Metal-Induced Higher-Ordered Structure Based on Planar Chiral Tetrasubstituted [2.2]Paracyclophane

Gon, M.; Morisaki, Y.; Chujo Y.

to be submitted

Chapter 10

Synthesis of Optically Active X-Shaped Conjugated Compounds and Dendrimers Based on Planar Chiral [2.2]Paracyclophane, Leading to Highly Emissive Circularly Polarized Luminescence Materials

Gon, M.; Morisaki, Y.; Sawada, R.; Chujo Y.

Chem.−Eur. J. accepted.

Other Publication

Stacked 1,3,5-Tris[(2,5-dimethylphenyl)ethynyl]benzenes: Dimer and Conjugated Microporous Polymer

Morisaki, Y.; Gon, M.; Tsuji, Y.; Kajiwara, Y.; Chujo, Y.

Tetrahedron Lett. **2011**, *52*, 5504−5507.